

Bombesin and Neurotensin Receptor Targeting Using Radiolabeled Peptide Analogs

ISBN: 978-90-8559-328-7

Cover picture: M. de Visser

Cover design: Optima Grafische Communicatie, Rotterdam, The Netherlands

Printed by: Optima Grafische Communicatie, Rotterdam, The Netherlands

© 2007, M. de Visser

All rights reserved. No part of this thesis may be reproduced, stored in a retrieval system of any nature, or transmitted in any form by any means, electronic, mechanical, photocopying, recording or otherwise, without the permission of the author.

Bombesin and Neurotensin Receptor Targeting Using Radiolabeled Peptide Analogs

Bombesine en neurotensine receptor targeting
met radiogelabelde peptide derivaten

Proefschrift

ter verkrijging van de graad van doctor aan de
Erasmus Universiteit Rotterdam
op gezag van de
rector magnificus

Prof.dr. S.W.J. Lamberts

en volgens besluit van het College voor Promoties.

De openbare verdediging zal plaatsvinden op

woensdag 12 december 2007 om 13.45 uur.

door

Monique de Visser

geboren te Bergen op Zoom



PROMOTIECOMMISSIE

Promotoren:

Prof. Dr. Ir. M. de Jong

Prof. Dr. E.P. Krenning

Overige leden:

Prof. Dr. B.J.M. Heijmen

Prof. Dr. C.H. Bangma

Prof. Dr. C. van de Wiele



Contents

- Chapter 1 General Introduction: Improvement strategies for peptide receptor scintigraphy and radionuclide therapy. 7
Cancer Biotherapy & Radiopharmaceuticals 2007; in press
- Part I Neurotensin analogs for in vivo targeting of exocrine pancreatic cancer**
- Chapter 2 Stabilised ¹¹¹In-labeled DTPA- and DOTA-conjugated neurotensin analogs for imaging and therapy of exocrine pancreatic cancer. 43
European Journal of Nuclear Medicine and Molecular Imaging 2003; Vol. 30(8): 1134-1139
- Chapter 3 Five stabilized ¹¹¹In-labeled neurotensin analogs in nude mice bearing HT29 tumors. 57
Cancer Biotherapy and Radiopharmaceuticals 2007; Vol. 22(3): 374-382
- Part II Bombesin analogs for in vivo targeting of prostate cancer**
- Chapter 4 Novel ¹¹¹In-labeled bombesin analogs for molecular imaging of prostate tumors. 73
European Journal of Nuclear Medicine and Molecular Imaging, 2007; Vol. 34(8):1228-1238
- Chapter 5 Molecular imaging of gastrin-releasing peptide receptor-positive tumors in mice using ⁶⁴Cu- and ⁸⁶Y-DOTA-(Pro¹,Tyr⁴)-bombesin(1-14). 93
Bioconjugate Chemistry 2007; Vol. 18(3): 724-730

Part III GRP receptor-expression during prostate cancer development

Chapter 6 Androgen-dependent expression of the gastrin-releasing peptide receptor in human prostate tumor xenografts. 115
Journal of Nuclear Medicine 2007; Vol. 48(1): 88-93

Chapter 7 Androgen-regulated gastrin-releasing peptide receptor expression in androgen-dependent human prostate tumor xenografts. 129
Manuscript submitted

Part IV Epilogue

Chapter 8 Summary and general discussion 145

Chapter 9 Nederlandse samenvatting voor niet-ingewijden 155

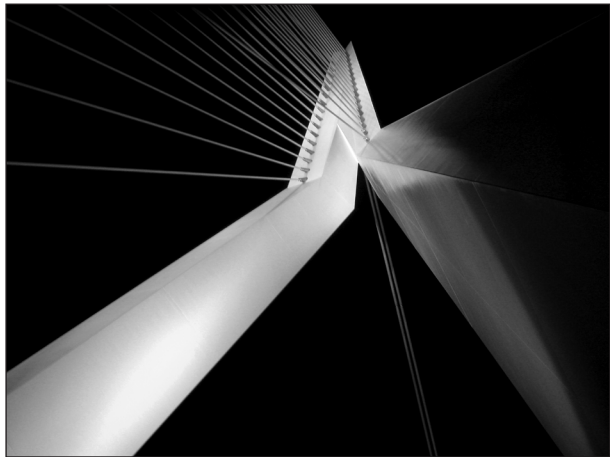
Dankwoord 163

Curriculum vitae 171

Publicaties 175

1

General introduction



Published as: Improvement strategies for peptide receptor scintigraphy and radionuclide therapy

Monique de Visser*

Suzanne M. Verwijnen*

Marion de Jong

*Both authors contributed equally to this manuscript.

Cancer Biotherapy & Radiopharmaceuticals 2007; in press

SUMMATION

Somatostatin receptor-targeting peptides are widely used for imaging and therapy of neuroendocrine tumors. Peptide receptor radionuclide therapy (PRRT) in neuroendocrine tumor patients with radiolabeled somatostatin analogs has resulted in symptomatic improvement, prolonged survival and enhanced quality of life. The side-effects of PRRT are few and mostly mild, certainly when using kidney protective agents. If more widespread use of PRRT is possible, such therapy might become the therapy of first choice in patients with metastasized or inoperable neuroendocrine GEP tumors.

Yet, much profit can be gained from improving the receptor-targeting strategies available and developing new strategies. This review presents an overview of several options to optimize receptor-targeted imaging and radionuclide therapy. These include optimization of peptide analogs, increasing the number of receptors on the tumor site, and combining PRRT with other treatment strategies.

The development of new peptide analogs with increased receptor binding affinity and improved stability might lead to higher accumulation of radioactivity inside tumor cells. Analogs of somatostatin have been widely studied. However, much profit can be gained in improving peptide analogs targeting other tumor related receptors, including gastrin-releasing peptide (GRP) receptors, neurotensin (NT) receptors, cholecystokinin (CCK) receptors, and glucagon-like peptide-1 (GLP-1) receptors. Several peptide analogs targeting these receptors are well on their way to clinical utilization.

Literature shows that it is possible to increase the receptor density on tumor cells using different methods which results in higher binding and internalization rates and thus a higher contrast during peptide-receptor-scintigraphy (PRS). In PRRT treatment, this would enable the administration of higher therapeutic doses to tumors, which might lead to a higher cure rate in patients.

Combinations of radionuclide therapy with other treatment modalities like chemotherapy or pre-treatment with radiosensitizers might increase the impact of the treatment. Furthermore, administration of higher dosages of radioactivity to the patient enabled by combinations of PRRT with strategies reducing the radiation dose to healthy organs will improve the outcome of tumor treatment. Also targeting one or several tumor-specific receptors by using combinations of therapeutic agents, as well as by reducing non-target uptake of radioactivity, will enlarge the therapeutic window of PRRT. Clinical studies will provide more insight in the effects of combining treatment strategies in cancer patients.

INTRODUCTION

Radiolabeled receptor-binding peptides are powerful tools for imaging and therapy of tumors expressing peptide binding receptors. Especially analogs of somatostatin are suitable for receptor-targeted localization, staging and treatment of somatostatin receptor (sst)-expressing neuroendocrine tumors [1]. The somatostatin receptor family consists of 5 receptor subtypes: sst₁-sst₅. The majority of neuroendocrine tumors feature a strong over-expression of sst, mainly subtype 2 (sst₂).

The introduction of radiolabeled somatostatin analogs started with the development of the sst-targeting somatostatin analog [¹¹¹In-DTPA⁰]octreotide (Octreoscan®). This analog is being used to visualize sst-receptor positive tumors and their metastases [2, 3]. The therapeutic efficacy of this analog was found promising, although no effects were found in patients with larger tumors and advanced disease [4]. The next generation of modified somatostatin analogs, including [DOTA⁰,Tyr³]octreotide, is being used for somatostatin receptor targeted radionuclide therapy as well. This analog has a higher affinity for sst₂, and has 1,4,7,10-tetraazacyclododecane-N',N'',N''',N''''-tetraacetic acid (DOTA) instead of diethylenetriaminepentaacetic acid (DTPA) as chelator, allowing stable radiolabeling with beta-emitting radionuclides such as ⁹⁰Y and ¹⁷⁷Lu. Several phase-1 and phase-2 peptide-receptor radionuclide therapy (PRRT) trials were performed using [⁹⁰Y-DOTA⁰,Tyr³]octreotide (⁹⁰Y-DOTA-TOC; OctreoTher®) [5-9], objective responses in patients with GEP tumors ranged from 9 - 33% [10]. These results were better than those obtained with [¹¹¹In-DTPA⁰]octreotide, despite differences in the [⁹⁰Y-DOTA⁰,Tyr³]octreotide protocols applied. [¹⁷⁷Lu-DOTA⁰,Tyr³]octreotate is a third generation somatostatin analog for PRRT and is being used in our medical center since the year 2000. [DOTA⁰,Tyr³]octreotate differs from [DOTA⁰,Tyr³]octreotide in that the C-terminal threoninol has been replaced with threonine. Compared with [DOTA⁰,Tyr³]octreotide, it shows considerable improvement in binding to sst₂-positive tissues *in vitro* and *in vivo* [11, 12]. [¹⁷⁷Lu-DOTA⁰,Tyr³]octreotate represents an important improvement because of the higher absorbed radiation doses that can be achieved to most tumors with about equal radiation doses to dose-limiting organs [13, 14]. ⁹⁰Y and ¹⁷⁷Lu-labeled peptides have greater therapeutic potential compared to ¹¹¹In-labeled peptides, for their emitted β-particle range exceeds the cell diameter, enabling irradiation of neighboring tumor cells, which is favorable in case of heterogeneous receptor expression. ¹⁷⁷Lu, as compared to ⁹⁰Y, has a lower tissue penetration range which is favorable for treatment of small tumors, whereas ⁹⁰Y might be more effective in tumors with a larger diameter [15, 16]. In contrast to ⁹⁰Y, ¹⁷⁷Lu also emits low energy γ-rays which directly allows imaging and dosimetry following [¹⁷⁷Lu-DOTA⁰,Tyr³]octreotate therapy. Treatment with [¹⁷⁷Lu-DOTA⁰,Tyr³]octreotate in patients with GEP tumors resulted in complete

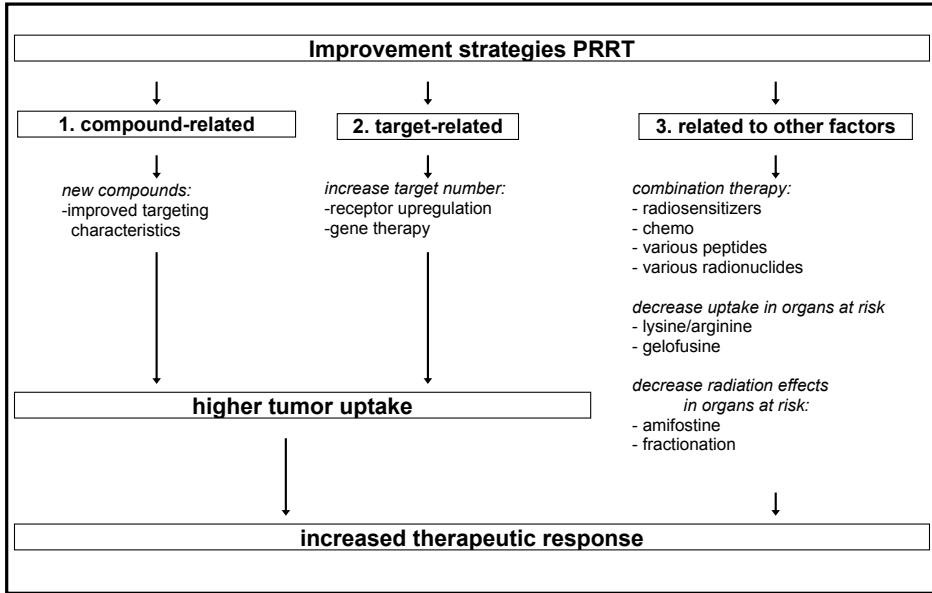


Figure 1: Improvement strategies for peptide receptor radionuclide therapy (PRRT).

or partial remission in 28% of patients [17]. Median time to progression was more than 36 months in patients who had either stable disease or tumor regression after treatment. In addition, patients treated with $[^{177}\text{Lu-DOTA}^0, \text{Tyr}^3]\text{octreotate}$ indicated a significant improvement of their quality of life [18].

In summary, PRRT with radiolabeled somatostatin analogs is a promising treatment option for patients with inoperable or metastasized neuroendocrine tumors. The side-effects of PRRT are few and mostly mild.

This review discusses several options to optimize receptor-targeted imaging and radionuclide therapy, outlining the efforts to develop optimized radiopharmaceuticals, to increase the target density and combine treatment modalities (see also Figure 1):

I. Developing new peptide analogs with increased receptor binding affinity and improved stability might lead to higher accumulation of radioactivity inside tumor cells. Many new nalogs of somatostatin have been developed and widely studied; much profit can also be gained by improving peptide analogs targeting other tumor related receptors, including gastrin-releasing peptide (GRP) receptors, neurotensin (NT) receptors, cholecystokinin (CCK) receptors, and glucagon-like peptide-1 (GLP-1) receptors.

II. Increasing the number of receptors that can be targeted on the tumor cells will result in a higher contrast during peptide-receptor-scintigraphy (PRS), and a higher radiation dose to the tumor during PRRT.

III. Combinations of radionuclide therapy with other treatment modalities such as chemotherapy or radiosensitizer pre-treatment might increase treatment impact. Also administration of higher radioactivity doses enabled by combinations of PRRT with strategies reducing the radiation dose to normal organs will improve the outcome of tumor treatment.

I. DEVELOPMENT OF NEW PEPTIDE ANALOGS

The natural structure of peptides makes them sensitive to peptidases. They are rapidly broken down in blood and other tissues, restricting their potential use as radiopharmaceuticals. Metabolically stable analogs are therefore preferable for clinical application. Strategies to stabilize peptides include the introduction of non-biodegradable peptide bonds, stabilized amino acid derivatives replacing the natural amino acids, and cyclization.

High *in vivo* stability is advantageous but not sufficient for good target-to-non target ratios. Important factors are also long retention time of radioactivity at the tumor site and rapid clearance of radioactivity from non-target tissues and blood. Internalization of radiolabeled peptides by tumor cells may lead to longer retention of radioactivity [19]. Peptide agonists often undergo receptor-mediated endocytosis enabling internalization of the radionuclide into tumor cells, whereas antagonists do most often not internalize [20]. The majority of research efforts to design peptide based radiopharmaceuticals have focused on receptor-agonists. Recently, somatostatin antagonists were shown most suitable for sst-targeting as well [21].

Subtle changes in peptide structures as described above, can have dramatic effects on the receptor-binding capacity and biodistribution of the compound. Attempts to improve the stability of the radiolabeled peptide can at the same time be fatal for its targeting abilities due to loss of receptor-binding affinity. Below we reviewed the most recent efforts to develop new radiolabeled peptides for imaging and therapy of receptor-expressing tumors.

SST receptor-targeting peptides

^{99m}Tc -labeled somatostatin analogs including hydrazinonicotinamide (Hynic)-derivatised ^{99m}Tc -[Hynic-Tyr³]octreotide, ^{99m}Tc -[Hynic-Tyr³]octreotate [22-26], and tetraamine-functionalized derivative ^{99m}Tc -[N₄⁰,Tyr³]octreotate (Demotate 1) [27-29], can be regarded as promising new radiopharmaceuticals for sst scintigraphy. Both Hynic- and N₄-derivatized analogs were capable of detecting sst-expressing lesions in patients.

Compared to single-photon emission computed tomography (SPECT) imaging, clinical positron emission tomography (PET) imaging provides a higher spatial resolution and the possibility to more accurately quantitate tumor and normal organ uptake. For PET imaging, peptides can be labeled with positron emitting radionuclides such as ^{68}Ga , ^{18}F , ^{64}Cu , ^{86}Y , ^{89}Zr , and ^{124}I . Several ^{18}F and ^{64}Cu labeled sst analogs have been reported, including Gluc-Lys(^{18}F)FP-TOCA [30] and ^{64}Cu -TETA-octreotide [31] which both appeared promising for imaging of patients bearing neuroendocrine tumors. In contrast to PET radionuclides that require a cyclotron for production, ^{68}Ga can be produced in-house using a $^{68}\text{Ge}/^{68}\text{Ga}$ generator [32]. PET imaging using ^{68}Ga -[DOTA⁰-Tyr³]octreotide has been shown preferable to SPECT imaging with Octreoscan®, especially in small lesions and tumors with low sst density [33, 34].

The radiolabeled analogs of octreotide and octreotate, including the analogs described above, have high binding-affinity for sst₂ [11], the most frequently expressed subtype in neuroendocrine cancers. In some cancers, however, sst₂ is not or only in low density expressed, whereas other subtype receptors can be present [35, 36]. The heterogeneous and concomitant sst receptor subtype expression strongly pleads for tracers, or combinations of tracers, that can target more than one sst. Ginj et al. evaluated 24 DOTA-somatostatin analogs, all based on octreotide, using a systematic modification at amino acid position 3 [37]. Two analogs, namely [DOTA⁰-Nal³]octreotide and [DOTA⁰-BzThi³]octreotide showed high binding affinity for sst₂, sst₃ and sst₅. ^{68}Ga -labeled [DOTA⁰-Nal³]octreotide has been shown to be a good tracer for primary diagnostic and follow-up studies in patients suspected from or with proven sst-expressing tumors [38].

As mentioned above, peptide agonists internalize into the cell after receptor-binding, which is thought to be essential for good retention of radionuclides in target cells. Ginj et al., however, recently reported promising results in a preclinical study comparing targeting characteristics of sst₂ or sst₃ binding agonists versus antagonists [21]. They found that these antagonists, even though they did not internalize, showed higher accumulation in tumor cells compared to agonists, whereas the receptor affinity of agonists and antagonists was in the same range. In addition, accumulation in non-tumor tissues, except for that in the kidneys, was less for antagonists than for agonists up to 24 hours after injection. These results suggest that antagonists may be better candidates to target tumors than agonists. The authors attribute the superior antagonist accumulation to binding of antagonists to a larger variety of receptor configurations. If the present observation can be translated to other receptors as well, the use of radiolabeled antagonists may considerably improve tumor imaging and PRRT efficacy.

GRP receptor-targeting peptides

Overexpression of GRP receptors has been demonstrated in a large number of human tumors, including prostate and breast tumors [39], which are among the major causes of cancer death worldwide [40]. Bombesin (BN) is a 14 amino acid peptide with high affinity for the GRP receptor, radiolabeled analogs of BN might therefore be useful for GRP receptor-targeted imaging and therapy. First attempts to develop radiolabeled BN analogs for diagnostic imaging aimed at radioiodinated peptides. These compounds were found to be very unstable and iodine was rapidly cleared from the tumor cells [41]. Now, more than 10 years later several ^{111}In and $^{99\text{m}}\text{Tc}$ labeled BN analogs have been developed with favorable *in vivo* characteristics for SPECT imaging of GRP receptor-expressing tumors [42-47].

$^{99\text{m}}\text{Tc}$ -labeled bombesin analogs have a tendency to accumulate in liver and intestines as a result of their high lipophilicity. This high unspecific accumulation of radioactivity interferes with detection of GRP receptor-positive lesions in the abdominal area. Much effort has been put into reducing the lipophilicity of the $^{99\text{m}}\text{Tc}$ -labeled BN analogs. Ferro-Flores et al. conjugated the bifunctional chelator HYNIC and the co-ligand EDDA (ethylenediamine-N,N'-diacetic acid) to bombesin for the preparation of $^{99\text{m}}\text{Tc}$ -EDDA/HYNIC-[Lys³]-BN. This conjugation resulted in less lipophilic properties of the peptide and consequently lower hepatobiliary and predominantly renal excretion [48]. Furthermore, Garcia Garayoa et al. recently showed that the introduction of a hydrophilic spacer between the peptide sequence and the $^{99\text{m}}\text{Tc}$ -binding complex can reduce the high lipophilicity and improve tumor-to-non tumor ratios [49].

Next to tumor diagnosis, staging, and localization, ^{111}In -labeled peptide analogs are often used as surrogates to determine the biodistribution and dosimetry of therapeutic radiopharmaceuticals labeled with radiometals like ^{90}Y . DTPA and DOTA are being used as chelating systems coupled to the BN analogs for this purpose [50]. ^{111}In -DTPA-BN analogs, e.g. [^{111}In -DTPA-Pro¹,Tyr⁴]BN [20, 47] were reported to have good tumor uptake and rapid clearance from non-target tissues and blood. Substitution of the DTPA chelator system in [DTPA-Pro¹,Tyr⁴]BN by DOTA was previously found to have favorable effects on the receptor-binding characteristics of this radioligand [47]. We recently synthesized a new DTPA-coupled BN analog, [^{111}In -DTPA-ACMpip⁵,Tha⁶, β Ala¹¹,Tha¹³,Nle¹⁴]BN(5-14) (Cmp 3) with a significantly higher GRP receptor-mediated tumor uptake *in vivo* in animal studies [51]. As ^{111}In -Cmp 3 seems promising for SPECT imaging of GRP receptor-expressing tumors, replacing the DTPA chelator by DOTA would enable therapeutic use of the compound and diagnostic PET imaging.

Most of the recent studies on newly developed BN peptide analogs focus on the DOTA-chelating system for its multipurpose utilization options: SPECT, PET, and

PRRT [19, 52-58]. For example, DOTA-PESIN (DOTA-PEG₄-BN(7-14)) showed to be a very promising new compound. Although it has only a moderate affinity for the GRP receptor, it showed good *in vivo* tumor uptake in animal studies [52]. Clearance of the compound proceeded via kidneys and urinary tract with fast washout from GRP receptor-negative tissues but rather high accumulation in the kidneys. The high kidney retention could not be reduced by lysine.

Another very promising DOTA-BN analog is ¹⁷⁷Lu-AMBA [58]. This compound consists of DOTA attached to BN(7-14) by a short linker. ¹⁷⁷Lu-AMBA, like DOTA-PESIN, showed in animals high GRP receptor-mediated tumor uptake and favorable tumor-to-background ratios. *In vivo* tumor treatment with ¹⁷⁷Lu-AMBA resulted in a significantly prolonged survival of tumor-bearing mice, and decreased tumor growth rate over that of controls. Like DOTA-PESIN, ¹⁷⁷Lu-AMBA is excreted via the kidneys, and the relatively high kidney retention cannot be reduced by co-injection of lysine, which is probably due to the lack of lysine residues in these peptide sequences. However, the accumulation of radioactivity in the kidneys is still 50% lower for DTPA- and DOTA-derivatized BN analogs compared to that of somatostatin analogs.

PRRT using BN analogs described above may be promising. Clinical scintigraphy with ^{99m}Tc- and ⁶⁸Ga-labeled BN analogs clearly delineated tumor lesions, including lymph nodes, and metastases [44, 59, 60]. However, also relatively high uptake in non-target, GRP receptor-positive, tissues such as pancreas and intestines was found which is unfavorable for PRRT. In a pre-clinical study using ¹¹¹In-Cmp 3 we found that increasing amounts of injected peptide mass in tumor-bearing rats decreased uptake in receptor-positive normal tissues more than that in the tumor. Also pre-injection of excess unlabeled peptide before administration of radiolabeled compound showed to be profitable for tumor uptake compared to that in receptor-expressing normal tissues (Figure 2) [61]. These effects were also found with ¹⁷⁷Lu-AMBA in tumor bearing mice [58]. Thus, injection of higher peptide mass and/or pre-injection of excess BN may increase tumor-to-non tumor ratios. Taking into account the biologic activity of BN agonists in patients, pre-injection of GRP receptor antagonists might be preferable.

Radiolabeled BN analogs are of particular interest for PRRT of advanced prostate cancer patients who do not respond to hormone therapy. So far, the best treatment strategies available for this group of patients are only marginally effective [62, 63]. However, in a study evaluating GRP receptor-expression in human prostate cancer xenograft models representing the different stages of prostate tumor development, including the shift from androgen-dependent towards androgen-independent tumor growth, we found high GRP receptor density only in androgen-dependent prostate cancer xenografts. These results suggest high GRP receptor expression in the early, androgen-dependent, stages of prostate tumor development and not in later stages.

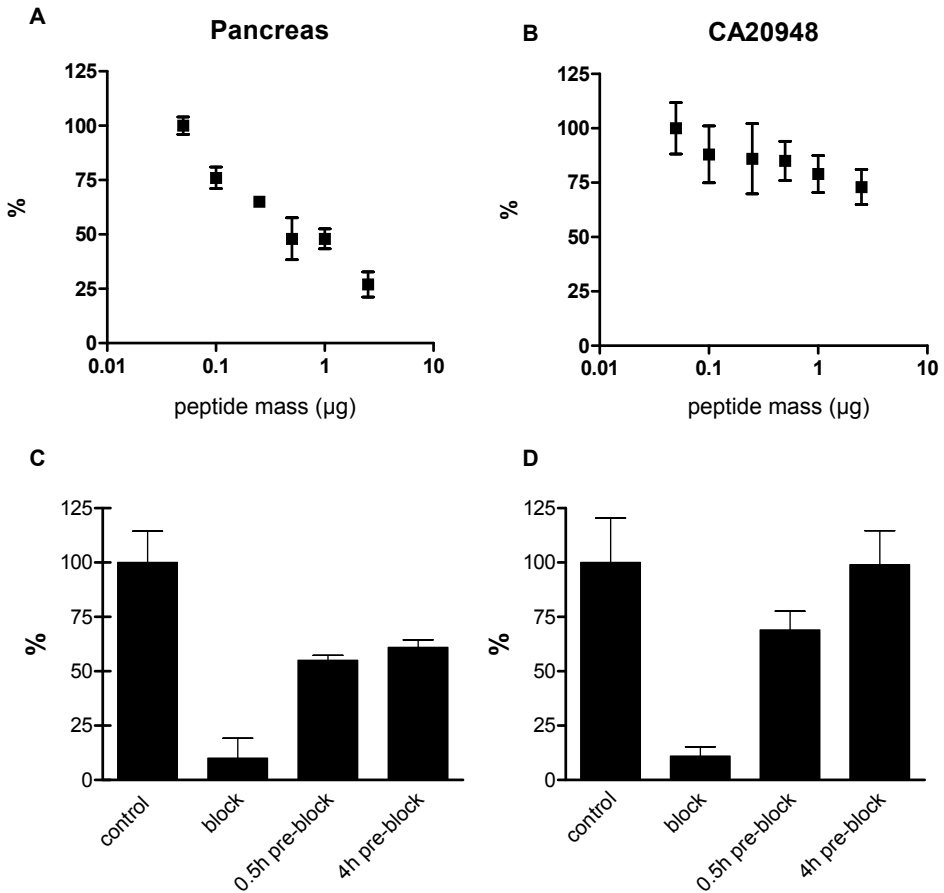


Figure 2: GRP receptor saturation: Uptake of ^{111}In -Cmp 3 in GRP receptor-expressing pancreas (A) and CA20948 tumor (B) in rats (4 hours p.i., lowest peptide mass is set at 100%). Receptor availability: Uptake of $0.1\mu\text{g}$ ^{111}In -Cmp 3 in rat pancreas (C) and tumor (D) without (control) or with $100\mu\text{g}$ unlabeled BN either coinjected (block) or pre-injected 0.5 (0.5h pre-block) or 4 hours (4h pre-block) prior to administration of radiolabeled compound (4 hours p.i., control is set at 100%). Injection of a higher peptide mass and/or pre-injection of excess BN affected the uptake in non-target GRP receptor-expressing tissues more than that in tumor.

In addition, simulation of androgen ablation treatment in the animal model (i.e. castration) strongly reduced GRP receptor-expression in androgen-dependent tumors, suggesting that GRP receptor expression in human prostate cancer is androgen-regulated [64]. Studies evaluating GRP receptor-expression on clinical prostate cancer tissue samples are underway to determine whether these results are clinically relevant.

The application of BN peptides in cancer patients is still in its infancy [44, 59, 60]. However, recent developments in the synthesis of new promising BN analogs are encouraging for further utilization in clinical studies.

NT receptor-targeting peptides

Neuroendocrine pancreatic tumors can be successfully localized and treated using radiolabeled somatostatin analogs [65-67]. Exocrine pancreatic cancer, however, does not express a sufficient level of sst for scintigraphic imaging. Reubi et al. reported that 75% of ductal pancreatic carcinomas over-expressed neurotensin (NT) receptors, whereas normal pancreatic tissue, pancreatitis and endocrine pancreatic cancers were NT receptor-negative [68]. Neurotensin is a 13-amino acid peptide localized in both the central nervous system and in peripheral tissues, mainly the gastrointestinal tract [69, 70]. The instability of native neurotensin prompted several groups [71-76] to synthesize neurotensin analogs less susceptible to degradation, while maintaining the binding affinity to NT receptors. Preclinical studies using ^{111}In -labeled DTPA (MP2530) and DOTA (MP2656) linked NT analogs demonstrated that subtle changes as introduction of non-natural amino acids on specific positions can be made in the C-terminal part of the peptide, the crucial part for binding and biological activity, without markedly affecting the binding properties [77]. These NT analogs showed good receptor-mediated uptake in NT receptor expressing HT29 xenografts and were thus promising tools for imaging of exocrine pancreatic tumors. PRRT using these analogs might however be hampered by the relatively high kidney uptake of ^{111}In -NT analogs. Recently, Maes et al. [73] reported a triply-stabilized $^{99\text{m}}\text{Tc}$ -labeled NT (NT-XIX) analog with high tumor uptake and reduced kidney uptake which led to a superior tumor-to-kidney ratio compared to ^{111}In -labeled analogs. Also $^{99\text{m}}\text{Tc}$ -Demotensin 4, a doubly-stabilized NT analog [72], showed a favorable tumor-to-kidney ratio. Still, the tumor-to-intestine and tumor-to-liver ratios were considerably higher for ^{111}In -labeled analogs, which is favorable for visualization of pancreatic tumors in patients [78].

Only one clinical evaluation study using a radiolabeled NT analog has been reported [79]. This study included four exocrine pancreatic cancer patients, who were injected with the NT analog: $^{99\text{m}}\text{Tc}$ -NT-XI. Scintigraphic imaging showed moderate tumor uptake in one patient whereas the other three patients showed no tumor uptake. Two out of these three patients were found to have a NT receptor-negative tumor.

CCK₂ receptor-targeting peptides

Unlike other neuroendocrine tumors, somatostatin receptor expression is rather low in medullary thyroid cancer (MTC) and is completely absent in clinically aggressive forms of the disease [80, 81]. The presence of cholecystokinin-2 (CCK₂) receptors was shown in more than 90% of MTCs, and in a high percentage of small cell lung cancers, stromal ovarian cancers, astrocytomas and several other tumor types [82]. On the basis of these findings, Behr et al. [83] evaluated the suitability of radioiodinated gastrin, a specific high affinity ligand for the CCK₂ receptor, for targeting CCK₂ receptor

expressing tumors *in vivo*. Their data suggested that gastrin analogs may represent a useful new class of receptor-binding peptides for diagnosis and therapy of a variety of tumor types, including MTC. Reubi et al. [84] developed DTPA-CCK₂ receptor binding CCK analogs, evaluated receptor-binding characteristics and obtained initial preclinical biodistribution data in non tumor-bearing rats. For the DOTA counterpart of the most promising analog [¹¹¹In-DOTA⁰]CCK₈, a high CCK₂ receptor affinity was found. The latter analog could visualize CCK₂ receptor-expressing tumors *in vivo* in rats [85], and also in patients with advanced metastatic MTC [¹¹¹In-DTPA⁰]CCK₈ was able to visualize the tumor lesions [86].

Besides CCK analogs, radiolabeled analogs of minigastrin have also shown to be suitable for CCK₂ receptor-targeting. For example, a clinical study in MTC patients showed that most tumor sites could be visualized with ¹¹¹In-DTPA-minigastrin [83,

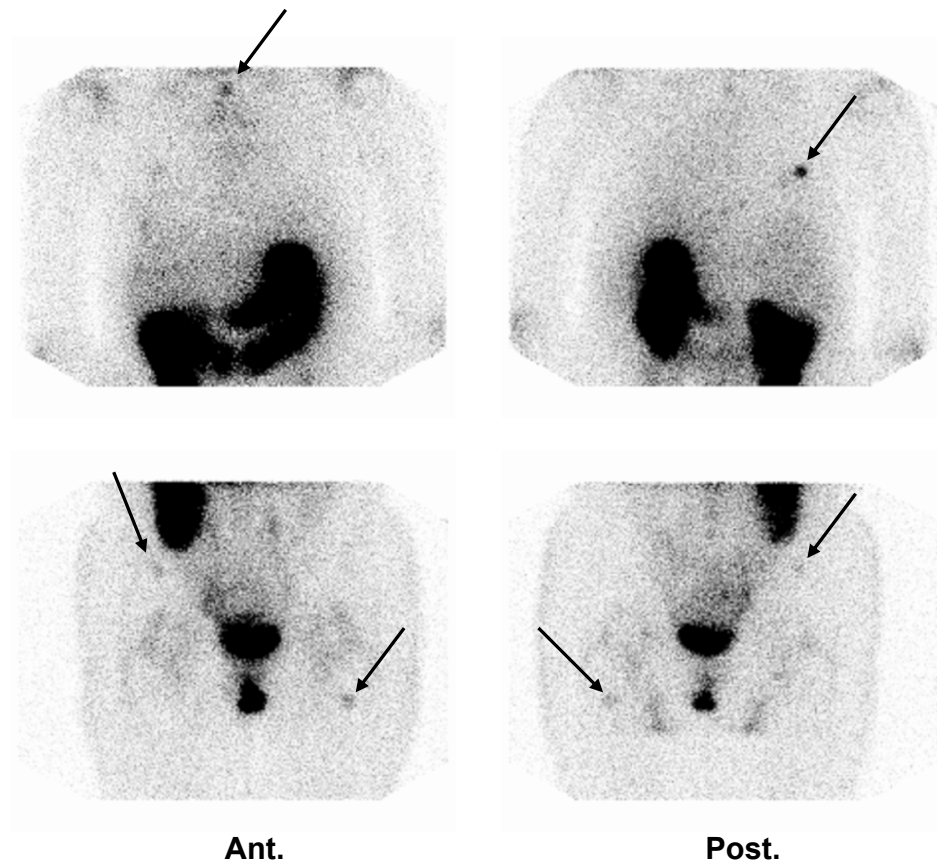


Figure 3: ^{99m}Tc-Demogastrin 2 scintigraphy (3 hours p.i.) in a 44 year old female MTC patient with elevated serum calcitonin. No tumor localization with ultrasound, SRS, CT, MRI and ¹⁸F¹⁸FDG-PET. Anterior (Ant) and posterior (Post) images of the thoracic (upper images) and pelvic (lower images) regions showing metastatic lesions (some marked with arrows).

87]. Nock et al. synthesized ^{99m}Tc -labeled N_4 -derivatized analogs of minigastrin [88]. Pre-clinical evaluation studies resulted in the selection of $[\text{N}_4^{0-1}, \text{Gly}^0, (\text{D})\text{Glu}^1]$ minigastrin (Demogastrin 2) as the most promising CCK_2 -targeting analog for tumor imaging. The qualities of ^{99m}Tc Demogastrin 2 could be confirmed in a patient with metastatic MTC; tumor deposits were clearly delineated (see also Figure 3).

More recent clinical studies by Gotthardt et al. [89, 90] in patients with metastatic/recurrent MTC compared the results of CCK_2 (gastrin) receptor scintigraphy (GRS), using ^{111}In -(D)Glu¹minigastrin, with somatostatin receptor scintigraphy (SRS), CT and ^{18}F -FDG PET. They found that GRS had a higher tumor detection rate than SRS and ^{18}F -FDG PET. GRS in combination with CT was most effective in the detection of metastatic MTC. Furthermore, GRS in patients bearing neuroendocrine tumors other than MTC detected additional tumor sites that were missed in SRS in 20% of patients. The authors concluded that GRS may become the scintigraphic imaging modality of choice in MTC patients. In conclusion, (pre)clinical studies have shown the suitability of radiolabeled CCK and gastrin analogs for scintigraphy of tumors such as MTC. PRRT using these radioligands is still preliminary but its future is promising.

GLP-1 receptor-targeting peptides

A new promising candidate for *in vivo* tumor targeting is glucagon-like peptide 1 (GLP-1) receptor, a member of the glucagon receptor family [91]. The GLP-1 receptor was recently shown to be highly overexpressed in human endocrine tumors, in particular insulinomas, gastrinomas [92], and pheochromocytomas [93].

Similar to other naturally occurring receptor-binding ligands, native GLP-1 receptor agonists are rapidly degraded in the blood [94, 95]. Therefore, Gotthardt et al. evaluated the more stable GLP-1 selective analog exendin, which showed to have potential for scintigraphic imaging of GLP-1 receptor-expressing tumors [96]. Recently, the exendin analog has been further optimized, which has led to two new, ^{111}In -DTPA-conjugated, Exendin-4 analogs: ^{111}In -DTPA-Lys⁴⁰-exendin-4 [97] and $[\text{Lys}^{40}(\text{Ahx-DTPA-}^{111}\text{In})\text{NH}_2]$ exendin-4 [98]. Both analogs showed encouraging preclinical characteristics with high GLP-1 receptor-mediated uptake in target tissues and good target-to-background ratios *in vivo* in animal models. In addition, Wicky et al. showed that $[\text{Lys}^{40}(\text{Ahx-DTPA-}^{111}\text{In})\text{NH}_2]$ exendin-4 efficiently repressed insulinoma growth in mice [99]. Kidney toxicity was found the limiting factor in this treatment strategy.

No clinical study using GLP-1 receptor-targeting analogs has been reported so far. For therapeutic purposes, high kidney retention of exendin-4 analogs could be problematic. Nevertheless, when this high accumulation in the kidneys can be overcome, high GLP-1 receptor-expression on tumors, in combination with the favorable

in vivo characteristics of the recent exendin-4 analogs, gives GLP-1 receptor-targeted PRRT serious potential.

$\alpha_v\beta_3$ integrin-targeting peptides

Cell matrix interactions are of fundamental importance for tumor invasion and formation of metastases as well as tumor-induced angiogenesis.

The $\alpha_v\beta_3$ integrin is a transmembrane protein which is preferentially expressed on proliferating endothelial cells [100], whereas it is absent on quiescent endothelial cells. For growth beyond the size of 1-2 mm in diameter, tumors require the formation of new blood vessels. The $\alpha_v\beta_3$ receptors are overexpressed on these newly formed blood vessels of actively growing tumors, and are therefore potential targets for receptor-mediated tumor imaging and therapy and for planning and monitoring of $\alpha_v\beta_3$ targeting treatment strategies.

It was found that the essential amino acid sequence for the binding of extracellular matrix proteins to $\alpha_v\beta_3$ receptors is arginine-glycine-aspartic acid (RGD) [101]. Several studies have been aimed to develop optimized $\alpha_v\beta_3$ targeting compounds. In summary, it was found that cyclic analogs of RGD containing 5 amino acids (RGD sequence + hydrophobic amino acid in position 4 + additional amino acid in position 5) have the highest $\alpha_v\beta_3$ binding affinities [102, 103]. Radiolabeled analogs containing this 5 amino acid sequence have been synthesized and evaluated for their $\alpha_v\beta_3$ targeting characteristics. Among them are DTPA and DOTA conjugated analogs for radiolabeling with ^{111}In , ^{90}Y , ^{177}Lu , ^{68}Ga and ^{64}Cu , enabling SPECT and PET imaging and PRRT [104, 105]. Also ^{18}F -labeled cyclic RGD analogs for PET imaging have been characterized [105-107]. In patients, Beer et al. showed that PET imaging using the RGD analog, ^{18}F -galacto-RGD, can effectively show the level of $\alpha_v\beta_3$ expression in man [108-110].

Dijkgraaf et al. [111] developed multivalent RGD peptides in an attempt to increase receptor-binding affinity. They synthesized and compared the *in vitro* and *in vivo* $\alpha_v\beta_3$ targeting characteristics of DOTA-linked monomeric, dimeric, and tetrameric RGD peptides radiolabeled with ^{111}In . They found enhanced receptor affinity *in vitro* and better tumor uptake *in vivo* for the tetrameric compound compared to its monomeric and dimeric analogs. Alternatively, they synthesized multimeric RGD peptides as dendrimers: macromolecules consisting of multiple perfectly branched monomers. Consistent with their previous results, the tetrameric RGD dendrimer showed enhanced affinity and significantly higher tumor uptake compared to its monomeric and dimeric analogs [112]. The authors ascribe the improved targeting characteristics of the multimer to the enhanced local concentration of RGD units in the vicinity of the receptor (statistical rebinding) and not to binding of the compound to multiple $\alpha_v\beta_3$ receptors. Unfortunately, the kidney retention of the

multimeric peptides was also increased resulting in unfavorable tumor-to-kidney ratios. Introduction of a linker in between the peptide moiety and the DOTA chelator, in an attempt to improve the target-to-background ratios of the peptide, led to a marginal enhancement of the tumor-to-kidney ratio only [113]. In a study evaluating the targeting potential of a cyclic RGD analog in an intraperitoneally (i.p.) growing tumor model, Dijkgraaf et al. found that i.p. vs. i.v injection of the radiolabeled RGD peptide resulted in markedly higher tumor uptake after i.p. administration whereas uptake in the other organs like kidneys were unaffected by the route of administration. PRRT experiments in this model indicated that i.p. growing tumors can be inhibited significantly by i.p. injection of a therapeutic dose of ^{177}Lu -labeled RGD analog [114]. Multimeric RGD peptides are promising tools for *in vivo* imaging of tumor angiogenesis in cancer patients. $\alpha_v\beta_3$ targeted PRRT with these compounds might particularly be used for i.p. growing tumors. Currently, ^{18}F -galacto-RGD is the only $\alpha_v\beta_3$ -targeting peptide shown effective for tumor imaging in patients [110].

II. IMPROVING THE THERAPEUTIC EFFECT: INCREASING RECEPTOR DENSITY ON TARGET CELLS

By increasing the receptor density on tumor cells in patients to be treated with radiolabeled peptides, and thereby increasing radioactivity uptake in the tumor, the therapeutic window can be enlarged.

Up-regulation of receptors

During the last three decades several reports have been published concerning hormones and growth factors inducing a higher number of receptors on tumor cells [115-123]. For an overview of references and findings, see table 1. In this review the focus will be on radiation-induced receptor up-regulation.

Up-regulation of peptide receptors on tumor cells after irradiation was first reported by Béhé et al. [124, 125], who showed that a total dose of 4 to 16 Gy of external beam irradiation led to time-dependent up-regulation of both sst_2 and gastrin receptors on AR42J cells, *in vitro* as well as *in vivo*. This phenomenon was also investigated *in vitro* in NCI-H69 small cell lung cancer cells [126]. which were irradiated with a total dose of 4 Gy and the subsequent internalization of [^{177}Lu -DTPA 0 ,Tyr 3]octreotate was 1.5-3 times increased compared to that in control cells.

Not only was the use of external beam radiation, but also low therapeutic doses of radiolabeled peptides found to induce sst_2 up-regulation. CA20948 rat pancreatic tumor-bearing rats [127, 128] were treated with a relatively low, non-curative dose of either [^{111}In -DTPA 0]octreotide [127] or [^{177}Lu -DOTA 0 ,Tyr 3]octreotate [128] and sst_2

Table 1: An overview of references concerning receptor up- and down-regulation.

Reference	Cell type	Origin of cell	Modulator	in vitro/ in vivo	Effect on expr.
¹¹⁵ Kimura, 1986	anterior pit. cells [†]	rat	estradiol	in vitro	up (2-fold)
¹¹⁶ Presky, 1988	GH ₄ C ₁	rat pit. tumor cells [†]	SRIF (chronic)	in vitro	up
¹¹⁷ Kimura, 1989	anterior pit. cells [†]	rat	estradiol	in vivo	up
¹¹⁸ Slama, 1992	arcuate nucleus	female rat brain	estradiol	in vivo	up
¹¹⁹ Vidal, 1994	AR42J	rat panc. tumor cells [‡]	EGF / Gastrin	in vitro	up
¹²⁰ Visser-Wisselaar, 1997	7315b	pituitary tumor cells [‡]	estradiol	in vitro + in vivo	up (+ up of sst ₂)
¹²¹ Froidevaux, 1999	AR42J	rat panc. tumor cells [‡]	octreotide (continuous)	in vivo	up
¹²² Viguerie, 1987	AR42J	rat panc. tumor cells [‡]	dexamethasone	in vitro	down
¹²¹ Froidevaux, 1999	AR42J	rat panc. tumor cells [‡]	octreotide	in vitro	down
			octreotide (single injection)	in vivo	down
			octreotide (discontinuous)	in vivo	down
¹²³ Gunn, 2006	IMR-32	human neuroblastoma	octreotide	in vitro	down
¹²⁴ Behe, 2003	AR42J	rat panc. tumor cells [‡]	external beam irradiation	in vitro + in vivo	up (also gastrin)
¹²⁵ Behe, 2004	AR42J	rat panc. tumor cells [‡]	external beam irradiation	in vivo	up (also gastrin)
¹²⁷ Capello, 2005	CA20948	rat panc. tumor cells [‡]	¹¹¹ In-octreotate (low dose)	in vivo	up (2-fold)
¹²⁶ Oddstig, 2006	NCI-H69	small cell lung cancer	x-ray (100 keV)	in vitro	up (1.5-3-fold)
¹²⁸ Melis, 2007	CA20948	rat panc. tumor cells [‡]	¹⁷⁷ Lu-octreotate (low dose)	in vivo	up (2-5-time)

Note; [†] pit. = pituitary, [‡] panc. = pancreatic

receptor expression in different phases of tumor response was determined versus base-line (control). Both studies revealed an increased sst₂ density on tumors regrowing after initial therapy-induced regression compared to control: treatment with [¹¹¹In-DTPA⁰]octreotide resulted in a 2-fold increase, while [¹⁷⁷Lu-DOTA⁰,Tyr³]octreotate treatment showed a more pronounced effect (2-5-fold increase). This radiation induced up-regulation of receptor expression might be important for improving the response rate in clinical PRRT, although the clinical value has to be determined.

Gene therapy

In general, gene transfer methods can be applied to induce expression of a desired gene in a cell. This concept has been used mostly for the treatment of cancer [129]. By using a vector, either viral or non-viral, a peptide receptor-encoding gene (or several genes) can be transferred into a tumor cell with the aim to enhance the uptake of radiolabeled peptide analogs. Gene therapy approaches in combination with PRRT might have some advantages: first, transduction of receptors is locally achieved (only in the tumor), leading to a higher tumor-to-background ratio. Second, constitutive receptor expression in the tumor is not required, therefore also receptor-negative tumors could theoretically be treated. And third, the therapeutic effect might be enormously increased by performing a dual gene transfer. For example, a “suicide” gene can be co-transferred with the receptor gene into the tumor cell, which can be simultaneously or subsequently used for treatment. On the other hand, patients with metastatic disease are probably difficult to treat with gene therapy, since this requires systemic administration of gene therapy vectors, with all related risks. Therefore, patients with circumscribed tumor lesions would probably benefit from gene therapy strategies, which is the case in ovarian and glioblastoma cancer patients.

Several groups have explored the possibility to increase sst expression on tumors using gene transfer modalities. One of the first studies using the adenoviral vector AdCMVhSSTr2, encoding the human sst₂, was performed in intraperitoneally growing SKOV3.ip1 human ovarian cancer tumor [130]. Biodistribution and gamma camera imaging showed higher uptake of various radiolabeled sst analogs in infected tumors than in control tumors.

Zinn et al. and Hemminki et al. introduced the concept of dual gene transfer using a replication-incompetent adenoviral vector encoding sst₂ and a so-called “suicide gene”: the herpes simplex virus type 1 thymidine kinase (HSV1-tk) [131, 132]. This gene encodes the thymidine kinase (tk) enzyme that, unlike mammalian tk, preferentially phosphorylates acycloguanosines, such as acyclovir (ACV) and ganciclovir (GCV), into monophosphate compounds, which are then converted into di- and triphosphates by cellular enzymes. The triphosphates are subsequently trapped inside the cell. Acycloguanosines are so-called “pro-drugs” since only the phosphorylated forms are incorporated as chain-terminating derivatives into the DNA and/or inhibit DNA polymerase activity, eventually leading to cell kills. Moreover, thymidine analogs (e.g. FIAU, FIRU) do not show toxic effects following phosphorylation and can therefore be used for imaging of HSV1-tk expression. Zinn and co-workers showed that expression of both sst₂ and HSV1-tk following AdTKSSTR infection could be measured with ^{99m}Tc-P2045 and radioiodinated FIAU, respectively, in mice bearing an A-427 tumor [133].

In 2002, Hemminki et al. reported the effects of gene transfer and subsequent treatment of s.c. and i.p. SKOV3.ip1 tumors *in vivo*: Mice were infected intra-tumorally with either AdTKSSTR, the infectivity-enhanced counterpart RGDTKSSTR or control virus [134], followed by GCV treatment. The use of the infectivity-enhanced virus RGDTKSSTR resulted in an improved therapeutic effect compared to controls. Sst₂ expression could be detected with ^{99m}Tc-P2045 imaging for 15 days after viral infection, although the uptake of the tracer decreased over time.

Using the same viral vector, our group showed a non-homogeneous uptake of specific sst₂ and HSV1-tk tracers in U87MG human glioma-bearing nude mice intra-tumorally infected with Ad5.tk.sst₂, using small animal SPECT/CT imaging (manuscript in progress). Herewith a major hurdle of gene therapy was visualized: poor viral spread is not favorable for the therapeutic outcome.

Rogers and co-workers transfected A-427 tumors *in vivo* with an adenovirus expressing sst₂, AdSSTr2. They performed therapy studies in animals, receiving AdSSTr2 and 400-500 µCi [⁹⁰Y]SMT-487 [135]. Animals that received viral infection, plus radiolabeled peptide treatment, showed a significantly reduced tumor quadrupling time compared to control animals.

Dual gene transfer modalities offer the use of two therapeutic pathways: 1) sst₂-targeted therapy with peptides radiolabeled with, for example, a β-particle emitting radionuclide, such as ¹¹⁷Lu or ⁹⁰Y, 2) suicide therapy with a pro-drug. Both possibilities can have a wide-spread effect: the first can lead to a high tumoricidal effect, since the cross-fire effect of ¹⁷⁷Lu and ⁹⁰Y can cause double stranded, unreparable DNA breaks, which leads to cell cycle arrest and eventually apoptosis [136]. In addition, non-infected cells are also treated, due to the long particle range of ¹⁷⁷Lu and ⁹⁰Y. In the second pathway, GCV-triphosphate can migrate through gap-junctions to the surrounding cells that might not have been transfected and apoptosis is induced: the co-called “bystander effect” [137]. These two effects are important since homogeneous transduction of a solid tumor has been rarely achieved [138, 139].

The use of molecular imaging in gene therapy experiments offers the opportunity to provide information about, for example, the location of vector delivery and the extent and magnitude of gene transfer and gene expression. Integrating imaging techniques such as SPECT and PET into these gene therapy protocols will make it possible to determine optimal treatment time points following vector administration. Furthermore, imaging will help to optimize treatment protocols for gene therapy modalities.

III. COMBINATION TREATMENT: RADIOLABELED PEPTIDES PLUS OTHER THERAPEUTIC AGENTS

Chemotherapeutics and Radiosensitizers

Recently, investigations have been started to combine PRRT with either chemotherapy or other radiosensitizing agents to increase therapeutic effects in patients with neuroendocrine tumors. Gotthardt et al. performed mono- and combination treatment in nude mice bearing AR42J tumors [140]. They examined [$^{177}\text{Lu-DOTA}^0, \text{Tyr}^3$]octreotide ($^{177}\text{Lu-DOTATOC}$) either alone or in combination with doxorubicin (DX) or cisplatin (CS) during a four-week period. They found that the combination of $^{177}\text{Lu-DOTATOC}$ plus DX was 14% and that of $^{177}\text{Lu-DOTATOC}$ plus CS was 23% more effective than $^{177}\text{Lu-DOTATOC}$ treatment alone, making the combination “PRRT plus chemotherapy” an effective approach to increase therapeutic efficacy in sst expressing tumors.

In patients, the radiosensitizing agent 5-fluorouracil (5-FU) was investigated in combination with high dose ^{111}In -labeled octreotide [141]. In 21 patients with neuroendocrine tumors, the efficacy and toxicity of this combination treatment was evaluated. The authors found that the combination of high dose [$^{111}\text{In-DTPA}^0$]octreotide and 5-FU was safe and symptomatic response rates were at least comparable to those reported for [$^{111}\text{In-DTPA}^0$]octreotide treatment alone. Stable disease or improvements in hormonal and functional scan abnormalities in patients with previous progression were achieved with the combination treatment. Our group recently started a pilot trial using the oral pro-drug of 5-FU, capecitabine, in combination with [$^{177}\text{Lu-DOTA}^0, \text{Tyr}^3$]octreotate in patients with GEP tumors to investigate the feasibility of combination treatment in these patients.

Johnson et al. recently investigated combination treatment of radiolabeled BN analogs with chemotherapy in a pre-clinical setting [56]. They examined the chemotherapeutic agents docetaxel (DC) and estramustine (EMP) in combination with ^{177}Lu labeled DOTA-8-AOC-BBN(7-14) NH_2 ($^{177}\text{Lu-BBN}$) in a PC-3 flank xenograft model. These chemotherapeutics were chosen since they are currently evaluated in clinical trials for the treatment of androgen independent prostate cancer. They work synergistically as microtubule inhibitors and offer an increased cytotoxic effect; they also exhibit radiosensitization properties. The results showed that mice treated with $^{177}\text{Lu-BBN}$ combined with either DC alone or DC + EMP showed a statistically significant longer survival, 107 and 109 days respectively, than the control animals (50 days). Furthermore, combination therapy demonstrated a significant survival advantage compared to the $^{177}\text{Lu-BBN}$ therapy alone. Blood was analyzed during the experiment until 2 weeks after the final therapy administration and no differences in blood cell counts were found.

Unfortunately, kidney damage was not evaluated in these studies. It is of interest to investigate the effect of chemotherapeutics combined with PRRT on radiation uptake in the kidneys and on the long term renal damage. Wild et al. reported therapy studies investigating the combination of the GLP-receptor binding analog [$^{111}\text{In-DTPA}^0$]Exendin-4 and the angiogenesis inhibitor PTK in Rip1Tag2 mice. They found that combination therapy resulted in a significantly lower median tumor volume compared to monotherapy. In addition, this study did not reveal renal toxicity in the group that was treated with the combination [142].

An issue that also needs to be addressed is the effect that chemotherapeutic agents might have on receptor expression on the tumor. Fueger and co-workers examined the possible influence of cytotoxic or cytostatic agents on binding characteristics of an sst ligand *in vitro* [143] and they found a reduced expression of high-affinity DOTA-LAN binding sites in response to the incubation with gemcitabine, camptotecin, mitomycin C and doxorubicin. In the case of gemcitabine, sst was again over-expressed after a 4-day recovery period, indicating that the down-regulation of receptor expression can be reversed. However, *in vivo* studies need to be performed to investigate the effect of chemotherapeutic agents on receptor expression, especially when combination treatment is given.

Combining different radionuclides

In preclinical studies, we found that the anti-tumor effect of radiolabeled sst analogs is dependent on tumor size [65, 66]. In a study comparing two radionuclides coupled to sst analogs, we demonstrated that [$^{177}\text{Lu-DOTA}^0\text{-Tyr}^3$]octreotate has a very good tumor cure rate in small tumors of approximately 0.5 cm², while larger tumors of about 7-9 cm² were better treated with [$^{90}\text{Y-DOTA-Tyr}^3$]octreotide [16]. These results agreed with the mathematical model proposed by O'Donoghue et al. [15]. For different radionuclide energies, the model predicts the chance of curation for different tumor diameters: according to this model, radionuclides with lower energies (e.g. ^{177}Lu) are optimal for small tumors and radionuclides with higher energies (e.g. ^{90}Y) are optimal for larger tumors. This indicates that PRRT in patients with sst₂-positive tumors of different sizes might have better potential with a combination of radionuclides with higher and lower energy β -particles. However, the feasibility of this combination treatment should be further evaluated in patients, preferably in a randomized clinical trial.

Hybrid molecules: apoptosis-inducing peptides

The receptor-targeted delivery of cytotoxic agents was first proposed to reduce toxicity of chemotherapeutic drugs in patients [144]. In order to achieve this, chemotherapeutic agents were linked to peptide analogs, resulting in the internalization of the complete molecule into the tumor cell. It is conceivable that these hybrid peptides can be

used to improve PRRT, for example in tumors with a low receptor expression or in non-responding receptor-expressing tumor types [145]. Hofland et al. and Nagy et al. have described the development and anti-tumor action of different cytotoxic sst analogs [145, 146]. Recently, new publications showed that the targeted cytotoxic analog AN-238, a conjugate based on the sst analog RC-121 coupled to a derivative of doxorubicin, could offer a more effective therapy than RC-121 treatment alone in mice bearing human melanoma tumors [147] or endometrial tumors [148]. In addition, the combination of targeted cytotoxic conjugates of luteinizing hormone-releasing hormone (LHRH) (AN-207), somatostatin (AN-238) and BN (AN-215) were tested in mice bearing ovarian tumors [149]. Results showed that AN-238 and AN-215 significantly inhibited tumor growth, the combination being equally effective. The authors concluded that combination treatment is feasible and effective with low toxicity risk [149]. Other studies showed that mice bearing human glioblastomas, U118MG and U87MG, could also be effectively treated with these agents. Both AN-215 and AN-238 strongly reduced tumor growth in glioblastoma-bearing mice [150-152]. These studies show that a wide variety of receptor-expressing tumors can be treated with receptor-targeted chemotherapeutic agents, although tumor cure was not achieved yet in these animal studies. It would be of great interest to investigate the effects on tumor growth with these agents radiolabeled with therapeutic radionuclides or combined with PRRT strategies. Meanwhile, clinical trials using these (unlabeled) targeted chemotherapeutic agents are ongoing [145, 148].

Other examples of hybrid peptides are camptothecin conjugated analogs of sst [153, 154] or BN [155, 156]. Several *in vitro* studies have shown increased efficacy of treatment with camptothecin-sst and camptothecin-BN conjugates compared to camptothecin alone [153-156]. This concept was further investigated in mice bearing NCI-H1299 human non-small cell lung tumors, which were treated with the camptothecin-BN conjugate and a camptothecin-BN analog that does not specifically bind the receptor. Tumor growth was significantly reduced after incubation with the camptothecin-BN conjugate, demonstrating the importance of receptor-specific binding and internalization of the conjugate to the tumor cell for therapeutic purposes [155].

Recently, we investigated the hybrid peptide [RGD-DTPA⁰]octreotate radiolabeled with ¹¹¹In [146, 157-159]. Arg-Gly-Asp (RGD) binds the integrin receptor $\alpha_v\beta_3$ and is known as an apoptosis-inducing agent by direct activation of caspase 3 [160]. We found that [RGD-¹¹¹In-DTPA⁰]octreotate predominantly internalizes via the sst₂, probably due to the higher affinity of octreotate for the sst₂ than that of RGD for the $\alpha_v\beta_3$ [157]. Furthermore, when [RGD-¹¹¹In-DTPA⁰]octreotate was compared with either [¹¹¹In-DTPA⁰]RGD or [¹¹¹In-DTPA⁰]octreotate in a clonogenic survival assay using sst₂/ $\alpha_v\beta_3$ expressing tumor cells, [RGD-¹¹¹In-DTPA⁰]octreotate showed the highest

tumoricidal effects [158]. Caspase 3 activity assays confirmed that [RGD-¹¹¹In-DTPA⁰]octreotate had the most pronounced activation of this executioner protease in the apoptosis pathway. Unfortunately, *in vivo* studies showed that renal uptake of [RGD-¹¹¹In-DTPA⁰]octreotate was high, a disadvantage for PRRT [159]. However, caspase-3 activity after incubation with the unlabeled hybrid peptide was higher than after RGD or DTPA-octreotide alone, making unlabeled [RGD-DTPA⁰]octreotate during or after PRRT interesting as well [159].

Combining different peptides: Multi-receptor targeting

Many cancer types simultaneously overexpress several peptide receptors [92]. There are a number of possible advantages in utilizing multiple radiolabeled ligands for therapeutic application of neuroendocrine tumors: 1) *in vivo* application of multi-receptor targeting selectively increases the radioactivity accumulation in tumors, 2) some of the receptors are not homogeneously expressed, and by multi-receptor targeting it is possible to achieve a higher tumoricidal effect, 3) there is a reduced risk of loss of some peptide receptors during therapy, due to tumor dedifferentiation and the subsequent loss of some peptide receptors [16].

Reubi et al. performed *in vitro* autoradiography on neuroendocrine tumors including ileal carcinoids, bronchial carcinoids, insulinomas, gastrinomas, glucagonomas and vipomas [92]. They found that all neuroendocrine tumors examined expressed two or more receptors; several combinations of peptides are of interest for optimal targeting of neuroendocrine tumors *in vivo*: 1) combination of ligands for the glucagon-like peptide-1 (GLP-1) and CCK₂ receptors for insulinomas, 2) a mixture of sst₂, GLP-1 and GRP radiolabeled ligands for gastrinomas.

Radiation protection in normal organs

Increasing the therapeutic window can also be achieved by reducing radiation toxicity to normal organs. In peptide(ss)-based therapy, the kidney is one of the dose-limiting organs and some clinical studies showed renal toxicity following PRRT ([161-163]). It is therefore favorable to reduce renal radiation, making it feasible to increase the total amount of injected radioactivity.

It has been found that radiolabeled somatostatin analogs are filtered and reabsorbed in the proximal tubules of rat kidneys [164]. Also, in the human kidney radioactivity was mostly concentrated in the cortex and the megalin/cubulin system was found to play an essential role in the reabsorption of octreotide [165, 166]. In addition, it was shown that 18% of the renal uptake of sst₂ targeting peptides can be dedicated to sst-mediated uptake [167].

Standard procedure to reduce renal uptake during PRRT in our institution is a 4-hour infusion of a mixture of lysine and arginine [17]. We investigated whether oral

administration of lysine could also reduce renal uptake [168]. In rats, oral administration of lysine reduced renal uptake with 40%, comparable to reduction found with intravenous administration of lysine [169]. Moreover, other agents, such as gefosine [170, 171], colchicine [172] and the radioprotective drug amifostine [173], could improve kidney protection strategies currently used in the clinic.

CONCLUSION

Many tumors overexpress one or more receptors which can be targeted using receptor-specific radiolabeled peptides. So far, sst-targeting peptides are widely used for imaging and therapy of cancer patients. PRRT with ^{177}Lu labeled somatostatin analogs has resulted in symptomatic improvement, prolonged survival and enhanced quality of life of neuroendocrine tumor patients. PRS and PRRT targeting other tumor-specific receptors, such as GRP and CCK receptors, are well on their way to clinical utilization as well.

Literature shows that it is possible to increase the receptor density on tumor cells using different methods. In PRRT treatment, this would enable the administration of higher therapeutic doses to tumors, which might lead to a higher cure rate in patients.

Targeting one or several tumor-specific receptors by combinations of therapeutic agents, as well as by reducing non-target uptake of radioactivity, will enlarge the therapeutic window of PRRT. Clinical studies will provide more insight in the effects of combination treatment strategies in cancer patients.

AIM AND OUTLINE OF THIS THESIS

This introduction provided an overview of several options to optimize peptide receptor scintigraphy (PRS) and peptide receptor radionuclide therapy (PRRT). One of these options is the development of new high potential peptide analogs targeting tumor specific receptors. Therefore the aims of this project were:

- I. To synthesize and evaluate radiolabeled neurotensin (NT) analogs for imaging and treatment of neurotensin receptor-1 (NTR-1) expressing exocrine pancreatic cancer.
- II. To develop and evaluate gastrin releasing peptide (GRP) receptor-targeting radiopharmaceuticals for prostate cancer imaging and therapy.
- III. To evaluate GRP receptor-expression during prostate cancer development.

Part I: Neurotensin analogs for *in vivo* targeting of exocrine pancreatic cancer

Exocrine pancreatic carcinoma is a very aggressive cancer. It grows extremely rapidly and early diagnosis allowing complete therapeutic surgical resection is rarely possible. There is, therefore, a significant need for new methods for visualization and therapy of exocrine pancreatic cancer. The expression of NT receptors has been manifested in several human cancers, including in 75% of exocrine ductal pancreatic adenocarcinomas. In this project we developed novel NT analogs with modified lysine and arginine derivatives to improve the stability and coupled to either the DTPA or the DOTA chelating system. **Chapters 2 and 3** describe the synthesis of the new peptide analogs and the *in vitro* evaluation of receptor-binding and stability. The peptide analogs with the most favorable *in vitro* characteristics for NTR-1 targeting were evaluated *in vivo* in tumor-bearing mice.

Part II: Bombesin analogs for *in vivo* targeting of prostate cancer

GRP receptors are expressed in high densities on several primary human tumors and their metastases, including prostate cancers. Prostate cancer is the second leading cause of cancer-related deaths and the most frequently diagnosed cancer in men in Western countries, and will increase to be a major health problem due to the aging of people in the Western world. Radiolabeled BN analogs targeting GRP receptors might be useful for diagnosis and treatment of prostate tumors.

In **chapter 4** we describe the pre-clinical evaluation of newly synthesized BN analogs. The outcome of the *in vitro* and *in vivo* studies led to the selection of one peptide analog with the most promising GRP receptor-targeting characteristics. This DTPA-conjugated analog can be radiolabeled with ^{111}In and is therefore suitable for scintigraphic tumor imaging, including single-photon emission computed tomography (SPECT). Compared to SPECT, positron-emission tomography (PET) produces higher resolution images in the clinic and enables more accurate quantification. As PET instrumentation becomes more and more available, there is a rising interest in the development of high potential GRP receptor-targeting PET tracers. We therefore radiolabeled a DOTA-conjugated BN analog with the positron-emitters ^{64}Cu and ^{86}Y , and evaluated their potential as GRP receptor-targeting PET tracers in tumor bearing mice (**chapter 5**).

Part III: GRP receptor-expression during prostate cancer development

GRP receptor-targeting radiopharmaceuticals appeared to be powerful tools for diagnosis, localization and staging of prostate cancer. In addition, these radiolabeled BN analogs are of particular interest for peptide receptor radionuclide therapy (PRRT) of advanced prostate cancer patients who do not respond anymore to hormone therapy. So far, the best treatment strategies available for this group of patients are only marginally

effective. As part of this project, we aimed to assess the value of GRP receptor-targeted imaging and treatment modalities in the various stages of prostate cancer progression, by evaluating GRP receptor expression in a panel of human prostate cancer xenograft models. This panel represents the various aspects of prostate tumor development, including the transition of androgen-dependent towards androgen-independent growth. In **chapter 6** we illustrate the *in vitro* autoradiographic evaluation of GRP receptor expression on frozen sections of the xenograft models using radiolabeled BN analogs. The results of this study suggested that GRP receptors are only expressed in the androgen-dependent and not in the androgen-independent xenograft models. This outcome led us to further evaluate GRP receptor expression in the androgen-dependent xenografts *in vivo* in mice and additionally assess the influence of hormone treatment on this receptor expression, as described in **chapter 7**.

This thesis concludes with a summarizing general discussion in which the impact of the results obtained from the different studies on clinical application of NT and BN has been discussed (**chapter 8**).

REFERENCES

1. Krenning, E.P., J.J. Teunissen, R. Valkema, et al., Molecular radiotherapy with somatostatin analogs for (neuro-)endocrine tumors. *J Endocrinol Invest* 2005; 28(11 Suppl): 146.
2. Krenning, E.P., D.J. Kwekkeboom, W.H. Bakker, et al., Somatostatin receptor scintigraphy with [111In-DTPA-D-Phe1]- and [123I-Tyr3]-octreotide: the Rotterdam experience with more than 1000 patients. *Eur J Nucl Med* 1993; 20(8): 716.
3. Kwekkeboom, D., E.P. Krenning and M. de Jong, Peptide receptor imaging and therapy. *J Nucl Med* 2000; 41(10): 1704.
4. Valkema, R., M. De Jong, W.H. Bakker, et al., Phase I study of peptide receptor radionuclide therapy with [In-DTPA]octreotide: the Rotterdam experience. *Semin Nucl Med* 2002; 32(2): 110.
5. Bodei, L., M. Cremonesi, S. Zoboli, et al., Receptor-mediated radionuclide therapy with 90Y-DOTATOC in association with amino acid infusion: a phase I study. *Eur J Nucl Med Mol Imaging* 2003; 30(2): 207.
6. Valkema, R., S. Pauwels, L.K. Kvols, et al., Survival and response after peptide receptor radionuclide therapy with [90Y-DOTA0,Tyr3]octreotide in patients with advanced gastroenteropancreatic neuroendocrine tumors. *Semin Nucl Med* 2006; 36(2): 147.
7. Otte, A., R. Herrmann, A. Heppeler, et al., Yttrium-90 DOTATOC: first clinical results. *Eur J Nucl Med* 1999; 26(11): 1439.
8. Waldherr, C., M. Pless, H.R. Maecke, et al., Tumor response and clinical benefit in neuroendocrine tumors after 7.4 GBq (90Y)-DOTATOC. *J Nucl Med* 2002; 43(5): 610.
9. Chinol, M., L. Bodei, M. Cremonesi, et al., Receptor-mediated radiotherapy with Y-DOTA-DPhe-Tyr-octreotide: the experience of the European Institute of Oncology Group. *Semin Nucl Med* 2002; 32(2): 141.
10. van Essen, M., E.P. Krenning, M. de Jong, et al., Peptide receptor radionuclide therapy with radiolabelled somatostatin analogues in patients with somatostatin receptor positive tumours. *Acta Oncologica* 2007.
11. Reubi, J.C., J.C. Schar, B. Waser, et al., Affinity profiles for human somatostatin receptor subtypes SST1-SST5 of somatostatin radiotracers selected for scintigraphic and radiotherapeutic use. *Eur J Nucl Med* 2000; 27(3): 273.
12. de Jong, M., W.A. Breeman, W.H. Bakker, et al., Comparison of (111)In-labeled somatostatin analogues for tumor scintigraphy and radionuclide therapy. *Cancer Res* 1998; 58(3): 437.
13. Esser, J.P., E.P. Krenning, J.J. Teunissen, et al., Comparison of [(177)Lu-DOTA(0),Tyr(3)]octreotate and [(177)Lu-DOTA(0),Tyr(3)]octreotide: which peptide is preferable for PRRT? *Eur J Nucl Med Mol Imaging* 2006; 33(11): 1346.
14. Kwekkeboom, D.J., W.H. Bakker, P.P. Kooij, et al., [177Lu-DOTAOTyr3]octreotate: comparison with [111In-DTPA]octreotide in patients. *Eur J Nucl Med* 2001; 28(9): 1319.
15. O'Donoghue, J.A., M. Bardies and T.E. Wheldon, Relationships between tumor size and curability for uniformly targeted therapy with beta-emitting radionuclides. *J Nucl Med* 1995; 36(10): 1902.
16. de Jong, M., W.A. Breeman, R. Valkema, et al., Combination radionuclide therapy using 177Lu- and 90Y-labeled somatostatin analogs. *J Nucl Med* 2005; 46 Suppl 1: 13S.
17. Kwekkeboom, D.J., J.J. Teunissen, W.H. Bakker, et al., Radiolabeled somatostatin analog [177Lu-DOTA0,Tyr3]octreotate in patients with endocrine gastroenteropancreatic tumors. *J Clin Oncol* 2005; 23(12): 2754.
18. Teunissen, J.J., D.J. Kwekkeboom and E.P. Krenning, Quality of life in patients with gastroenteropancreatic tumors treated with [177Lu-DOTA0,Tyr3]octreotate. *J Clin Oncol* 2004; 22(13): 2724.

19. Zhang, H., J. Chen, C. Waldherr, et al., Synthesis and evaluation of bombesin derivatives on the basis of pan-bombesin peptides labeled with indium-111, lutetium-177, and yttrium-90 for targeting bombesin receptor-expressing tumors. *Cancer Res* 2004; 64(18): 6707.
20. Breeman, W.A., L.J. Hofland, M. de Jong, et al., Evaluation of radiolabelled bombesin analogues for receptor-targeted scintigraphy and radiotherapy. *Int J Cancer* 1999; 81(4): 658.
21. Ginj, M., H. Zhang, B. Waser, et al., Radiolabeled somatostatin receptor antagonists are preferable to agonists for in vivo peptide receptor targeting of tumors. *Proc Natl Acad Sci U S A* 2006; 103(44): 16436.
22. Gabriel, M., C. Decristoforo, E. Donnemiller, et al., An inpatient comparison of ^{99m}Tc-EDDA/HYNIC-TOC with ¹¹¹In-DTPA-octreotide for diagnosis of somatostatin receptor-expressing tumors. *J Nucl Med* 2003; 44(5): 708.
23. Bangard, M., M. Behe, S. Guhlke, et al., Detection of somatostatin receptor-positive tumours using the new ^{99m}Tc-tricine-HYNIC-D-Phe1-Tyr3-octreotide: first results in patients and comparison with ¹¹¹In-DTPA-D-Phe1-octreotide. *Eur J Nucl Med* 2000; 27(6): 628.
24. Hubalewska-Dydejczyk, A., K. Fross-Baron, F. Golkowski, et al., ^{99m}Tc-EDDA/HYNIC-octreotate in detection of atypical bronchial carcinoid. *Exp Clin Endocrinol Diabetes* 2007; 115(1): 47.
25. Hubalewska-Dydejczyk, A., K. Fross-Baron, R. Mikolajczak, et al., ^{99m}Tc-EDDA/HYNIC-octreotate scintigraphy, an efficient method for the detection and staging of carcinoid tumours: results of 3 years' experience. *Eur J Nucl Med Mol Imaging* 2006; 33(10): 1123.
26. Hubalewska-Dydejczyk, A., P. Szybinski, K. Fross-Baron, et al., (^{99m}Tc-EDDA/HYNIC-octreotate - a new radiotracer for detection and staging of NET: a case of metastatic duodenal carcinoid. *Nucl Med Rev Cent East Eur* 2005; 8(2): 155.
27. Gabriel, M., C. Decristoforo, T. Maina, et al., ^{99m}Tc-N⁴-[Tyr3]Octreotate Versus ^{99m}Tc-EDDA/HYNIC-[Tyr3]Octreotide: an inpatient comparison of two novel Technetium-99m labeled tracers for somatostatin receptor scintigraphy. *Cancer Biother Radiopharm* 2004; 19(1): 73.
28. Nikolopoulou, A., T. Maina, P. Sotiriou, et al., Tetraamine-modified octreotide and octreotate: labeling with ^{99m}Tc and preclinical comparison in AR4-2J cells and AR4-2J tumor-bearing mice. *J Pept Sci* 2006; 12(2): 124.
29. Decristoforo, C., T. Maina, B. Nock, et al., ^{99m}Tc-Demotate 1: first data in tumour patients-results of a pilot/phase I study. *Eur J Nucl Med Mol Imaging* 2003; 30(9): 1211.
30. Meisetschlager, G., T. Poethko, A. Stahl, et al., Gluc-Lys([¹⁸F]FP)-TOCA PET in patients with SSTR-positive tumors: biodistribution and diagnostic evaluation compared with [¹¹¹In]DTPA-octreotide. *J Nucl Med* 2006; 47(4): 566.
31. Anderson, C.J., F. Dehdashti, P.D. Cutler, et al., ⁶⁴Cu-TETA-octreotide as a PET imaging agent for patients with neuroendocrine tumors. *J Nucl Med* 2001; 42(2): 213.
32. Breeman, W.A., M. de Jong, E. de Blois, et al., Radiolabelling DOTA-peptides with ⁶⁸Ga. *Eur J Nucl Med Mol Imaging* 2005; 32(4): 478.
33. Kowalski, J., M. Henze, J. Schuhmacher, et al., Evaluation of positron emission tomography imaging using [⁶⁸Ga]-DOTA-D Phe(1)-Tyr(3)-Octreotide in comparison to [¹¹¹In]-DTPAOC SPECT. First results in patients with neuroendocrine tumors. *Mol Imaging Biol* 2003; 5(1): 42.
34. Gabriel, M., C. Decristoforo, D. Kendler, et al., ⁶⁸Ga-DOTA-Tyr3-octreotide PET in neuroendocrine tumors: comparison with somatostatin receptor scintigraphy and CT. *J Nucl Med* 2007; 48(4): 508.
35. Kulaksiz, H., R. Eissele, D. Rossler, et al., Identification of somatostatin receptor subtypes 1, 2A, 3, and 5 in neuroendocrine tumours with subtype specific antibodies. *Gut* 2002; 50(1): 52.
36. Reubi, J.C., B. Waser, J.C. Schaefer, et al., Somatostatin receptor sst1-sst5 expression in normal and neoplastic human tissues using receptor autoradiography with subtype-selective ligands. *Eur J Nucl Med* 2001; 28(7): 836.
37. Ginj, M., J.S. Schmitt, J. Chen, et al., Design, synthesis, and biological evaluation of somatostatin-based radiopeptides. *Chem Biol* 2006; 13(10): 1081.

38. Wild, D., H.R. Macke, B. Waser, et al., ⁶⁸Ga-DOTANOC: a first compound for PET imaging with high affinity for somatostatin receptor subtypes 2 and 5. *Eur J Nucl Med Mol Imaging* 2005; 32(6): 724.
39. Reubi, J.C., S. Wenger, J. Schmuckli-Maurer, et al., Bombesin receptor subtypes in human cancers: detection with the universal radioligand (125)I-[D-TYR(6), beta-ALA(11), PHE(13), NLE(14)] bombesin(6-14). *Clin Cancer Res* 2002; 8(4): 1139.
40. Jemal, A., R. Siegel, E. Ward, et al., Cancer statistics, 2007. *CA Cancer J Clin* 2007; 57(1): 43.
41. Breeman, W.A., M. de Jong, B. Bernard, et al., Tissue distribution and metabolism of radioiodinated DTPA0, D-Tyr1 and Tyr3 derivatives of octreotide in rats. *Anticancer Res* 1998; 18(1A): 83.
42. Nock, B., A. Nikolopoulou, E. Chiotellis, et al., [(99m)Tc]Demobesin 1, a novel potent bombesin analogue for GRP receptor-targeted tumour imaging. *Eur J Nucl Med Mol Imaging* 2003; 30(2): 247.
43. Nock, B.A., A. Nikolopoulou, A. Galanis, et al., Potent bombesin-like peptides for GRP-receptor targeting of tumors with 99mTc: a preclinical study. *J Med Chem* 2005; 48(1): 100.
44. Van de Wiele, C., F. Dumont, R. Vanden Broecke, et al., Technetium-99m RP527, a GRP analogue for visualisation of GRP receptor- expressing malignancies: a feasibility study. *Eur J Nucl Med* 2000; 27(11): 1694.
45. van Bokhoven, A., M. Varella-Garcia, C. Korch, et al., Molecular characterization of human prostate carcinoma cell lines. *Prostate* 2003; 57(3): 205.
46. Hoffman, T.J., H. Gali, C.J. Smith, et al., Novel series of ¹¹¹In-labeled bombesin analogs as potential radiopharmaceuticals for specific targeting of gastrin-releasing peptide receptors expressed on human prostate cancer cells. *J Nucl Med* 2003; 44(5): 823.
47. Breeman, W.A., M. de Jong, J.L. Erion, et al., Preclinical comparison of (111)In-labeled DTPA- or DOTA-bombesin analogs for receptor-targeted scintigraphy and radionuclide therapy. *J Nucl Med* 2002; 43(12): 1650.
48. Ferro-Flores, G., C. Arteaga de Murphy, J. Rodriguez-Cortes, et al., Preparation and evaluation of ^{99m}Tc-EDDA/HYNIC-[Lys 3]-bombesin for imaging gastrin-releasing peptide receptor-positive tumours. *Nucl Med Commun* 2006; 27(4): 371.
49. Garcia Garayoa, E., D. Ruegg, P. Blauenstein, et al., Chemical and biological characterization of new Re(CO)(3)/[(99m)Tc](CO)(3) bombesin analogues. *Nucl Med Biol* 2007; 34(1): 17.
50. Reubi, J.C., H.R. Macke and E.P. Krenning, Candidates for peptide receptor radiotherapy today and in the future. *J Nucl Med* 2005; 46 Suppl 1: 67S.
51. de Visser, M., H.F. Bernard, J.L. Erion, et al., Novel (111)In-labelled bombesin analogues for molecular imaging of prostate tumours. *Eur J Nucl Med Mol Imaging* 2007.
52. Zhang, H., J. Schuhmacher, B. Waser, et al., DOTA-PESIN, a DOTA-conjugated bombesin derivative designed for the imaging and targeted radionuclide treatment of bombesin receptor-positive tumours. *Eur J Nucl Med Mol Imaging* 2007.
53. Yang, Y.S., X. Zhang, Z. Xiong, et al., Comparative in vitro and in vivo evaluation of two ⁶⁴Cu-labeled bombesin analogs in a mouse model of human prostate adenocarcinoma. *Nucl Med Biol* 2006; 33(3): 371.
54. Smith, C.J., H. Gali, G.L. Sieckman, et al., Radiochemical investigations of (177)Lu-DOTA-8-Aoc-BBN[7-14]NH(2): an in vitro/in vivo assessment of the targeting ability of this new radiopharmaceutical for PC-3 human prostate cancer cells. *Nucl Med Biol* 2003; 30(2): 101.
55. Rogers, B.E., H.M. Bigott, D.W. McCarthy, et al., MicroPET imaging of a gastrin-releasing peptide receptor-positive tumor in a mouse model of human prostate cancer using a ⁶⁴Cu-labeled bombesin analogue. *Bioconjug Chem* 2003; 14(4): 756.
56. Johnson, C.V., T. Shelton, C.J. Smith, et al., Evaluation of combined (177)Lu-DOTA-8-AOC-BBN (7-14)NH(2) GRP receptor-targeted radiotherapy and chemotherapy in PC-3 human prostate tumor cell xenografted SCID mice. *Cancer Biother Radiopharm* 2006; 21(2): 155.

57. Biddlecombe, G.B., B.E. Rogers, M.D. Visser, et al., Molecular Imaging of Gastrin-Releasing Peptide Receptor-Positive Tumors in Mice Using (64)Cu- and (86)Y-DOTA-(Pro(1),Tyr(4))-Bombesin(1-14). *Bioconjug Chem* 2007.
58. Lantry, L.E., E. Cappelletti, M.E. Maddalena, et al., 177Lu-AMBA: Synthesis and characterization of a selective 177Lu-labeled GRP-R agonist for systemic radiotherapy of prostate cancer. *J Nucl Med* 2006; 47(7): 1144.
59. Van de Wiele, C., F. Dumont, S. van Belle, et al., Is there a role for agonist gastrin-releasing peptide receptor radioligands in tumour imaging? *Nucl Med Commun* 2001; 22(1): 5.
60. Baum, R., V. Prasad, N. Mutloka, et al., Molecular imaging of bombesin receptors in various tumors by Ga-68 AMBA PET/CT: First results *J Nucl Med* 2007; 48(supplement 2): 79P.
61. de Visser, M., W.M. van Weerden, M. Melis, et al., Radiolabeled bombesin analogs in preclinical studies. *J Nucl Med* 2007; 48, suppl 2: 24P.
62. Mancuso, A., S. Oudard and C.N. Sternberg, Effective chemotherapy for hormone-refractory prostate cancer (HRPC): present status and perspectives with taxane-based treatments. *Crit Rev Oncol Hematol* 2007; 61(2): 176.
63. Oudard, S., E. Banu, P. Beuzebec, et al., Multicenter randomized phase II study of two schedules of docetaxel, estramustine, and prednisone versus mitoxantrone plus prednisone in patients with metastatic hormone-refractory prostate cancer. *J Clin Oncol* 2005; 23(15): 3343.
64. de Visser, M., W.M. van Weerden, C.M. de Ridder, et al., Androgen-dependent expression of the gastrin-releasing Peptide receptor in human prostate tumor xenografts. *J Nucl Med* 2007; 48(1): 88.
65. de Jong, M., W.A. Breeman, B.F. Bernard, et al., Tumor response after [(90)Y-DOTA(0),Tyr(3)] octreotide radionuclide therapy in a transplantable rat tumor model is dependent on tumor size. *J Nucl Med* 2001; 42(12): 1841.
66. de Jong, M., W.A. Breeman, B.F. Bernard, et al., [177Lu-DOTA(0),Tyr3] octreotate for somatostatin receptor-targeted radionuclide therapy. *Int J Cancer* 2001; 92(5): 628.
67. De Jong, M., R. Valkema, F. Jamar, et al., Somatostatin receptor-targeted radionuclide therapy of tumors: preclinical and clinical findings. *Semin Nucl Med* 2002; 32(2): 133.
68. Reubi, J.C., B. Waser, H. Friess, et al., Neurotensin receptors: a new marker for human ductal pancreatic adenocarcinoma. *Gut* 1998; 42(4): 546.
69. Kuhar, M.J., Imaging receptors for drugs in neural tissue. *Neuropharmacology* 1987; 26(7B): 911.
70. Ehlers, R.A., S. Kim, Y. Zhang, et al., Gut peptide receptor expression in human pancreatic cancers. *Ann Surg* 2000; 231(6): 838.
71. Zhang, K., R. An, Z. Gao, et al., Radionuclide imaging of small-cell lung cancer (SCLC) using 99mTc-labeled neurotensin peptide 8-13. *Nucl Med Biol* 2006; 33(4): 505.
72. Nock, B.A., A. Nikolopoulou, J.C. Reubi, et al., Toward stable N4-modified neurotensins for NTS1-receptor-targeted tumor imaging with 99mTc. *J Med Chem* 2006; 49(15): 4767.
73. Maes, V., E. Garcia-Garayoa, P. Blauenstein, et al., Novel 99mTc-labeled neurotensin analogues with optimized biodistribution properties. *J Med Chem* 2006; 49(5): 1833.
74. Garcia-Garayoa, E., V. Maes, P. Blauenstein, et al., Double-stabilized neurotensin analogues as potential radiopharmaceuticals for NTR-positive tumors. *Nucl Med Biol* 2006; 33(4): 495.
75. Garcia-Garayoa, E., L. Allemann-Tannahill, P. Blauenstein, et al., In vitro and in vivo evaluation of new radiolabeled neurotensin(8-13) analogues with high affinity for NT1 receptors. *Nucl Med Biol* 2001; 28(1): 75.
76. Lugin, D., F. Vecchini, S. Doulut, et al., Reduced peptide bond pseudopeptide analogues of neurotensin: binding and biological activities, and in vitro metabolic stability. *Eur J Pharmacol* 1991; 205(2): 191.
77. de Visser, M., P.J. Janssen, A. Srinivasan, et al., Stabilised 111In-labelled DTPA- and DOTA-conjugated neurotensin analogues for imaging and therapy of exocrine pancreatic cancer. *Eur J Nucl Med Mol Imaging* 2003; 30(8): 1134.

78. Emami, B., J. Lyman, A. Brown, et al., Tolerance of normal tissue to therapeutic irradiation. *Int J Radiat Oncol Biol Phys* 1991; 21(1): 109.
79. Buchegger, F., F. Bonvin, M. Kosinski, et al., Radiolabeled neurotensin analog, ^{99m}Tc-NT-XI, evaluated in ductal pancreatic adenocarcinoma patients. *J Nucl Med* 2003; 44(10): 1649.
80. Reubi, J.C., J.A. Chayvialle, B. Franc, et al., Somatostatin receptors and somatostatin content in medullary thyroid carcinomas. *Lab Invest* 1991; 64(4): 567.
81. Kwekkeboom, D.J., J.C. Reubi, S.W. Lamberts, et al., In vivo somatostatin receptor imaging in medullary thyroid carcinoma. *J Clin Endocrinol Metab* 1993; 76(6): 1413.
82. Reubi, J.C., J.C. Schaer and B. Waser, Cholecystokinin(CCK)-A and CCK-B/gastrin receptors in human tumors. *Cancer Res* 1997; 57(7): 1377.
83. Behr, T.M., N. Jenner, S. Radetzky, et al., Targeting of cholecystokinin-B/gastrin receptors in vivo: preclinical and initial clinical evaluation of the diagnostic and therapeutic potential of radiolabelled gastrin. *Eur J Nucl Med* 1998; 25(4): 424.
84. Reubi, J.C., B. Waser, J.C. Schaer, et al., Unsulfated DTPA- and DOTA-CCK analogs as specific high-affinity ligands for CCK-B receptor-expressing human and rat tissues in vitro and in vivo. *Eur J Nucl Med* 1998; 25(5): 481.
85. de Jong, M., W.H. Bakker, B.F. Bernard, et al., Preclinical and initial clinical evaluation of ¹¹¹In-labeled nonsulfated CCK8 analog: a peptide for CCK-B receptor-targeted scintigraphy and radionuclide therapy. *J Nucl Med* 1999; 40(12): 2081.
86. Kwekkeboom, D.J., W.H. Bakker, P.P. Kooij, et al., Cholecystokinin receptor imaging using an octapeptide DTPA-CCK analogue in patients with medullary thyroid carcinoma. *Eur J Nucl Med* 2000; 27(9): 1312.
87. Behr, T.M., N. Jenner, M. Behe, et al., Radiolabeled peptides for targeting cholecystokinin-B/gastrin receptor-expressing tumors. *J Nucl Med* 1999; 40(6): 1029.
88. Nock, B.A., T. Maina, M. Behe, et al., CCK-2/gastrin receptor-targeted tumor imaging with (^{99m}Tc)-labeled minigastrin analogs. *J Nucl Med* 2005; 46(10): 1727.
89. Gotthardt, M., M.P. Behe, D. Beuter, et al., Improved tumour detection by gastrin receptor scintigraphy in patients with metastasised medullary thyroid carcinoma. *Eur J Nucl Med Mol Imaging* 2006; 33(11): 1273.
90. Gotthardt, M., M.P. Behe, J. Grass, et al., Added value of gastrin receptor scintigraphy in comparison to somatostatin receptor scintigraphy in patients with carcinoids and other neuroendocrine tumours. *Endocr Relat Cancer* 2006; 13(4): 1203.
91. Mayo, K.E., L.J. Miller, D. Bataille, et al., International Union of Pharmacology. XXXV. The glucagon receptor family. *Pharmacol Rev* 2003; 55(1): 167.
92. Reubi, J.C. and B. Waser, Concomitant expression of several peptide receptors in neuroendocrine tumours: molecular basis for in vivo multireceptor tumour targeting. *Eur J Nucl Med Mol Imaging* 2003; 30(5): 781.
93. Korner, M., M. Stockli, B. Waser, et al., GLP-1 Receptor Expression in Human Tumors and Human Normal Tissues: Potential for In Vivo Targeting. *J Nucl Med* 2007; 48(5): 736.
94. Meier, J.J. and M.A. Nauck, Glucagon-like peptide 1(GLP-1) in biology and pathology. *Diabetes Metab Res Rev* 2005; 21(2): 91.
95. Hassan, M., A. Eskilsson, C. Nilsson, et al., In vivo dynamic distribution of ¹³¹I-glucagon-like peptide-1 (7-36) amide in the rat studied by gamma camera. *Nucl Med Biol* 1999; 26(4): 413.
96. Gotthardt, M., M. Fischer, I. Naeher, et al., Use of the incretin hormone glucagon-like peptide-1 (GLP-1) for the detection of insulinomas: initial experimental results. *Eur J Nucl Med Mol Imaging* 2002; 29(5): 597.
97. Gotthardt, M., G. Lalyko, J. van Eerd-Vismale, et al., A new technique for in vivo imaging of specific GLP-1 binding sites: First results in small rodents. *Regul Pept* 2006.
98. Wild, D., M. Behe, A. Wicki, et al., [Lys40(Ahx-DTPA-¹¹¹In)NH2]exendin-4, a very promising ligand for glucagon-like peptide-1 (GLP-1) receptor targeting. *J Nucl Med* 2006; 47(12): 2025.

99. Wicki, A., D. Wild, D. Storch, et al., [Lys40(Ahx-DTPA-111In)NH2]-Exendin-4 Is a Highly Efficient Radiotherapeutic for Glucagon-Like Peptide-1 Receptor-Targeted Therapy for Insulinoma. *Clin Cancer Res* 2007; 13(12): 3696.
100. Brooks, P.C., Role of integrins in angiogenesis. *Eur J Cancer* 1996; 32A(14): 2423.
101. Plow, E.F., T.A. Haas, L. Zhang, et al., Ligand binding to integrins. *J Biol Chem* 2000; 275(29): 21785.
102. Gurrath, M., G. Muller, H. Kessler, et al., Conformation/activity studies of rationally designed potent anti-adhesive RGD peptides. *Eur J Biochem* 1992; 210(3): 911.
103. Aumailley, M., M. Gurrath, G. Muller, et al., Arg-Gly-Asp constrained within cyclic pentapeptides. Strong and selective inhibitors of cell adhesion to vitronectin and laminin fragment P1. *FEBS Lett* 1991; 291(1): 50.
104. van Hagen, P.M., W.A. Breeman, H.F. Bernard, et al., Evaluation of a radiolabelled cyclic DTPA-RGD analogue for tumour imaging and radionuclide therapy. *Int J Cancer* 2000; 90(4): 186.
105. Chen, X., R. Park, M. Tohme, et al., MicroPET and autoradiographic imaging of breast cancer alpha v-integrin expression using 18F- and ⁶⁴Cu-labeled RGD peptide. *Bioconjug Chem* 2004; 15(1): 41.
106. Cai, W., X. Zhang, Y. Wu, et al., A thiol-reactive 18F-labeling agent, N-[2-(4-18F-fluorobenzamido)ethyl]maleimide, and synthesis of RGD peptide-based tracer for PET imaging of alpha v beta 3 integrin expression. *J Nucl Med* 2006; 47(7): 1172.
107. Haubner, R., B. Kuhnast, C. Mang, et al., [18F]Galacto-RGD: synthesis, radiolabeling, metabolic stability, and radiation dose estimates. *Bioconjug Chem* 2004; 15(1): 61.
108. Beer, A.J., R. Haubner, M. Sarbia, et al., Positron emission tomography using [18F]Galacto-RGD identifies the level of integrin alpha(v)beta3 expression in man. *Clin Cancer Res* 2006; 12(13): 3942.
109. Beer, A.J., R. Haubner, I. Wolf, et al., PET-based human dosimetry of 18F-galacto-RGD, a new radiotracer for imaging alpha v beta3 expression. *J Nucl Med* 2006; 47(5): 763.
110. Beer, A.J., R. Haubner, M. Goebel, et al., Biodistribution and pharmacokinetics of the alphav-beta3-selective tracer 18F-galacto-RGD in cancer patients. *J Nucl Med* 2005; 46(8): 1333.
111. Dijkgraaf, I., J.A. Kruijtzter, S. Liu, et al., Improved targeting of the alpha(v)beta (3) integrin by multimerisation of RGD peptides. *Eur J Nucl Med Mol Imaging* 2007; 34(2): 267.
112. Dijkgraaf, I., A.Y. Rijnders, A. Soede, et al., Synthesis of DOTA-conjugated multivalent cyclic-RGD peptide dendrimers via 1,3-dipolar cycloaddition and their biological evaluation: implications for tumor targeting and tumor imaging purposes. *Org Biomol Chem* 2007; 5(6): 935.
113. Dijkgraaf, I., S. Liu, J.A. Kruijtzter, et al., Effects of linker variation on the in vitro and in vivo characteristics of an 111In-labeled RGD peptide. *Nucl Med Biol* 2007; 34(1): 29.
114. Dijkgraaf, I., J.A. Kruijtzter, C. Frielink, et al., Alpha v beta 3 integrin-targeting of intraperitoneally growing tumors with a radiolabeled RGD peptide. *Int J Cancer* 2007; 120(3): 605.
115. Kimura, N., C. Hayafuji, H. Konagaya, et al., 17 beta-estradiol induces somatostatin (SRIF) inhibition of prolactin release and regulates SRIF receptors in rat anterior pituitary cells. *Endocrinology* 1986; 119(3): 1028.
116. Presky, D.H. and A. Schonbrunn, Somatostatin pretreatment increases the number of somatostatin receptors in GH4C1 pituitary cells and does not reduce cellular responsiveness to somatostatin. *J Biol Chem* 1988; 263(2): 714.
117. Kimura, N., C. Hayafuji and N. Kimura, Characterization of 17-beta-estradiol-dependent and -independent somatostatin receptor subtypes in rat anterior pituitary. *J Biol Chem* 1989; 264(12): 7033.
118. Slama, A., C. Videau, C. Kordon, et al., Estradiol regulation of somatostatin receptors in the arcuate nucleus of the female rat. *Neuroendocrinology* 1992; 56(2): 240.
119. Vidal, C., I. Raully, M. Zeggari, et al., Up-regulation of somatostatin receptors by epidermal growth factor and gastrin in pancreatic cancer cells. *Mol Pharmacol* 1994; 46(1): 97.

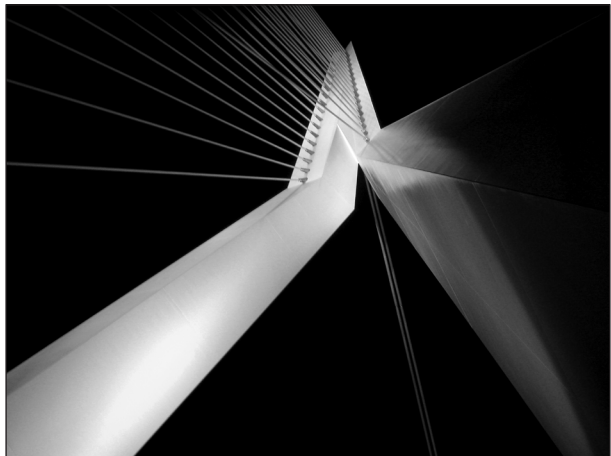
120. Visser-Wisselaar, H.A., C.J. Van Uffelen, P.M. Van Koetsveld, et al., 17-beta-estradiol-dependent regulation of somatostatin receptor subtype expression in the 7315b prolactin secreting rat pituitary tumor in vitro and in vivo. *Endocrinology* 1997; 138(3): 1180.
121. Froidevaux, S., E. Hintermann, M. Torok, et al., Differential regulation of somatostatin receptor type 2 (sst 2) expression in AR4-2J tumor cells implanted into mice during octreotide treatment. *Cancer Res* 1999; 59(15): 3652.
122. Viguerie, N., J.P. Esteve, C. Susini, et al., Dexamethasone effects on somatostatin receptors in pancreatic acinar AR4-2J cells. *Biochem Biophys Res Commun* 1987; 147(3): 942.
123. Gunn, S.H., J.E. Schwimer, M. Cox, et al., In vitro modeling of the clinical interactions between octreotide and 111In-pentetreotide: is there evidence of somatostatin receptor downregulation? *J Nucl Med* 2006; 47(2): 354.
124. Behe, M., M. Püsken, M. Henzel, et al., Upregulation of gastrin and somatostatin receptor after irradiation. *Eur J Nucl Med Mol Imaging* 2003; 30: S218.
125. Behe, M., S. Koller, M. Püsken, et al., Irradiation-induced upregulation of somatostatin and gastrin receptors in vitro and in vivo. *Eur J Nucl Med Mol Imaging* 2004; 31: S237.
126. Oddstig, J., P. Bernhardt, O. Nilsson, et al., Radiation-induced up-regulation of somatostatin receptor expression in small cell lung cancer in vitro. *Nucl Med Biol* 2006; 33(7): 841.
127. Capello, A., E. Krenning, B. Bernard, et al., 111In-labelled somatostatin analogues in a rat tumour model: somatostatin receptor status and effects of peptide receptor radionuclide therapy. *Eur J Nucl Med Mol Imaging* 2005; 32(11): 1288.
128. Melis, M., F. Forrer, A. Capello, et al., Up-regulation of somatostatin receptor density on rat CA20948 tumours escaped from low dose [177Lu-DOTA0,Tyr3]octreotate therapy. *QJ Nucl Med* 2007.
129. Seth, P., Vector-mediated cancer gene therapy: an overview. *Cancer Biol Ther* 2005; 4(5): 512.
130. Rogers, B.E., S.F. McLean, R.L. Kirkman, et al., In vivo localization of [(111)In]-DTPA-D-Phe1-octreotide to human ovarian tumor xenografts induced to express the somatostatin receptor subtype 2 using an adenoviral vector. *Clin Cancer Res* 1999; 5(2): 383.
131. Zinn, K.R., T.R. Chaudhuri, D.J. Buchsbaum, et al., Simultaneous evaluation of dual gene transfer to adherent cells by gamma-ray imaging. *Nucl Med Biol* 2001; 28(2): 135.
132. Hemminki, A., N. Belousova, K.R. Zinn, et al., An adenovirus with enhanced infectivity mediates molecular chemotherapy of ovarian cancer cells and allows imaging of gene expression. *Mol Ther* 2001; 4(3): 223.
133. Zinn, K.R., T.R. Chaudhuri, V.N. Krasnykh, et al., Gamma camera dual imaging with a somatostatin receptor and thymidine kinase after gene transfer with a bicistronic adenovirus in mice. *Radiology* 2002; 223(2): 417.
134. Hemminki, A., K.R. Zinn, B. Liu, et al., In vivo molecular chemotherapy and noninvasive imaging with an infectivity-enhanced adenovirus. *J Natl Cancer Inst* 2002; 94(10): 741.
135. Rogers, B.E., K.R. Zinn, C.Y. Lin, et al., Targeted radiotherapy with [(90)Y]-SMT 487 in mice bearing human nonsmall cell lung tumor xenografts induced to express human somatostatin receptor subtype 2 with an adenoviral vector. *Cancer* 2002; 94(4 Suppl): 1298.
136. Payne, C.M., C.G. Bjore, Jr. and D.A. Schultz, Change in the frequency of apoptosis after low- and high-dose X-irradiation of human lymphocytes. *J Leukoc Biol* 1992; 52(4): 433.
137. Freeman, S.M., C.N. Abboud, K.A. Whartenby, et al., The "bystander effect": tumor regression when a fraction of the tumor mass is genetically modified. *Cancer Res* 1993; 53(21): 5274.
138. Buchsbaum, D.J., T.R. Chaudhuri, M. Yamamoto, et al., Gene expression imaging with radiolabeled peptides. *Ann Nucl Med* 2004; 18(4): 275.
139. ter Horst, M., S.M. Verwijnen, E. Brouwer, et al., Locoregional delivery of adenoviral vectors. *J Nucl Med* 2006; 47(9): 1483.

140. Gotthardt, M., D. Librizzi, D. Wolf, et al., Increased therapeutic efficacy through combination of Lu-177-DOTATOC and chemotherapy in neuroendocrine tumours in vivo. *Eur J Nucl Med Mol Imaging* 2006; 33(suppl 2): S115.
141. Kong, G., E. Lau, S. Ramdave, et al., High-dose In-111 octreotide therapy in combination with radiosensitizing 5-FU chemotherapy for treatment of SSR-expressing neuroendocrine tumors. *J Nucl Med* 2005; 46(suppl 2): 151P.
142. Wild, D., A. Wicki and G. Christofori, Combination therapy with [(Dys40(Ahx-[111In-DTPA)])-Exendin-4 and VEGF-receptor tyrosine kinase inhibitor PTK in a glucagon-like-peptide-1 receptor-positive transgenic mouse tumor model. *J Nucl Med* 2007; 48, suppl 2: 83P.
143. Fueger, B.J., G. Hamilton, M. Raderer, et al., Effects of chemotherapeutic agents on expression of somatostatin receptors in pancreatic tumor cells. *J Nucl Med* 2001; 42(12): 1856.
144. Schally, A.V. and A. Nagy, Cancer chemotherapy based on targeting of cytotoxic peptide conjugates to their receptors on tumors. *Eur J Endocrinol* 1999; 141(1): 1.
145. Nagy, A. and A.V. Schally, Targeting cytotoxic conjugates of somatostatin, luteinizing hormone-releasing hormone and bombesin to cancers expressing their receptors: a "smarter" chemotherapy. *Curr Pharm Des* 2005; 11(9): 1167.
146. Hofland, L.J., A. Capello, E.P. Krenning, et al., Induction of apoptosis with hybrids of Arg-Gly-Asp molecules and peptides and antimetabolic effects of hybrids of cytostatic drugs and peptides. *J Nucl Med* 2005; 46 Suppl 1: 191S.
147. Keller, G., A.V. Schally, A. Nagy, et al., Effective therapy of experimental human malignant melanomas with a targeted cytotoxic somatostatin analogue without induction of multi-drug resistance proteins. *Int J Oncol* 2006; 28(6): 1507.
148. Engel, J.B., A.V. Schally, G. Halmos, et al., Targeted therapy with a cytotoxic somatostatin analog, AN-238, inhibits growth of human experimental endometrial carcinomas expressing multidrug resistance protein MDR-1. *Cancer* 2005; 104(6): 1312.
149. Buchholz, S., G. Keller, A.V. Schally, et al., Therapy of ovarian cancers with targeted cytotoxic analogs of bombesin, somatostatin, and luteinizing hormone-releasing hormone and their combinations. *Proc Natl Acad Sci U S A* 2006; 103(27): 10403.
150. Kanashiro, C.A., A.V. Schally, A. Nagy, et al., Inhibition of experimental U-118MG glioblastoma by targeted cytotoxic analogs of bombesin and somatostatin is associated with a suppression of angiogenic and antiapoptotic mechanisms. *Int J Oncol* 2005; 27(1): 169.
151. Kiaris, H., A.V. Schally, A. Nagy, et al., Regression of U-87 MG human glioblastomas in nude mice after treatment with a cytotoxic somatostatin analog AN-238. *Clin Cancer Res* 2000; 6(2): 709.
152. Szereday, Z., A.V. Schally, A. Nagy, et al., Effective treatment of experimental U-87MG human glioblastoma in nude mice with a targeted cytotoxic bombesin analogue, AN-215. *Br J Cancer* 2002; 86(8): 1322.
153. Moody, T.W., J. Fuselier, D.H. Coy, et al., Camptothecin-somatostatin conjugates inhibit the growth of small cell lung cancer cells. *Peptides* 2005; 26(9): 1560.
154. Sun, L.C., J. Luo, L.V. Mackey, et al., A conjugate of camptothecin and a somatostatin analog against prostate cancer cell invasion via a possible signaling pathway involving PI3K/Akt, alphaVbeta3/alphaVbeta5 and MMP-2/-9. *Cancer Lett* 2007; 246(1-2): 157.
155. Moody, T.W., L.C. Sun, S.A. Mantey, et al., In vitro and in vivo antitumor effects of cytotoxic camptothecin-bombesin conjugates are mediated by specific interaction with cellular bombesin receptors. *J Pharmacol Exp Ther* 2006; 318(3): 1265.
156. Sun, L.C., J. Luo, V.L. Mackey, et al., Effects of camptothecin on tumor cell proliferation and angiogenesis when coupled to a bombesin analog used as a targeted delivery vector. *Anticancer Drugs* 2007; 18(3): 341.
157. Bernard, B., A. Capello, M. van Hagen, et al., Radiolabeled RGD-DTPA-Tyr3-octreotate for receptor-targeted radionuclide therapy. *Cancer Biother Radiopharm* 2004; 19(2): 173.

158. Capello, A., E.P. Krenning, B.F. Bernard, et al., Increased cell death after therapy with an Arg-Gly-Asp-linked somatostatin analog. *J Nucl Med* 2004; 45(10): 1716.
159. Capello, A., E.P. Krenning, B.F. Bernard, et al., Anticancer activity of targeted proapoptotic peptides. *J Nucl Med* 2006; 47(1): 122.
160. Buckley, C.D., D. Pilling, N.V. Henriquez, et al., RGD peptides induce apoptosis by direct caspase-3 activation. *Nature* 1999; 397(6719): 534.
161. Lambert, B., M. Cybulla, S.M. Weiner, et al., Renal toxicity after radionuclide therapy. *Radiat Res* 2004; 161(5): 607.
162. Kwekkeboom, D.J., J. Mueller-Brand, G. Paganelli, et al., Overview of results of peptide receptor radionuclide therapy with 3 radiolabeled somatostatin analogs. *J Nucl Med* 2005; 46 Suppl 1: 62S.
163. Valkema, R., S.A. Pauwels, L.K. Kvols, et al., Long-term follow-up of renal function after peptide receptor radiation therapy with (90)Y-DOTA(0),Tyr(3)-octreotide and (177)Lu-DOTA(0), Tyr(3)-octreotate. *J Nucl Med* 2005; 46 Suppl 1: 83S.
164. Melis, M., E.P. Krenning, B.F. Bernard, et al., Localisation and mechanism of renal retention of radiolabelled somatostatin analogues. *Eur J Nucl Med Mol Imaging* 2005; 32(10): 1136.
165. De Jong, M., R. Valkema, A. Van Gameren, et al., Inhomogeneous Localization of Radioactivity in the Human Kidney After Injection of [(111)In-DTPA]Octreotide. *J Nucl Med* 2004; 45(7): 1168.
166. de Jong, M., R. Barone, E. Krenning, et al., Megalin is essential for renal proximal tubule reabsorption of (111)In-DTPA-octreotide. *J Nucl Med* 2005; 46(10): 1696.
167. Rolleman, E.J., P.P. Kooij, W.W. de Herder, et al., Somatostatin receptor subtype 2 mediated uptake of radiolabelled somatostatin analogues in the human kidney. *Eur J Nucl Med Mol Imaging* 2007; in press.
168. Verwijnen, S.M., E.P. Krenning, R. Valkema, et al., Oral versus intravenous administration of lysine: equal effectiveness in reduction of renal uptake of [111In-DTPA]octreotide. *J Nucl Med* 2005; 46(12): 2057.
169. Bernard, B.F., E.P. Krenning, W.A. Breeman, et al., D-lysine reduction of indium-111 octreotide and yttrium-90 octreotide renal uptake. *J Nucl Med* 1997; 38(12): 1929.
170. van Eerd, J.E., E. Vegt, J.F. Wetzels, et al., Gelatin-based plasma expander effectively reduces renal uptake of 111In-octreotide in mice and rats. *J Nucl Med* 2006; 47(3): 528.
171. Vegt, E., J.F. Wetzels, F.G. Russel, et al., Renal uptake of radiolabeled octreotide in human subjects is efficiently inhibited by succinylated gelatin. *J Nucl Med* 2006; 47(3): 432.
172. Rolleman, E.J., E.P. Krenning, A. Van Gameren, et al., Uptake of [111In-DTPA0]octreotide in the rat kidney is inhibited by colchicine and not by fructose. *J Nucl Med* 2004; 45(4): 709.
173. Rolleman, E.J., F. Forrer, B. Bernard, et al., Amifostine protects rat kidneys during peptide receptor radionuclide therapy with [(177)Lu-DOTA (0),Tyr (3)]octreotate. *Eur J Nucl Med Mol Imaging* 2006.

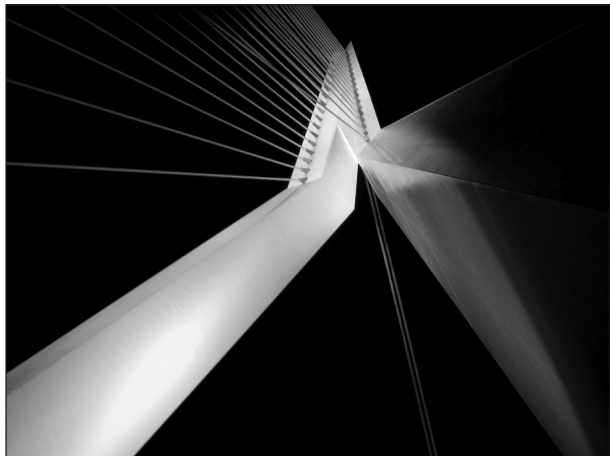
I

Neurotensin analogs for in vivo
targeting of exocrine pancreatic
cancer



2

Stabilized ^{111}In -labeled DTPA- and DOTA-conjugated neurotensin analogs for imaging and therapy of exocrine pancreatic cancer



Monique de Visser
Paul J.J.M. Janssen
Ananthachari Srinivasan
Jean-Claude Reubi
Beatrice Waser
Jack L. Erion
Michelle A. Schmidt
Eric P. Krenning
Marion de Jong

European Journal of Nuclear Medicine and Molecular Imaging
2003; Vol. 30(8): 1134-1139

ABSTRACT

Neurotensin (NT) receptors are overexpressed in exocrine pancreatic cancer and Ewing's sarcoma. The potential utility of native NT in cancer diagnosis and therapy is, however, limited by its rapid degradation *in vivo*. Therefore, NT analogs were synthesized with modified lysine and arginine derivatives to enhance stability and coupled either to DTPA, to enable high specific activity labeling with indium-111 for imaging, or to DOTA, to enable high specific activity labeling with β -emitting radionuclides, such as lutetium-177 and yttrium-90. Based on serum stability (4 h incubation at 37°C in human serum) and receptor binding affinity, the five most promising analogs were selected and further evaluated in *in vitro* internalization studies in human colorectal adenocarcinoma HT29 cells, which overexpress NT receptors. All five NT analogs bound with high affinity to NT receptors on human exocrine pancreatic tumor sections. The analogs could be labeled with ^{111}In to a high specific activity. The ^{111}In -labeled compounds were found to be very stable in serum. Incubation of HT29 cells with the ^{111}In -labeled analogs at 37°C showed rapid receptor-mediated uptake and internalization. The most promising analog, peptide 2530 [DTPA-(Pip)Gly-Pro-(PipAm)Gly-Arg-Pro-Tyr-tBuGly-Leu-OH] was further tested *in vivo* in a biodistribution study using HT29 tumor-bearing nude mice. The results of this study showed low percentages of injected dose per gram tissue of this ^{111}In -labeled 2530 analog in receptor-negative organs like blood, spleen, pancreas, liver, muscle and femur. Good uptake was found in the receptor-positive HT29 tumor and high uptake was present in the kidneys. Co-injection of excess unlabeled NT significantly reduced tumor uptake, showing that tumor uptake is a receptor-mediated process. With their enhanced stability, maintained high receptor affinity and rapid receptor-mediated internalization, the ^{111}In -labeled DTPA- and DOTA-conjugated NT analogs are excellent candidates for imaging and therapy of exocrine pancreatic cancer, peptide 2530 being the most promising analog.

INTRODUCTION

Exocrine pancreatic carcinoma is a very aggressive tumor. It grows extremely rapidly and early diagnosis, allowing complete therapeutic surgical resection, is rarely possible. There is, therefore, a significant need for new methods for the visualization and therapy of exocrine pancreatic cancer.

Neuroendocrine pancreatic tumors, like gastrinoma, can be successfully localized and treated using radiolabeled somatostatin analogs, which bind with high affinity to the ss_{t_2} somatostatin receptor [1-3]. These receptors are expressed at high density in neuroendocrine cancer. This method, however, cannot be used for the diagnosis of exocrine pancreatic cancer since this cancer does not express a sufficient level of somatostatin receptors. Therefore, to use a similar strategy, it is necessary to find receptors for other small regulatory peptides that are overexpressed in exocrine pancreatic carcinomas.

It has been previously reported that 75% of all ductal pancreatic carcinomas overexpress neurotensin (NT) receptors, and that normal pancreatic tissue, pancreatitis and endocrine pancreatic cancers do not express NT receptors [4]. NT is a 13-amino acid peptide localized in both the central nervous system and peripheral tissues, mainly the gastrointestinal tract [5, 6]. Three subtypes of NT receptors have been cloned [7]. NTR1 and NTR2 belong to the family of G-protein-coupled receptors. NTR1 has a higher affinity for NT compared with the other receptor subtypes and is of particular interest for the development of receptor-based radiopharmaceuticals [8]. Structure-activity relationships have shown that the C-terminal sequence NT(8–13) is sufficient for preservation of receptor binding [8]. Barroso et al. described the NT(8–13) binding site for NTR1 in which the N-terminal tetrapeptide of NT(8–13) fits in the third extracellular loop and the C-terminal dipeptide binds to residues at the junction between the extracellular and transmembrane domains of the receptor [8]. High-affinity NTR1 receptors are expressed in different kinds of tumors, such as Ewing's sarcomas, astrocytomas and meningiomas, but especially high levels are found in pancreatic tumors [4, 5, 9-12]. The corresponding ^{111}In -DTPA-NT(8–13) analog has been examined as a radioligand for *in vivo* detection of NT receptors. However, rapid enzymatic degradation of this derivative precluded its use as a scintigraphic agent for NT receptors. The $\text{Pro}^{10}\text{-Tyr}^{11}$ and the $\text{Arg}^8\text{-Arg}^9$ bonds in the NT sequence are easily cleaved, and it is reasonable to assume that these are the most labile sites in NT(8–13) when attacked by serum and tissue peptidases [13]. Our objective here was to design serum-stable NT analogs for imaging and therapy of exocrine pancreatic cancer. There have been several reports by other groups on technetium-99m and fluorine-18 labeled NT analogs, which have increased stability [13-18]. In this study we developed NT peptides containing either DTPA- or DOTA-

linked chelators, which allow labeling with indium-111, lutetium-177, yttrium-90, gallium-68 and cobalt-57, as well as other radionuclides. This strategy for radiolabeling provides versatile NT analogues that may be useful for visualization and/or receptor-mediated radionuclide therapy of exocrine pancreatic tumors.

In this study we describe the synthesis, receptor affinity, serum stability and in vitro internalization of new NT analogues. In addition, the most promising analogue is further evaluated in a biodistribution study using HT29 tumor-bearing nude mice.

MATERIALS AND METHODS

Synthesis

Solid phase peptide synthesis was performed using an Applied Biosystems Model 432A “Synergy” peptide synthesizer (Applied Biosystems, Foster City, Calif., USA) employing the Fmoc (9-fluorenylmethoxy-carbonyl) strategy. The instrument protocol required 25 μmol of starting resin and 75 μmol of subsequent Fmoc-protected amino acids activated by a combination of N-hydroxybenzotriazole (HOBt) and (2-(1-H benzotriazol-1-yl)-1,1,3,3-tetramethyluronium hexafluorophosphate (HBTU). Tri-*t*-butyl DTPA (75 μmol) or tri-*t*-butyl DOTA (75 μmol) [19] was placed in an “amino acid column” at the appropriate location to prepare DTPA or DOTA derivatives, respectively. The arginine and lysine derivatives employed were purchased from RSP Amino Acid Analogs (Hopkinton, Mass., USA). Cleavage and deprotection were accomplished using 85% TFA:5% thioanisole:5% phenol:5% water. The crude peptide was isolated by precipitation with *t*-butyl methyl ether (Sigma, St. Louis, Miss., USA) and purified by reverse phase high-performance liquid chromatography (HPLC) using an acetonitrile/water gradient containing 0.1% TFA. Molecular weight determination was accomplished by mass spectrometry operating in the electrospray mode (Varian, Palo Alto, California, USA).

Receptor affinity

Receptor affinity of the NT analogs was determined as described previously [4]. In short, ductal pancreatic adenocarcinoma sections were incubated for 1 h at 4°C with 40,000 dpm/100 μl monoiodo ^{125}I -[Tyr³]-NT [74 TBq/mmol (2,000 Ci), Anawa] in 50 mM Tris/HCl buffer, pH 7.6, containing 5 mM MgCl₂, 0.2% bovine serum albumin and 5 \times 10⁻⁵ M bacitracin. To generate competitive inhibition curves, the sections were incubated in the presence of increasing amounts of non-radioactive NT analogs. After incubation, the sections were washed in cold 50 mM Tris/HCl buffer, pH 7.6. The sections were then dried under a stream of cold air, apposed to 3H hyperfilms (Amersham, Little Chalfont, Bucks, UK) for exposure in X-ray film cassettes. The autoradiograms

were quantified using a computer-assisted image processing system, as described elsewhere [20].

Labeled peptides

The NT analogs were radiolabeled with ^{111}In ($^{111}\text{InCl}_3$, Tyco Healthcare, Petten, The Netherlands, DRN 4901, 370 MBq/ml in HCl, pH 1.5–1.9). The DTPA-conjugated analogs were labeled with ^{111}In to a maximum specific activity of 200 MBq/nmol as described previously [21]. The DOTA-conjugated analog was labeled with ^{111}In to a maximum specific activity of 200 MBq/nmol at 100°C for 25 min as described previously [22]. Consecutive quality control by instant thin-layer chromatography and SEP-PAK C_{18} reverse phase chromatography (Waters) was performed as described previously [23]. The radiolabeling yield and radiochemical purity were >95%.

Serum stability

The serum stability of ^{111}In -labeled NT analogs was evaluated by incubation in human serum [50% serum:50% phosphate-buffered saline (PBS)] of healthy donors at 37°C for 4 h. The percentage intact peptide after incubation was determined by separating degradation products by reverse phase HPLC using a Vydac C-18 column connected to a radiometric detector, and using a 15 min, 0–70% linear acetonitrile gradient (0.1% TFA/water).

Cell culture

The NTR1-expressing human HT29 cell line was obtained from European Collection of Cell Cultures (Salisbury, England) [24]. Cells were maintained in Dulbecco's modified Eagle's medium (Gibco, Life Technologies, Breda, The Netherlands) supplemented with 10% heat-inactivated fetal bovine serum, 2 mM glutamine, 1 mM sodium pyruvate, 0.1 mg/l fungizone and 50 IU/ml penicillin/streptomycin. Subconfluent cell cultures were transferred to six-well plates 24 h before internalization experiments.

Internalization

Studies of internalization of the ^{111}In -labeled NT analogs were performed as previously described [25]. HT29 cells were incubated in triplicate with 1 ml incubation medium (RPMI supplemented with 20 mM HEPES and 1% bovine serum albumin) containing 40–80 kBq of ^{111}In -labeled peptide (concentration as indicated) during increasing incubation times.

Cellular uptake was stopped by removing medium from the cells and washing with 2 ml of ice-cold PBS. Surface bound activity was removed by incubation with 1 ml of 20 mM sodium acetate in PBS (pH 5.0) for 10 min. Internalized and surface bound radioactivity was determined by measuring the different fractions in an LKB-1282-

compugamma system (Perkin Elmer, Oosterhout, The Netherlands) and expressed as a percentage of the applied dose per milligram cellular protein. Protein was determined using a commercially available kit (BioRad, Veenendaal, The Netherlands). To test the receptor specificity of internalization, an increasing concentration (10^{-10} M to 10^{-6} M) of unlabeled NT was added to the incubation medium to compete with the binding of radiolabeled NT analogs to the NT receptor.

Biodistribution experiments

The biodistribution experiments were done with male NMRI nude mice implanted with an average of 1 million HT29 cells. After 14–21 days the animals were injected with 2 MBq/0.1 μ g of ^{111}In -2530. The injection volume was 0.25 ml. In order to discriminate between specific (receptor-mediated) and non-specific binding, some animals were co-injected with a thousand-fold excess of unlabeled NT (100 μ g). One, 4 or 24 h after injection, animals were sacrificed and selected organs and tissues were collected for counting.

RESULTS

Peptides

Figure 1 shows the sequences of the peptides used in this study and the structure of the amino acid derivatives.

Receptor affinity

An IC_{50} value of 1.3 nM was determined for the native NT peptide for NTR1. All five NT analogs were shown to have high affinity for the receptor; the IC_{50} values varied between 3.4 nM and 5.2 nM (Table 1).

Table 1. Receptor affinity ($\text{IC}_{50} \pm \text{SEM}$; $n = 4$) of the native NT and the five NT analogs.

No	Sequence	$\text{IC}_{50} \pm \text{SEM}$ (nM)
	Neurotensin	1.3 ± 0.27
2530	DTPA-(Pip)Gly-Pro-(PipAm)Gly-Arg-Pro-Tyr-tBuGly-Leu-OH	4.4 ± 0.20
2577	DTPA-DTyr-Glu-Asn-Lys-Pro-(PipAm)Gly-Arg-Pro-Tyr-tBuGly-Leu-OH	5.2 ± 0.60
2578	DTPA-DTyr-Glu-Asn-Lys-Pro-(PipAm)Gly-Arg-Pro-Tyr-tBuGly-Cha-OH	5.2 ± 0.67
2579	DTPA-DTyr-Glu-Asn-Lys-Pro-(PipAm)Gly-Arg-Pro-Tyr-tBuGly-tBuAla-OH	4.7 ± 0.97
2656	DOTA-(Pip)Gly-Pro-(PipAm)Gly-Arg-Pro-Tyr-tBuGly-Leu-OH	3.4 ± 0.40

Serum stability

The percentage intact peptide of the ^{111}In -DTPA-NT(8–13) analog, without stabilizing amino acid derivatives, was found to be only 2% after 4 h incubation in human serum.

No	Sequence
2433	DTPA-Arg-Arg-Pro-Tyr-Ile-Leu-OH
2530	DTPA-(Pip)Gly-Pro-(PipAm)Gly-Arg-Pro-Tyr-tBuGly-Leu-OH
2577	DTyr-Glu-Asn-Lys-Pro-(PipAm)Gly-Arg-Pro-Tyr-tBuGly-Leu-OH
2578	DTPA-DTyr-Glu-Asn-Lys-Pro-(PipAm)Gly-Arg-Pro-Tyr-tBuGly-Cha-OH
2579	DTPA-DTyr-Glu-Asn-Lys-Pro-(PipAm)Gly-Arg-Pro-Tyr-tBuGly-tBuAla-OH
2656	DOTA-(Pip)Gly-Pro-(PipAm)Gly-Arg-Pro-Tyr-tBuGly-Leu-OH

tBuGly – t-butylglycine; tBuAla – t-butylalanine; Cha – cyclohexylalanine;

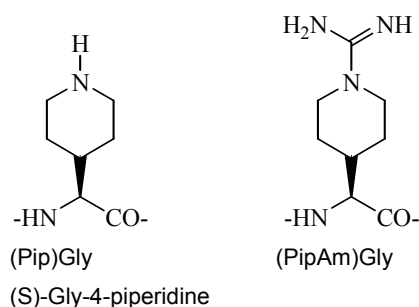


Fig. 1. Sequences of DTPA-NT(8–13) (2433) and five NT analogs.

Table 2. Serum stability of NT(8–13) and the NT analogs. Percentage intact peptide was determined after 4 h incubation in human serum at 37°C.

No	Sequence	% intact
2433	DTPA-Arg-Arg-Pro-Tyr-Ile-Leu-OH	2
2530	DTPA-(Pip)Gly-Pro-(PipAm)Gly-Arg-Pro-Tyr-tBuGly-Leu-OH	96
2577	DTPA-DTyr-Glu-Asn-Lys-Pro-(PipAm)Gly-Arg-Pro-Tyr-tBuGly-Leu-OH	95
2578	DTPA-DTyr-Glu-Asn-Lys-Pro-(PipAm)Gly-Arg-Pro-Tyr-tBuGly-Cha-OH	94
2579	DTPA-DTyr-Glu-Asn-Lys-Pro-(PipAm)Gly-Arg-Pro-Tyr-tBuGly-tBuAla-OH	98

On the other hand, the ^{111}In -labeled peptide 2530 was 96% intact, and the ^{111}In -labeled peptides 2577, 2578 and 2579 were more than 94% intact after incubation under the same conditions, as shown in Table 2.

Internalization

All of the ^{111}In -NT analogs were shown to be very rapidly internalized into HT29 cells. Figure 2A shows the time course of internalization into the cell expressed as % dose/mg cellular protein of the different NT peptides. All analogs internalized time dependently, with peptide 2530 having the highest rate of internalization. The internalization of the DOTA-linked analog, peptide 2656, was comparable to that of peptide 2530,

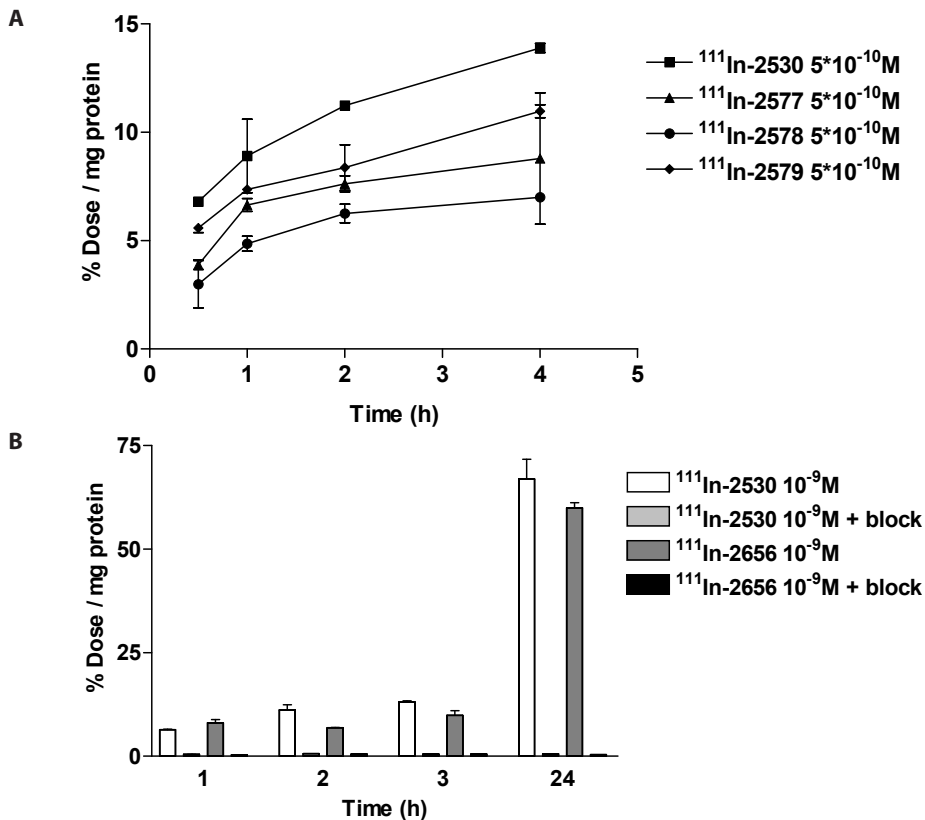


Fig. 2A,B. Time course of the internalization of $^{111}\text{In-DTPA-NT}$ (A, B) and $^{111}\text{In-DOTA-NT}$ (B) analogs into HT29 cells at 37°C . Unlabeled NT was added to the ^{111}In -labeled peptides 2530 and 2656 at a concentration of $1 \mu\text{M}$ (block) (B). Results are % of the total dose given to the cells per milligram protein at indicated incubation times. Each data point represents the mean \pm SD of three replicas.

which was about 65% of the dose per milligram protein after 24 h (Figure 2B). Addition of micromolar amounts of unlabeled NT to the incubation medium (Figure 3A) effectively competed for the binding and internalization of radiolabeled peptide into HT29 cells.

Peptide 2530 again showed the highest internalization of the four DTPA-conjugated analogs, and comparison of peptide 2530 (DTPA-coupled) with peptide 2656 (DOTA-coupled) revealed no significant difference (Figure 3B). Therefore we performed a biodistribution study in nude mice with peptide 2530.

Biodistribution

Injection of $^{111}\text{In-2530}$ in nude mice bearing HT29 tumors resulted in a relatively low uptake after 4 h in blood, spleen, pancreas, liver, muscle and femur. Average uptake was found in intestine, colon and HT29 tumor and relatively high uptake in the kidneys (Table 3).

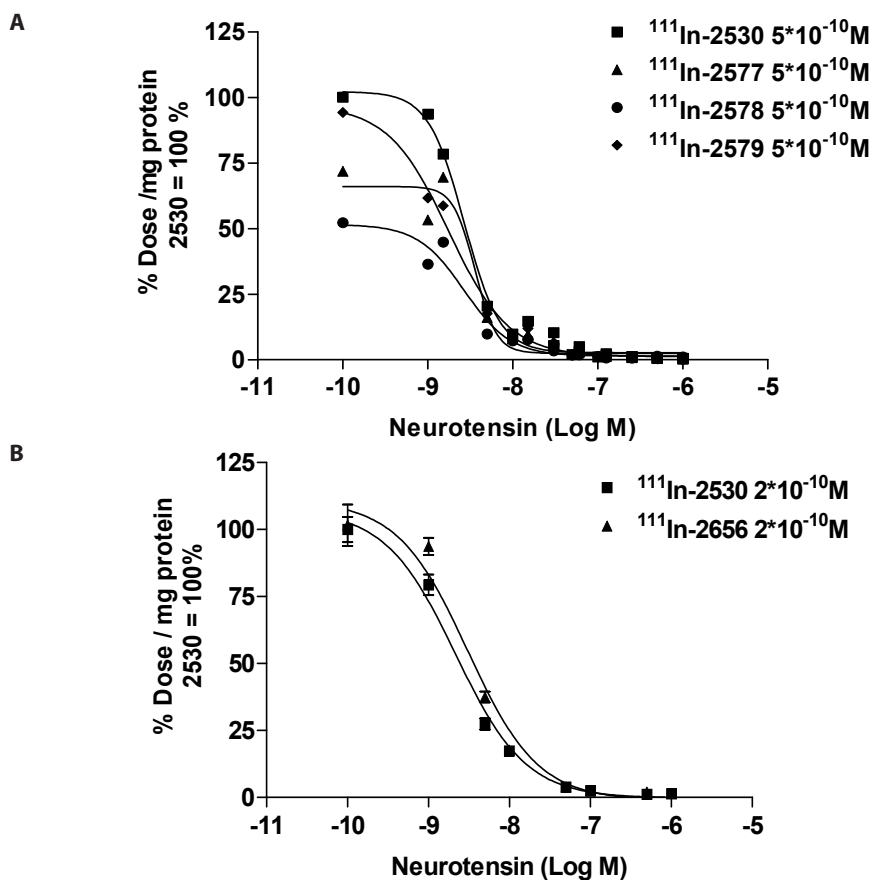


Fig. 3A,B. Internalization of $^{111}\text{In-DTPA-NT}$ (A, B) and $^{111}\text{In-DOTA-NT}$ (B) analogs in HT29 cells at 37°C in the presence of an increasing concentration of unlabeled NT. Results are % of the total dose given to the cells per milligram protein. Each data point represents the mean \pm SD of three replicas.

Twenty-four hours postinjection, the uptake (percentage of the injected dose per gram tissue) of $^{111}\text{In-2530}$ in the HT29 tumor was $0.66 (\pm 0.27)$, while 4 h postinjection the uptake was $1.10 (\pm 0.64)$, showing a slow washout from the tumor.

One, 4 and 24 h postinjection, the tumor to blood ratio (T/B) of $^{111}\text{In-2530}$ was, respectively, $11 (\pm 5)$, $51 (\pm 27)$ and $126 (\pm 44)$ (Table 4).

In order to establish whether the uptake in the HT29 tumor is receptor mediated, we performed co-injection experiments using the radiolabeled DTPA analog (MP2530) and excess unlabeled NT. If excess unlabeled NT was co-injected, the uptake of the analog in the HT29 tumor at 4 h postinjection was significantly reduced [$1.10 (\pm 0.64)$ vs. $0.22 (\pm 0.06)$ ($P=0.001$) respectively]. The uptake in the colon also was significantly reduced ($P=0.02$) when cold NT was added [$0.27 (\pm 0.10)$ vs. $0.16 (\pm 0.09)$]. Other tissues did not show significant reductions, although a tendency towards a reduction in the intestine could be observed.

Table 3. Percentage of injected dose of ^{111}In -2530 per gram tissue (%ID/g tissue \pm SD) in nude mice with HT29 xenografts, 1 h, 4 h, 4 h coinjected with 100 μg unlabeled neurotensin and 24 h postinjection. Animals received i.v. a dose of 2 MBq/0.1 μg of ^{111}In -2530.

	1 h (n=3)	4 h (n=20-23)	4 h + unlabeled NT (n=7)	24 h (n=9)
blood	0.190 \pm 0.079	0.023 \pm 0.011	0.030 \pm 0.028	0.006 \pm 0.002
spleen	0.169 \pm 0.021	0.070 \pm 0.022	0.093 \pm 0.064	0.062 \pm 0.032
pancreas	0.195 \pm 0.021	0.029 \pm 0.017	0.069 \pm 0.090	0.015 \pm 0.007
liver	0.122 \pm 0.032	0.063 \pm 0.028	0.089 \pm 0.058	0.042 \pm 0.015
muscle	0.651 \pm 0.927	0.023 \pm 0.022	0.122 \pm 0.260	0.010 \pm 0.013
femur	1.205 \pm 1.685	0.051 \pm 0.031	0.112 \pm 0.177	0.027 \pm 0.012
intestine	0.716 \pm 0.066	0.317 \pm 0.145	0.200 \pm 0.153	0.200 \pm 0.091
colon	0.350 \pm 0.046	0.267 \pm 0.096	0.165 \pm 0.088	0.233 \pm 0.345
kidneys	7.913 \pm 1.398	5.309 \pm 2.662	5.395 \pm 3.150	2.081 \pm 0.748
HT-29 tumor	1.898 \pm 0.311	1.098 \pm 0.637	0.224 \pm 0.065	0.663 \pm 0.272

Table 4. Tumor to blood ratios (\pm SD) of ^{111}In -2530 injected nude mice with HT29 xenografts, 1 h, 4 h and 24 h postinjection. Animals received i.v. a dose of 2 MBq/0.1 μg of ^{111}In -2530.

	1 h (n=3)	4 h (n=17)	24 h (n=9)
tumor / blood	11.1 \pm 4.9	51.7 \pm 26.6	126.0 \pm 43.9

DISCUSSION

New NT derivatives were designed and synthesized in order to develop peptides with increased metabolic stability [13]. The peptides were synthesized by replacing naturally occurring amino acids with more stable amino acid derivatives. In this work we focused on the five most promising analogs based on their receptor affinity and *in vitro* serum stability. The sequences of the five peptides all contain the C-terminal hexapeptide NT(8–13), which is crucial for preserving receptor binding, with stabilized amino acid derivatives at positions 8 and 12.

Replacing amino acids by derivatives in the NT analogs did not compromise the receptor affinity. All analogs exhibited high *in vitro* binding affinity in the low nanomolar range to NTR1 expressed on human HT29 tumors. The IC_{50} value of peptide 2530 was 3.9 nM, whereas the IC_{50} of the original NT, which was used as a competitive inhibitor, was 1.3 nM (Table 1).

All changes in the peptide chain had a beneficial influence on stability in human serum. DTPA-linked NT(8–13) was almost entirely metabolized in human serum; only 2% peptide was intact after 4 h incubation at 37°C. The stability of peptide 2530 was increased up to 96% intact peptide after incubation. The other analogs were found to be nearly as stable as peptide 2530 (Table 2).

To be useful for scintigraphic and radionuclide therapy, radiopeptides must be internalized into tumor cells, where the radionuclide will be retained and, in the

case of radionuclide therapy, cause more lethal damage to the tumor cells. The new stabilized NT analogs reported here, internalized rapidly into NTR1-expressing HT29 cells. Incubation of the new peptides at 37°C produced a time-dependent accumulation in cells. Peptide 2530 was the most active peptide, with 14% accumulation in cells after 4 h and 65% in cells after 24 h (Figure 2). The internalization of all five analogs could be blocked with an increasing concentration of unlabeled NT in the incubation medium, which demonstrates the receptor specificity of the internalization. The uptake of the radiolabeled NT analog 2530 *in vivo* was determined in nude mice bearing human HT29 xenografts. The involvement of the NT receptor in the tumor uptake was shown by our experiments with excess unlabeled NT co-injected. In accordance with the internalization studies, we found the uptake in the HT29 tumor to be receptor mediated. We also found a receptor-mediated uptake in the normal mice colon (Table 3).

The uptake of our analog in the kidneys is comparable to the results found with other NT analogs [13, 16, 17]. As expected, the accumulation found in the kidney was relatively high. NT analogs were conjugated to the metal chelator DTPA in order to allow labeling with ^{111}In for scintigraphy. Peptide 2656 is linked with DOTA, which is capable of forming stable chelates with metals such as ^{111}In , ^{177}Lu , ^{67}Ga , ^{68}Ga , ^{86}Y , ^{90}Y , ^{64}Cu and ^{57}Co and can therefore be used for not only scintigraphy but also radionuclide therapy. In this study, conjugation of a DTPA (peptide 2530) or a DOTA (peptide 2656) chelating molecule to a stabilized NT analog had essentially no effect on receptor affinity or internalization into cells.

In conclusion, the five most promising NT analogs were identified based on their high receptor affinity, enhanced serum stability and high level of receptor-mediated internalization into NTR1-overexpressing HT29 tumor cells *in vitro*. In addition, peptide 2530 showed receptor-mediated tumor uptake *in vivo* in mice bearing HT29 tumors.

This DTPA-conjugated NT analog can be labeled with ^{111}In and is therefore an excellent candidate for scintigraphic imaging of tumors overexpressing NT receptors, such as exocrine pancreatic adenocarcinomas. The DOTA-conjugated compound, peptide 2656, has the ability to form stable complexes with β -particle emitters, such as ^{177}Lu and ^{90}Y , and is therefore a candidate for peptide-receptor radionuclide therapy of these tumors.

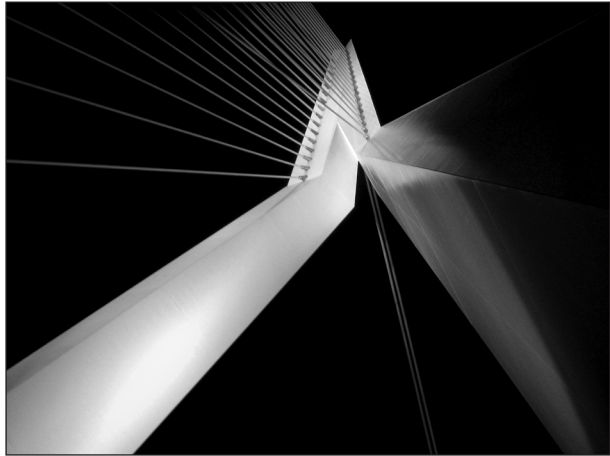
REFERENCES

1. de Jong, M., W.A. Breeman, B.F. Bernard, et al., [177Lu-DOTA(0),Tyr3] octreotate for somatostatin receptor-targeted radionuclide therapy. *Int J Cancer* 2001; 92(5): 628.
2. de Jong, M., W.A. Breeman, B.F. Bernard, et al., Tumor response after [(90)Y-DOTA(0),Tyr(3)] octreotide radionuclide therapy in a transplantable rat tumor model is dependent on tumor size. *J Nucl Med* 2001; 42(12): 1841.
3. De Jong, M., R. Valkema, F. Jamar, et al., Somatostatin receptor-targeted radionuclide therapy of tumors: preclinical and clinical findings. *Semin Nucl Med* 2002; 32(2): 133.
4. Reubi, J.C., B. Waser, H. Friess, et al., Neurotensin receptors: a new marker for human ductal pancreatic adenocarcinoma. *Gut* 1998; 42(4): 546.
5. Ehlers, R.A., S. Kim, Y. Zhang, et al., Gut peptide receptor expression in human pancreatic cancers. *Ann Surg* 2000; 231(6): 838.
6. Kuhar, M.J., Imaging receptors for drugs in neural tissue. *Neuropharmacology* 1987; 26(7B): 911.
7. Vincent, J.P., J. Mazella and P. Kitabgi, Neurotensin and neurotensin receptors. *Trends Pharmacol Sci* 1999; 20(7): 302.
8. Barroso, S., F. Richard, D. Nicolas-Etheve, et al., Identification of residues involved in neurotensin binding and modeling of the agonist binding site in neurotensin receptor 1. *J Biol Chem* 2000; 275(1): 328.
9. Wang, L., H. Friess, Z. Zhu, et al., Neurotensin receptor-1 mRNA analysis in normal pancreas and pancreatic disease. *Clin Cancer Res* 2000; 6(2): 566.
10. Reubi, J.C., B. Waser, A. Schmassmann, et al., Receptor autoradiographic evaluation of cholecystokinin, neurotensin, somatostatin and vasoactive intestinal peptide receptors in gastrointestinal adenocarcinoma samples: where are they really located? *Int J Cancer* 1999; 81(3): 376.
11. Reubi, J.C., S. Wenger, J. Schmuckli-Maurer, et al., Bombesin receptor subtypes in human cancers: detection with the universal radioligand (125)I-[D-TYR(6), beta-ALA(11), PHE(13), NLE(14)] bombesin(6-14). *Clin Cancer Res* 2002; 8(4): 1139.
12. Reubi, J.C., A. Zimmermann, S. Jonas, et al., Regulatory peptide receptors in human hepatocellular carcinomas. *Gut* 1999; 45(5): 766.
13. Bergmann, R., M. Scheunemann, C. Heichert, et al., Biodistribution and catabolism of (18) F-labeled neurotensin(8-13) analogs. *Nucl Med Biol* 2002; 29(1): 61.
14. Bruehlmeier, M., E.G. Garayoa, A. Blanc, et al., Stabilization of neurotensin analogues: effect on peptide catabolism, biodistribution and tumor binding. *Nucl Med Biol* 2002; 29(3): 321.
15. Egli, A., R. Alberto, L. Tannahill, et al., Organometallic 99mTc-aquaion labels peptide to an unprecedented high specific activity. *J Nucl Med* 1999; 40(11): 1913.
16. Garcia-Garayoa, E., L. Allemann-Tannahill, P. Blauenstein, et al., In vitro and in vivo evaluation of new radiolabeled neurotensin(8-13) analogues with high affinity for NT1 receptors. *Nucl Med Biol* 2001; 28(1): 75.
17. Garcia-Garayoa, E., P. Blauenstein, M. Bruehlmeier, et al., Preclinical evaluation of a new, stabilized neurotensin(8-13) pseudopeptide radiolabeled with (99m)Tc. *J Nucl Med* 2002; 43(3): 374.
18. Schubiger, P.A., L. Allemann-Tannahill, A. Egli, et al., Catabolism of neurotensins. Implications for the design of radiolabeling strategies of peptides. *Q J Nucl Med* 1999; 43(2): 155.
19. Srinivasan, A. and M. Schmidt, Tri-t-butyl DTPA: a versatile synthon for the incorporation of DTPA by solid phase. *American Peptide Symposium* 1997: P 110.
20. Reubi, J.C., L.K. Kvols, B. Waser, et al., Detection of somatostatin receptors in surgical and percutaneous needle biopsy samples of carcinoids and islet cell carcinomas. *Cancer Res* 1990; 50(18): 5969.

21. Bakker, W.H., R. Albert, C. Bruns, et al., [111In-DTPA-D-Phe1]-octreotide, a potential radiopharmaceutical for imaging of somatostatin receptor-positive tumors: synthesis, radiolabeling and in vitro validation. *Life Sci* 1991; 49(22): 1583.
22. de Jong, M., W.A. Breeman, W.H. Bakker, et al., Comparison of (111)In-labeled somatostatin analogues for tumor scintigraphy and radionuclide therapy. *Cancer Res* 1998; 58(3): 437.
23. Bakker, W.H., E.P. Krenning, J.C. Reubi, et al., In vivo application of [111In-DTPA-D-Phe1]-octreotide for detection of somatostatin receptor-positive tumors in rats. *Life Sci* 1991; 49(22): 1593.
24. Maoret, J.J., Y. Anini, C. Rouyer-Fessard, et al., Neurotensin and a non-peptide neurotensin receptor antagonist control human colon cancer cell growth in cell culture and in cells xenografted into nude mice. *Int J Cancer* 1999; 80(3): 448.
25. De Jong, M., B.F. Bernard, E. De Bruin, et al., Internalization of radiolabelled [DTPA0]octreotide and [DOTA0,Tyr3]octreotide: peptides for somatostatin receptor-targeted scintigraphy and radionuclide therapy. *Nucl Med Commun* 1998; 19(3): 283.

3

Five stabilized ^{111}In -labeled neurotensin analogs in nude mice bearing HT29 tumors



Paul J.J.M. Janssen*
Monique de Visser*
Suzanne M. Verwijnen
Bert F. Bernard
Ananthachari Srinivasan
Jack L. Erion
Wouter A.P. Breeman
Arnold G. Vulto
Eric P. Krenning
Marion de Jong

*Both authors contributed equally to this manuscript.

Cancer Biotherapy & Radiopharmaceuticals 2007; Vol.
22(3):374-381

ABSTRACT

Neurotensin (NT) receptors are overexpressed in different human tumors, such as human ductal pancreatic adenocarcinoma. New stable neurotensin analogs with high receptor affinity have been synthesized by replacing arginine residues with lysine and arginine derivatives. The aim of this study was to explore the biodistribution, tumor uptake, kidney localization, and stability characteristics of these new analogs in order to develop new diagnostic tools for exocrine pancreatic cancer. Four ^{111}In -labeled DTPA-chelated NT analogs and one ^{111}In -labeled DOTA-chelated NT analog were evaluated in NMRI nude mice bearing NT receptor-positive HT29 tumors. Experiments with a coinjection of unlabeled NT or lysine were performed to investigate receptor-mediated uptake and kidney protection, respectively. In addition, the *in vivo* serum stability of the most promising analog was analyzed. In the biodistribution study in mice, at 4 hours postinjection, a low percentage of the injected dose per gram (%ID/g) of tissue for all compounds was found in NT receptor-negative organs, such as the blood, spleen, pancreas, liver, muscle, and femur. A high uptake was found in the colon, intestine, kidneys, and in implanted HT29 tumors. The coinjection of excess unlabeled neurotensin significantly reduced tumor uptake, showing tumor uptake to be receptor-mediated. To a lesser extent, this was also observed for the colon, but not for other tissues. We concluded that DTPA-(Pip)Gly-Pro-(PipAm)Gly-Arg-Pro-Tyr-tBuGly-Leu-OH and the DOTA-linked counterpart have the most favorable biodistribution properties regarding tumor uptake.

INTRODUCTION

Exocrine adenocarcinoma of the pancreas is a major cause of death from cancer in western countries. Because of difficulties in diagnosis, the aggressiveness of pancreatic tumors, and the lack of effective systemic treatment, generally less than 5% of patients with adenocarcinoma of the pancreas survive 5 years after diagnosis [1, 2]. So there is a clear demand for new diagnostics, preferably enabling for the discrimination between pancreas carcinoma and pancreatitis.

A variety of neuropeptide receptors is overexpressed on tumors, and the use of radiolabeled peptides to detect malignancies at an early stage has been proven to be very attractive. One example is the possibility of the early detection of endocrine pancreatic tumors by the specific binding of [¹¹¹In-DTPA]octreotide (OctreoScan®) to somatostatin receptors, which are overexpressed in high density in this type of tumor [3]. Unfortunately, these receptors are not overexpressed in the exocrine pancreatic adenocarcinomas.

In 1980, Gutniak et al. [4] described a patient with watery diarrhea caused by a pancreatic tumor. This tumor contained many cells with an immunoreactivity to enkephalin and neurotensin (NT), whereas for calcitonin and vasoactive intestinal peptide (VIP), the immunoreactivity was low to absent. It was the first report on the presence of NT receptors in a pancreatic tumor. Ehlers et al. [5] showed that NT receptors are expressed in 88% of surgical specimens of exocrine pancreatic tumor. The expression of VIP, substance P, and gastrin-releasing peptide (GRP) receptors are substantially lower. Reubi et al. showed that NT receptors are overexpressed in different human tumors, such as human ductal pancreatic adenocarcinoma (75%) [6], Ewing's sarcoma (65%), meningioma (52%), astrocytoma (43%), medulloblastoma (38%), medullary thyroid carcinoma (29%), and small-cell lung cancer (25%) [7]. Of great clinical importance is the fact that neurotensin receptors are overexpressed in ductal pancreatic adenocarcinoma, whereas in normal pancreas and chronic pancreatitis, these receptors are absent, thus enabling for the discrimination between malignant and nonmalignant tissue. Buchegger et al. [8] delivered proof of this concept when in 1 of 4 patients the tumor could be visualized by tomoscintigraphy following an injection of a radiolabeled NT analog.

NT is a tridecapeptide in humans, localized in endocrine cells of the distal gut. After binding to its different receptors (NTS1, NTS2, and NTS3), this peptide exerts several actions in the gastrointestinal tract and brain. The stimulation of the NTS1 receptor improves pancreatic and biliary secretion, colonic motility and the growth of normal intestinal mucosa and pancreas [9]. *In vivo* and *in vitro* NT stimulates the growth of human colon cancer cell lines. In addition, the growth of pancreatic cancer cells was shown to be stimulated by NT through its receptor [10, 11].

The native neurotensin is very unstable in plasma. Several endogenous peptidases and proteases cause the rapid degradation of this neuropeptide [12]. The instability of native neurotensin, prompted several groups [13-18] and us to synthesize NT analogs that were less susceptible to degradation, while maintaining the binding affinity to the NT receptors. The results of the binding and internalization studies demonstrate that subtle changes, by introducing non-natural amino acids on specific positions, can be made in the C-terminal part of the peptide, which is the crucial part for binding and biologic activity, without markedly affecting the binding properties. The effect of amino acid substitutions on the biologic activity cannot be predicted, although a high correlation between binding and biologic potencies of the NT analogs has been described [15].

We presented five new NT analogs with positive receptor affinity and internalization characteristics in a NT receptor-positive cell line [19]. In this paper, we expand these studies to *in vivo* experiments to explore the tumor-binding characteristics, clearance, *in vivo* degradation, and a possible reduction of high kidney uptake of these analogs.

MATERIALS AND METHODS

Peptides

NT analogs were synthesized by Tyco Healthcare, Inc. (St. Louis, MO, USA), as described earlier [19]. Nonnatural amino acids were used in this procedure to augment the stability of these compounds in plasma, compared to the native neurotensin. The following non-natural amino acids were used: S-Gly-4-piperidine ([Pip]Gly), (S)-Gly-4-piperidine[N-amidino] ([PipAm]Gly), t-butylglycine (tBuGly), t-butylalanine (tBuAla), and cyclohexylalanine (Cha). These compounds are derivatives of lysine, arginine, glycine, and alanine, respectively. The affinity for NT receptors was tested and resulted in the selection of five promising NT analogs with a comparable IC_{50} to the native neurotensin (IC_{50} : 1.3 ± 0.27 nM [19]). The following analogs were used in the *in vivo* experiments (with their corresponding IC_{50} values [nM] [19]):

1. DTPA-(Pip)Gly-Pro-(PipAm)Gly-Arg-Pro-Tyr-tBuGly-Leu-OH ;(MP2530, IC_{50} : 4.4 ± 0.20);
2. DTPA-Dtyr-Glu-Asn-Lys-Pro-(PipAm)Gly-Arg-Pro-Tyr-tBuGly-Leu-OH (MP2577, IC_{50} : 5.2 ± 0.60);
3. DTPA-Dtyr-Glu-Asn-Lys-Pro-(PipAm)Gly-Arg-Pro-Tyr-tBuGly-Cha-OH (MP2578, IC_{50} : 5.2 ± 0.67);
4. DTPA-Dtyr-Glu-Asn-Lys-Pro-(PipAm)Gly-Arg-Pro-Tyr-tBuGly-tBuAla-OH (MP2579, IC_{50} : 4.7 ± 0.97);
5. DOTA-(Pip)Gly-Pro-(PipAm)Gly-Arg-Pro-Tyr-tBuGly-Leu-OH (MP2656, IC_{50} : 3.4 ± 0.40).

Radiolabeling NT-analogs and quality control

Radiolabeling with $^{111}\text{InCl}_3$ (Tyco Healthcare; Petten, The Netherlands) of the NT analogs and subsequent quality control was performed, as described earlier [20]. The labeling of the DOTA compound was performed at 100°C during 30 minutes. The incorporation of ^{111}In always exceeded 95%. The incorporation of ^{111}In and radiochemical purity of the NT analogs were analyzed by a combination of instant thin-layer chromatography (ITLC) and high-performance liquid chromatography (HPLC). ITLC was performed with ITLC-silica gel (SG) and 0.1 M of Na-citrate at a pH of 5 as eluents. An aliquot of the reaction mixture was placed on the lower part of the ITLCSG strip and developed up to 10 cm from the origin. Peptide-bound ^{111}In stays at the origin ($R_f = 0.0\text{--}0.3$), whereas free $^{111}\text{In}^{3+}$ migrates with the solvents front ($R_f = 1$). ITLC strips were cut in two sections: a lower part (= origin + 4 cm) and an upper part, containing the nonincorporated ^{111}In . Radioactivity of both parts was quantified in a dose calibrator. (Veenstra VDC-202; Veenstra, Joure, The Netherlands).

The incorporation of ^{111}In in MP2656 was also performed by ITLC, as described above, in the presence of DTPA: after cooling the reaction vial ambient temperature, 10 μL of 4 mM DTPA was added. This addition was crucial to avoid false positive quality control results, owing to colloid formation [21, 22]. In addition, in the presence of DTPA, the nonincorporated radionuclide would be rapidly transformed to ^{111}In -DTPA before an intravenous (i.v.) administration and excreted through the kidneys, as described earlier, for ^{90}Y or ^{177}Lu -radiolabeled analogs [20, 23].

A chromatographic analysis of radiolabeled analogs was performed on a Waters Breeze HPLC system (Waters; Etten-Leur, The Netherlands), based on a 1525 binary HPLC pump that was also connected to a Unispec MCA γ -detector (Canberra; Zellik, Belgium). A Symmetry C_{18} 4.6 • 250 mm 5 μm HPLC column (Waters; Etten-Leur, The Netherlands) was used as the stationary phase, whereas the eluent system consisted of 0.1% TFA in H_2O (solvent A) and methanol (solvent B), applying the following gradient protocol: 0–2 minutes 100% A (flow rate, 1 mL/minute), 2–3 minutes of 55% B, 3–30 minutes of 65% B (flow rate, 0.5 mL/minute), 30–38 minutes of 100% B (flow rate, 1 mL/minute), 38–40 minutes of 100% B flow rate, 1 mL/minute), and 40–46 minutes of 100% A (flow rate, 1 mL/minute).

Biodistribution experiments

The experiments were performed with male NMRI nude mice that were implanted with an average of 1 million HT29 cells. These cells express NTR1 receptors and were obtained from the European Collection of Cell Culture (Salisbury, England). After 14–21 days, the animals were injected with 2 MBq/0.1 μg of [^{111}In -DTPA] NT (MP2530, MP2577, MP2578, or MP2579) or the [^{111}In -DOTA] NT (MP2656) analog. The injection volume was 0.25 mL. To discriminate between specific (receptor-mediated)

and nonspecific binding, some animals ($n = 4$) were coinjected with a 1000-fold excess of unlabeled NT (100 μg). Four (4) ($n = 8$) and 24 ($n = 8$) hours following the injection, the animals were sacrificed and selected organs and tissues were collected for counting.

To study the kidney-protective properties of lysine, we coinjected D-lysine (400 mg/kg) with the different analogs in nude mice ($n = 4$). We performed an *ex vivo* autoradiography on the kidney samples in order to determine the location of the radioactivity in this organ. The samples were taken 4 hours postinjection of labeled MP2530. Radioactivity was measured during 24 hours, using the Cyclone System (Packard Bioscience Company; Groningen, The Netherlands).

In vivo stability in plasma

A HPLC system from Waters, Inc. (Milford, MA, USA) was used, with a C_{18} column (5 μm , 4.6 mm in diameter, 250 mm in length). Solvent A was acetonitril with 0.1% trifluoroacetic acid (Merck, Gernsheim, Germany), and solvent B was 0.1% trifluoroacetic acid (Merck) in MilliQ water. A gradient with solvent A and B was run as follows: 5% A/95% B to 70% A/30% B in 20 minutes; thereafter, the HPLC run was isocratic 70% A/30% B during 5 minutes. Two thousand (2000) μL of 96% ethanol was added to 1000 μL plasma of mice, who were sacrificed 10 ($n = 3$) or 30 ($n = 3$) minutes following an injection of 2 MBq [^{111}In -DTPA] NT (MP2530). Two (2) minutes after an addition of the ethanol, the sample was centrifuged and the supernatant was filtered through a 0.22- μm filter. To 200 μL of filtered supernatant 1800 μL of phosphate-buffered saline (PBS) with 5% ethanol was added. This fluid was injected into the HPLC and 91 aliquots (0–23.92 minutes) were collected. One aliquot was 0.2615 mL and after collection, the activity was counted. The standard addition method was carried out by adding four times the measured activity of [^{111}In -DTPA] NT to the plasma sample.

Statistical analysis

Data were expressed as the mean \pm standard deviation. A statistical analysis was performed using the analysis of variance (ANOVA), Fisher LSD, and the Student's (two sample) *t* test, using the program SPSS (version 10.1 for Windows, Chicago, IL, USA). A probability of less than 0.05 was considered significant.

RESULTS

Biodistribution

The percentage of the injected dose per gram (%ID/g) tissue 4 hours after injection varies between 0.04 (\pm 0.03) in the blood and 7.05 (\pm 2.28) in the kidneys. Tissues with a relative low radioactivity uptake after 4 hours are the blood, the spleen, the pancreas, the liver, muscle, and femur. Average uptake is found in the intestine, colon, and HT29 tumor and relatively high uptake in the kidneys (Table 1). This differentiation in uptake is observed for all ¹¹¹In-labeled analogs. The MP2530 radiolabeled compound shows significantly ($p = 0.019$) higher uptake in the HT29 tumor, compared to the other DTPA-chelated analogs. The difference in uptake in the tumor, 4 hours postinjection, between the DTPA analog with the highest tumor uptake (MP2530) and the DOTA compound (MP2656) was in favor of the latter ($p = 0.011$). Twenty-four (24) hours postinjection, the uptake in the HT29 tumor of [¹¹¹In-DTPA] NT (MP2530) was 0.66 (\pm 0.27), whereas at 4 hours postinjection, the uptake was 1.04 (\pm 0.56), showing a slow washout from the tumor.

Four (4) and 24 hours postinjection the tumor-to-blood ratio of the MP2530 compound was respectively: 51 (\pm 27) and 126 (\pm 44). At these time points, the DOTA analog showed better tumor-to-blood ratios of 179 (\pm 123) and 452 (\pm 238), whereas the tumor-to-blood ratio of the analogs MP2577, MP2578, and MP2579 4 hours postinjection were, respectively, 18 (\pm 15), 17 (\pm 12), and 28 (\pm 24). To establish whether the uptake in the HT29 tumor was receptor-mediated, we performed

Table 1. Biodistribution ¹¹¹In-Labeled NT Analogs in HT-29 Bearing Nude Mice.

	MP2530		MP2577	MP2578	MP2579	MP2656	
	4 hours	24 hours	4 hours	4 hours	4 hours	4 hours	24 hours
Blood	0.023 \pm 0.011	0.006 \pm 0.002	0.036 \pm 0.041	0.064 \pm 0.062	0.036 \pm 0.029	0.013 \pm 0.009	0.004 \pm 0.003
Spleen	0.070 \pm 0.022	0.062 \pm 0.032	0.042 \pm 0.031	0.100 \pm 0.072	0.087 \pm 0.038	0.109 \pm 0.027	0.104 \pm 0.040
Pancreas	0.029 \pm 0.017	0.015 \pm 0.007	0.026 \pm 0.027	0.039 \pm 0.033	0.035 \pm 0.022	0.038 \pm 0.015	0.031 \pm 0.023
Liver	0.063 \pm 0.028	0.042 \pm 0.015	0.066 \pm 0.074	0.070 \pm 0.042	0.058 \pm 0.029	0.089 \pm 0.021	0.079 \pm 0.030
Muscle	0.023 \pm 0.022	0.010 \pm 0.013	0.013 \pm 0.017	0.022 \pm 0.024	0.022 \pm 0.013	0.022 \pm 0.017	0.006 \pm 0.003
Femur	0.051 \pm 0.031	0.027 \pm 0.012	0.047 \pm 0.055	0.086 \pm 0.065	0.050 \pm 0.028	0.089 \pm 0.051	0.060 \pm 0.023
Intestine	0.32 \pm 0.15	0.20 \pm 0.09	0.14 \pm 0.07	0.24 \pm 0.13	0.39 \pm 0.15	0.56 \pm 0.21	0.31 \pm 0.08
Colon	0.27 \pm 0.10	0.23 \pm 0.34	0.09 \pm 0.06	0.24 \pm 0.16	0.26 \pm 0.12	0.32 \pm 0.14	0.31 \pm 0.18
HT29 tumor	1.10 \pm 0.64	0.66 \pm 0.27	0.50 \pm 0.31	0.58 \pm 0.46	0.66 \pm 0.18	1.59 \pm 0.60	1.37 \pm 0.27
Kidneys	5.31 \pm 2.66	2.08 \pm 0.75	4.16 \pm 2.27	6.09 \pm 4.82	6.29 \pm 2.08	7.05 \pm 2.28	3.77 \pm 1.75

Note; Figures reflect the percentage of injected dose of ¹¹¹In-labeled-NT analogs per gram of tissue (%ID/g tissue \pm standard deviation) in nude mice with HT29 xenografts at 4 and 24 hours postinjection ($n = 8$). All animals received an intravenous dose of 2 MBq/0.1 μ g of the corresponding peptide. (See the Results section for significant differences.)

NT, neurotensin.

Table 2. Kidney Uptake of Different ^{111}In -Labeled Analogs.

Analog	%ID/g tissue (without D-Lysine)	%ID/g tissue (with D-Lysine)
MP2530	2.84 ± 1.04	2.85 ± 0.92
MP2577	2.68 ± 1.62	1.45 ± 0.86
MP2578	2.93 ± 0.75	2.04 ± 0.93
MP2579	4.31 ± 1.66	1.94 ± 0.74
MP2656	4.29 ± 2.25	4.24 ± 1.09

Note; Figures represent the reduction in kidney uptake by coinjection of D-lysine (400 mg/kg). Values are the percent injected dose per gram (%ID/g) of tissue \pm the standard deviation. All animals received an intravenous dose of 2 MBq/0.1 μg of ^{111}In -labeled analogs with or without D-lysine ($n = 4$).

coinjection experiments, using the radiolabeled DTPA analog (MP2530) or the radiolabeled DOTA analog (MP2656) and excess unlabeled NT. If excess unlabeled NT was coinjected, the uptake 4 hours postinjection in the HT29 tumor of the DTPA and the DOTA analog was significantly reduced by $1.10 (\pm 0.56)$ versus $0.22 (\pm 0.06)$ ($p = 0.001$) and $1.59 (\pm 0.60)$ versus $0.58 (\pm 0.40)$, respectively. The uptake in the colon also was significantly reduced ($p = 0.02$) when unlabeled NT was added $0.27 (\pm 0.10)$ versus $0.16 (\pm 0.09)$. Other tissues did not show significant reductions, although a tendency in reduction in the intestine could be observed.



Figure 1. *Ex vivo* autoradiogram of 3 sections of 2 different kidneys (4 hours postinjection of labeled MP2530). Sections from top to bottom: the cortex to the medulla of the kidney. The uptake is predominantly present in the cortex of the organ.

Effects of D-Lysine

The effect of coinjection of D-lysine, together with the labeled analogs on the kidney uptake, is shown in table 2. The uptake in the kidney of the labeled analogs, MP2530 and MP2656, was not reduced, whereas the uptake of the labeled MP2577, MP2578, and MP2579 analogs was reduced by an average of 40%. As shown in figure 1, the radioactivity was predominantly present in the cortex of the kidney.

In vivo stability in plasma

Three typical HPLC runs of the [^{111}In -DTPA] NT (MP2530) analog in plasma are shown in figure 2. Ten (10) minutes after the injection of the labeled analog, $40.4\% \pm 3.8\%$ of the injected activity was found at the same retention time as the intact [^{111}In -DTPA] NT (see standard addition curve). The amount of intact [^{111}In -DTPA] NT 30 minutes after injection was only $10.5\% \pm 3.1\%$, showing a rapid decline in circulating intact radiolabeled NT.

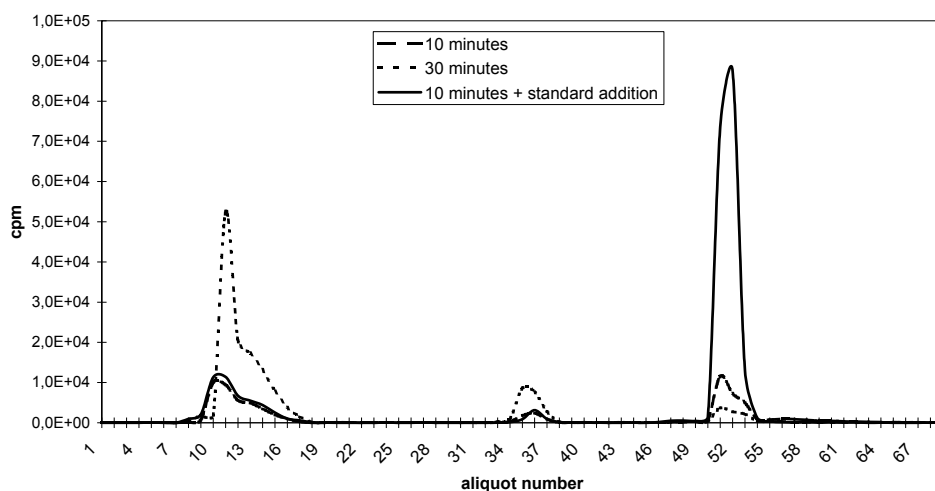


Figure 2. Metabolic stability of [^{111}In]-NT (MP2530) following an injection in nude mice. The samples taken were 10 and 30 minutes following an injection of $2 \text{ MBq}/0.1 \mu\text{g}$ of the labeled analog. The intact peptide is eluted in aliquot 52-56, as shown by the standard addition.

DISCUSSION

We synthesized five promising NT analogs, coupled to the conjugating groups, DTPA or DOTA. We included non-natural amino acids to enhance serum stability. An ideal compound would have augmented plasma stability, compared to the native NT, whereas the affinity for NT receptors would not be compromised. We tested four DTPA-NT analogs and one DOTA-NT analog *in vitro* that met these properties the

best [19]. The amino acids at positions 9, 10, and 11 (of the native NT) of the used analogs were not changed, compared to the native NT (Arg⁹-Pro¹⁰-Tyr¹¹), as this sequence was thought to be essential for receptor-binding. The bond between Pro¹⁰ and Tyr¹¹ in these analogs was thus as susceptible for neutral endopeptidase and metalloendopeptidase as the native NT. The amino acid at position 8 in the native NT was changed in all used analogs into (PipAm)Gly, with the aim of making the bond between position 8 and 9 (Arg-Arg of the native NT) less prone degradation by a metalloendopeptidase. The amino acid on position 12 was altered into tBuGly, with the aim of making it more difficult to cleave the bond between amino acids 11 and 12 by neutral endopeptidase and angiotensin converting enzyme. *In vitro*, all analogs were found to be very stable in serum. After 4 hours of incubation at 37°C in human serum, at least 94% of the analogs were intact, whereas only 2% of the native DTPA-NT(8–13) remained intact after 4 hours [19]. However, at 10 and 30 minutes after an injection of 2 MBq/0.1 µg labeled MP2530 in nude mice, respectively, 40.4% and 10.5% of intact, radiolabeled neuropeptide was recovered. These findings were in accordance with the first studies in humans (unpublished results), which also showed a rapid decline of intact MP2530 after injection. This dramatic difference between the plasma half-life determined in *in vitro* experiments and the observed plasma half-life in patients was also reported by Buchegger et al. [8]. They found a plasma half-life of 21 days *in vitro*, whereas the half-life in patients ranged between 17 and 62 minutes. The discrepancy between the *in vitro* and *in vivo* results on the stability of the compound might be explained by the lack of excretion in *in vitro* experiments and the absence or inactivity of proteolytic enzymes in plasma *in vitro*. Kitabgi et al. [12] described the possible mechanism of proteolytic inactivation by peptidases, which were bound to the membrane located near the peptide receptor. Garcia-Garayoa et al. [13] also found marked differences in the stability of their compounds in whole blood versus plasma in their *in vitro* metabolic stability experiments. In the latter solution, the analogs were more stable. *In vivo*, the presence and effectiveness of the degrading enzymes was certainly higher, thus explaining the differences in stability of the analogs found in the *in vitro* and *in vivo* experiments.

The uptake in 10 different tissues of the five radiolabeled NT analogs was determined in nude mice bearing human HT-29 xenografts. The uptake in the harvested organs at 4 hours postinjection did not show any significant differences between the investigated analogs, with the exception of the HT29 tumor. The uptake in the tumor of the radiolabeled DTPA analog (MP2530) and of the labeled DOTA analog (MP2656) was significantly better than the uptake of the other analogs investigated in this study. Also, in *in vitro* internalization experiments, the MP2530 compound showed the best results [19]. The involvement of the NT receptor in the tumor uptake was shown by our experiments with excess unlabeled NT that was coinjected. In

accordance with the internalization studies, we found the uptake in the HT29 tumor to be receptor-mediated. We also found a receptor-mediated uptake in the normal mice colon and intestine. Rettenbacher and Reubi showed that NT receptors are also strongly expressed in the mesenteric and submucosal plexus of the colon, suggesting a major physiologic role for these peptides [24]. In the study of Buchegger et al. [8] in 4 patients with ductal pancreatic adenocarcinoma, 2 (with positive receptor expression) of 4 patients showed a significant radioactivity uptake in the intestinal tissue. Our experiments were in accordance with these results.

Compared to the results reported in other papers, the percentage of injected activity in the tumor of the analogs in our study was lower compared to other reported $^{99\text{m}}\text{Tc}$ -labeled NT analogs. However, the tumor-to-normal tissue ratios of our analogs were markedly better (except for the kidneys). For example, the tumor-to-blood ratio with the [$^{99\text{m}}\text{Tc}$]-NT analogs reported by Garcia-Garayoa et al. [14, 25] 5 hours postinjection was approximately 21, whereas we found tumor-to-blood ratios (4 hours postinjection) up to 179, owing to a rapid clearance from the blood. A high tumor-to-blood ratio is advantageous for tumor imaging.

As expected, the accumulation found in the kidney was relatively high. The uptake of the labeled peptides in the kidney was in the cortex, which was also shown for various other peptides. The peptides were reabsorbed by the proximal tubular cells by carrier-mediated endocytosis and the radioactive degradation products were trapped in the lysosomes, resulting in a high kidney radioactivity. As demonstrated by various authors, the uptake of somatostatin analogs in this organ can be substantially reduced by the pre- or coadministration of D-lysine [26-29]. This was also shown for the analogs MP2577, MP2578, and MP2579 in the same order of magnitude as described by these authors. The kidney uptake of MP2530 and MP2656, however, is not reduced by a coinjection of D-lysine. This can be explained by the absence of a lysine residue in the MP2530 and MP2656 analogs.

Recently, Maes et al. [16] reported an improved $^{99\text{m}}\text{Tc}$ -labeled NT analog with a high tumor uptake and a reduced kidney uptake, which led to a higher tumor-to-kidney ratio, compared to the ^{111}In -labeled analogs described in this paper. High tumor-to-kidney ratios are favorable for future tumor treatment strategies with NT analogs, as the kidneys are often considered to be the dose-limiting organs. Still, the tumor-to-intestine and tumor-to-liver ratios were considerably higher for the ^{111}In -labeled analogs, which would be favorable for the visualization of pancreatic tumors in patients [30]

The analogs we investigated showed a low liver uptake, whereas other groups reported liver uptakes of sometimes even higher than the kidney uptake, which was possibly related to stability and/or lipophilicity [31]. Bruehlmeier et al. [32] also found a positive correlation between stability and higher ratios of specific to non-specific (e.g., the liver) uptake.

CONCLUSIONS

In conclusion, the five new ^{111}In -labeled neuropeptide analogs showed a receptor-specific tumor uptake *in vivo*. MP2530 and its DOTA-linked counterpart showed the highest tumor uptake and tumor-to-blood ratios, and have superior characteristics in comparison to NT analogs reported thus far. We chose the MP2530 analog for clinical experiments, which have since commenced. If the diagnostic properties of the labeled DTPA-NT (MP2530) are adequate, the use of the DOTA compound, labeled with radionuclides, such as ^{177}Lu or ^{90}Y , might be feasible for peptide-receptor radionuclide therapy.

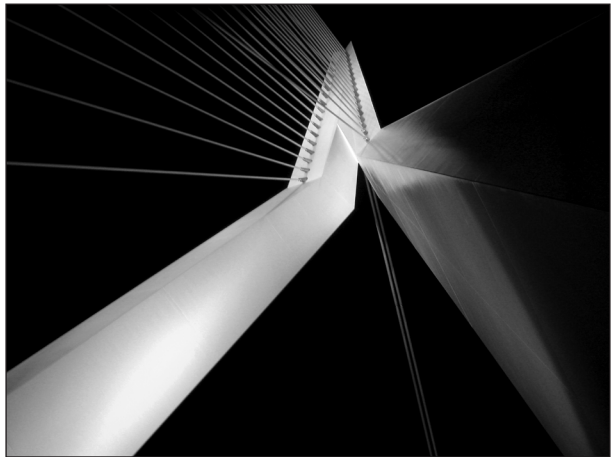
REFERENCES

1. Krenning EP, Kwkkeboom DJ, Pauwels S, et al., Somatostatin receptor scintigraphy. *Nuclear Medicine Annual*, ed. L. Freeman. 1995, New York: Raven Press. 1.
2. Williamson, R.C., Pancreatic cancer: the greatest oncological challenge. *Br Med J (Clin Res Ed)* 1988; 296(6620): 445.
3. Gold, E.B. and S.B. Goldin, Epidemiology of and risk factors for pancreatic cancer. *Surg Oncol Clin N Am* 1998; 7(1): 67.
4. Gutniak, M., U. Rosenqvist, L. Grimelius, et al., Report on a patient with watery diarrhoea syndrome caused by a pancreatic tumour containing neurotensin, enkephalin and calcitonin. *Acta Med Scand* 1980; 208(1-2): 95.
5. Ehlers, R.A., S. Kim, Y. Zhang, et al., Gut peptide receptor expression in human pancreatic cancers. *Ann Surg* 2000; 231(6): 838.
6. Reubi, J.C., B. Waser, H. Friess, et al., Neurotensin receptors: a new marker for human ductal pancreatic adenocarcinoma. *Gut* 1998; 42(4): 546.
7. Reubi, J.C., B. Waser, J.C. Schaer, et al., Neurotensin receptors in human neoplasms: high incidence in Ewing's sarcomas. *Int J Cancer* 1999; 82(2): 213.
8. Buchegger, F., F. Bonvin, M. Kosinski, et al., Radiolabeled neurotensin analog, ^{99m}Tc-NT-XI, evaluated in ductal pancreatic adenocarcinoma patients. *J Nucl Med* 2003; 44(10): 1649.
9. Vincent, J.P., J. Mazella and P. Kitabgi, Neurotensin and neurotensin receptors. *Trends Pharmacol Sci* 1999; 20(7): 302.
10. Ishizuka, J., C.M. Townsend, Jr. and J.C. Thompson, Neurotensin regulates growth of human pancreatic cancer. *Ann Surg* 1993; 217(5): 439.
11. Wang, L., H. Friess, Z. Zhu, et al., Neurotensin receptor-1 mRNA analysis in normal pancreas and pancreatic disease. *Clin Cancer Res* 2000; 6(2): 566.
12. Kitabgi, P., F. De Nadai, C. Rovere, et al., Biosynthesis, maturation, release, and degradation of neurotensin and neuromedin N. *Ann N Y Acad Sci* 1992; 668: 30.
13. Garcia-Garayoa, E., L. Allemann-Tannahill, P. Blauenstein, et al., In vitro and in vivo evaluation of new radiolabeled neurotensin(8-13) analogues with high affinity for NT1 receptors. *Nucl Med Biol* 2001; 28(1): 75.
14. Garcia-Garayoa, E., V. Maes, P. Blauenstein, et al., Double-stabilized neurotensin analogues as potential radiopharmaceuticals for NTR-positive tumors. *Nucl Med Biol* 2006; 33(4): 495.
15. Lugin, D., F. Vecchini, S. Doulut, et al., Reduced peptide bond pseudopeptide analogues of neurotensin: binding and biological activities, and in vitro metabolic stability. *Eur J Pharmacol* 1991; 205(2): 191.
16. Maes, V., E. Garcia-Garayoa, P. Blauenstein, et al., Novel ^{99m}Tc-labeled neurotensin analogues with optimized biodistribution properties. *J Med Chem* 2006; 49(5): 1833.
17. Nock, B.A., A. Nikolopoulou, J.C. Reubi, et al., Toward stable N⁴-modified neurotensins for NTS1-receptor-targeted tumor imaging with ^{99m}Tc. *J Med Chem* 2006; 49(15): 4767.
18. Zhang, K., R. An, Z. Gao, et al., Radionuclide imaging of small-cell lung cancer (SCLC) using ^{99m}Tc-labeled neurotensin peptide 8-13. *Nucl Med Biol* 2006; 33(4): 505.
19. de Visser, M., P.J. Janssen, A. Srinivasan, et al., Stabilised ¹¹¹In-labelled DTPA- and DOTA-conjugated neurotensin analogues for imaging and therapy of exocrine pancreatic cancer. *Eur J Nucl Med Mol Imaging* 2003; 30(8): 1134.
20. Breeman, W.A., M. De Jong, T.J. Visser, et al., Optimising conditions for radiolabelling of DOTA-peptides with ⁹⁰Y, ¹¹¹In and ¹⁷⁷Lu at high specific activities. *Eur J Nucl Med Mol Imaging* 2003; 30(6): 917.
21. Breeman, W.A., K. D.J., E. De Blois, et al., Radiolabelled regulatory peptides for imaging and therapy. *Anti-Cancer Agents in Medicinal Chemistry* 2007; 7: In press.

22. Liu, S. and D.S. Edwards, Bifunctional chelators for therapeutic lanthanide radiopharmaceuticals. *Bioconjug Chem* 2001; 12(1): 7.
23. Breeman, W.A., M.T. De Jong, E. De Blois, et al., Reduction of skeletal accumulation of radioactivity by co-injection of DTPA in [90Y-DOTA0,Tyr3]octreotide solutions containing free 90Y3+. *Nucl Med Biol* 2004; 31(6): 821.
24. Rettenbacher, M. and J.C. Reubi, Localization and characterization of neuropeptide receptors in human colon. *Naunyn Schmiedebergs Arch Pharmacol* 2001; 364(4): 291.
25. Garcia-Garayoa, E., P. Blauenstein, M. Bruehlmeier, et al., Preclinical evaluation of a new, stabilized neurotensin(8--13) pseudopeptide radiolabeled with (99m)tc. *J Nucl Med* 2002; 43(3): 374.
26. Bernard, B.F., E.P. Krenning, W.A. Breeman, et al., D-lysine reduction of indium-111 octreotide and yttrium-90 octreotide renal uptake. *J Nucl Med* 1997; 38(12): 1929.
27. de Jong, M., E.J. Rolleman, B.F. Bernard, et al., Inhibition of renal uptake of indium-111-DTPA-octreotide in vivo. *J Nucl Med* 1996; 37(8): 1388.
28. Kobayashi, H., T.M. Yoo, I.S. Kim, et al., L-lysine effectively blocks renal uptake of 125I- or 99mTc-labeled anti-Tac disulfide-stabilized Fv fragment. *Cancer Res* 1996; 56(16): 3788.
29. Lang, L., E. Jagoda, C. Wu, et al., Factors influencing the in vivo pharmacokinetics of peptides and antibody fragments: the pharmacokinetics of two PET-labeled low molecular weight proteins. *Q J Nucl Med* 1997; 41(2): 53.
30. Emami, B., J. Lyman, A. Brown, et al., Tolerance of normal tissue to therapeutic irradiation. *Int J Radiat Oncol Biol Phys* 1991; 21(1): 109.
31. Bergmann, R., M. Scheunemann, C. Heichert, et al., Biodistribution and catabolism of (18)F-labeled neurotensin(8-13) analogs. *Nucl Med Biol* 2002; 29(1): 61.
32. Bruehlmeier, M., E.G. Garayoa, A. Blanc, et al., Stabilization of neurotensin analogues: effect on peptide catabolism, biodistribution and tumor binding. *Nucl Med Biol* 2002; 29(3): 321.

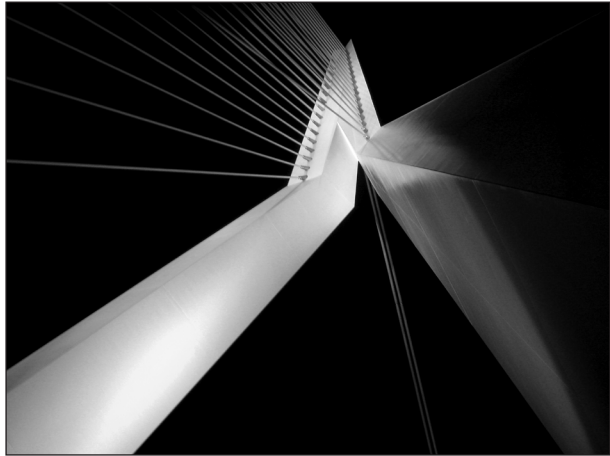
III

Bombesin analogs for in vivo targeting of prostate cancer



4

Novel ^{111}In -labeled bombesin analogs for molecular imaging of prostate tumors



Monique. de Visser
Bert. F. Bernard
Jack. L. Erion
Michelle. A. Schmidt
Ananthachari Srinivasan
Beatrice Waser
Jean-Claude Reubi
Eric. P. Krenning
Marion de Jong

European Journal of Nuclear Medicine and Molecular Imaging
2007; Vol. 34(8):1228–1238

ABSTRACT

It has been shown that some primary human tumors and their metastases, including prostate and breast tumors, overexpress gastrin-releasing peptide (GRP) receptors. Bombesin (BN) is a neuropeptide with a high affinity for these GRP receptors. We demonstrated successful scintigraphic visualization of BN receptor-positive tumors in preclinical studies using the radiolabeled BN analog [^{111}In -DTPA-Pro¹,Tyr⁴]BN. However, the receptor affinity as well as the serum stability of this analog leaves room for improvement. Therefore new ^{111}In -labeled BN analogs were synthesized and evaluated *in vitro* and *in vivo*.

The receptor affinity of the new BN analogs was tested on human GRP receptor-expressing prostate tumor xenografts and rat colon sections. Analogs with high receptor affinity (low nM range) were selected for further evaluation. Incubation *in vitro* of GRP receptor-expressing rat CA20948 and human PC3 tumor cells with the ^{111}In -labeled analogs resulted in rapid receptor-mediated uptake and internalization. The BN analog with the best receptor affinity and *in vitro* internalization characteristics, Cmp 3 ([^{111}In -DTPA-ACMpip⁵,Tha⁶, β Ala¹¹,Tha¹³,Nle¹⁴]BN(5–14)), was tested *in vivo* in biodistribution studies using rats bearing GRP receptor-expressing CA20948 tumors, and nude mice bearing human PC3 xenografts. Injection of ^{111}In -labeled Cmp 3 in these animals showed high, receptor-mediated uptake in receptor-positive organs and tumors which could be visualized using planar gamma camera and microSPECT/CT imaging.

With their enhanced receptor affinity and their rapid receptor-mediated internalization *in vitro* and *in vivo*, the new BN analogs, and especially Cmp 3, are promising candidates for use in diagnostic molecular imaging and targeted radionuclide therapy of GRP receptor-expressing cancers.

INTRODUCTION

Bombesin-like peptides, including gastrin-releasing peptide (GRP) and neuromedin B (NMB), are involved in the regulation of a large number of biological processes in the gut and central nervous system (CNS) [1]. They mediate their action by binding to G protein-coupled receptors [2].

Four subtypes of the bombesin (BN) receptor are known. Three of them, the NMB receptor (BB_1), the GRP receptor (BB_2) and BN receptor subtype 3 (BRS-3 or BB_3), are mammalian receptors, whereas the fourth subtype (BB_4) is found only in amphibians [3-6]. Except for the GRP receptor, these receptor subtypes are not characterized very well with regard to their distribution and function in human tissues [7, 8].

BN receptors are expressed in high densities on several primary human tumors and their metastases, including prostate, breast, small cell lung and pancreatic cancers [9-16]. Prostate cancer is the most frequently diagnosed malignancy and the third leading cause of cancer mortality among men in the Western world [17]. Although the commonly used hormonal therapies increase the survival of patients with hormone-dependent prostate tumors, patients with hormone-independent tumors still have a poor prognosis. Therefore new diagnosis and treatment methods for these tumors are still very welcome.

Prostate tumors overexpress GRP receptors [11, 14, 18-21]. In an autoradiographic study, Markwalder and Reubi found the GRP receptor to be expressed in high density on invasive prostate carcinomas and proliferative intraepithelial prostate lesions, mostly prostatic intraepithelial neoplasias, whereas normal prostate tissue and, in most cases, hyperplastic prostate tissue were GRP receptor-negative [11]. These findings suggest that the GRP receptor can be used as a molecular basis for diagnosing and treating prostate tumors with, for example, GRP receptor-targeted scintigraphy, radionuclide therapy and cytotoxic therapy [11, 22]. It has been proposed that GRP receptor-expressing tumors can be visualized and treated using radiolabeled BN analogs in a manner similar to what has been found for somatostatin receptor-expressing tumors, which have been successfully imaged and treated using radiolabeled somatostatin analogs [23-25].

A number of researchers continue to work on the development of radiolabeled BN analogs that specifically target GRP receptor-expressing tumors. For example, $^{99\text{m}}\text{Tc}$ - and ^{111}In -coupled BN analogs have been developed for diagnostic SPECT imaging and ^{64}Cu - and ^{68}Ga -labeled analogs for PET imaging of GRP receptor-expressing tumors [26-39]. In addition, ^{90}Y - and ^{177}Lu -labeled analogs have been described as promising tools for targeted radiotherapy of these tumors [32, 40].

We previously developed and evaluated the radiolabeled peptide [^{111}In -DTPA-Pro¹,Tyr⁴]BN, a BN analog which internalized rapidly into GRP receptor-positive

tumor cells *in vitro* and *in vivo* [33-35]. In addition, GRP receptor-expressing CA20948 and AR42J tumors could be visualized using gamma camera imaging in rats after injection with this radiolabeled BN analog [33, 34].

Our goal in this study was to extend our previous study by developing an improved BN analog with an increased uptake in GRP receptor-expressing tumors. Because the BN analog, Cmp 1 [DTPA-Pro¹,Tyr⁴]BN is an analog with minimal modifications of the native peptide, we synthesized new BN analogs with shortened amino acid sequences including stable amino acid derivatives to increase the receptor affinity of these peptides. We selected five of these new BN analogs on the basis of their receptor affinity and compared their *in vitro* characteristics with the characteristics of Cmp 1. We determined the *in vivo* tumor uptake and tissue biodistribution of the compound found to have the most promising *in vitro* characteristics.

MATERIALS AND METHODS

Peptide synthesis

The new BN analogs were synthesized by solid phase peptide synthesis using an Applied Biosystems Model 432A “Synergy” Peptide synthesizer (Applied Biosystems, Foster City, CA, USA) employing the Fmoc (9-fluorenylmethoxy-carbonyl) strategy. The instrument protocol required 25 μmol of starting resin and 75 μmol of subsequent Fmoc-protected amino acids activated by a combination of N-hydroxybenzotriazole (HOBt) and (2-(1-H-benzotriazol-1-yl)-1,1,3,3-tetramethyluronium hexafluorophosphate (HBTU). Tri-t-butyl DTPA (75 μmol) was placed at the appropriate location in an amino acid column to prepare DTPA-coupled derivatives [19]. The arginine and lysine derivatives used were purchased from RSP Amino Acid Analogs (Hopkinton, MA, USA). All other Fmoc-protected amino acids were purchased from Novobiochem/EMD Biosciences (Madison, WI, USA).

The cleavage and deprotection were accomplished using 85% TFA:5% thioanisole:5% phenol:5% water. We isolated the crude peptide by precipitating with t-butyl methyl ether (Sigma, St. Louis, MO, USA), and purified the peptide by reverse phase high-performance liquid chromatography (HPLC) using an acetonitrile/water gradient containing 0.1% TFA, with final yields ranging from 10% to 25% of the starting resin scale. The molecular weights of compounds 1 through 6 were determined by mass spectrometry operating in the electrospray mode (Varian, Palo Alto, CA, USA); M/z determined for the peptides were: Cmp 1, 1,016.0 (M+2H), consistent for a compound of expected MW of 2,030.0; Cmp 2, 1,515.6 (M+H); Cmp 3, 1,644.7 (M+H); Cmp 4, 1,638.8 (M+H), Cmp 5, 1,504.8 (M+H); Cmp 6, 1,431.8 (M+H). Peptide radiolabeling The DTPA-conjugated BN analogs were radiolabeled with ¹¹¹In

($^{111}\text{InCl}_3$, Tyco Healthcare, Petten, the Netherlands, DRN 4901, 370 MBq/ml in HCl, pH 1.5–1.9) to a maximum specific activity of 200 MBq/nmol as described previously [41]. Consecutive quality control by instant thin-layer chromatography and SEP-PAK C18 reverse phase chromatography (Waters) was performed as described previously [42]. The radiolabeling yield and radiochemical purity were always >95%.

Receptor affinity

Receptor affinity of the BN analogs was determined on frozen sections of the GRP receptor-expressing human prostate tumor xenograft PC-295 [43] and rat colon using *in vitro* autoradiography. The 10- μm sections were incubated for 1 h at room temperature with 0.1 nM ^{111}In -Cmp 1 (^{111}In -DTPA-Pro¹,Tyr⁴-bombesin) (200 MBq/nmol) in 167 mM Tris (pH 7.6), 5 mM MgCl_2 , 1% bovine serum albumin (BSA), 40 $\mu\text{g}/\text{ml}$ bacitracin. To generate competitive inhibition curves, the sections were incubated in the presence of increasing amounts of the selected nonradioactive ^{115}In -labeled BN analogs. After incubation, the sections were washed two times for 5 min each in 167 mM Tris (pH 7.6), 5 mM MgCl_2 , 0.25% BSA (4°C), for 5 min in 167 mM Tris (pH 7.6), 5 mM MgCl_2 (4°C) and finally rinsed in MilliQ water (4°C). The sections were then dried and exposed to phosphor imaging screens for 72 h. The imaging screens were read using the Cyclone Storage Phosphor System and the autoradiograms were quantified using Optiquant Software (Packard, Meriden, USA).

Cell culture

The BN analogs were tested using the GRP receptor-expressing rat pancreatic tumor cell lines CA20948 and AR42J [44] and the human prostate tumor cell line PC3. We have previously used the CA20948 tumor model to characterize BN analogs. Many other groups, however, have used the AR42J tumor model. In this study we used both models to enable comparisons with other studies.

The CA20948 cells were grown in Dulbecco's modified Eagle's medium (Gibco, Life Technologies, Breda, the Netherlands) supplemented with 10% fetal bovine serum, Glutamax I (1x), 0.2 mM sodium pyruvate, 0.25 mg/l Fungizone and 200 IU/ml penicillin/streptomycin (Gibco, Life Technologies, Breda, the Netherlands). The AR42J and PC3 cells were grown in RPMI medium (Gibco, Life Technologies, Breda, the Netherlands) supplemented with 10% fetal bovine serum, Glutamax I (1x), 0.2 mM sodium pyruvate, 0.25 mg/l Fungizone and 200 IU/ml penicillin/streptomycin (Gibco, Life Technologies, Breda, the Netherlands).

Internalization

The internalization characteristics of the ^{111}In -labeled BN analogs were determined as previously described [45]. Subconfluent cell cultures were transferred to six-well

plates 24 h before internalization experiments. For increasing incubation times, the CA20948 and PC3 cells were incubated in triplicate with 1 ml incubation medium (RPMI supplemented with 20 mM HEPES and 1% bovine serum albumin) containing 80–100 kBq of ^{111}In -labeled peptide (concentration as indicated).

Cellular uptake was stopped by removing medium from the cells and washing with 2 ml of ice-cold PBS. Surfacebound activity was removed by incubation with 1 ml of 20 mM sodium acetate in PBS (pH 5.0) for 10 min. Internalized and surface-bound radioactivity was determined separately by measuring the different fractions in an LKB-1282-Compugamma system (Perkin Elmer, Oosterhout, the Netherlands) and expressed as a percentage of the total dose applied per milligram cellular protein. Protein was determined using a commercially available kit (Protein assay, BioRad, Veenendaal, the Netherlands). To test the receptor specificity of internalization, an increasing concentration (10^{-10} M to 10^{-6} M) of unlabeled [Tyr⁴]BN was added to the incubation medium to compete with the binding of radiolabeled BN analogs to the GRP receptor.

Biodistribution experiments

The biodistribution experiments were done using male Lewis rats implanted with an average of 1 million CA20948 cells and male NMRI nu/nu mice implanted with an average of 5 million PC3 cells. After 14–21 days (tumor size ca. 2–4 cm² for CA20948 and 1 cm² for PC3) the animals were injected intravenously with 2–4 MBq/0.1 µg of ^{111}In -labeled peptide. In this biodistribution study we compared the uptake of the most promising compound (based on the binding affinity and internalization results), ^{111}In -Cmp 3, with the uptake of compound ^{111}In -Cmp 1 in the selected organs and tumors. The injection volume was 0.50 ml in rats and 0.20 ml in mice. To discriminate between receptor-specific (receptor-mediated) and non-specific binding, some animals were co-injected with an excess of unlabeled [Tyr⁴]BN (100 µg in rats and 50 µg in mice). We sacrificed the animals 4, 24, 48 and 72 h (mice only 4 h) after injection and collected the organs and tissues of interest for counting radioactivity and calculating the uptake (% injected dose per mg tissue). Statistical analysis was performed using the Mann Whitney and unpaired t test. A probability of less than 0.05 was considered significant.

Serum stability

The serum stability of ^{111}In -Cmp 1 and 3 was evaluated by incubation in human serum [50% serum:50% phosphate-buffered saline (PBS)] of healthy donors at 37°C for 4 h. The percentage of intact peptide after incubation was determined by separating degradation products by reverse phase HPLC using a Vydac C-18 column connected

to a radiometric detector, and using a 15 min, 0–70% linear acetonitrile gradient (0.1% TFA/water).

Tumor visualization

The tumor visualization experiments were done using a male Lewis rat implanted with an average of 1 million CA20948 cells in the right flank and AR42J cells in the left flank. After 14–21 days, the rat was intravenously injected with 4 MBq/0.1 μg ^{111}In -Cmp 3. Directly after injection of the radiotracer, a dynamic planar scan of the rat was made over 1 h using a one-headed gamma camera (Siemens, Erlangen, Germany). At 4 h after injection, a static image was acquired for 1 min. Immediately after imaging at 4 h postinjection, the rat was sacrificed and a biodistribution study was performed.

For microSPECT/CT imaging a female Swiss nu/nu mouse was injected with ca. 1 million CA20948 cells. After 14 days the mouse was intravenously injected with 10 MBq/0.1 μg ^{111}In -Cmp 3. Four hours after injection, SPECT/CT imaging was performed with a four-headed multiplexing multi-pinhole NanoSPECT/CT (Bioscan Inc., Washington D.C.). After the acquisition, the data were reconstructed iteratively with the HiSPECT software (Bioscan Inc., Washington D.C., USA), a dedicated ordered subsets-expectation maximization (OSEM) software package for multiplexing multi-pinhole reconstruction. The CT and SPECT images were fused using Pmod image fusion software (Mediso Ltd., Budapest, Hungary). Immediately after imaging at 4 h postinjection the mouse was sacrificed and a biodistribution study was performed.

RESULTS

Peptides

Figure 1 shows the sequences and the molecular weights of compounds 1–6 used in this study and the structures of the non-natural amino acid derivatives.

Receptor affinity

The receptor affinity of the BN analogs was determined on GRP receptor-expressing human prostate tumor xenografts (PC-295) and rat colon sections. The IC_{50} values of the BN analogs are presented in table 1. Cmp 2, Cmp 3 and Cmp 4 show increased receptor affinity for both the human (0.50, 0.36 and 0.41 nM respectively) and rat (0.22, 0.08 and 0.31 nM respectively) GRP receptor compared with analog Cmp 1 (human 1.40 nM and rat 2.28 nM). However, all analogs show improved receptor affinity for the rat GRP receptor.

Analog	Sequence	MW
Compound 1	DTPA-Pro-Gln-Arg-Tyr-Gly-Asn-Gln-Trp-Ala-Val-Gly-His-Leu-Met-NH ₂	2030
Compound 2	DTPA-Acp-Gln-Trp-Ala-Val-βAla-His-Phe-Nle-NH ₂	1514
Compound 3	DTPA-ACMpip-Tha-Gln-Trp-Ala-Val-βAla-His-Tha-Nle-NH ₂	1644
Compound 4	DTPA-ACMpip-Tha-Gln-Trp-Ala-Val-βAla-His-Phe-Nle-NH ₂	1638
Compound 5	DTPA- _D Tha-Gln-Trp-Ala-Val-βAla-His-Tha-Nle-NH ₂	1504
Compound 6	_D Dpr(DTPA)-Gln-Trp-Ala-Val-βAla-His-Phe-Nle-NH ₂	1431

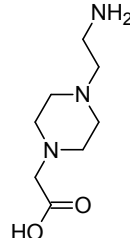
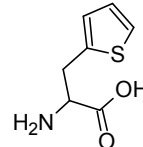
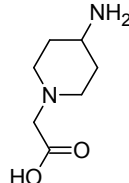
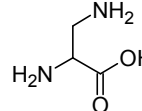
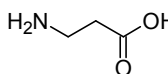
 <p>Acp 1-Aminoethyl,4-carboxymethyl-piperazine</p>	 <p>Tha β-(2-Thienyl)-alanine</p>	 <p>ACMpip 4-Amino-carboxymethyl-piperidine</p>	 <p>Dpr 1,2-Diaminopropionic acid</p>	 <p>βAla β-Alanine</p>
---	---	---	---	---

Figure. 1 Sequences of [DTPA-Pro¹,Tyr⁴]BN (compound 1) and five new BN analogs, including non-natural amino acid derivatives.

Table 1. GRP receptor-binding affinity (IC₅₀, mean ± SD) of BN analogs, determined on human PC-295 and rat colon sections.

Analog	Sequence	r Colon IC ₅₀ (nM)	h PC-295 IC ₅₀ (nM)
Compound 1	DTPA-Pro ¹ ,Tyr ⁴ -bombesin	2.28 ± 0.57	1.40 ± 0.07
Compound 2	DTPA-Acp ⁶ , βA ¹¹ F ¹³ , Nle ¹⁴ -bombesin (6-14)	0.22 ± 0.05	0.50 ± 0.05
Compound 3	DTPA-aCMpip ⁵ ,Tha ⁶ ,βA ¹¹ ,Tha ¹³ ,Nle ¹⁴ -bombesin (5-14)	0.08 ± 0.01	0.36 ± 0.01
Compound 4	DTPA-aCMpip ⁵ ,Tha ⁶ ,βA ¹¹ ,F ¹³ ,Nle ¹⁴ -bombesin (5-14)	0.31 ± 0.02	0.41 ± 0.01
Compound 5	DTPA- _D Tha ⁶ ,βA ¹¹ ,Tha ¹³ ,Nle ¹⁴ -bombesin (6-14)	0.43 ± 0.04	2.54 ± 0.34
Compound 6	_D Dpr(DTPA) ⁶ , βA ¹¹ F ¹³ , Nle ¹⁴ -bombesin (6-14)	1.20 ± 0,01	15.39 ± 2,81

Internalization

All the ¹¹¹In-labeled BN analogs internalized into CA20948 and PC3 cells. Figure 2 shows the time course of internalization into the CA20948 (a) and PC3 (b) cells expressed as percent of the dose per milligram cellular protein of the different radiolabeled peptides. All the ¹¹¹In-labeled BN analogs internalized time dependently, but, compared with ¹¹¹In-Cmp 1, the new BN analogs were more rapidly internalized into the CA20948 tumor cells. The internalization characteristics of the analogs in the human PC3 cells were in some cases significantly different from those found in the rat CA20948 cells. In addition, the rank orders of the analogs based on these internalization data of the areas under the curve (AUC) are notably different in the rat and human tumor cells (Figure 2).

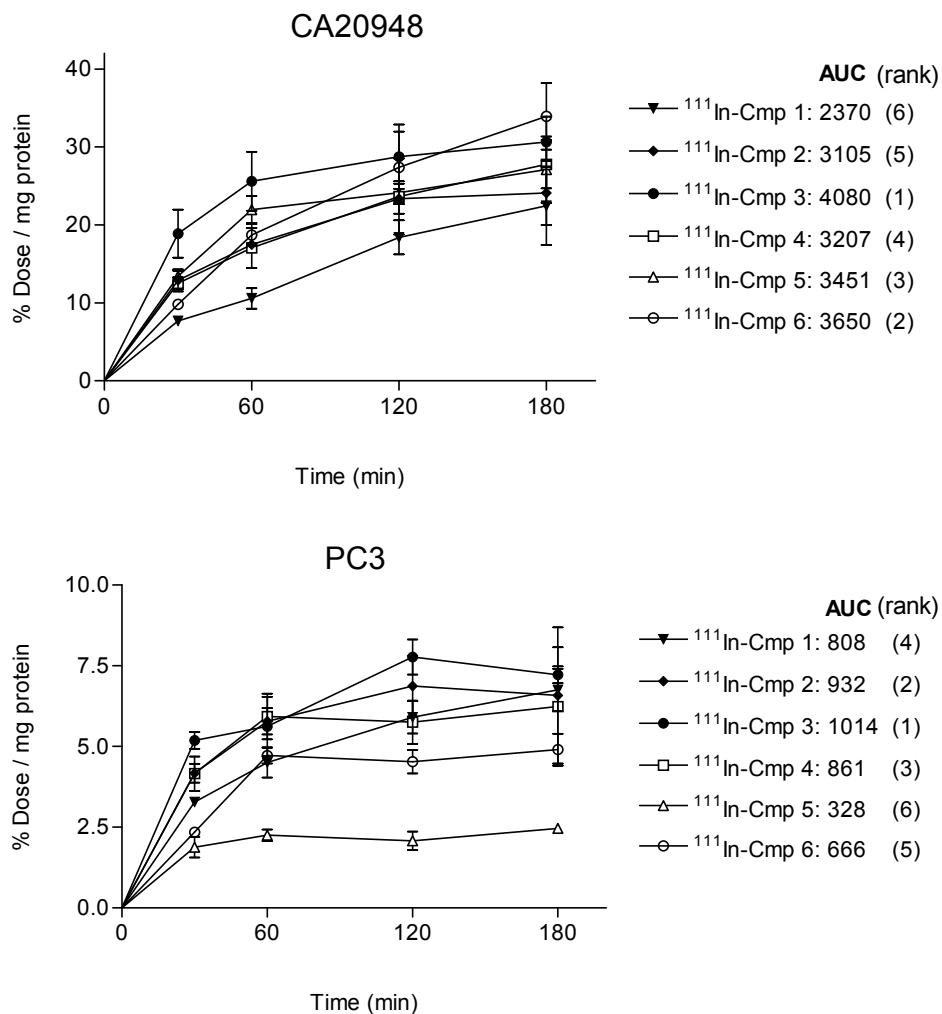


Figure. 2 Time curve of internalization of 0.5 nM ^{111}In -Cmp 1 and four new ^{111}In -labeled BN analogs in rat CA20948 tumor cells (a) and human PC3 tumor cells (b). Results are presented as the average percentage of the total dose per milligram cellular protein (% dose/mg protein; mean \pm SD). AUC: area under the curve

^{111}In -Cmp 3 showed the highest rate of internalization in the first hours of incubation and had the highest AUC in both the rat and the human tumor model. On the basis of these internalization data and the data on receptor affinity for the human and the rat GRP receptor, we selected analog ^{111}In -Cmp 3 for further *in vitro* and *in vivo* characterization.

To prove that the internalization of ^{111}In -Cmp 3 was receptor-mediated, we added increasing amounts of unlabeled [Tyr⁴]BN to the incubation medium, which contained 10^{-10} M ^{111}In -Cmp 1 or ^{111}In -Cmp 3. The results in figure. 3 show that addition

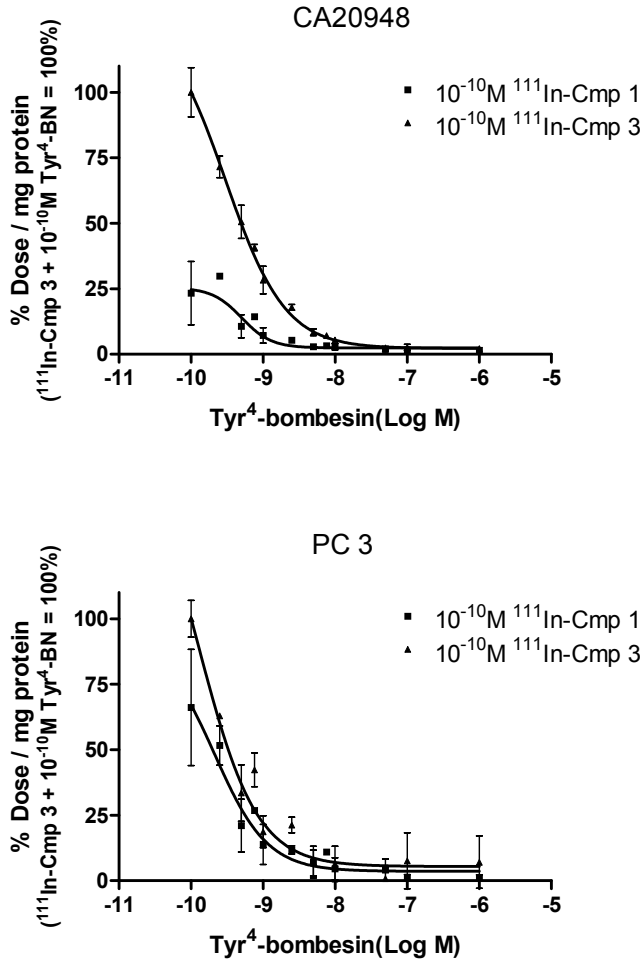


Figure. 3 Internalization of 0.1 nM ^{111}In -Cmp 1 and ^{111}In -Cmp 3 in the rat CA20948 (a) and human PC3 (b) tumor cells after 1-h incubation with increasing amounts of unlabeled [Tyr⁴]BN. Results are the average percentage of the total dose per milligram cellular protein (% dose/mg protein); mean \pm SD of three experiments.

of 1^{-10} nM unlabeled [Tyr⁴] BN effectively caused this peptide to compete with the uptake of either ^{111}In -Cmp 1 or ^{111}In -Cmp 3 for receptor binding and internalization into CA20948 cells and PC3 cells. Consistent with the findings in the time curve internalization study (Figure 2), the superior internalization characteristics of ^{111}In -Cmp 3 over ^{111}In -Cmp 1 are less impressive in the human PC3 cells than in the rat CA20948 cells.

Biodistribution

In the *in vivo* biodistribution studies we compared the uptake of ¹¹¹In-Cmp 3 with that of ¹¹¹In-Cmp 1 in rats bearing CA20948 tumors and nude mice bearing PC3 tumors. Compared with ¹¹¹In-Cmp 1, the uptake of ¹¹¹In-Cmp 3 was two to three times higher (4 h postinjection) in the rat BN receptor-positive pancreas, stomach, caecum, small intestine and colon (p<0.007) (Table 2). The same was true for the uptake in the receptor-positive CA20948 tumor (p<0.015). The radioactivity in the background organs and blood, except for the kidneys, was also two to three times higher for ¹¹¹In-Cmp 3 than for ¹¹¹In-Cmp 1, but was still very low, indicating rapid clearance. Coinjection of 100 µg unlabeled [Tyr⁴]BN resulted in an 89% reduction in ¹¹¹In-Cmp 3 uptake in the CA20948 tumor and also in a reduction in uptake in other GRP receptor-positive organs, e.g. 94% in the pancreas and 88% in the colon. The uptake reduction found for ¹¹¹In-Cmp 1 was comparable to that for ¹¹¹In-Cmp 3: 90% in the tumor, 99% in the pancreas and 88% in the colon. As presented in table 2, ¹¹¹In-Cmp 3 showed good retention in receptor-positive organs and tumor up to 72 h postinjection. Due to rapid clearance from the body, good tumor-to-background ratios were found (Table 2). The

Table 2 Uptake of ¹¹¹In-Cmp 1 and ¹¹¹In-Cmp 3 in rats bearing CA20948 tumors at 4, 24, 48 and 72 h p.i. (0.1 µg /4 MBq with or without coinjection of 100 µg unlabeled [Tyr⁴]BN).

	¹¹¹ In-Cmp 1		¹¹¹ In-Cmp 3				
	4 h	4 h + unlabeled BN	4 h	4 h + unlabeled BN	24 h	48 h	72 h
	(n=6)	(n=3)	(n=27)	(n=20)	(n=6)	(n=3)	(n=3)
Blood	0.005±0.001	0.005±0.002	0.012±0.006	0.012±0.006	0.007±0.002	0.003±0.000	0.002±0.000
Spleen	0.023±0.018	0.020±0.003	0.029±0.014	0.033±0.008	0.034±0.014	0.031±0.006	0.029±0.009
Pancreas	1.307±0.260	0.018±0.005	2.883±1.135	0.185±0.520	2.227±0.347	1.332±0.629	1.165±0.169
Kidney	1.085±0.195	1.546±0.309	1.145±0.352	1.188±0.553	1.203±0.250	0.834±0.086	0.698±0.046
Liver	0.024±0.007	0.023±0.004	0.040±0.013	0.041±0.014	0.035±0.006	0.027±0.007	0.028±0.005
Stomach	0.054±0.021	0.015±0.007	0.136±0.068	0.068±0.049	0.085±0.023	0.051±0.030	0.036±0.005
Ceacum	0.248±0.035	0.138±0.010	0.692±0.162	0.179±0.134	0.487±0.104	0.186±0.082	0.140±0.010
Small intestine	0.103±0.047	0.050±0.007	0.375±0.207	0.219±0.364	0.192±0.056	0.122±0.065	0.060±0.022
Colon	0.229±0.013	0.028±0.023	0.550±0.195	0.068±0.058	0.337±0.101	0.137±0.057	0.088±0.016
Muscle	0.002±0.001	0.002±0.001	0.004±0.002	0.004±0.002	0.004±0.001	0.004±0.000	0.003±0.000
Femur	0.006±0.002	0.007±0.001	0.013±0.004 ⁽²³⁾	0.009±0.004 ⁽¹⁷⁾	0.013±0.003	0.013±0.003	0.012±0.001
CA20948	0.251±0.277	0.026±0.005	0.583±0.244 ⁽²⁵⁾	0.067±0.088	0.521±0.115	0.277±0.167	0.266±0.082
Tumor to normal tissue radioactivity ratios							
Tumor/blood	50		49	74		92	133
Tumor/muscle	126		146	130		69	89
Tumor/kidney	0.2		0.5	0.4		0.3	0.4

Note; Results are the average uptake values of one to five experiments presented as percent of the injected dose per gram tissue (%ID/g) ± SD.

(^x) =n

respective tumor-to-blood and tumor-to-muscle ratios were 50 and 126 for ^{111}In -Cmp at 1 and 4 h postinjection, and 49 and 146 for ^{111}In -Cmp 3 at 4 h postinjection; for ^{111}In -Cmp 3 these ratios respectively reached 133 and 89 at 72 h postinjection.

The results found in the PC3 tumor-bearing nude mice at 4 h postinjection were partly consistent with the results found in the CA20948 tumor-bearing rats; ^{111}In -Cmp 3 showed a two times higher uptake in the BN receptor-positive organs compared with ^{111}In -Cmp 1 ($p < 0.005$ for pancreas, caecum, small intestine and colon). The uptake of ^{111}In -Cmp 3 in the human PC3 tumor was 1.3-fold higher compared with ^{111}In -Cmp 1 (Table 3). However, the radioactivity accumulation in the mouse kidneys was four times lower for the new compound ^{111}In -Cmp 3 ($p < 0.0001$). The uptake reduction in the blocking experiments in the mice was consistent with the uptake reductions found in the rats: 86% in PC3 tumor for both compounds, 96% for Cmp 3 in mouse pancreas (Cmp 1: 99%) and 95% for Cmp 3 in mouse colon (Cmp 1: 96%). Respective tumor-to-blood and tumor-to-muscle ratios in these PC3 tumor-bearing mice were 28 and 36 for ^{111}In -Cmp 1 and 18 and 49 for ^{111}In -Cmp 3 at 4 h postinjection.

Table 3 Uptake of ^{111}In -Cmp 1 and ^{111}In -Cmp 3 in nude mice bearing PC3 tumors at 4 h p.i. (0.1 μg /4 MBq with or without co-injection of 100 μg unlabeled [$^{14}\text{Tyr}^4$]BN)

	^{111}In -Cmp 1		^{111}In -Cmp 3	
	4 h	4 h + unlabeled BN	4 h	4 h + unlabeled BN
	(n=17)	(n=10)	(n=11)	(n=7)
	0.023 \pm 0.007	0.029 \pm 0.014	0.047 \pm 0.012	0.035 \pm 0.020
Spleen	0.371 \pm 0.207	0.069 \pm 0.029	0.482 \pm 0.251	0.060 \pm 0.026 ⁽⁶⁾
Pancreas	8.486 \pm 3.983	0.100 \pm 0.042	15.010 \pm 3.930	0.553 \pm 0.312
Kidney	4.750 \pm 1.248	3.849 \pm 1.215	1.072 \pm 0.293	0.727 \pm 0.283
Liver	0.082 \pm 0.025	0.117 \pm 0.040	0.223 \pm 0.085	0.226 \pm 0.124
Stomach	0.666 \pm 0.528	0.070 \pm 0.048 ⁽⁶⁾	0.550 \pm 0.233 ⁽⁵⁾	0.056 \pm 0.061 ⁽³⁾
Ceacum	1.556 \pm 0.620	0.120 \pm 0.075 ⁽⁹⁾	3.306 \pm 0.530 ⁽⁹⁾	0.409 \pm 0.130 ⁽⁵⁾
Small intestine	0.769 \pm 0.296	0.116 \pm 0.054	1.560 \pm 0.512	0.152 \pm 0.179
Colon	2.457 \pm 1.119	0.090 \pm 0.076	3.986 \pm 1.227	0.187 \pm 0.114
Muscle	0.040 \pm 0.094	0.019 \pm 0.011	0.017 \pm 0.016 ⁽¹⁰⁾	0.009 \pm 0.006 ⁽⁶⁾
Femur	0.018 \pm 0.016 ⁽¹⁶⁾	0.033 \pm 0.015	0.083 \pm 0.028 ⁽⁸⁾	0.026 \pm 0.010 ⁽⁴⁾
PC3	0.651 \pm 0.243 ⁽⁶⁾	0.089 \pm 0.070 ⁽⁷⁾	0.838 \pm 0.577 ⁽⁸⁾	0.120 \pm 0.122 ⁽⁶⁾
Tumor to normal tissue radioactivity ratios				
Tumor/blood	28		18	
Tumor/muscle	36		49	
Tumor/kidney	0.1		0.8	

Note; Results are the average uptake values of three or four experiments presented as percent of the injected dose per gram tissue (%ID/g) \pm SD.

(x) =n

Serum stability

The *in vitro* serum stability of the ^{111}In -Cmp 3 was determined and compared with the stability of ^{111}In -Cmp 1. The percentage of intact peptide after the 4-hour incubation of ^{111}In -Cmp 1 in human serum was 67%. Under the same conditions ^{111}In -Cmp 3 showed a slightly increased stability of 74% intact peptide.

Tumor visualization

To visualize GRP receptor-expressing tumors in rats using the newly developed BN analog, we injected a Lewis rat bearing GRP receptor-expressing tumors [CA20948 (right flank) and AR42J, which is commonly used by many other research groups (left flank)] with 4 MBq/0.1 μg ^{111}In -Cmp 3. Gamma camera imaging was performed directly after injection and at 4 h after injection. Figure 4 shows scan images at 1, 10, 30 and 60 min and at 4 h after injection. The images in figure 4 demonstrate rapid uptake of ^{111}In -Cmp 3 in GRP receptor-positive AR42J tumor; uptake in this tumor could already be detected at 1 min postinjection. At 4 h postinjection, the AR42J tumor was still clearly visible. In this experiment the uptake of ^{111}In -Cmp 3 in the CA20948 tumor was much lower than the uptake in the AR42J tumor. This was probably due to necrosis of the huge CA20948 tumor and higher GRP receptor density of the AR42J tumor.

The background radioactivity rapidly decreased after the first hour, which resulted in increasing tumor-to-background ratios. As ^{111}In -Cmp 3 is excreted via the kidneys and the urinary system, radioactivity rapidly accumulated in the kidneys in the first hour after injection. At 4 h postinjection, the radioactivity in the kidneys had decreased, and therefore the tumor-to-kidney ratio was more favorable at this time point.

In addition to the dynamic gamma camera imaging we also performed a microSPECT/CT imaging study with a nude mouse bearing the CA20948 tumor. The mouse was injected with 10 MBq/0.1 μg ^{111}In -Cmp 3 and was scanned at 4 h postinjection. Immediately after imaging at 4 h postinjection, the mouse was sacrificed for determination of the *in vivo* biodistribution of the compound. Figure 5 shows the fused SPECT/CT images of the mouse. Biodistribution results are presented in the adjacent table. The sagittal, coronal and transaxial slices show a clear localization of the CA20948 tumor on the right shoulder of the mouse, with no interfering background radioactivity. On the sagittal slice, bowel activity is visible which is probably caused by the GRP receptor-positive pancreas and intestines.

The tumor uptake in the CA20948 tumor-bearing nude mouse was much higher than that found in the CA20948 tumor-bearing rats, which resulted in very high tumor-to-background ratios.

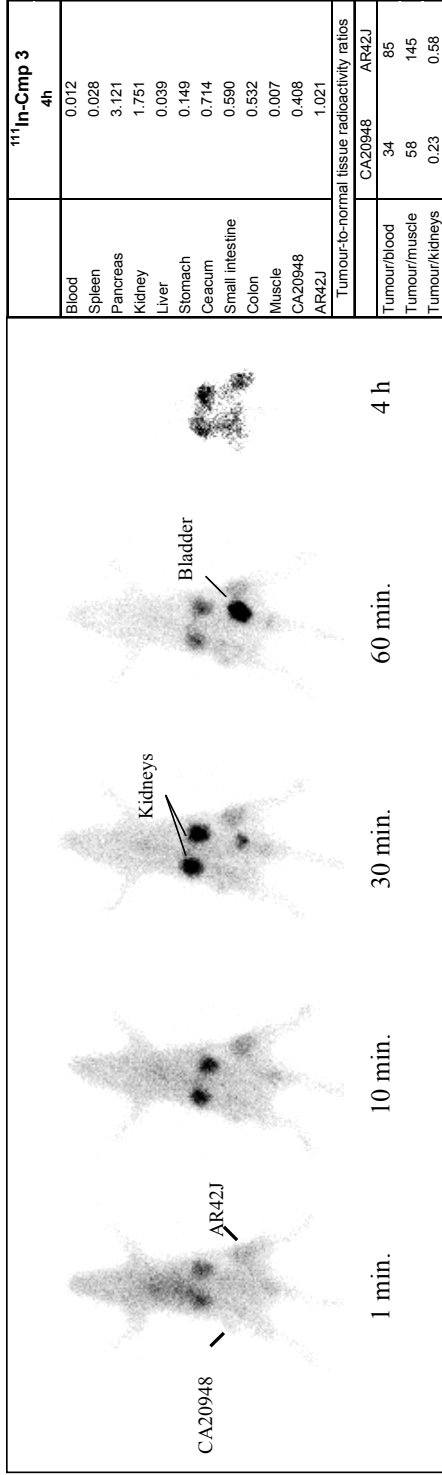


Figure 4 Planar gamma camera images of a rat bearing a CA20948 tumor in the right flank and an AR42J tumor at the left flank 1, 10, 30 and 60 min and 4 h after injection of 0.1 µg ¹¹¹In-Cmp 3 (4 MBq). Biodistribution data obtained from this rat immediately after imaging at 4 h postinjection are shown in the adjacent table. The uptake values are presented as %ID/g tissue.

DISCUSSION

The overexpression of peptide receptors in human tumors is of considerable clinical interest [46]. It has been shown that the overexpression of somatostatin receptors on human neuroendocrine tumors can be targeted successfully. On the one hand, long-term octreotide treatment of patients with somatostatin receptor-expressing tumors has been successful in relieving the symptoms related to excessive hormone production by these tumors [47]. On the other hand, the use of radiolabeled somatostatin analogs has permitted visualization of *in vivo* neuroendocrine tumors and their metastases in patients [23]. In addition, ^{177}Lu - and ^{90}Y -labeled somatostatin analogs have been used in radionuclide therapy in this group of patients [48-55].

It has been reported that the GRP receptor is expressed in high densities on prostate cancers [11, 14, 18-21]. Based on this fact, and the experience with somatostatin receptors, we conclude that targeting the GRP receptor could be the molecular basis for clinical applications such as diagnostic scintigraphy and targeted radionuclide therapy of prostate tumors.

With its 27 amino acid sequence, the GRP peptide has poor *in vivo* stability and has not been found to be useful as a diagnostic or therapeutic agent. The carboxyl-terminal decapeptide of GRP is similar to that of the 14-amino acid peptide BN [56]. BN has a high affinity for the GRP receptor, which makes the development of optimized radiolabeled analogs of the BN peptide a very interesting goal.

As we previously reported, BN analog [DTPA-Pro¹,Tyr⁴]BN (Cmp 1) is capable of visualizing GRP receptor-positive tumors *in vivo*. In this study we developed new DTPA-coupled BN analogs with shortened amino acid sequences containing non-natural amino acid derivatives to improve the receptor binding affinity of the compounds.

The results of the present study show that shortening the amino acid sequence and replacing amino acids by derivatives in the BN analogs improves the receptor affinity for both the rat and the human GRP receptor (Table 1). The new compounds internalized rapidly into GRP-receptor expressing rat and human tumor cells *in vitro*. In *in vivo* biodistribution studies, ^{111}In -Cmp 3 showed a two to three times higher uptake in the GRP receptor-positive pancreas, CA20948 tumor (1.3 times for PC3) and also the whole gastro-intestinal tract compared with ^{111}In -Cmp 1, with a good retention up to 72 h postinjection. This good receptor-mediated tumor uptake and retention of ^{111}In -Cmp 3 combined with its rapid clearance from the body (Table 2) resulted in good tumor-to-blood and tumor-to-muscle ratios ranging from 49 and 146 respectively at 4 h postinjection up to 133 and 89 respectively at 72 h postinjection in the CA20948 tumor-bearing rats. In the CA20948 mouse model the respective CA20948 tumor-to-blood and tumor-to-muscle ratios even reached 99 and 234 (Figure 5). These ratios compare well with those reported for other radiolabeled BN analogs

in the literature [27-30, 32, 36, 40]. For example, the recently published ^{111}In -BZH1 and ^{111}In -BZH2 showed tumor-to-muscle ratios in AR42J tumor-bearing rats of 171 and 99 respectively, compared with 146 for ^{111}In -Cmp 3 at 4 h postinjection [32].

This study shows that shortening the amino acid sequence and replacing specific amino acids in the BN sequence can yield compounds with improved receptor affinity (Table 1). In preliminary studies we found that substitution of the native asparagine at position 6 with other amino acid derivatives did not always adversely affect receptor binding affinity, and the derivatives presented here are examples of modifications which were found to be beneficial. Additionally, not all shortened peptides have improved stability. For example, a peptide identical to Cmp 3, except with the aCmpip at position 5 deleted, has only 32.9% intact peptide left after 4-h incubation in human serum (data not shown), indicating that minor changes in the BN amino acid sequence can have a marked effect on the peptide's stability. In the case of Cmp 3, the characteristic responsible for the increased internalization *in vitro* and *in vivo* is the enhanced receptor affinity and not the serum stability, for the stability of this compound was only marginally improved compared with Cmp 1.

Gamma camera imaging of a CA20948 and AR42J tumor-bearing rat injected with ^{111}In -Cmp 3 showed that the tumor could be visualized as early as at 1 min postinjection (Figure 4). MicroSPECT imaging of a CA20948 tumor-bearing nude mouse injected with the same compound resulted in clear tumor detection with very high tumor-to-background ratios (Figure 5).

The dose-limiting organs in peptide receptor radionuclide therapy using somatostatin analogs are the kidneys, owing to the reabsorption and retention of these radiolabeled peptides. In this case, the kidneys can be protected by infusion of amino acids and by applying individual dosimetry in order to keep the kidney radiation dose below the maximum tolerated dose of 23–27 Gy [57]. However, the effect of amino acid infusion on kidney retention of BN analogs has not been published as yet. Nevertheless, compared with somatostatin analogs these BN analogs have an almost three times lower retention of radioactivity in the kidneys, which is very favorable possible use in radionuclide therapy.

It should be noticed that the *in vitro* and *in vivo* characteristics of some of the analogs obtained in the rat tumor models are sometimes the opposite of those found in the human tumor model. These findings are in agreement with the findings of Maina et al., who recently reported that there are interspecies differences in structure and pharmacology of human and animal GRP receptors [58]. This could be a major pitfall when using rat receptor models for selection of optimized analogs. Human receptor models should therefore always be used to verify the results obtained in rat receptor models. In this study, Cmp 3 has superior receptor binding and internalization characteristics in both rat and human tumor models *in vitro* as well as *in vivo*. In

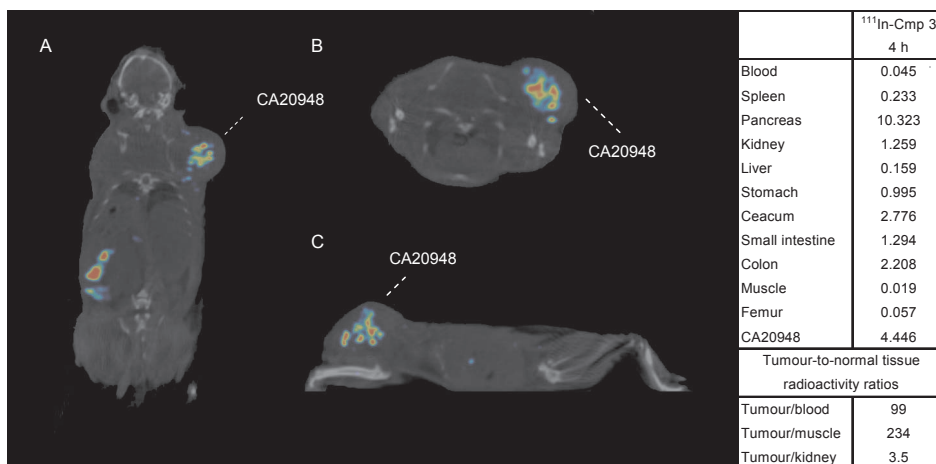


Figure. 5 MicroSPECT/CT images of a Swiss nu/nu mouse bearing a CA20948 tumor on the right shoulder at 4 h postinjection of $0.1 \mu\text{g } ^{111}\text{In}$ -Cmp 3 (10 MBq). Biodistribution data obtained from this mouse immediately after imaging at 4 h postinjection are shown in the adjacent table. The uptake values are presented as %ID/g tissue.

addition, Cmp 3 also showed remarkable binding characteristics in primary human prostate cancer sections ($\text{IC}_{50}=1.3 \text{ nM}$, data not shown).

We plan to study further improvement of the tumor uptake of Cmp 3, e.g. by conjugating this BN analog with the DOTA chelator. Breeman et al. reported an increased GRP receptor affinity and tumor uptake when replacing the DTPA chelator with the DOTA chelator coupled to the $[\text{Pro}^1, \text{Tyr}^4]\text{BN}$ analog (Cmp 1) [34]. Besides radiolabeling with ^{111}In , this DOTA chelator enables radiolabeling with positron emitters like ^{68}Ga and ^{64}Cu for diagnostic PET imaging and also with β -emitters like ^{177}Lu and ^{90}Y ; this may permit their use for radiotherapy to treat GRP receptor-positive tumors [26, 32, 36, 38-40], comparable to the use of ^{90}Y -labeled octreotide and ^{177}Lu -labeled octreotate to treat somatostatin receptor-expressing tumors [48-55]. Also increasing the receptor density on the tumors using gene therapy and, even more interestingly, delivering the radiolabeled analog directly to the tumor using intratumoral injections to improve tumor uptake are to be studied.

In conclusion, the five new BN analogs were compared with analog Cmp 1 concerning receptor binding affinity and *in vitro* internalization into GRP receptor-expressing tumor cells. In addition, Cmp 3, with the best prospects based on the results of these studies, was further characterized *in vivo* for biodistribution and retention characteristics in tumor-bearing rats and mice. We found that ^{111}In -Cmp 3 has good uptake in both rat and human GRP receptor-expressing tumors, which makes this analog a good candidate for molecular imaging and therapy of GRP receptor-positive prostate tumors.

REFERENCES

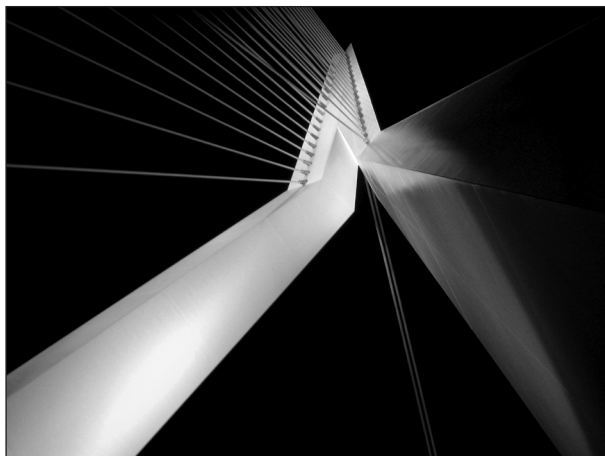
1. Erspamer, V., G.F. Erpamer and M. Inselvini, Some pharmacological actions of alytesin and bombesin. *J Pharm Pharmacol* 1970; 22(11): 875.
2. Kroog, G.S., R.T. Jensen and J.F. Battey, Mammalian bombesin receptors. *Med Res Rev* 1995; 15(5): 389.
3. Fathi, Z., M.H. Corjay, H. Shapira, et al., BRS-3: a novel bombesin receptor subtype selectively expressed in testis and lung carcinoma cells. *J Biol Chem* 1993; 268(8): 5979.
4. Nagalla, S.R., B.J. Barry, K.C. Creswick, et al., Cloning of a receptor for amphibian [Phe¹³] bombesin distinct from the receptor for gastrin-releasing peptide: identification of a fourth bombesin receptor subtype (BB4). *Proc Natl Acad Sci U S A* 1995; 92(13): 6205.
5. Spindel, E.R., E. Giladi, P. Brehm, et al., Cloning and functional characterization of a complementary DNA encoding the murine fibroblast bombesin/gastrin-releasing peptide receptor. *Mol Endocrinol* 1990; 4(12): 1956.
6. Wada, E., J. Way, H. Shapira, et al., cDNA cloning, characterization, and brain region-specific expression of a neuromedin-B-preferring bombesin receptor. *Neuron* 1991; 6(3): 421.
7. Ferris, H.A., R.E. Carroll, D.L. Lorimer, et al., Location and characterization of the human GRP receptor expressed by gastrointestinal epithelial cells. *Peptides* 1997; 18(5): 663.
8. Rettenbacher, M. and J.C. Reubi, Localization and characterization of neuropeptide receptors in human colon. *Naunyn Schmiedebergs Arch Pharmacol* 2001; 364(4): 291.
9. Gugger, M. and J.C. Reubi, Gastrin-releasing peptide receptors in non-neoplastic and neoplastic human breast. *Am J Pathol* 1999; 155(6): 2067.
10. Halmos, G., J.L. Wittliff and A.V. Schally, Characterization of bombesin/gastrin-releasing peptide receptors in human breast cancer and their relationship to steroid receptor expression. *Cancer Res* 1995; 55(2): 280.
11. Markwalder, R. and J.C. Reubi, Gastrin-releasing peptide receptors in the human prostate: relation to neoplastic transformation. *Cancer Res* 1999; 59(5): 1152.
12. Reubi, C., M. Gugger and B. Waser, Co-expressed peptide receptors in breast cancer as a molecular basis for in vivo multireceptor tumour targeting. *Eur J Nucl Med Mol Imaging* 2002; 29(7): 855.
13. Reubi, J.C., S. Wenger, J. Schmuckli-Maurer, et al., Bombesin receptor subtypes in human cancers: detection with the universal radioligand (125)I-[D-TYR(6), beta-ALA(11), PHE(13), NLE(14)] bombesin(6-14). *Clin Cancer Res* 2002; 8(4): 1139.
14. Sun, B., G. Halmos, A.V. Schally, et al., Presence of receptors for bombesin/gastrin-releasing peptide and mRNA for three receptor subtypes in human prostate cancers. *Prostate* 2000; 42(4): 295.
15. Toi-Scott, M., C.L. Jones and M.A. Kane, Clinical correlates of bombesin-like peptide receptor subtype expression in human lung cancer cells. *Lung Cancer* 1996; 15(3): 341.
16. Qin, Y., T. Ertl, R.Z. Cai, et al., Inhibitory effect of bombesin receptor antagonist RC-3095 on the growth of human pancreatic cancer cells in vivo and in vitro. *Cancer Res* 1994; 54(4): 1035.
17. Jemal, A., R. Siegel, E. Ward, et al., Cancer statistics, 2006. *CA Cancer J Clin* 2006; 56(2): 106.
18. Aprikian, A.G., K. Han, S. Chevalier, et al., Bombesin specifically induces intracellular calcium mobilization via gastrin-releasing peptide receptors in human prostate cancer cells. *J Mol Endocrinol* 1996; 16(3): 297.
19. Bartholdi, M.F., J.M. Wu, H. Pu, et al., In situ hybridization for gastrin-releasing peptide receptor (GRP receptor) expression in prostatic carcinoma. *Int J Cancer* 1998; 79(1): 82.
20. Reile, H., P.E. Armatis and A.V. Schally, Characterization of high-affinity receptors for bombesin/gastrin releasing peptide on the human prostate cancer cell lines PC-3 and DU-145: internalization of receptor bound 125I-(Tyr⁴) bombesin by tumor cells. *Prostate* 1994; 25(1): 29.
21. Xiao, D., J. Wang, L.L. Hampton, et al., The human gastrin-releasing peptide receptor gene structure, its tissue expression and promoter. *Gene* 2001; 264(1): 95.

22. Plonowski, A., A. Nagy, A.V. Schally, et al., In vivo inhibition of PC-3 human androgen-independent prostate cancer by a targeted cytotoxic bombesin analogue, AN-215. *Int J Cancer* 2000; 88(4): 652.
23. Krenning, E.P., D.J. Kwekkeboom, W.H. Bakker, et al., Somatostatin receptor scintigraphy with [¹¹¹In-DTPA-D-Phe¹]- and [¹²³I-Tyr³]-octreotide: the Rotterdam experience with more than 1000 patients. *Eur J Nucl Med* 1993; 20(8): 716.
24. Kwekkeboom, D., E.P. Krenning and M. de Jong, Peptide receptor imaging and therapy. *J Nucl Med* 2000; 41(10): 1704.
25. Otte, A., E. Jermann, M. Behe, et al., DOTATOC: a powerful new tool for receptor-mediated radionuclide therapy. *Eur J Nucl Med* 1997; 24(7): 792.
26. Hoffman, T.J., H. Gali, C.J. Smith, et al., Novel series of ¹¹¹In-labeled bombesin analogs as potential radiopharmaceuticals for specific targeting of gastrin-releasing peptide receptors expressed on human prostate cancer cells. *J Nucl Med* 2003; 44(5): 823.
27. La Bella, R., E. Garcia-Garayoa, M. Langer, et al., In vitro and in vivo evaluation of a ^{99m}Tc(I)-labeled bombesin analogue for imaging of gastrin releasing peptide receptor-positive tumors(1). *Nucl Med Biol* 2002; 29(5): 553.
28. Nock, B., A. Nikolopoulou, E. Chiotellis, et al., [(^{99m}Tc)Demobesin 1, a novel potent bombesin analogue for GRP receptor-targeted tumour imaging. *Eur J Nucl Med Mol Imaging* 2003; 30(2): 247.
29. Nock, B.A., A. Nikolopoulou, A. Galanis, et al., Potent bombesin-like peptides for GRP-receptor targeting of tumors with ^{99m}Tc: a preclinical study. *J Med Chem* 2005; 48(1): 100.
30. Smith, C.J., G.L. Sieckman, N.K. Owen, et al., Radiochemical investigations of gastrin-releasing peptide receptor-specific [(^{99m}Tc(X)(CO)₃-Dpr-Ser-Ser-Ser-Gln-Trp-Ala-Val-Gly-His-Leu-Met-(NH₂)] in PC-3, tumor-bearing, rodent models: syntheses, radiolabeling, and in vitro/in vivo studies where Dpr = 2,3-diaminopropionic acid and X = H₂O or P(CH₂OH)₃. *Cancer Res* 2003; 63(14): 4082.
31. Van de Wiele, C., F. Dumont, R.A. Dierckx, et al., Biodistribution and dosimetry of (^{99m}Tc-RP527, a gastrin-releasing peptide (GRP) agonist for the visualization of GRP receptor-expressing malignancies. *J Nucl Med* 2001; 42(11): 1722.
32. Zhang, H., J. Chen, C. Waldherr, et al., Synthesis and evaluation of bombesin derivatives on the basis of pan-bombesin peptides labeled with indium-111, lutetium-177, and yttrium-90 for targeting bombesin receptor-expressing tumors. *Cancer Res* 2004; 64(18): 6707.
33. Breeman, W.A., M. De Jong, B.F. Bernard, et al., Pre-clinical evaluation of [(¹¹¹In-DTPA-Pro(1), Tyr(4))bombesin, a new radioligand for bombesin-receptor scintigraphy. *Int J Cancer* 1999; 83(5): 657.
34. Breeman, W.A., M. de Jong, J.L. Erion, et al., Preclinical comparison of (¹¹¹In)-labeled DTPA- or DOTA-bombesin analogs for receptor-targeted scintigraphy and radionuclide therapy. *J Nucl Med* 2002; 43(12): 1650.
35. Breeman, W.A., L.J. Hofland, M. de Jong, et al., Evaluation of radiolabelled bombesin analogues for receptor-targeted scintigraphy and radiotherapy. *Int J Cancer* 1999; 81(4): 658.
36. Chen, X., R. Park, Y. Hou, et al., microPET and autoradiographic imaging of GRP receptor expression with ⁶⁴Cu-DOTA-[Lys³]bombesin in human prostate adenocarcinoma xenografts. *J Nucl Med* 2004; 45(8): 1390.
37. Meyer, G.J., H. Macke, J. Schuhmacher, et al., ⁶⁸Ga-labelled DOTA-derivatised peptide ligands. *Eur J Nucl Med Mol Imaging* 2004; 31(8): 1097.
38. Rogers, B.E., H.M. Bigott, D.W. McCarthy, et al., MicroPET imaging of a gastrin-releasing peptide receptor-positive tumor in a mouse model of human prostate cancer using a ⁶⁴Cu-labeled bombesin analogue. *Bioconjug Chem* 2003; 14(4): 756.
39. Schuhmacher, J., H. Zhang, J. Doll, et al., GRP receptor-targeted PET of a rat pancreas carcinoma xenograft in nude mice with a ⁶⁸Ga-labeled bombesin(6-14) analog. *J Nucl Med* 2005; 46(4): 691.

40. Smith, C.J., H. Gali, G.L. Sieckman, et al., Radiochemical investigations of (177)Lu-DOTA-8-Aoc-BBN[7-14]NH(2): an in vitro/in vivo assessment of the targeting ability of this new radiopharmaceutical for PC-3 human prostate cancer cells. *Nucl Med Biol* 2003; 30(2): 101.
41. Bakker, W.H., R. Albert, C. Bruns, et al., [111In-DTPA-D-Phe1]-octreotide, a potential radiopharmaceutical for imaging of somatostatin receptor-positive tumors: synthesis, radiolabeling and in vitro validation. *Life Sci* 1991; 49(22): 1583.
42. Bakker, W.H., E.P. Krenning, J.C. Reubi, et al., In vivo application of [111In-DTPA-D-Phe1]-octreotide for detection of somatostatin receptor-positive tumors in rats. *Life Sci* 1991; 49(22): 1593.
43. Bernard, B.F., E. Krenning, W.A. Breeman, et al., Use of the rat pancreatic CA20948 cell line for the comparison of radiolabelled peptides for receptor-targeted scintigraphy and radionuclide therapy. *Nucl Med Commun* 2000; 21(11): 1079.
44. van Weerden, W.M., C.M. de Ridder, C.L. Verdaasdonk, et al., Development of seven new human prostate tumor xenograft models and their histopathological characterization. *Am J Pathol* 1996; 149(3): 1055.
45. De Jong, M., B.F. Bernard, E. De Bruin, et al., Internalization of radiolabelled [DTPA0]octreotide and [DOTA0,Tyr3]octreotide: peptides for somatostatin receptor-targeted scintigraphy and radionuclide therapy. *Nucl Med Commun* 1998; 19(3): 283.
46. Reubi, J.C., Peptide receptors as molecular targets for cancer diagnosis and therapy. *Endocr Rev* 2003; 24(4): 389.
47. Lamberts, S.W., E.P. Krenning and J.C. Reubi, The role of somatostatin and its analogs in the diagnosis and treatment of tumors. *Endocr Rev* 1991; 12(4): 450.
48. Bodei, L., M. Cremonesi, S. Zoboli, et al., Receptor-mediated radionuclide therapy with 90Y-DOTATOC in association with amino acid infusion: a phase I study. *Eur J Nucl Med Mol Imaging* 2003; 30(2): 207.
49. de Jong, M., D. Kwekkeboom, R. Valkema, et al., Radiolabelled peptides for tumour therapy: current status and future directions. Plenary lecture at the EANM 2002. *Eur J Nucl Med Mol Imaging* 2003; 30(3): 463.
50. De Jong, M., R. Valkema, F. Jamar, et al., Somatostatin receptor-targeted radionuclide therapy of tumors: preclinical and clinical findings. *Semin Nucl Med* 2002; 32(2): 133.
51. Kwekkeboom, D.J., W.H. Bakker, B.L. Kam, et al., Treatment of patients with gastro-entero-pancreatic (GEP) tumours with the novel radiolabelled somatostatin analogue [177Lu-DOTA(0),Tyr3]octreotate. *Eur J Nucl Med Mol Imaging* 2003; 30(3): 417.
52. Kwekkeboom, D.J., W.H. Bakker, P.P. Kooij, et al., [177Lu-DOTAOTyr3]octreotate: comparison with [111In-DTPA0]octreotide in patients. *Eur J Nucl Med* 2001; 28(9): 1319.
53. Otte, A., J. Mueller-Brand, S. Dellas, et al., Yttrium-90-labelled somatostatin-analogue for cancer treatment. *Lancet* 1998; 351(9100): 417.
54. Paganelli, G., S. Zoboli, M. Cremonesi, et al., Receptor-mediated radiotherapy with 90Y-DOTA-D-Phe1-Tyr3-octreotide. *Eur J Nucl Med* 2001; 28(4): 426.
55. Waldherr, C., M. Pless, H.R. Maecke, et al., The clinical value of [90Y-DOTA]-D-Phe1-Tyr3-octreotide (90Y-DOTATOC) in the treatment of neuroendocrine tumours: a clinical phase II study. *Ann Oncol* 2001; 12(7): 941.
56. Sunday, M.E., L.M. Kaplan, E. Motoyama, et al., Gastrin-releasing peptide (mammalian bombesin) gene expression in health and disease. *Lab Invest* 1988; 59(1): 5.
57. Emami, B., J. Lyman, A. Brown, et al., Tolerance of normal tissue to therapeutic irradiation. *Int J Radiat Oncol Biol Phys* 1991; 21(1): 109.
58. Maina, T., B.A. Nock, H. Zhang, et al., Species differences of bombesin analog interactions with GRP-R define the choice of animal models in the development of GRP-R-targeting drugs. *J Nucl Med* 2005; 46(5): 823.

5

Molecular imaging of gastrin-releasing peptide receptor-positive tumors in mice using ^{64}Cu - and ^{86}Y -DOTA-(Pro¹,Tyr⁴)-bombesin(1-14)



Gráinne B. Biddlecombe
Buck E. Rogers
Monique de Visser
Jesse J. Parry
Marion de Jong
Jack L. Erion
Jason S. Lewis

Bioconjugate Chemistry 2007; Vol. 18(3):724–730

ABSTRACT

Bombesin is a tetradecapeptide neurohormone that binds to gastrin releasing peptide receptors (GRPR). GRPRs have been found in a variety of cancers including invasive breast and prostate tumors. The peptide MP2346 (DOTA-(Pro¹,Tyr⁴)-Bombesin(1-14)) was designed to bind to these GRP receptors. This study was undertaken to evaluate radiolabeled MP2346 as a Positron Emission Tomography (PET) imaging agent. MP2346 was radiolabeled, in high radiochemical purity, with the positron-emitting nuclides ⁶⁴Cu ($t_{1/2} = 12.7$ h, $\beta^+ = 19.3\%$, $E_{\text{avg}} = 278$ keV) and ⁸⁶Y ($t_{1/2} = 14.7$ h, $\beta^+ = 33\%$, $E_{\text{avg}} = 664$ keV). ⁶⁴Cu-MP2346 and ⁸⁶Y-MP2346 were studied *in vitro* for cellular internalization by GRPR expressing PC-3 (human prostate adenocarcinoma) cells. Both ⁶⁴Cu- and ⁸⁶Y-MP2346 were studied *in vivo* for tissue distribution in nude mice with PC-3 tumors. Biodistribution in PC3 tumor-bearing mice demonstrated higher tumor uptake, but lower liver retention, in animals injected with ⁸⁶Y-MP2346 compared to ⁶⁴Cu-MP2346. Receptor mediated uptake was confirmed by a significant reduction in uptake in the PC-3 tumor and other receptor-rich tissues by co-injection of a blockade. Small animal PET/CT imaging was carried out in mice bearing PC-3 tumors and rats bearing AR42J tumors. It was possible to delineate PC-3 tumors *in vivo* with ⁶⁴Cu-MP2346, but superior ⁸⁶Y-MP2346-PET images were obtained due to lower uptake in clearance organs and lower background activity. The ⁸⁶Y analog demonstrated excellent PET image quality in models of prostate cancer for the delineation of the GRPR-rich tumors and warrants further investigation.

INTRODUCTION

Gastrin-releasing peptide (GRP), a 27-amino acid mammalian peptide, is responsible for the release of gastrin from stomach cells. The receptor for GRP (GRPR) has been found in a variety of cancers including ovarian, lung, gastrointestinal and colon [1-6]. GRPRs have also been shown to be present on invasive breast and prostate tumors [7, 8]. Bombesin (BN) is a 14-amino acid neuropeptide that was originally isolated from the skin of the Bombina frog and binds with high affinity to GRPR [9]. A non-invasive method of detecting (by imaging) and treating GRPR-positive tumors has been achieved by the radiolabeling of BN analogs with diagnostic and therapeutic radionuclides [10-12].

Indium-111 and ^{99m}Tc -labeled BN analogs have been studied as potential single-photon emission computed tomography (SPECT) radiopharmaceuticals [13-20]. BN analogs radiolabeled with ^{131}I , ^{188}Re and ^{177}Lu [21-23] have been evaluated for potential radiotherapy applications. Positron emission tomography (PET) is a more quantitative imaging method compared to SPECT with better spatial resolution and image contrast. Animal studies have been carried out using ^{68}Ga -, ^{18}F - and ^{64}Cu -labeled BN analogs utilizing PET and have shown good tumor localization and visualization [24-28].

Copper-64 ($t_{1/2} = 12.7$ h, $\beta^+ = 19.3\%$, $E_{\text{avg}} = 278$ keV) and ^{86}Y ($t_{1/2} = 14.7$ h, $\beta^+ = 33\%$, $E_{\text{avg}} = 664$ keV), can both be prepared on small cyclotrons utilizing the $^{64}\text{Ni}(\text{p},\text{n})^{64}\text{Cu}$ and $^{86}\text{Sr}(\text{p},\text{n})^{86}\text{Y}$ reactions, respectively [29, 30]. Due to the decay scheme of ^{64}Cu (17.4% β^+ , 41% EC, 40% β^-) it has the potential to be used both for diagnostic and therapeutic applications [31]. Yttrium-86 is a PET-emitting nuclide and can act as an imaging surrogate for ^{90}Y , which has been used extensively in nuclear medicine as a therapeutic nuclide. DOTA-(Pro¹, Tyr⁴)-Bombesin(1-14) (MP2346), where DOTA = 1,4,7,10-tetraazacyclododecan-*N,N,N',N''*-tetraacetic acid, (Figure 1) was previously synthesized and demonstrated promise for scintigraphic imaging of GRPR-expressing

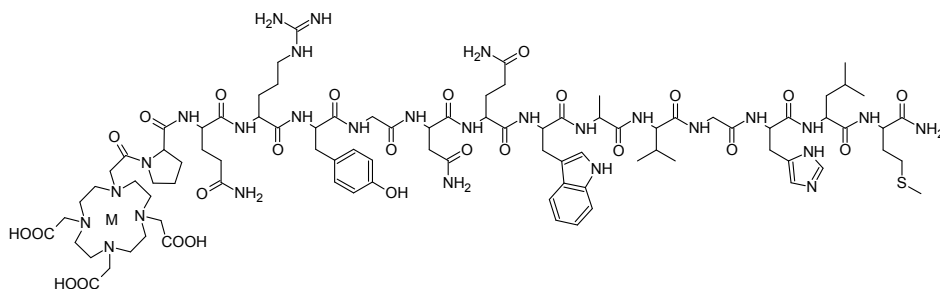


Figure 1. Structure of MP2346 (DOTA-Pro-Gln-Arg-Tyr-Gly-Asn-Gln-Trp-Ala-Val-Gly-His-Leu-Met-NH₂) with M corresponding to the chelated ^{64}Cu or ^{86}Y metal.

tumors after radiolabeling with ^{111}In [13]. The goal of this study was to evaluate both ^{64}Cu - and ^{86}Y -radiolabeled MP2346 as candidates for the non-invasive detection of GRPR-positive tumors using PET.

EXPERIMENTAL PROCEDURES

General methods and materials

All chemicals unless otherwise stated were purchased from the Sigma-Aldrich Chemical Company (St. Louis, MO, USA). Water was distilled and then deionized ($18\text{ M}\Omega/\text{cm}^2$) by passing through a milli-Q® water filtration system (Millipore Corp., Milford, MA, USA). Copper-64 and ^{86}Y were produced on a CS-15 biomedical cyclotron at Washington University School of Medicine, using published methods [29, 30]. PC-3 (human prostate adenocarcinoma) cells were obtained from American Type Culture Collection (ATCC) (Manassas, VA, USA) and maintained in our laboratories by serial cell culture. Radioactivity was counted with a Beckman Gamma 8000 counter containing a NaI crystal (Beckman Instruments, Inc., Irvine, CA, USA).

Radiolabeling of MP2346.

The GRPR binding peptide MP2346 (CAS 593287-40-2) was synthesized by a solid phase method as described and its purity was confirmed with HPLC and mass spectrometry [14]. Labeling of MP2346 (10 μg) with $^{64}\text{CuCl}_2$ (11.15 mCi) took place in a 100 μl aliquot of 0.5M NH_4OAc (pH 5.5) incubated at 80°C for 30 min. Quality control of the product was performed using radio thin-layer chromatography on MKC_{18}F silica gel plates using NH_4OAc /methanol (30:70) as the mobile phase ($^{64}\text{CuCl}_2$ $R_f = 0$; ^{64}Cu -MP2346 $R_f = 0.7$). The reaction between MP2346 (1.8 μg) with $^{86}\text{YCl}_3$ (2.1 mCi) took place in 0.5M NH_4OAc (pH 6.5) incubated at 80°C for 30 min. Quality control was performed using the same TLC conditions as with the ^{64}Cu analog ($^{86}\text{YCl}_3$ $R_f = 0$; ^{86}Y -MP2346 $R_f = 0.5$). Reaction progress and purity were also monitored by analytical reversed-phase HPLC, which was performed on an Waters Alliance 2695 Separations Module (Milford, MA, USA) with a Waters 996 photodiode array detector (PDA) and an Carroll & Ramsey 105-S1 radioactivity detector (Berkeley, CA, USA) with a Waters XTerra™ MS C_{18} 3.5 μm (2.1 \times 50 mm) column. The mobile phase was H_2O (0.1% formic acid) and CH_3CN (solvent B). The gradient consisted of 15% B to 85% A in 60 min (0.5 mL/min flow rate) (^{64}Cu -MP2346, $t_R = 5.8$ min; ^{86}Y -MP2346, $t_R = 6.9$ min; unreacted ^{64}Cu or ^{86}Y were eluted in the void volume, $t_R < 1.0$ min; uncomplexed MP2346, $t_R = 16.4$ min).

Internalization studies

PC-3 cells were harvested and seeded into 6-well plates at 5×10^5 cells per well. On the following day, the cells were washed with Hank's balanced salt solution (HBSS), and 1 ml of internalization media (DMEM plus 30 mM HEPES, 2 mM L-glutamine, 1 mM sodium pyruvate, and 1% BSA) was added to each well. The ^{64}Cu -MP2346 or ^{86}Y -MP2346 was then added such that the final concentration of peptide was approximately 1 nM. To three of the six wells per plate, an excess (10 μg) of [Tyr⁴]-Bombesin (Sigma Chemical Co., St. Louis, MO) was added to act as an inhibitor. The plates (one per time point) were then incubated at 37°C for 15, 30, 60, 120, 240, or 1200 min. At each time point, the corresponding plate was removed, the radioactive media was aspirated, and the cells were washed with cold HBSS. This was followed by an acid wash (HBSS plus 20 mM sodium acetate, pH 4.0), which was collected for the determination of surface bound radioactivity. Immediately after collection of the acid wash, 1 ml of 10 mM sodium borate/1.0% SDS was added to the wells and allowed to incubate for 2-3 minutes at room temperature to facilitate cell lysis. The lysates were collected and, along with the surface fractions, were counted on a gamma counter. Protein amounts were determined using the Pierce BCA™ Protein Assay Kit (Rockford, IL, USA) in a separate set of plates in which all of the steps were followed, but no radioactivity was added. The data are presented as fmol of internalized radioactivity normalized to protein amount. Maximum internalizations were determined from non-linear curve fitting using Prism software and the one site binding hyperbola equation provided.

Biodistribution studies

All animal experiments were conducted in compliance with the Guidelines for the Care and Use of Research Animals established by Washington University's Animal Studies Committee. Biodistribution studies were carried out on male athymic nude mice (Charles River Laboratories, Wilmington, MA, USA) that had been implanted with 3×10^6 PC-3 cells into either the upper-right or lower-left flank of the animal. Tumors were allowed to grow for 36 days after implantation, at which time the animals received either 8-10 μCi of ^{64}Cu -MP2346 or ^{86}Y -MP2346 (7-10 ng) in 50 μL of saline via lateral tail vein injection. Animals were then euthanized at desired time points (1, 4 and 24 h, $n = 5$ per group). Two additional groups of mice (1 h time point only) were pre-injected with unlabeled peptide to act as a receptor-blockade (100 μg of [Tyr⁴]-Bombesin) immediately prior to administering ^{64}Cu -MP2346 or ^{86}Y -MP2346. This constitutes a 10,000 or 15,000 fold increase over the mass of peptide injected with ^{64}Cu -MP2346 or ^{86}Y -MP2346 respectively. Following sacrifice, selected tissues and organs of interest were then removed and weighed and radioactivity measured in a gamma counter. The percent dose per gram (%ID/g) was then calculated.

Imaging studies

Small animal PET images were obtained on a microPET-FOCUS 220 (Siemens Medical Solutions USA, Inc) [32] and were co-registered with CT images from a MicroCAT II System (ImTek Inc., Knoxville, Tennessee, USA). Mice were anesthetized with 1-2% isoflurane prior to scanning, positioned supine and immobilized in a custom prepared cradle. To reduce scattering caused by the prompt gammas of ^{86}Y the energy window of the small animal PET (typically 250-750 keV) was narrowed to 470-580 keV, and the data obtained normalized to a ^{86}Y cylinder phantom. The image registration between microCT and PET images was accomplished by using a landmark registration technique with AMIRA image display software (AMIRA, TGS Inc, San Diego, CA, USA). The registration method proceeds by rigid transformation of the microCT images from landmarks provided by fiducial markers directly attached to the animal bed. Images were obtained of male athymic nude mice (Charles River Laboratories, Wilmington, MA, USA) that had been implanted with 3×10^6 PC-3 cells into the right flank. Images of male Lewis rats (Charles River Laboratories, Wilmington, MA, USA) that had been implanted with AR42J tumor pieces in the left flank of the rat 10 days before the study were also obtained. In these studies, the mice received either ^{64}Cu -MP2346 ($n = 3$, 125 μCi , 125 ng) or ^{86}Y -MP2346 ($n = 3$, 200 μCi , 200 ng). These mice were imaged side by side with mice ($n = 3$ per group) that had been co-administered with 100 μg of [Tyr⁴]-Bombesin along with the radiolabeled peptide. The Lewis rats in the ^{86}Y -MP2346 PET study were imaged individually. One group ($n = 3$) was given ^{86}Y -MP2346 (200 μCi , 200 ng) and another group ($n = 3$) was co-administered 100 μg of [Tyr⁴]-Bombesin. For imaging studies tumor, kidney and liver standard uptake values (SUV, defined as the ratio of activity in tissue per milliliter to the activity in the injected dose per subject body weight; $(\text{nCi/ml}) \times [\text{weight (g)}/\text{injected dose (nCi)}]$) of ^{64}Cu - or ^{86}Y -activity were generated by measuring regions of interest that encompassed the entire organ from the small animal PET images.

Statistical methods

All of the data are presented as mean \pm SD. For statistical classification, a Student's *t* test was performed using GraphPad PRISM (San Diego, CA, USA). Differences at the 95% confidence level ($p < 0.05$) were considered significant.

RESULTS

Radiolabeling of MP2346

Radiolabeling of MP2346 with ^{64}Cu and ^{86}Y was performed over a range of temperatures, incubation times and buffer pH's. The optimal conditions for labeling MP2346

with $^{64}\text{CuCl}_2$ in 0.5M NH_4OAc (pH 5.5) were found to be 80°C degrees for 30 minutes. Radiochemical yields >99% at a specific activity of 0.99 mCi/ μg (1958 mCi/ μmol) were achieved. The ^{86}Y analog was labeled with $^{86}\text{YCl}_3$ in 0.5M NH_4OAc (pH 6.5) at 80°C over 30 minutes. Radiochemical yields >94% (1.0 mCi/ μg ; 2000 mCi/ μmol) were obtained by this method.

Internalization studies

The internalization of ^{64}Cu -MP2346 and ^{86}Y -MP2346 into PC-3 (human prostate adenocarcinoma) cells is shown in figure 2. The internalization of ^{64}Cu -MP2346 and ^{86}Y -MP2346 were monitored over a 20 h period. The amount of specifically internalized peptide normalized to the protein content of the cells was 121.83 ± 33.74 fmol/mg for ^{64}Cu -MP2346 and 28.09 ± 30.76 fmol/mg for ^{86}Y -MP2346 after 15 min incubation. Internalization increased steadily for both compounds and after 20 h of incubation, 512.04 ± 83.41 fmol/mg of ^{64}Cu -MP2346 and 1420.419 ± 129.94 fmol/mg of ^{86}Y -MP2346 were internalized into the PC-3 cells. The amount of surface-bound radioactivity was <100 fmol/mg for all time points (data not shown). Non-linear curve fitting showed that the maximum internalization was 535 fmol/mg for ^{64}Cu -MP2346 and 1945 fmol/mg for ^{86}Y -MP2346.

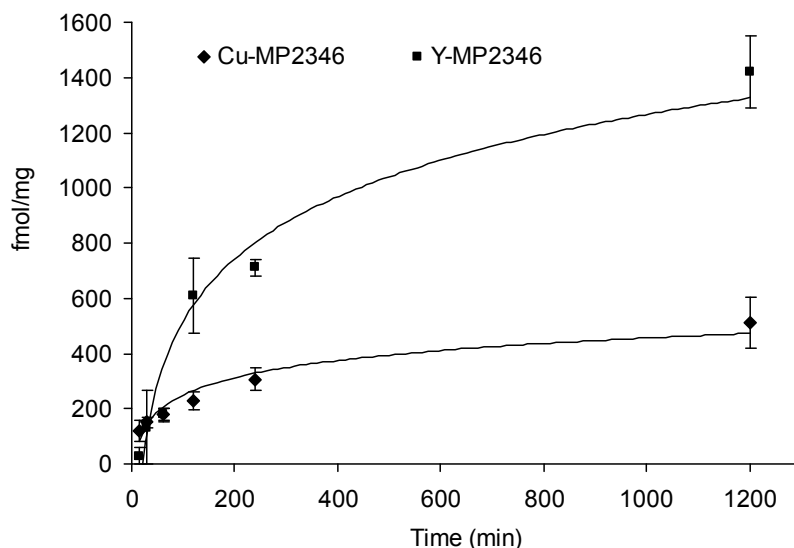


Figure 2. Internalization of ^{64}Cu -MP2346 and ^{86}Y -MP2346 into PC-3 cells. ^{64}Cu -MP2346 or ^{86}Y -MP2346 was added to the cells and incubated at 37 °C. At various time points, the media was removed, the cells acid-washed to remove surface bound radioactivity, and harvested. The cell pellets (internalized) and acid wash (surface bound) were counted. The data are presented as fmol of internalized radioactivity normalized to protein amount against time. The data are shown as the mean of 3 experiments \pm SD with each experiment being performed in triplicate.

Biodistribution studies

Biodistribution studies were carried out on male athymic nude mice that had been implanted with PC-3 tumors into the right flank of the animals. Tumors were allowed to grow for 36 days, at which time the animals either received 8-10 μCi (~8-10 ng) of ^{64}Cu -MP2346 or 8-10 μCi (~8-10 ng) of ^{86}Y -MP2346 via tail vein injection. The mass of the injected peptide was the same for the two radiocompounds and therefore differences between the biodistribution profiles are not due to the mass of the peptide

Table 1. Biodistribution of ^{64}Cu -MP2346 and ^{86}Y -MP2346 in male nude mice bearing day-36 PC-3 tumors (%ID/g \pm standard deviation, $n = 5$) at 1, 4 and 24 h^a

Tissue	1 hour	4 hour	24 hour
^{64}Cu -MP2346			
blood	0.128 \pm 0.015	0.076 \pm 0.024	0.069 \pm 0.007
lung	0.426 \pm 0.117	0.409 \pm 0.166	0.218 \pm 0.043
liver(all)	1.329 \pm 0.304	1.412 \pm 0.345	1.089 \pm 0.429
spleen	0.278 \pm 0.098	0.332 \pm 0.135	0.175 \pm 0.049
kidney	6.148 \pm 1.067	4.936 \pm 0.810	1.222 \pm 0.296
muscle	0.316 \pm 0.255	0.084 \pm 0.120	0.034 \pm 0.013
fat	0.071 \pm 0.038	0.045 \pm 0.046	0.012 \pm 0.017
heart	0.160 \pm 0.048	0.121 \pm 0.038	0.185 \pm 0.024
bone	0.885 \pm 0.928	0.131 \pm 0.101	0.038 \pm 0.026
pancreas	4.387 \pm 1.090	3.339 \pm 0.463	1.155 \pm 0.327
PC-3 tumor	0.793 \pm 0.181	0.421 \pm 0.214	0.309 \pm 0.199
pancreas ^a	0.464 \pm 0.259		
PC-3 tumor ^a	0.099 \pm 0.134		
^{86}Y -MP2346			
blood	0.219 \pm 0.098	0.009 \pm 0.002	0.001 \pm 0.001
lung	0.302 \pm 0.062	0.097 \pm 0.060	0.030 \pm 0.020
liver(all)	0.170 \pm 0.027	0.145 \pm 0.048	0.152 \pm 0.069
spleen	0.742 \pm 0.296	0.803 \pm 0.241	0.463 \pm 0.105
kidney	8.309 \pm 2.412	8.789 \pm 2.106	2.623 \pm 0.391
muscle	0.089 \pm 0.010	0.016 \pm 0.002	0.005 \pm 0.004
fat	0.059 \pm 0.007	0.006 \pm 0.006	0.003 \pm 0.002
heart	0.091 \pm 0.030	0.022 \pm 0.010	0.002 \pm 0.002
bone	0.336 \pm 0.228	0.087 \pm 0.025	0.044 \pm 0.012
pancreas	14.456 \pm 5.719	13.358 \pm 2.954	12.965 \pm 2.229
PC-3 tumor	2.646 \pm 1.228	1.243 \pm 0.658	1.405 \pm 0.222
pancreas ^a	0.304 \pm 0.018		
PC-3 tumor ^a	0.667 \pm 0.179		

Note; ^aTwo additional groups were pre-administered blockade (100 μg of [Tyr⁴]-Bombesin) immediately prior to administering ^{64}Cu -MP2346 or ^{86}Y -MP2346. Similar trends were also observed for the other receptor-rich tissues, the stomach and intestines, where uptake of the two radiocompounds was significantly reduced by administration of blockade.

Table 2. Selected tumor/organ ratios for ^{64}Cu - and ^{86}Y -MP2346 in male nude mice bearing day-36 PC-3 tumors (%ID/g \pm standard deviation, $n = 5$) at 1, 4 and 24 h.

Compound (h)	^{64}Cu (1 h)	^{86}Y (1 h)	^{64}Cu (4 h)	^{86}Y (4 h)	^{64}Cu (24 h)	^{86}Y (24 h)
Tumor/Blood	6.192	12.074	5.511	134.3	4.487	1680
Tumor/Muscle	2.718	29.89	4.996	79.20	9.056	271.4
Tumor/Liver	0.597	15.60	0.298	8.590	0.284	9.223
Tumor/Kidney	0.129	0.318	0.085	0.141	0.253	0.536

administered. Table 1 shows the summary of the biodistribution data of ^{64}Cu -MP2346 and ^{86}Y -MP2346 in male nude mice bearing PC-3 tumors at 1, 4 and 24 h. Table 2 gives selected tumor/organ ratios for ^{64}Cu -MP2346 and ^{86}Y -MP2346.

Both ^{64}Cu -MP2346 and ^{86}Y -MP2346 demonstrated rapid clearance of radioactivity from the blood over the 24 h period. Although blood levels of ^{86}Y -MP2346 were initially higher at 1 h compared to the ^{64}Cu -analog (0.219 ± 0.098 vs. 0.128 ± 0.015 %ID/g, $p < 0.005$) by 24 h there was a significant reduction in the blood levels of ^{86}Y -MP2346 compared to ^{64}Cu -MP2346 (0.001 ± 0.001 vs. 0.069 ± 0.007 %ID/g, $p < 0.0001$). This combined with the increased uptake of ^{86}Y -MP2346 in the tumor resulted in over a 300-fold increase in the T/B ratio for ^{86}Y -MP2346 compared to ^{64}Cu -MP2346 at 24 h.

The liver activity of ^{64}Cu -MP2346 is consistently higher at all time points (1 h, 1.329 ± 0.304 %ID/g; 4 h, 1.412 ± 0.345 %ID/g; 24 h, 1.089 ± 0.429 %ID/g) compared to ^{86}Y -MP2346 (1 h, 0.170 ± 0.027 %ID/g; 4 h, 0.145 ± 0.048 %ID/g; 24 h, 0.152 ± 0.069 %ID/g). These data result in superior tumor/liver ratios for the ^{86}Y -MP2346 (Table 2). It is also important to note that for both agents, there is very little liver clearance of activity over 24 h. Kidney uptake of ^{64}Cu -MP2346 was initially high but reduced ~5-fold by 24 h (1 h, 6.148 ± 1.067 %ID/g; 4 h, 4.936 ± 0.810 %ID/g; 24 h, 1.222 ± 0.296 %ID/g). In contrast ^{86}Y -MP2346 showed slightly higher kidney retention at 1 h (8.309 ± 2.412 %ID/g), which remained constant over 4 h (8.789 ± 2.106 %ID/g) and then only showed a 3-fold decrease by 24 h (2.623 ± 0.391 %ID/g).

The GRPR-rich pancreas demonstrated uptake of ^{64}Cu -MP2346 (1 h, 4.387 ± 1.090 %ID/g; 4 h, 3.339 ± 0.463 %ID/g; 24 h, 1.155 ± 0.327 %ID/g) which was significantly lower ($p < 0.001$) than values obtained for ^{86}Y -MP2346 at all time points (1 h, 14.456 ± 5.719 %ID/g; 4 h, 13.358 ± 2.954 %ID/g; 24 h, 12.965 ± 2.229 %ID/g). To demonstrate receptor mediated targeting of the agents two additional groups were pre-administered blockade (100 μg of [Tyr⁴]-Bombesin) immediately prior to administering ^{64}Cu -MP2346 or ^{86}Y -MP2346 and were sacrificed at 1 h postinjection. In these animals, the pancreas demonstrated receptor mediated blocking with a significant decrease in tissue retention of the tracers in the receptor-rich pancreas compared to the non-blocked animals (^{64}Cu -MP2346, 0.464 ± 0.259 vs. 4.387 ± 1.090 %ID/g, $p < 0.0005$; ^{86}Y -MP2346, 0.304 ± 0.018 vs. 14.456 ± 5.719 %ID/g, $p < 0.0005$). Similar trends were also observed for the other receptor-rich tissues, the stomach and the

intestines, where uptake of the tracers was significantly reduced by administration of blockade (data not shown).

Uptake of ^{86}Y -MP2346 into the GRPR-rich PC-3 tumor was significantly higher at all time points compared to ^{64}Cu -MP2346 (1 h, 2.646 ± 1.228 vs. 0.793 ± 0.181 %ID/g, $p < 0.0005$; 4 h, 1.243 ± 0.658 vs. 0.421 ± 0.214 %ID/g, $p < 0.0005$; 24 h, 1.405 ± 0.222 vs. 0.309 ± 0.199 %ID/g, $p < 0.0005$), resulting in superior tumor/blood, tumor/muscle and tumor/liver ratios for ^{86}Y -MP2346 compared to ^{64}Cu -MP2346 (Table 2). Administration of blockade (100 μg of [Tyr⁴]-Bombesin) immediately prior to administering ^{64}Cu -MP2346 or ^{86}Y -MP2346 resulted in significant reduction in PC-3 tumor accumulation for both agents (^{64}Cu -MP2346, 0.099 ± 0.134 vs. 0.793 ± 0.181 %ID/g, $p < 0.0005$; ^{86}Y -MP2346, 0.667 ± 0.179 vs. 2.646 ± 1.228 %ID/g, $p < 0.0005$) confirming receptor-mediated accumulation of the compounds into the tumor.

Imaging studies

Small animal PET/CT images of ^{64}Cu -MP2346 and ^{86}Y -MP2346 in PC-3 tumor-bearing mice and ^{86}Y -MP2346 in AR42J bearing rats are shown in figures 3A and 3B. SUV data for ^{64}Cu -MP2346 over 24 hours is shown in figure 4. Small animal PET/CT images of ^{64}Cu -MP2346 in the PC-3 model allows for clear delineation of the PC-3 tumor in the upper-right flank of the animal after 1 h and as far out as 24h post-injection (Figure 3A). Also noted in these images is the accumulated activity in the liver of the mice consistent with the data obtained from the acute biodistribution data (Table 1). In the ^{86}Y -MP2346 images, low background accumulation is observed (i.e., low non-target tissue accumulation), and this is consistent with the biodistribution data and the tumor/tissue ratios reported (Tables 1 and 2). In all cases the ^{86}Y -MP2346 images in the PC-3 bearing mice are superior to the ^{64}Cu -MP2346 images due to the high tumor/tissues ratios reported from the biodistribution data (Table 2). Due to the excellent image quality obtained with ^{86}Y -MP2346 in the PC-3 bearing mice, we wanted to confirm this in a second rodent model and therefore undertook imaging in Lewis Rats bearing AR42J tumors. The low tumor/background ratio associated with ^{86}Y -MP2346 also allows for excellent tumor visualization in the AR42J rats (Figure 3B), where the tumor is easily delineated in the lower-left flank of the rat at 4 and 24 h post-injection.

In figure 3A the significant reduction in tumor accumulation in the blocked animals confirmed specific uptake of the ^{64}Cu -MP2346 and ^{86}Y -MP2346 in the receptor-rich tumor tissue. SUV data were calculated for the tumors in both blocked and non-blocked animals (Figures 3 and 4). This analysis showed that there were statistical differences ($p < 0.001$) between tumor concentration of mice that did and did not receive a co-injection of blockade at all time points examined and that the PET data were consistent with the trends and relationships observed with the acute biodistribution data.

DISCUSSION

Peptide based agents targeting the GRPRs on tumors have been developed and studied in animals and humans for diagnostic and therapeutic applications [10-26]. The breadth of work undertaken on GRPR-targeting radiopharmaceuticals has been comprehensively reviewed by Smith *et al.* in 2003 and 2005 [11, 12]. Multiple BN analogs have been explored and compared [11, 12] and have demonstrated the potential of these systems for use in humans. In this current report we evaluated both ^{64}Cu - and ^{86}Y -radiolabeled MP2346 [DOTA-(Pro¹, Tyr⁴)-Bombesin(1-14)] as candidates for the non-invasive detection of GRPR-positive tumors using PET. DOTA is able to chelate a variety of β -, β^+ or α -particle-emitting radiometals, remaining stable under a variety of physiologic conditions.

Both agents were radiolabeled in high specific activity by the addition of the radionuclides of choice to the peptide in ammonium acetate buffer. The specific activities obtained (~ 1 mCi/ μg) are high but higher values are achievable, especially if the HPLC conditions used are utilized for an additional purification step, removing unlabeled peptide from labeled peptide. Figure 2 shows that the ^{64}Cu -peptide, ^{64}Cu -MP2346, internalized into PC-3 cells with $\sim 34\%$ of the maximum internalized reached by 1h. This is similar to the 1h internalization of ^{111}In -MP2346 into CA20948 and AR42J cells [13]. ^{86}Y -MP2346 internalized into PC-3 cells with only $\sim 13\%$ of the maximum internalized reached by 1h. However, after 20 h of incubation, nearly a 3-fold higher level of internalization is noted for the ^{86}Y -MP2346 analog compared with ^{64}Cu -MP2346. It has been reported that the level of peptide internalization is crucial for *in vivo* targeting with radiolabeled peptides [33, 34]. For example, in the well-defined model of somatostatin receptor targeting, a significant correlation exists between the level of somatostatin peptide internalization into receptor positive tissues and the *in vivo* uptake [35]. It is reasonable to assume that the bombesin receptor-targeting peptides discussed in this current work will follow similar patterns to those reported for somatostatin peptides, and, therefore, the higher level of internalization of the ^{86}Y -analog explains in part the superior *in vivo* properties of ^{86}Y -MP2346 compared to ^{64}Cu -MP2346.

The biodistribution data presented in Table 1 for ^{64}Cu -MP2346 and ^{86}Y -MP2346 show distinct differences in the kinetics of the two compounds in both receptor-rich and non-target organs. This can be attributed to inherent differences in the physical and chemical properties of the individual agents (e.g., overall charge, pKa) due to the different metals incorporated into MP2346, and not the mass of the peptide administered since this was identical in the comparative experiments. As discussed above, it is likely that cellular internalization is the most influential factor in the uptake and retention of the agents in the tumor and other receptor-positive tissues.

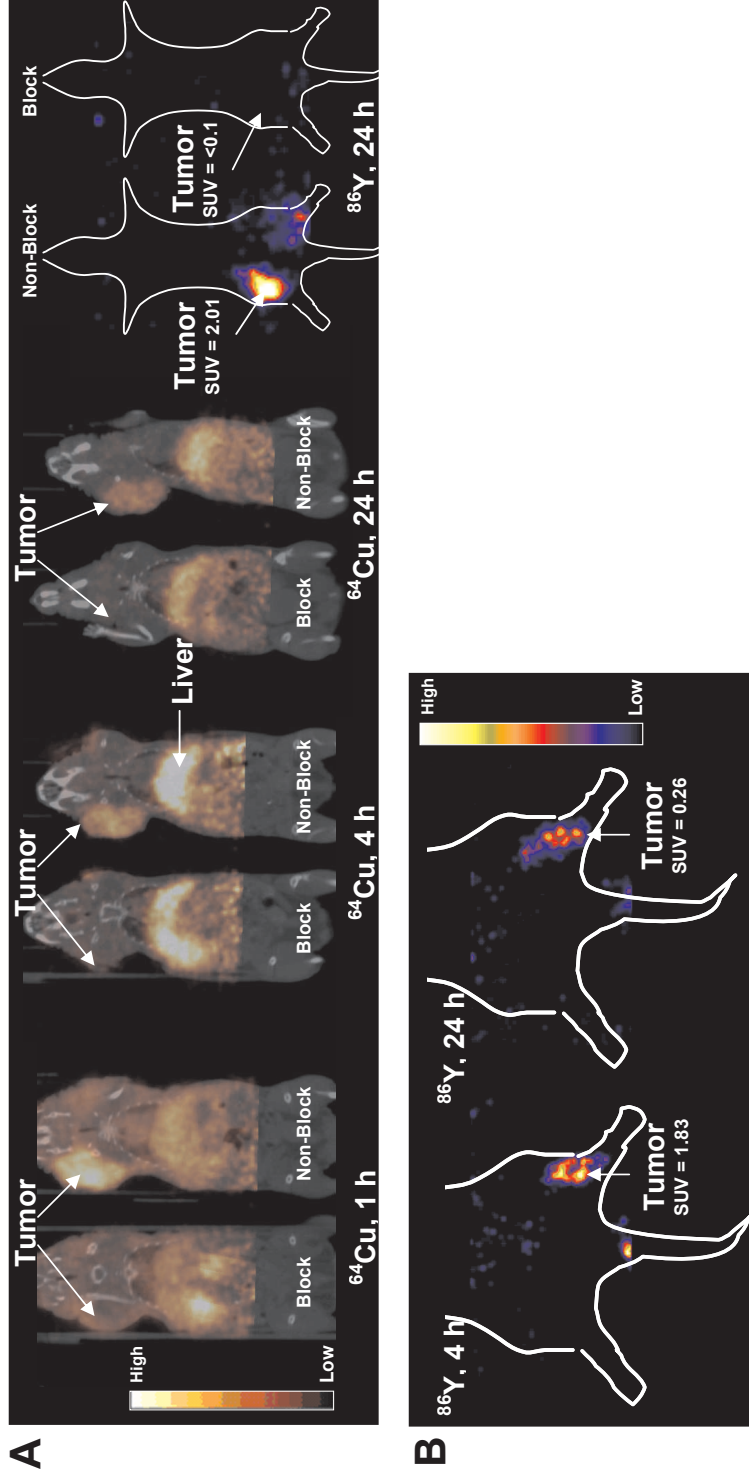


Figure 3. (A) ^{64}Cu -MP2346 PET with co-registered CT at 1, 4 and 24 h in nude mice with PC-3 tumors in the right neck (SUV values not shown on figure). At each time point a mouse that received blockade (left) was co-imaged with a mouse that did not receive blockade (right). Also shown is ^{86}Y -MP2346 PET (without CT co-registration) in nude mice with PC-3 tumors in right flank. At each time point a mouse that received blockade (right) was co-imaged with a mouse that did not receive blockade (left). The PET images also show that the administration of a blockade dose substantially reduces tumor uptake of both agents by such an extent that the tumor cannot be delineated for either compound at any time point. (B) ^{86}Y -MP2346 PET at 4 and 24 h post-injection in male Lewis Rats with AR42J tumors in left leg. In both the mice and rats PET imaging it is evident that background accumulation is very low (i.e., low non-target tissue uptake) and that in the non-blockade mouse very little tumor tracer accumulation is noted.

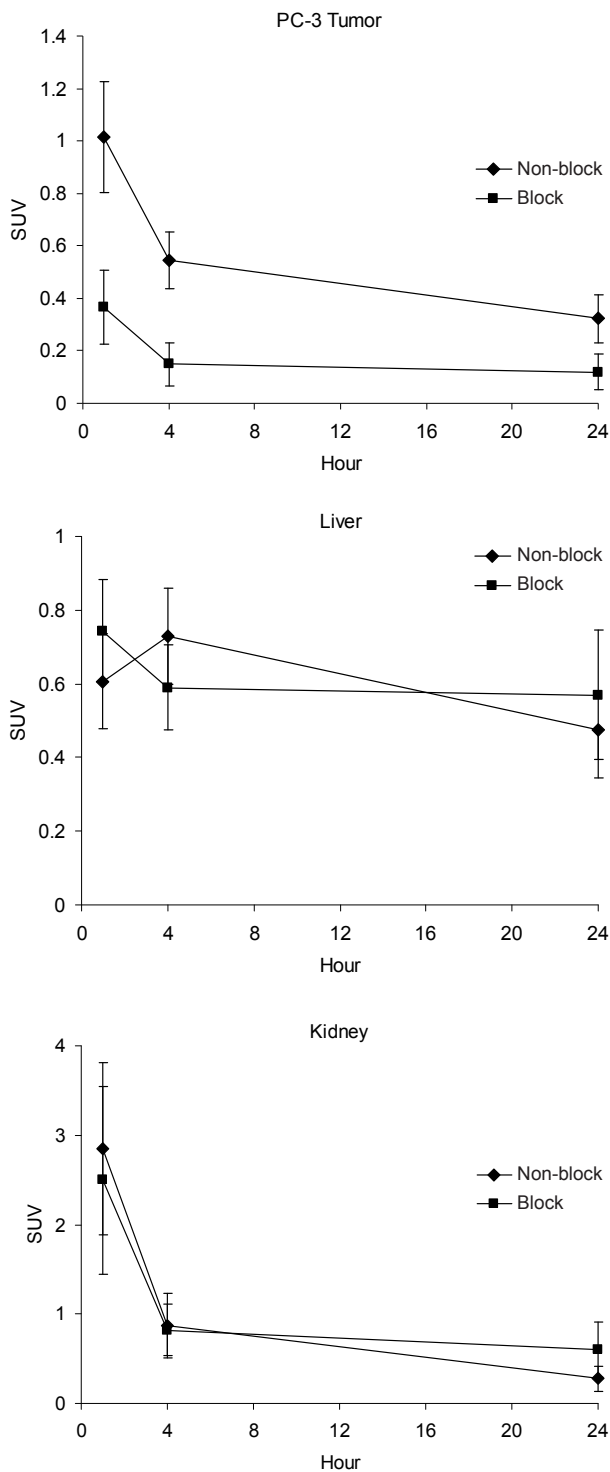


Figure 4. SUV data obtained for PET analysis of ^{64}Cu -MP2346 in mice implanted with PC-3 tumors. In these studies, the mice received ^{64}Cu -MP2346 ($n = 3$, $125 \mu\text{Ci}$, 125 ng). These mice were imaged side by side with mice ($n = 3$ per group) that had been co-administered with $100 \mu\text{g}$ of $[\text{Tyr}^4]$ -Bombesin along with the radiolabeled peptide.

In other non-target tissues, the ^{86}Y analog in general showed a more favorable biodistribution compared with ^{64}Cu -MP2346. This was most notable in the higher tumor uptake and lower non-target tissue (in particular the liver) accumulation resulting in superior tumor/tissue ratios (Table 2). The reasons for these differences are not due to cellular internalization but are consequences of the different chemical and physical properties of ^{86}Y -MP2346 and ^{64}Cu -MP2346.

The kidney uptake of ^{86}Y -MP2346 is not optimal and is higher than ^{64}Cu -MP2346 and could be a problem in the translation of this agent to the clinic due to high absorbed doses. Although these kidney values are lower than those found for the ^{18}F -labeled peptides, ^{18}F -FB[Lys³]BBN (1 h, ~16 %ID/g) and ^{18}F -FB-Aca-BBN(7-14) (1 h, ~8 %ID/g) [27] they are comparable to those found with other ^{64}Cu -BN systems [24-26]. The uptake of ^{86}Y -MP2346 and subsequent retention, compared to the uptake and washout noted with the ^{64}Cu analog could be attributed to the net charge of the compound. It has been reported that the renal retention of ^{64}Cu - and ^{111}In -labeled chelates was higher for positively charged peptides and lower for neutral and negatively charged ones [36-38]. Given the expected charge of ^{86}Y -MP2346 is +1 and ^{64}Cu -MP2346 is neutral (at slightly acid pH), this could account for the difference in renal uptake and clearance. Subtle alteration of ^{86}Y -MP2346 to present an overall neutral or negative charge could reduce renal uptake and improve clearance. If this strategy does not work tracer accumulation could possibly be tempered by the use of D-lysine or a similar agent to decrease this retention [39].

The liver burden associated with ^{64}Cu -MP2346 (1 h, 1.329 %ID/g), although significantly lower than that found with other ^{64}Cu -BN peptide systems, (^{64}Cu -DOTA-[Lys³]BBN, ~4.5 %ID/g [26]; ^{64}Cu -DOTA-Aca-BBN(7-14), ~13 %ID/g [25]; ^{64}Cu -DOTA-Aoc-BN(7-14), ~13 %ID/g [24]) could still hinder the delineation of GRPR-positive tumors in anatomical regions in close proximity to the liver and could also lead to high radiation absorbed doses. Although DOTA is a promiscuous chelator for many 2+ and 3+ charged metals, ^{64}Cu has been shown to dissociate *in vivo* from DOTA and DOTA-conjugates [40]. Copper-64 then undergoes metabolism and transchelation to superoxide dismutase and other proteins causing increased blood and liver accumulation [41, 42]. The cross-bridged cyclam chelator, CBTE2A, has demonstrated improved *in vivo* stability and consequently a reduction in transchelation [40-43]. CBTE2A has been conjugated to the somatostatin peptide analog Tyr³-octreotate (Y3-TATE) and ^{64}Cu -CBTE2A-Y3-TATE showed improved non-target organ clearance and higher tumor ratios compared with ^{64}Cu -TETA-analog [42]. By incorporation of the CBTE2A moiety (replacing DOTA) on to the peptide system used in this study, an improved biodistribution would be anticipated.

The tumor uptake of ^{86}Y -MP2346 at all time points is superior to that found with ^{64}Cu -MP2346 (Table 1) and can be attributed to the superior cellular internalization of

this agent (Figure 2). These values compare well with those found for other analogs in the same tumor model; for example, La Bella *et al* showed with two ^{99m}Tc -labeled BN analogs showed 0.3-0.6 %ID/g at 24 h postinjection in the PC-3 tumor [17, 20]. These values are similar to that found with ^{64}Cu -MP2346 but ~2- fold lower than those for ^{86}Y -MP2346. The PET agents ^{18}F -FB[Lys³]BBN and ^{18}F -FB-Aca-BBN(7-14) showed PC-3 uptake values at 1 h of 5.94 ± 0.78 %ID/g and 0.43 ± 0.18 %ID/g, respectively [27]. ^{177}Lu -DOTA-Aoc-BN(7-14) was reported to have 4.2 %ID/g in the PC-3 tumor with a tumor/blood ratio of 11.1 at 1 h, an uptake value slightly higher than that found with ^{86}Y -MP2346 but resulting in a similar tumor/blood ratio (Table 2) [23]. The ^{64}Cu analog of DOTA-Aoc-BN(7-14) was shown to have 5.5 %ID/g at 2 h in the PC-3 tumor, a value much higher than that found with ^{64}Cu -MP2346, but only ~2-fold higher than that determined with ^{86}Y -MP2346. However, on comparison of the tumor/blood ratios, ^{64}Cu -DOTA-Aoc-BN(7-14) had a tumor/blood ratio of 4.2, a value lower than that for ^{64}Cu -MP2346 (6.192 at 1 h, Table 2) and 3-fold lower than that for ^{86}Y -MP2346 (12.074 at 1 h, Table 2). ^{64}Cu -DOTA-[Lys³]BBN demonstrated 3.97 ± 0.15 %ID/g in the PC-3 tumor [26] with the truncated analog showing ~3.0 %ID/g [25]. These values are comparable to those found for ^{86}Y -MP2346, but higher than those for ^{64}Cu -MP2346, but as discussed above the liver burden, with the other analogs, is significantly higher. In all of these studies non-target tissue accumulation differed again presumably due to peptide affinity, overall charge and metal-chelate stability. Overall differences in tumor accumulation could also be attributed to the amount of peptide mass administered to the animals, the tumor volume and the status of the PC-3 cells maintained within each laboratory so care must be taken in the comparison of the current studies with those previously reported.

The PET imaging confirms the data obtained in the biodistribution studies. The less than optimal biodistribution of ^{64}Cu -MP2346 results in high background and liver accumulation. ^{86}Y -MP2346 produces high quality PET images (Figure 2 and 3) in PC-3 bearing mice and this excellent image quality was confirmed in AR42J bearing rats where tumor activity is high even after 1 h against very low background activity. The liver shows very low accumulation of the ^{86}Y -labeled peptide suggesting that the Y-DOTA chelate is more stable than the Cu-analog and is not susceptible to transchelation *in vivo*. It is important to note that these images have been produced following the administration of larger amounts of peptide due to the higher dose (~20 fold) than that given in the biodistribution studies. Nevertheless, the observed tissue distribution in the rat images is consistent with the biodistribution found in sampled tissues in mice. Additionally, in both studies, animals that were preinjected with a large quantity of [Tyr⁴]-Bombesin had significantly reduced uptake of the agents in the receptor positive tumors with little change in uptake in receptor negative tissue. This further confirms the receptor-mediated uptake of the agents *in vivo*.

CONCLUSION

In conclusion, ^{64}Cu -MP2346 and ^{86}Y -MP2346 were evaluated as agents for the PET imaging of the GRP receptor. In particular ^{86}Y -MP2346 due to its good tumor concentration and low non-target tissue accumulation allows for the excellent delineation of the GRPR-positive PC-3 tumor and warrants further evaluation for diagnostic purposes as a GRPR PET imaging agent.

ACKNOWLEDGEMENTS

We are very grateful for the technical assistance of Lori Strong, Nicole Fettig, Jerrel R. Rutlin, Laura Meyer, Susan Adams, Rebecca Andrews, Todd Perkins and Dr. Jeongsoo Yoo. This work was supported by the National Cancer Institute (R24 CA86307). Small animal PET imaging is supported by an NIH/NCI SAIRP grant (R24 CA83060) with additional support from the Small Animal Imaging Core of the Alvin J. Siteman Cancer Center at Washington University and Barnes-Jewish Hospital. The SAIC Core is supported by an NCI Cancer Center Support Grant # 1 P30 CA91842.

REFERENCES

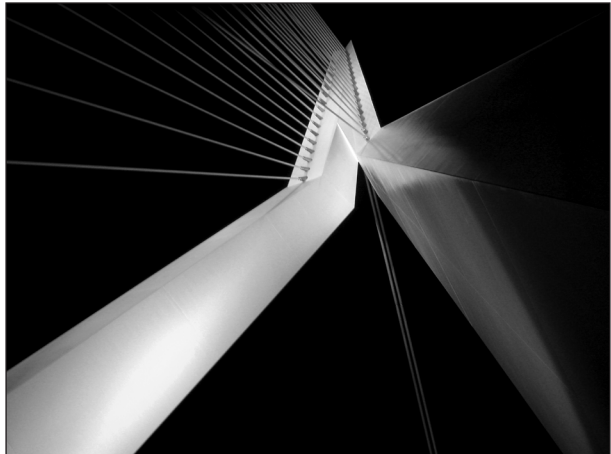
1. Carroll, R.E., K.A. Matkowskyj, S. Chakrabarti, et al., Aberrant expression of gastrin-releasing peptide and its receptor by well-differentiated colon cancers in humans. *Am J Physiol* 1999; 276(3 Pt 1): G655.
2. Chave, H.S., A.C. Gough, K. Palmer, et al., Bombesin family receptor and ligand gene expression in human colorectal cancer and normal mucosa. *Br J Cancer* 2000; 82(1): 124.
3. Corjay, M.H., D.J. Dobrzanski, J.M. Way, et al., Two distinct bombesin receptor subtypes are expressed and functional in human lung carcinoma cells. *J Biol Chem* 1991; 266(28): 18771.
4. Ferris, H.A., R.E. Carroll, D.L. Lorimer, et al., Location and characterization of the human GRP receptor expressed by gastrointestinal epithelial cells. *Peptides* 1997; 18(5): 663.
5. Reubi, J.C., S. Wenger, J. Schmuckli-Maurer, et al., Bombesin receptor subtypes in human cancers: detection with the universal radioligand ¹²⁵I-[D-TYR(6), beta-ALA(11), PHE(13), NLE(14)] bombesin(6-14). *Clin Cancer Res* 2002; 8(4): 1139.
6. Sun, B., A.V. Schally and G. Halmos, The presence of receptors for bombesin/GRP and mRNA for three receptor subtypes in human ovarian epithelial cancers. *Regulatory Peptides* 2000; 90(1-3): 77.
7. Gugger, M. and J.C. Reubi, Gastrin-releasing peptide receptors in non-neoplastic and neoplastic human breast. *Am J Pathol* 1999; 155(6): 2067.
8. Markwalder, R. and J.C. Reubi, Gastrin-releasing peptide receptors in the human prostate: relation to neoplastic transformation. *Cancer Res* 1999; 59(5): 1152.
9. Anastasi, A., V. Erspamer and M. Bucci, Isolation and amino acid sequences of alytesin and bombesin, two analogous active tetradecapeptides from the skin of European discoglossid frogs. *Arch Biochem Biophys* 1972; 148(2): 443.
10. Varvarigou, A., P. Bouziotis, C. Zikos, et al., Gastrin-releasing peptide (GRP) analogues for cancer imaging. *Cancer Biotherapy Radiopharm* 2004; 19(2): 219.
11. Smith, C.J., W.A. Volkert and T.J. Hoffman, Gastrin releasing peptide (GRP) receptor targeted radiopharmaceuticals: A concise update. *Nucl Med Biol* 2003; 30: 861.
12. Smith, C.J., W.A. Volkert and T.J. Hoffman, Radiolabeled peptide conjugates for targeting of the bombesin receptor superfamily subtypes. *Nucl Med Biol* 2005; 32(7): 733.
13. Breeman, W.A., M. de Jong, J.L. Erion, et al., Preclinical comparison of ¹¹¹In-labeled DTPA- or DOTA-bombesin analogs for receptor-targeted scintigraphy and radionuclide therapy. *J Nucl Med* 2002; 43(12): 1650.
14. Breeman, W.A., L.J. Hofland, M. de Jong, et al., Evaluation of radiolabelled bombesin analogues for receptor-targeted scintigraphy and radiotherapy. *Int J Cancer* 1999; 81(4): 658.
15. Breeman, W.A.P., M. de Jong, B.F. Bernard, et al., Pre-clinical evaluation of [¹¹¹In-DTPA-Pro¹, Tyr⁴]bombesin, a new radioligand for bombesin-receptor scintigraphy. *Int J Cancer* 1999; 83: 657.
16. Karra, S.R., R. Schibli, H. Gali, et al., ^{99m}Tc-labeling and in vivo studies of a bombesin analogue with a novel water-soluble dithiadiphosphine-based bifunctional chelating agent. *Bioconjug Chem* 1999; 10(2): 254.
17. La Bella, R., E. Garcia-Garayoa, M. Bahler, et al., A ^{99m}Tc-postlabeled high affinity bombesin analogue as a potential tumor imaging agent. *Bioconjug Chem* 2002; 13: 599.
18. Van de Wiele, C., F. Dumont, R.A. Dierckx, et al., Biodistribution and dosimetry of ^{99m}Tc-RP527, a gastrin-releasing peptide (GRP) agonist for the visualization of GRP receptor-expressing malignancies. *J Nucl Med* 2001; 42: 1722.
19. Van de Wiele, C., F. Dumont, R. Vanden Broecke, et al., Technetium-99m RP527, a GRP analogue for visualisation of GRP receptor- expressing malignancies: a feasibility study. *Eur J Nucl Med* 2000; 27(11): 1694.

20. La Bella, R., E. Garcia-Garayoa, M. Langer, et al., In vitro and in vivo evaluation of a ^{99m}Tc (I)-labeled bombesin analogue for imaging of gastrin releasing peptide receptor-positive tumors. *Nucl Med Biol* 2002; 29: 553.
21. Rogers, B.E., D.T. Curiel, M.S. Mayo, et al., Tumor localization of a radiolabeled bombesin analogue in mice bearing human ovarian tumors induced to express the gastrin releasing peptide receptor by an adenoviral vector. *Cancer* 1997; 80: 2419.
22. Safavy, A., M.B. Khazaeli, H. Qin, et al., Synthesis of bombesin analogues for radiolabeling with rhenium-188. *Cancer* 1997; 80(12 Suppl): 2354.
23. Smith, C.J., T.J. Hoffman, D.L. Hayes, et al., Radiochemical investigations of ^{177}Lu -DOTA-8-Aoc-BBN[7-14] NH_2 : A new gastrin releasing peptide receptor (GRPr) targeting radiopharmaceutical. *J Label Comp Radiopharm* 2001; 44: S706.
24. Rogers, B.E., H.M. Bigott, D.W. McCarthy, et al., MicroPET imaging of a gastrin-releasing peptide receptor-positive tumor in a mouse model of human prostate cancer using a ^{64}Cu -labeled bombesin analogue. *Bioconjug Chem* 2003; 14(4): 756.
25. Yang, Y.S., X. Zhang, Z. Xiong, et al., Comparative in vitro and in vivo evaluation of two ^{64}Cu -labeled bombesin analogs in a mouse model of human prostate adenocarcinoma. *Nucl Med Biol* 2006; 33(3): 371.
26. Chen, X., R. Park, Y. Hou, et al., microPET and Autoradiographic Imaging of GRP Receptor Expression with ^{64}Cu -DOTA-[Lys³]Bombesin in Human Prostate Adenocarcinoma Xenografts. *J Nucl Med* 2004; 45: 1390.
27. Zhang, X., W. Cai, F. Cao, et al., ^{18}F -labeled bombesin analogs for targeting GRP receptor-expressing prostate cancer. *J Nucl Med* 2006; 47(3): 492.
28. Breeman, W.A., M. de Jong, E. de Blois, et al., Radiolabelling DOTA-peptides with ^{68}Ga . *Eur J Nucl Med Mol Imaging* 2005; 32(4): 478.
29. McCarthy, D.W., R.E. Shefer, R.E. Klinkowstein, et al., Efficient production of high specific activity ^{64}Cu using a biomedical cyclotron. *Nucl Med Biol* 1997; 24(1): 35.
30. Yoo, J., L. Tang, T.A. Perkins, et al., Preparation of high specific activity (^{86}Y) using a small biomedical cyclotron. *Nucl Med Biol* 2005; 32(8): 891.
31. Blower, P.J., J.S. Lewis and J. Zweit, Copper radionuclides and radiopharmaceuticals in nuclear medicine. *Nucl Med Biol* 1996; 23: 957.
32. Tai, Y.C., A. Ruangma, D. Rowland, et al., Performance evaluation of the microPET focus: a third-generation microPET scanner dedicated to animal imaging. *J Nucl Med* 2005; 46(3): 455.
33. Hofland, L.J. and S.W.J. Lamberts, The Pathophysiological Consequences of Somatostatin Receptor Internalization and Resistance. *Endocr. Rev* 2003; 24: 28.
34. Reubi, J.C., Peptide Receptors as Molecular Targets for Cancer Diagnosis and Therapy. *Endocr. Rev* 2003; 24: 389.
35. Storch, D., M. Béhé, M.A. Walter, et al., Evaluation of [^{99m}Tc /EDDA/HYNIC 0]Octreotide Derivatives Compared with [^{111}In -DOTA 0 ,Tyr³, Thr⁸]Octreotide and [^{111}In -DTPA 0]Octreotide: Does Tumor or Pancreas Uptake Correlate with the Rate of Internalization? *J Nucl Med* 2005 46: 1561.
36. Akizawa, H., Y. Arano, M. Mifune, et al., Effect of molecular charges on renal uptake of ^{111}In -DTPA-conjugated peptides. *Nucl Med Biol* 2001; 28: 761.
37. Jones-Wilson, T.M., K.A. Deal, C.J. Anderson, et al., The in vivo behavior of copper-64-labeled azamacrocyclic complexes. *Nucl Med Biol* 1998; 25(6): 523.
38. Rogers, B.E., C.J. Anderson, J.M. Connett, et al., Comparison of four bifunctional chelates for radiolabeling monoclonal antibodies with copper radioisotopes: biodistribution and metabolism. *Bioconjugate Chem* 1996; 7(4): 511.
39. de Jong, M., W.H. Bakker, W.A.P. Breeman, et al., Preclinical comparison of [DTPA 0]octreotide, [DTPA 0 ,Tyr³]octreotide and [DOTA 0 ,Tyr³]octreotide as carriers for somatostatin receptor-targeted scintigraphy and radionuclide therapy. *Int J Cancer* 1998; 75: 406.

40. Wadas, T.J., E.H. Wong, G.R. Weisman, et al., Copper chelation chemistry and its role in copper radiopharmaceuticals. *Current Pharmaceutical Design* in press.
41. Boswell, C.A., X. Sun, W. Niu, et al., Comparative in vivo stability of copper-64-labeled cross-bridged and conventional tetraazamacrocyclic complexes. *J Med Chem* 2004; 47: 1465.
42. Sprague, J.E., Y. Peng, X. Sun, et al., Preparation and biological evaluation of copper-64-labeled Tyr³-octreotate using a cross-bridged macrocyclic chelator. *Clin Cancer Res* 2004; 10: 8674.
43. Sun, X., M. Wuest, G.R. Weisman, et al., Radiolabeling and in vivo behavior of copper-64-labeled cross-bridged cyclam ligands. *J Med Chem* 2002; 45(2): 469.

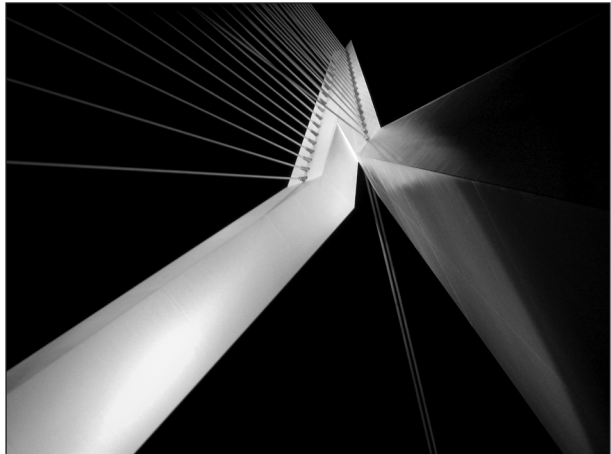
III

GRP receptor-expression during
prostate cancer development



6

Androgen-dependent expression of the gastrin-releasing peptide receptor in human prostate tumor xenografts



Monique de Visser
Wytske M. van Weerden
Corrina M. A. de Ridder
Suzanne Reneman
Marleen Melis
Eric P. Krenning
Marion de Jong

Journal of Nuclear Medicine 2007; Vol. 48(1):88-93

ABSTRACT

Human prostate cancers (PC) overexpress gastrin-releasing peptide (GRP) receptors. This observation suggests that GRP receptors may be used as new visualization and treatment modalities for these tumors. Radiolabeled GRP receptor-targeting analogs of GRP and bombesin (BN) have successfully been developed for these purposes. Expression of GRP receptors in human prostate tumors is, however, primarily evaluated in early stages of tumor development and information on expression in the more progressive prostate tumors is uncertain. To evaluate GRP receptor expression in all stages of PC, we investigated GRP receptor expression using a panel of 12 established human PC xenograft models representing the different stages of human PC and the effect of antiandrogen treatment (castration).

Methods: Human PC xenografts were grown in male nude mice, and GRP receptor density in the tumors was evaluated using displacement receptor autoradiography with the universal BN receptor analog ^{125}I -[D-Tyr⁶, β -Ala¹¹,Phe¹³,Nle¹⁴]BN(6–14) and the BN analog ^{111}In -[DTPA-Pro¹,Tyr⁴]BN (DTPA is diethylenetriaminepentaacetic acid) before and after castration.

Results: Autoradiography showed high-density GRP receptor expression in the androgen-dependent tumors (3/12 models), whereas only very low receptor expression was found in the androgen-responsive and -independent tumors (9/12 models). Castration resulted in GRP receptor downregulation (11%–36% of initial values) in the 3 androgen-dependent tumors.

Conclusion: High GRP receptor density was only observed in androgen-dependent PC xenografts, indicating high GRP receptor expression in the early, androgen-dependent, stages of prostate tumor development and not in later stages. In addition, castration strongly reduced GRP receptor expression in androgen-dependent tumors, indicating that GRP receptor expression in human PC is androgen-regulated.

INTRODUCTION

Prostate cancer (PC) is the third leading cause of cancer related deaths and the most frequently diagnosed cancer in men in Western countries [1]. Early screening for PC has resulted in a sharp increase in the number of locally confined tumors, although the micrometastatic stage of these tumors is often uncertain. Lymph node metastases have a significant impact on the prognosis of PC patients as it dictates the available treatment options: Locally confined tumors can be treated by radical prostatectomy or radiation therapy, whereas tumors that are no longer confined to the prostate require androgen ablation treatment by surgical or chemical castration or treatment with antiandrogens. Most PC patients are initially androgen sensitive and will respond to androgen ablation therapy. However, a major problem in the treatment of metastasized PC is the transition of this androgen-responsive characteristic toward hormone-independent growth. This shift from androgen dependence to androgen-independent tumor growth is not well understood [2, 3], and effective treatment of androgen-independent PC is not available [4]. Consequently, accurate staging of early-diagnosed PC is a crucial step in the management of PC. Besides the need for accurate staging at presentation, a sensitive diagnostic technique is urgently needed to detect local relapse or metastatic disease of PC patients who have undergone local therapy but are faced with rising prostate-specific antigen (PSA). In case of a local recurrence after radical prostatectomy additional local radiotherapy can be given. This therapy is often initiated on the basis of PSA kinetics, without any direct evidence for a local recurrence because it is very difficult to demonstrate. Clearly, there is a clinical need to find a target present in early stages of PC as well as in metastases that may be used for molecular imaging.

It has been shown that prostate tumors overexpress gastrin releasing peptide (GRP) receptors while normal and hyperplastic prostate tissue was receptor-negative [5, 6]. This GRP receptor expression is predominantly evaluated on primary human prostate tumor tissue from radical prostatectomy specimens. In these cases, the state of androgen dependence has not been published. Among the 7 androgen-independent bone metastases tested, 4 cases were GRP receptor-positive with very diverse receptor densities [5]. Nevertheless, the GRP receptor expression in later stages of PC is unclear, and, therefore, the value of GRP receptor-targeted therapy in androgen-independent PC remains uncertain.

The GRP receptor is a member of the bombesin (BN) receptor family, which consists of 4 known receptor subtypes. Three of them, the neuromedin B (NMB) receptor (BB_1), the GRP receptor (BB_2), and the BN receptor subtype 3 (BRS-3 or BB_3), are mammalian receptors, whereas the fourth subtype (BB_4) is found only in amphibians [7-10]. Except for the GRP receptor, these receptor subtypes are not very well characterized with regard to their distribution and function in human tissues [11, 12].

BN-like peptides, including BN, GRP, and NMB, are involved in the regulation of a large number of biologic processes in the gut and central nervous system [13] and mediate their action by binding to BN receptors. It has been proposed that radiolabeled analogs of these BN-like peptides may be used to image and treat GRP receptor-expressing tumors, such as prostate tumors [14, 15]. This peptide-based receptor-targeted imaging and treatment of tumors have been demonstrated successfully for somatostatin receptor-expressing tumors using radiolabeled somatostatin analogs [16-18].

A number of researchers are working on the development of radiolabeled BN analogs that specifically target GRP receptor-expressing tumors *in vitro* and *in vivo* [15, 19-22]. Most of these research groups use human GRP receptor-expressing prostate tumor models such as PC-3 and DU-145. These cell lines grow independent of androgen and do not express androgen receptor or secrete PSA, which in itself is an uncharacteristic feature of most PC patients [23]. Therefore, it is questionable whether these cell lines can be considered representative models for clinical PC. To determine the value of newly developed BN analogs in the various stages of prostate tumor development, more realistic prostate tumor models would add significant value.

The availability of experimental human prostate tumor models is rather limited. A unique panel of human prostate tumor xenograft models has been established and reviewed by Van Weerden et al. [24, 25]. This panel comprises 12 xenograft models from 9 different patients. The xenografts represent the various aspects of human PC and, therefore, are excellent tools to study PC progression from androgen-dependent to androgen-independent stages. Three models (PC-295, PC-310, PC-82) are strictly dependent on androgens for their development and growth: These tumors do not develop in castrated male mice, and castration of tumor-bearing animals results in regression without tumor relapse [26, 27]. Two models, PC-346 (including the sublines PC-346 P, PC-346 I, PC-346 B, and PC-346 iB) and PC-374, are androgen-responsive but not androgen-dependent: Tumors do develop and continue to grow in castrated male mice, but at a lower growth rate. Finally 4 xenografts (PC-133, PC-135, PC-324, and PC-339) are representatives of androgen-independent PC. These tumors develop identically in intact or castrated male mice, and their growth rate does not change on testosterone depletion or supplementation.

In this study we evaluated the expression of GRP receptors and its androgen regulation throughout the various stages of prostate tumor development using the panel of 12 human prostate tumor xenograft models. *In vitro* BN receptor-binding studies were performed on frozen xenograft sections using radiolabeled BN analogs.

MATERIALS AND METHODS

Prostate Cancer Xenografts

The panel of human PC xenografts is listed in Table 1. Xenografts were routinely propagated in intact male nude NMRI mice (Taconic M&B) [24, 25]. Mice were kept in 14 x 13 x 33.2 cm³ individually ventilated cages (Techniplast) with 3 or 4 mice per cage, on sawdust (Woody-Clean, type BK8/15; Technilab-BMI) on a 12-h light–dark cycle, at 50% relative humidity, in a temperature-controlled (22°C) room. Mice received irradiated chow and acidified drinking water ad libitum. The experiment was approved by the Animal Experimental Committee (DEC) of the Erasmus University and performed in agreement with The Netherlands Experiments on Animals Act (1977) and the European Convention for Protection of Vertebrate Animals used for Experimental Purposes (Strasbourg; March 18, 1986).

Mice were implanted subcutaneously with small fragments of human prostate tumor. In the case of androgen-dependent tumor transplantation, mice were supplemented with testosterone to obtain optimal tumor take (80%–85%) and tumor growth. Hormonal substitution was achieved by implanting Silastic tubings filled with crystalline steroid (6 mg/tubing; AppliChem). These testosterone implants lead to testosterone levels exceeding the low physiologic levels in intact male nude mice for at least 75 d [28].

Androgen withdrawal was performed by surgical castration under ketamine (Alfasan) and Rompun (Bayer AG) anesthesia (1:1 mixture), which was followed

Table 1 PC xenograft panel

Tumor model	Origin	AD/AR/AI	Androgen receptor	PSA
PC-295	LN	AD	+	+
PC-310	PC	AD	+	+
PC-82	PC	AD	+	+
PC-346 p*	TURP	AR	+	+
PC-346 I		AR	+ [†]	+
PC-346 B		AR	+	+
PC-346 BI		AR	+	+
PC-374	SSM	AR	+	+
PC-133	Bone	AI	–	–
PC-135	PC	AI	–	–
PC-324	TURP	AI	–	–
PC-339	TURP	AI	–	–

Note; *PC-346 p is derived from a nonprogressive TURP patient, and the 3 sublines were derived from this xenograft. [†]Androgen receptor mutation (T877A). AD = androgen-dependent; AR = androgen-independent but androgen-responsive; AI = androgen-independent; PSA = prostate-specific antigen; PC = primary prostate tumor; LN = lymph node metastasis; TURP = transurethral resection of the prostate; SSM = scrotal skin metastasis.

by removal of the Silastic testosterone implants. Mice were sacrificed 8–10 d after castration. Tumors were removed and snap frozen in liquid nitrogen for *in vitro* autoradiography.

Radiolabeled Peptides

BN analog [D-Tyr⁶,β-Ala¹¹,Phe¹³,Nle¹⁴]BN(6–14), referred to as universal ligand, was provided by Biosynthema Inc., and radiolabeled with ¹²⁵I as described previously [29].

Analog [DTPA-Pro¹,Tyr⁴]BN (DTPA is diethylenetriaminepentaacetic acid) was provided by Mallinckrodt Inc. and radiolabeled with ¹¹¹In (¹¹¹InCl₃ [DRN 4901], Tyco Healthcare; 370 MBq/mL in HCl, pH 1.5–1.9) as described earlier [30].

In Vitro Autoradiography

In vitro autoradiography with the radiolabeled BN receptor-binding ¹²⁵I-universal ligand was performed on PC xenograft sections to detect the expression of all members of the BN receptor family. Displacement with GRP (only GRP receptor binding), NMB (only NMB receptor binding), or BN (mainly GRP receptor and some NMB receptor binding) was used to discriminate between binding to the different receptor subtypes. This is an established method to detect BN receptor subtype expression on several human tissues, as described by Reubi et al. [6].

Frozen PC xenograft sections (10 mm) were incubated for 1 h at room temperature with 0.1 nmol/L ¹²⁵I-universal ligand (¹²⁵I-[D-Tyr⁶, β-Ala¹¹,Phe¹³,Nle¹⁴]BN(6–14)) (74 TBq/mmol) in 167 mmol/L Tris (pH 7.6), supplemented with 5 mmol/L MgCl₂, 1% bovine serum albumin (BSA), and 40 mg/mL bacitracin. To differentiate between binding of the universal ligand to the different members of the BN receptor family, the sections were incubated in the presence of excess amounts (1 mmol/L) of either universal ligand, GRP, NMB, or BN (Sigma-Aldrich). After incubation, the sections were washed 2 times for 5 min each in 167 mmol/L Tris (pH 7.6), 5 mmol/L MgCl₂, and 0.25% BSA (4°C), 5 min in 167 mmol/L Tris (pH 7.6) and 5 mmol/L MgCl₂ (4°C), and finally rinsed in MilliQ water (Millipore) (4°C). The sections were then dried and exposed to phosphor imaging screens (Perkin Elmer) for 72 h. The imaging screens were read using a Cyclone Storage Phosphor System (Packard), and the autoradiograms were quantified using Optiquant Software (Packard).

In vitro receptor binding of ¹¹¹In-[DTPA-Pro¹,Tyr⁴]BN (200 MBq/nmol) was determined on PC xenograft sections as described. Sections were incubated for 1 h with 1 nmol/L of the ¹¹¹In-labeled peptide with or without 1 mmol/L [Tyr⁴]BN (Sigma-Aldrich). The imaging screens were read after an overnight exposure of the xenograft sections.

RESULTS

BN receptor expression was determined on the 12 human prostate tumor xenografts using ^{125}I -universal ligand and ^{111}In -[DTPA-Pro¹, Tyr⁴]BN. The results of the *in vitro* autoradiography studies are shown in figures 1 and 2, respectively.

The androgen-dependent PC xenografts PC-295, PC-310, and PC-82 showed high binding of ^{125}I -universal ligand, which could be almost completely blocked by 1026 mol/L of universal ligand, GRP, and BN and to a much lesser extent by 1026 mol/L NMB (Figure 1A). This blocking pattern indicates high receptor-mediated binding of ^{125}I -universal ligand to predominantly GRP receptors (Figure 1B). The androgen-

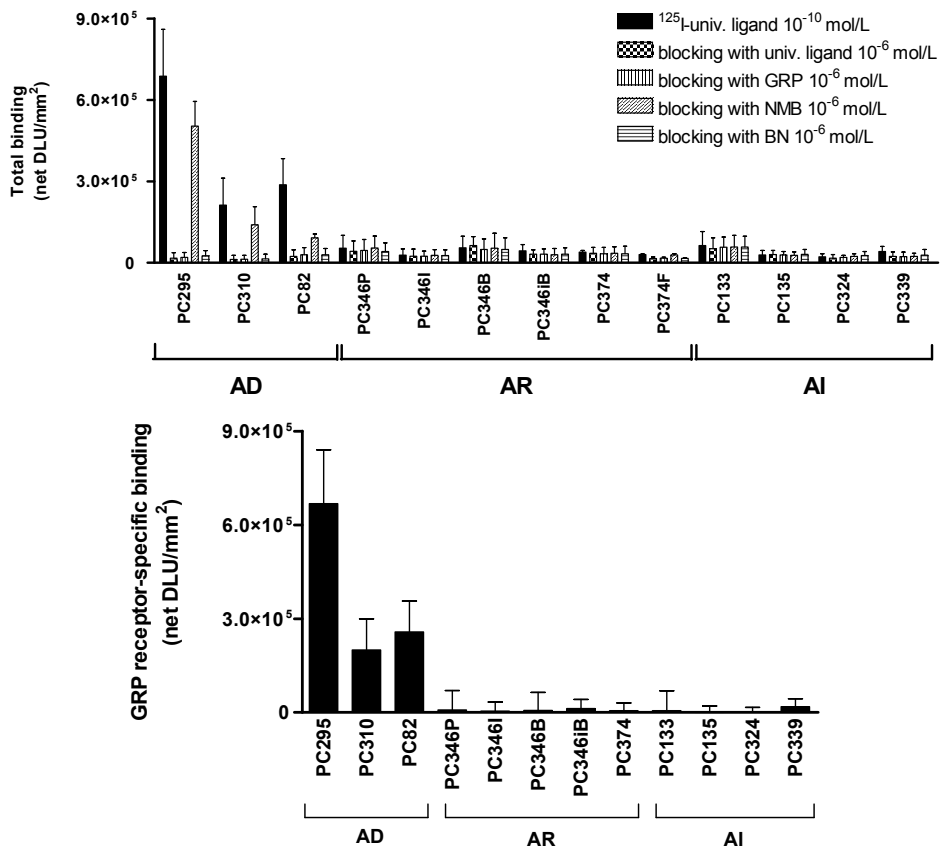


Figure 1. Total binding of 10^{-10} mol/L ^{125}I -universal (univ.) ligand with or without a blocking concentration (10^{-6} mol/L) of unlabeled universal ligand, GRP, NMB, or BN (A) and GRP receptor-specific binding (= total binding [^{125}I -universal ligand 10^{-10} mol/L] minus unspecific binding [blocking with GRP 10^{-6} mol/L]) (B) to androgen-dependent (AD), androgen-independent but responsive (AR), and androgen-independent (AI) PC xenograft sections. Results are shown as average net density light units per square millimeter (net DLU/mm²) \pm SD. Results are average of 3 independent experiments (n = 2–4 sections/experiment).

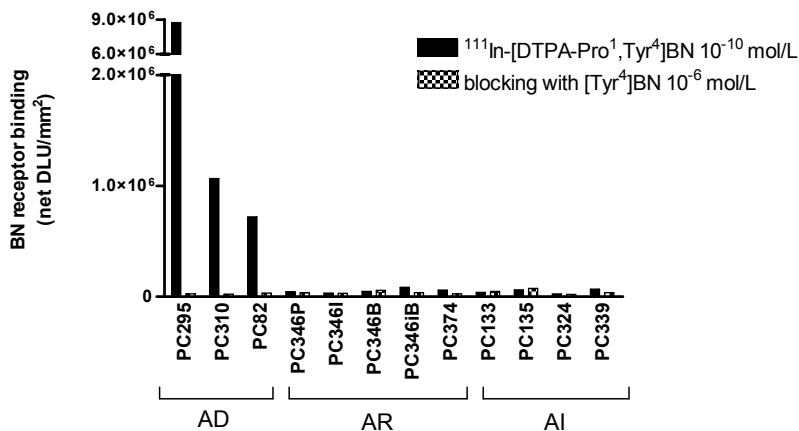


Figure 2. Total binding of 10^{-9} mol/L ^{111}In -[DTPA-Pro¹,Tyr⁴]BN with or without a blocking concentration (10^{-6} mol/L) of unlabeled [Tyr⁴]BN, to androgen-dependent (AD), androgen-independent but responsive (AR), and androgen-independent (AI) PC xenograft sections. Results are shown as average net density light units per square millimeter (net DLU/mm²). Results are average of 1 experiment (n = 2 sections/experiment).

independent, but responsive and the completely androgen-independent, PC xenografts showed very low receptor-mediated binding of ^{125}I -universal ligand (Figures 1A and 1B). These results suggest that these xenografts express GRP receptors only at very low density. The other members of the BN receptor family, NMB and BB₃, are not, or to a much lesser degree, expressed in this panel of PC xenografts.

Similar results were found in the ^{111}In -[DTPA-Pro¹,Tyr⁴]BN *in vitro* autoradiography: high receptor-mediated binding in androgen-dependent PC xenografts and only very low binding in androgen-responsive and androgen-independent PC-xenografts (Figure 2).

To determine hormonal regulation of the BN receptor family members, PC xenograft-bearing mice were androgen ablated by castration and implant removal. The effect of this treatment on the expression of BN receptors was determined 8–10 d after castration using ^{125}I -universal ligand and ^{111}In -[DTPA-Pro¹,Tyr⁴]BN in an *in vitro* autoradiographic study. The GRP receptor-mediated binding in the androgen-dependent PC xenografts was drastically reduced after castration (Figures 3A and 3B). The androgen-independent but responsive and the androgen-independent PC xenografts showed no alteration in their binding profile of the radiolabeled peptides after castration of the animals (data not shown).

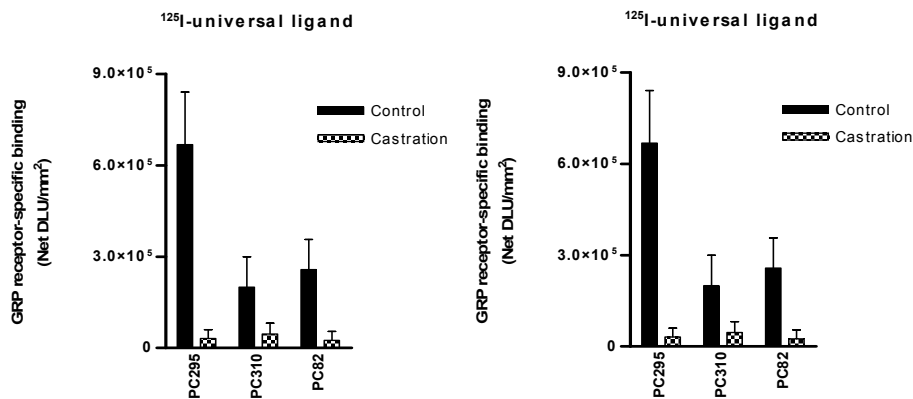


Figure 3. Receptor-specific binding of ^{125}I -universal ligand (= total binding [^{125}I -universal ligand 10^{-10} mol/L] minus unspecific binding [blocking with GRP 10^{-6} mol/L]) (A) and ^{111}In -[DTPA-Pro¹,Tyr⁴]BN (= [^{111}In -[DTPA-Pro¹,Tyr⁴]BN 10^{-9} mol/L] minus [blocking with [Tyr⁴]BN 10^{-6} mol/L]) (B) to androgen-dependent (AD), androgen-independent but responsive (AR), and androgen-independent (AD) PC xenograft sections. Xenografts were obtained from control mice or castrated mice (castration 8–10 d before tumor collection). Results are shown as average net density light units square millimeter (net DLU/mm²). Results are average of 3 independent experiments with ^{125}I -universal ligand (1 experiment with ^{111}In -[DTPA-Pro¹,Tyr⁴]BN) (n = 2 sections/experiment).

DISCUSSION

The overexpression of peptide receptors in human tumors is of considerable clinical interest [31]. For example, the overexpression of somatostatin receptors on human neuroendocrine tumors has enabled successful receptor-targeted visualization and treatment of these tumors. The long-term octreotide treatment of patients with somatostatin receptor-expressing tumors has been successful in relieving the symptoms related to excessive hormone production by these tumors [32]. Also the use of radiolabeled somatostatin analogs has permitted visualization of neuroendocrine tumors and their metastases in patients [16]. Additionally, ^{177}Lu and ^{90}Y -labeled somatostatin analogs have successfully been used in radionuclide therapy in this group of patients [33-35].

BN is a neuropeptide with a high affinity for the GRP receptor. This opens attractive clinical applications using the GRP receptor as a target, such as treatment with BN receptor antagonists, targeted chemotherapy with cytotoxic BN analogs, and peptide-receptor scintigraphy and radionuclide therapy using radiolabeled BN analogs. It has been reported that the GRP receptor is expressed in high densities on PC cells [5, 6, 36, 37]. Markwalder and Reubi described high GRP receptor expression in primary PC and prostatic intraepithelial neoplasias, whereas normal prostate tissue and, in most cases, prostatic hyperplasia were GRP receptor-negative. They also found GRP receptor expression in 4 of 7 bone metastases derived from hormone refractory patients, albeit with very diverse receptor densities [5].

The panel of PC xenografts used in this study represents the different stages in tumor progression from androgen-dependent to androgen-independent [24, 25]. This panel is well established and has been used in a variety of PC-related studies showing their relevance as perfect tools in basic and translational research [27, 38-40].

In vitro autoradiography on sections of all tumors of the panel using the radio-labeled BN receptor-binding ^{125}I -universal ligand and the ^{111}In -labeled BN analog [DTPA-Pro¹,Tyr⁴]BN has shown that GRP receptors are predominantly expressed in the androgen-dependent xenografts. This GRP receptor binding largely disappeared in the androgen-independent but responsive and the completely androgen-independent tumors. Also, castration (androgen ablation) of mice bearing the androgen-dependent PC xenografts resulted in strongly reduced GRP receptor expression. GRP receptor expression of the androgen-responsive and androgen-independent xenografts was not altered. These results suggest that GRP receptor expression is regulated by androgens.

Further preclinical and clinical studies are required to determine whether androgen regulation of GRP receptor expression found in these PC xenograft models can also be established in PC patients. Androgen-regulated GRP receptor expression in PC patients would imply that PC patients having received standard hormonal therapy may have very low levels of GRP receptor. As a result, GRP receptor-based technologies may not be relevant in patients who have been pretreated by hormonal therapy. On the other hand, it should not be omitted that the androgen-independent PC-3 and DU-145 cell lines, though not clinically representative, express GRP receptors and that some bone metastases derived from hormone-refractory patients were found to be GRP receptor-positive [5].

The results of this study provide strong support for the use of GRP receptors for a sensitive new image modality for PC patients at the earliest time possible. Early detection and accurate staging at the time of diagnosis is essential and determines the treatment options available, as the presence of lymph node metastasis will make local treatment needless. Also, a significant number of patients who have been treated locally by radical prostatectomy or radiation therapy will sooner or later show increasing levels of PSA of unknown origin and require additional therapy. These patients who have not yet been treated with additional hormonal therapy, but who are faced with generally low-volume metastases, may benefit from new systemic treatments using GRP receptor-based, BN-radiolabeled therapeutic analogs.

CONCLUSION

The results of this study suggest that in this model the overexpression of GRP receptors on prostate tumors is limited only to the androgen-dependent stages of PC. This overexpression of receptors is drastically reduced after androgen ablation in the animal model, indicating androgen regulation of the GRP receptor. Further studies are underway to determine GRP receptor density in tumor tissue derived from both hormonally treated and untreated patients as well as from patients at different stages of tumor progression. We are currently investigating the reversibility of castration-induced GRP receptor downregulation using the PC xenograft models.

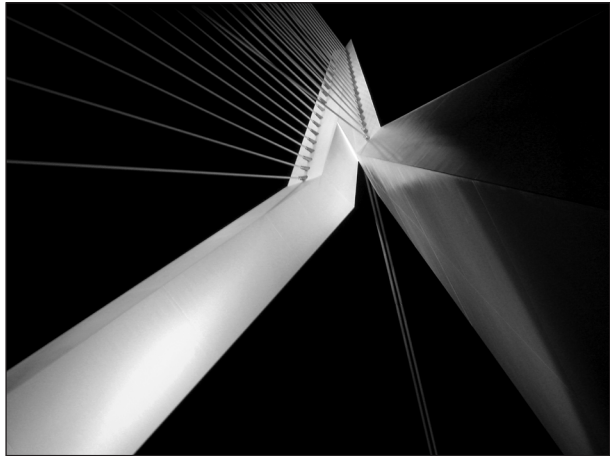
REFERENCES

1. Jemal A, Siegel R, Ward E, et al. Cancer statistics, 2007. *CA Cancer J Clin* 2007;57:43.
2. Arnold JT, Isaacs JT. Mechanisms involved in the progression of androgen-independent prostate cancers: it is not only the cancer cell's fault. *Endocr Relat Cancer* 2002;9:61.
3. Feldman BJ, Feldman D. The development of androgen-independent prostate cancer. *Nat Rev Cancer* 2001;1:34.
4. Martel CL, Gumerlock PH, Meyers FJ, et al. Current strategies in the management of hormone refractory prostate cancer. *Cancer Treat Rev* 2003;29:171.
5. Markwalder R, Reubi JC. Gastrin-releasing peptide receptors in the human prostate: relation to neoplastic transformation. *Cancer Res* 1999;59:1152.
6. Reubi JC, Wenger S, Schmockli-Maurer J, et al. Bombesin receptor subtypes in human cancers: detection with the universal radioligand (125)I-[D-TYR(6), beta-ALA(11), PHE(13), NLE(14)] bombesin(6-14). *Clin Cancer Res* 2002;8:1139.
7. Fathi Z, Corjay MH, Shapira H, et al. BRS-3: a novel bombesin receptor subtype selectively expressed in testis and lung carcinoma cells. *J Biol Chem* 1993;268:5979.
8. Nagalla SR, Barry BJ, Creswick KC, et al. Cloning of a receptor for amphibian [Phe13]bombesin distinct from the receptor for gastrin-releasing peptide: identification of a fourth bombesin receptor subtype (BB4). *Proc Natl Acad Sci U S A* 1995;92:6205.
9. Spindel ER, Giladi E, Brehm P, et al. Cloning and functional characterization of a complementary DNA encoding the murine fibroblast bombesin/gastrin-releasing peptide receptor. *Mol Endocrinol* 1990;4:1956.
10. Wada E, Way J, Shapira H, et al. cDNA cloning, characterization, and brain region-specific expression of a neuromedin-B-preferring bombesin receptor. *Neuron* 1991;6:421.
11. Ferris HA, Carroll RE, Lorimer DL, et al. Location and characterization of the human GRP receptor expressed by gastrointestinal epithelial cells. *Peptides* 1997;18:663.
12. Rettenbacher M, Reubi JC. Localization and characterization of neuropeptide receptors in human colon. *Naunyn Schmiedebergs Arch Pharmacol* 2001;364:291.
13. Erspamer V, Erpamer GF, Inselvini M. Some pharmacological actions of alytesin and bombesin. *J Pharm Pharmacol* 1970;22:875.
14. De Vincentis G, Scopinaro F, Varvarigou A, et al. Phase I trial of technetium [Leu13] bombesin as cancer seeking agent: possible scintigraphic guide for surgery? *Tumori* 2002;88:S28.
15. Van de Wiele C, Dumont F, Vanden Broecke R, et al. Technetium-99m RP527, a GRP analogue for visualisation of GRP receptor-expressing malignancies: a feasibility study. *Eur J Nucl Med* 2000;27:1694.
16. Krenning EP, Kwekkeboom DJ, Bakker WH, et al. Somatostatin receptor scintigraphy with [111In-DTPA-D-Phe1]- and [123I-Tyr3]-octreotide: the Rotterdam experience with more than 1000 patients. *Eur J Nucl Med* 1993;20:716.
17. Kwekkeboom D, Krenning EP, de Jong M. Peptide receptor imaging and therapy. *J Nucl Med* 2000;41:1704.
18. Otte A, Jermann E, Behe M, et al. DOTATOC: a powerful new tool for receptor-mediated radionuclide therapy. *Eur J Nucl Med* 1997;24:792.
19. Nock BA, Nikolopoulou A, Galanis A, et al. Potent bombesin-like peptides for GRP-receptor targeting of tumors with 99mTc: a preclinical study. *J Med Chem* 2005;48:100.
20. Smith CJ, Gali H, Sieckman GL, et al. Radiochemical investigations of (177)Lu-DOTA-8-Aoc-BBN[7-14]NH(2): an in vitro/in vivo assessment of the targeting ability of this new radiopharmaceutical for PC-3 human prostate cancer cells. *Nucl Med Biol* 2003;30:101.
21. Zhang X, Cai W, Cao F, et al. 18F-labeled bombesin analogs for targeting GRP receptor-expressing prostate cancer. *J Nucl Med* 2006;47:492.

22. Hoffman TJ, Gali H, Smith CJ, et al. Novel series of ¹¹¹In-labeled bombesin analogs as potential radiopharmaceuticals for specific targeting of gastrin-releasing peptide receptors expressed on human prostate cancer cells. *J Nucl Med* 2003;44:823.
23. van der Kwast TH, Schalken J, Ruizeveld de Winter JA, et al. Androgen receptors in endocrine-therapy-resistant human prostate cancer. *Int J Cancer* 1991;48:189.
24. van Weerden WM, de Ridder CM, Verdaasdonk CL, et al. Development of seven new human prostate tumor xenograft models and their histopathological characterization. *Am J Pathol* 1996;149:1055.
25. van Weerden WM, Romijn JC. Use of nude mouse xenograft models in prostate cancer research. *Prostate* 2000;43:263.
26. Jongsma J, Oomen MH, Noordzij MA, et al. Kinetics of neuroendocrine differentiation in an androgen-dependent human prostate xenograft model. *Am J Pathol* 1999;154:543.
27. van Weerden WM, van Kreuningen A, Elissen NM, et al. Castration-induced changes in morphology, androgen levels, and proliferative activity of human prostate cancer tissue grown in athymic nude mice. *Prostate* 1993;23:149.
28. van Steenbrugge GJ, Groen M, de Jong FH, et al. The use of steroid-containing Silastic implants in male nude mice: plasma hormone levels and the effect of implantation on the weights of the ventral prostate and seminal vesicles. *Prostate* 1984;5:639.
29. Bakker WH, Krenning EP, Breeman WA, et al. Receptor scintigraphy with a radioiodinated somatostatin analogue: radiolabeling, purification, biologic activity, and in vivo application in animals. *J Nucl Med* 1990;31:1501.
30. Bakker WH, Albert R, Bruns C, et al. [¹¹¹In-DTPA-D-Phe¹]-octreotide, a potential radiopharmaceutical for imaging of somatostatin receptor-positive tumors: synthesis, radiolabeling and in vitro validation. *Life Sci* 1991;49:1583.
31. Reubi JC. Peptide receptors as molecular targets for cancer diagnosis and therapy. *Endocr Rev* 2003;24:389.
32. Lamberts SW, Krenning EP, Reubi JC. The role of somatostatin and its analogs in the diagnosis and treatment of tumors. *Endocr Rev* 1991;12:450.
33. de Jong M, Kwekkeboom D, Valkema R, et al. Radiolabelled peptides for tumour therapy: current status and future directions. Plenary lecture at the EANM 2002. *Eur J Nucl Med Mol Imaging* 2003;30:463.
34. Kwekkeboom DJ, Bakker WH, Kooij PP, et al. [¹⁷⁷Lu-DOTAOTyr³]octreotate: comparison with [¹¹¹In-DTPA]octreotide in patients. *Eur J Nucl Med* 2001;28:1319.
35. Bodei L, Cremonesi M, Zoboli S, et al. Receptor-mediated radionuclide therapy with ⁹⁰Y-DOTA-TOC in association with amino acid infusion: a phase I study. *Eur J Nucl Med Mol Imaging* 2003;30:207.
36. Sun B, Halmos G, Schally AV, et al. Presence of receptors for bombesin/gastrin-releasing peptide and mRNA for three receptor subtypes in human prostate cancers. *Prostate* 2000;42:295.
37. Xiao D, Wang J, Hampton LL, et al. The human gastrin-releasing peptide receptor gene structure, its tissue expression and promoter. *Gene* 2001;264:95.
38. Hendriksen PJ, Dits NF, Kokame K, et al. Evolution of the androgen receptor pathway during progression of prostate cancer. *Cancer Res* 2006;66:5012.
39. Jongsma J, Oomen MH, Noordzij MA, et al. Different profiles of neuroendocrine cell differentiation evolve in the PC-310 human prostate cancer model during long-term androgen deprivation. *Prostate* 2002;50:203.
40. Marques RB, Erkens-Schulze S, de Ridder CM, et al. Androgen receptor modifications in prostate cancer cells upon long-term androgen ablation and antiandrogen treatment. *Int J Cancer* 2005;117:221.

7

Androgen-regulated gastrin-releasing peptide receptor expression in androgen-dependent human prostate tumor xenografts



Monique de Visser
Wytske M. van Weerden
Corrina M.A. de Ridder
Suzanne Reneman
Marleen Melis
Wout A.P. Breeman
Eric P. Krenning
Marion de Jong



Manuscript submitted

ABSTRACT

Human prostate cancer (PC) overexpresses gastrin releasing peptide (GRP) receptors. Radiolabeled GRP receptor-targeting analogs of bombesin (BN) have successfully been introduced as potential new visualization and treatment modalities for these tumors. In a previous study, human PC xenograft models representing different stages of tumor development showed high GRP receptor density in androgen-dependent PC tumor models, whereas androgen-independent tumors were found to be GRP receptor-negative. In the present study we investigated the effect of modulation of the androgen status of the animals on the expression of GRP receptors in three androgen-dependent human PC models PC-295, PC-310 and PC-82. The androgen-independent, GRP receptor-expressing, PC-3 model was used as reference model.

Methods: A biodistribution study was performed using the radiolabeled BN analog [^{111}In -DTPA-ACMpip⁵,Tha⁶, β Ala¹¹,Tha¹³,Nle¹⁴]BN(5-14) (^{111}In -Cmp 3 [1]) in xenograft-bearing male nude mice at different time points between 0-7 days after castration with or without subsequent supplementation of testosterone during 2-14 days. Tumor uptake of the radiolabeled BN analog was recorded and subsequently GRP receptor expression was evaluated *ex vivo* by autoradiography in tumor samples using the bombesin analogs ^{125}I -GRP and [^{111}In -DTPA-Pro¹,Tyr⁴]BN.

Results: For all three tumor models studied, a significantly decreased tumor uptake was found after castration of tumor-bearing animals (41-73% of control at 7 days after castration). When testosterone was subsequently supplemented to the castrated animals for up to 14 days, GRP receptor-mediated tumor uptake was restored to control level. The androgen-independent PC-3 xenograft showed no-decrease in GRP receptor-expression after castration and no subsequent response to testosterone supplementation.

Conclusion: Androgen manipulation strongly affected GRP receptor-expression in androgen-dependent tumor models, indicating that GRP receptor-expression in these human PC models is androgen-regulated.

INTRODUCTION

Prostate cancer (PC) is the second leading cause of cancer-related deaths and the most frequently diagnosed cancer in men in Western countries [2]. PC will increase to be a major health problem due to the aging of people in the Western world. Metastatic PC is a major oncological problem and is not curable, although initially hormone deprivation therapy is effective in the majority of patients [3]. PC patients will however eventually relapse, due to progression towards hormone independent growth of the tumor. Unfortunately, PC responds poorly to chemotherapeutic agents of which taxane-based treatments are nowadays considered the standard second-line treatment of hormone-resistant PC [4, 5]. Eventually, most patients will die of progressive, hormone-independent disease. Early diagnosis of localized tumors and improved staging of (metastatic) disease are essential determinants that will improve treatment decisions by better judging the need for systemic therapies.

Furthermore, early screening for PC using prostate specific antigen (PSA), as a biomarker will result in a stage shift towards the detection of early organ-confined tumors. Early treatment of these tumors will demand for new concepts of local treatment modalities using tumor-specific targets as future strategies for the clinical management of PC.

It has been shown that prostate tumors overexpress gastrin releasing peptide (GRP) receptors [6-9]. The overexpression of these receptors in prostate tumors is restricted to the malignant cells, as normal and hyperplastic prostate tissue were shown to be GRP receptor-negative [6]. The GRP receptor is a member of the bombesin (BN) receptor family, which consists of four known receptor subtypes. Three of them, the neuromedin B (NMB) receptor (BB₁), the GRP receptor (BB₂) and BN receptor subtype 3 (BRS-3 or BB₃), are mammalian receptors, whereas the fourth subtype (BB₄) is found only in amphibians [10-13]. Except for the GRP receptor, these receptor subtypes are not very well characterized with regard to their distribution and function in human tissues [14, 15]. Bombesin-like peptides, such as BN, GRP and NMB, are involved in the regulation of a large number of biological processes in the gut and central nervous system (CNS) [16] and mediate their action by binding to the BN receptor subtypes. This opens attractive clinical applications using the GRP receptor as a target, using BN receptor antagonists, targeted chemotherapy with cytotoxic BN analogs and peptide-receptor scintigraphy (PRS) and radionuclide therapy (PRRT) using radiolabeled BN analogs.

In a previous study we evaluated the expression of GRP receptors in different stages of tumor development using a panel of 12 xenograft models from 9 different patients representing the various stages of human PC ranging from androgen-dependent to androgen-independent disease (Table 1) [17, 18]. We found GRP receptor-

mediated binding of radiolabeled BN analogs only in androgen-dependent but not in androgen-independent xenografts representing the more advanced stages of prostate tumor development [19]. These results suggest that GRP receptor-expression is related to the state of androgen-dependency of PC.

In the present study we investigated the influence of androgens on GRP receptor-expression in three androgen-dependent human PC xenograft models PC-82, PC-295 and PC-310, and in the reference androgen-independent PC-3 xenograft model. In contrast to the androgen responsive xenograft models, the PC-3 cell line is not considered to be a very relevant model for human prostate disease as this cell line, does not express androgen receptor and PSA, features that are very characteristic for most PC patients [20]. However, PC-3 cells do express GRP receptors in high density and is a suitable model for evaluation of GRP receptor-targeting agents. The PC-3 cell line is often used in GRP receptor-related studies, and therefore is chosen as a reference model in our studies. Androgen regulation of GRP receptor-expression was evaluated by manipulation of the androgen status of the animal by androgen ablation treatment and subsequent supplementation with testosterone. GRP receptor-expression was determined *in vivo* in a biodistribution study using the radiolabeled BN analog [^{111}In -DTPA-ACMpip⁵,Tha⁶, β Ala¹¹,Tha¹³,Nle¹⁴]BN(5-14), referred to as ^{111}In -Cmp 3, followed by autoradiographic analyses of tissue samples with ^{125}I -GRP and [^{111}In -DTPA-Pro¹,Tyr⁴]BN.

MATERIAL AND METHODS

PC Xenografts

Xenografts were routinely propagated in intact male nude NMRI (Naval Medical Research Institute) mice (Taconic M&B, Ry, Denmark) as described previously [17-19]. The experiment was approved by the Animal Experimental Committee (DEC) of the Erasmus University and performed in agreement with The Netherlands Experiments on Animals Act (1977) and the European Convention for protection of Vertebrate Animals used for Experimental Purposes (Strasbourg, 18 March 1986).

Mice were implanted subcutaneously with small fragments of human prostate tumor. In the case of androgen dependent tumor transplantation, mice were supplemented with testosterone to obtain optimal tumor take (80-85%) and tumor growth. Hormonal substitution was achieved by implanting silastic tubings filled with crystalline steroid (6mg/tubing; AppliChem, Darmstadt, Germany). These testosterone implants result in constant supraphysiological levels of testosterone exceeding the low physiological levels in intact male nude mice for at least 75 days [21].

Table 1. PC xenograft panel

Tumor model	Origin	AD/AR/AI	Androgen receptor	PSA	GRP receptor-binding [#]
PC-295	LN	AD	+	+	+
PC-310	PC	AD	+	+	+
PC-82	PC	AD	+	+	+
PC-346 p*	TURP	AS	+	+	-
PC-346 I		AS	+ [†]	+	-
PC-346 B		AS	+	+	-
PC-346 BI		AS	+	+	-
PC-374	SSM	AS	+	+	-
PC-133	Bone	AI	-	-	-
PC-135	PC	AI	-	-	-
PC-324	TURP	AI	-	-	-
PC-339	TURP	AI	-	-	-

Note; *PC-346 p is derived from a nonprogressive TURP patient, and the 3 sublines were derived from this xenograft. [†]Androgen receptor mutation (T877A). [#]GRP receptor-mediated binding of ¹²⁵I-universal ligand [19]. AD = androgen-dependent; AS = androgen-sensitive; AI = androgen-independent; PSA = prostatespecific antigen; PC = primary prostate tumor; LN = lymph node metastasis; TURP = transurethral resection of the prostate; SSM = scrotal skin metastasis.

Androgen Ablation and Testosterone Supplementation

Androgen withdrawal was performed by surgical castration under ketamin (Alfasan, Woerden, The Netherlands) and Rompun (Bayer AG, Leverkusen, Germany) anesthesia (mix of 1:1), followed by removal of the silastic testosterone implants. Supplementation of testosterone was accomplished by subsequent re-implantation of testosterone implants at different days after castration.

Radiolabeled Peptides

Iodine-125 labeled GRP was obtained commercially from Amersham Biosciences (Buckinghamshire, United Kingdom). Bombesin analog [D-Tyr⁶, βAla¹¹, Phe¹³, Nle¹⁴]BN(6-14), referred to as universal ligand, was provided by Biosynthema Inc. (St. Louis, USA) and radiolabeled with ¹²⁵I as described previously [22]. Bombesin analogs [DTPA-Pro¹, Tyr⁴]BN and [DTPA-ACMpip⁵, Tha⁶, βAla¹¹, Tha¹³, Nle¹⁴]BN(5-14) (Cmp 3) were provided by Mallinckrodt Inc. (St. Louis, USA), and radiolabeled with ¹¹¹In (¹¹¹InCl₃, Tyco Healthcare, Petten, the Netherlands, DRN 4901, 370 MBq/ml in HCl, pH 1.5-1.9) as described earlier [23-25].

Biodistribution Studies

Tumor-bearing mice were testosterone supplemented (control), or castrated at 2, 4, or 7 days (cas 2, cas 4, cas 7). Additionally, 3 groups of mice were castrated and after 7 days supplemented with testosterone for 2, 4, and 14 days (cas 7 T 2, cas 7 T 4, cas 7 T 14). Mice were injected intravenously with 4 MBq/0.1 μg/200 μl of the radiolabeled

BN analog ^{111}In -Cmp 3, and sacrificed 4 hours after injection. Tumor tissue and other organs of interest, including GRP receptor-positive organs, background tissue and clearance organs, were collected for counting of radioactivity (LKB-1282-compugamma system, Perkin Elmer, Oosterhout, the Netherlands) and calculation of the uptake (% injected dose per g of tissue). Immediately after counting, the tumors were snap frozen in liquid nitrogen for *in vitro* autoradiography.

After decay of radioactivity, tumors were evaluated in an *in vitro* autoradiographic experiment using ^{125}I -GRP (74 TBq/mmol) and ^{111}In -[DTPA-Pro¹,Tyr⁴]BN (200 MBq/nmol)

Autoradiographic Analyses

PC xenograft tumor tissues were evaluated in an *in vitro* autoradiographic experiment as described previously [19]. In short, frozen xenograft sections (10 μm) were incubated for 1 hour at room temperature with 0.1 nM ^{125}I -universal ligand (74 TBq/mmol), ^{125}I -GRP (74 TBq/mmol) or ^{111}In -[DTPA-Pro¹,Tyr⁴]BN (200 MBq/nmol). To discriminate between GRP receptor-mediated binding and non-receptor-mediated binding sections were incubated in the presence of an excess (1 μM) of GRP or [Tyr⁴]BN (Sigma Aldrich, Zwijndrecht, The Netherlands). The sections were exposed to phosphor imaging screens (Perkin Elmer, Boston USA) for 16-72 hours. The screens were read using a Cyclone Storage Phosphor System (Packard, Meriden, USA) and the autoradiograms were quantified using Optiquant Software (Packard, Meriden, USA). Results are indicated as average GRP receptor-mediated binding (net Density Light Units/ mm^2 of total binding minus non-specific binding) as percentage of intact animals (control, 100%) of radiolabeled peptide.

Statistical analysis was performed using the Mann Whitney and unpaired t-test. A probability of less than 0.05 was considered significant.

RESULTS

Effect of Androgen Ablation on GRP Receptor-Binding: Autoradiographic Analyses

GRP receptor-expression was determined by *in vitro* autoradiography on tumor sections of 3 androgen-dependent human PC xenografts. Tumors were derived from intact hormonally supplemented, castrated male nude mice, or castrated mice subsequently supplemented with testosterone. The results of the *in vitro* autoradiography studies using ^{125}I -universal ligand are shown in figure 1.

The androgen-dependent PC xenografts PC-295, PC-310 and PC-82 derived from intact, testosterone supplemented mice showed high binding of ^{125}I -universal ligand, which was almost completely blocked by 10^{-6} M of universal ligand, GRP and BN,

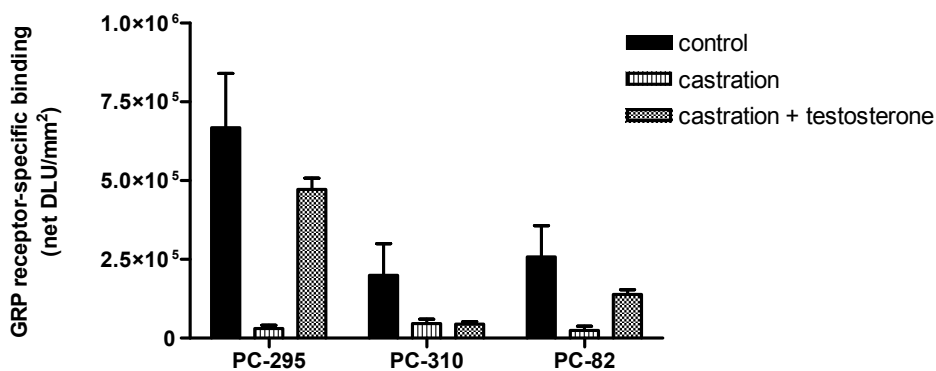


Figure 1. GRP receptor-specific binding of ^{125}I -universal ligand (= total binding (^{125}I -universal ligand 10^{-10}M) minus non-specific binding (^{125}I -universal ligand 10^{-10}M + GRP 10^{-6}M) to androgen-dependent PC xenograft sections. Xenografts were obtained from control mice, castrated mice (castration 7-10 days before tumor collection) or castrated mice that received testosterone (castration + testosterone = 57 + 38 days, 29 + 13 days and 20 + 22 days respectively for PC-295, PC-310 and PC-82). Results are shown as average net Density Light Units per mm^2 (net DLU/ mm^2). Results are average from 3 independent experiments (1 experiment for the castration + testosterone group) (n = 2-4 sections/experiment).

and to a much lesser extent by 10^{-6}M NMB (data not shown). This blocking pattern indicates high receptor-mediated binding of ^{125}I -universal ligand to predominantly GRP receptors, as described by Reubi et al. [7]. This is consistent with our previous findings [19].

GRP receptor-mediated binding of ^{125}I -universal ligand was drastically reduced after androgen ablation in all 3 androgen-dependent PC xenografts resulting in 95, 77, and 90% reduction of GRP receptor-binding in PC-295, PC-310, and PC-82 respectively. Reversing the androgen ablation treatment was achieved by re-supplementation of testosterone implants in tumor bearing mice (57, 29, and 20 days post-castration for PC-295, PC-310 and PC-82, respectively). Animals were sacrificed and tumors were collected at 38, 13, and 22 days for PC-295, PC-310 and PC-82 respectively. A partial recovery of GRP receptor-mediated ligand binding to 70 and 54% of control level was observed for PC-295 and PC-82 respectively. PC-310 showed no regain of ligand binding compared to the ablated PC-310 tumor after 13 days of testosterone administration.

Effect of Androgen Ablation on GRP Receptor-Mediated Tumor Uptake: Biodistribution Studies

A similar study set-up was chosen to evaluate *in vivo* biodistribution of the radiolabeled BN analog, ^{111}In -Cmp 3, in PC xenografts bearing mice under hormonal manipulation. The uptake of the ^{111}In -labeled peptide at 4 hours after injection in the GRP receptor-positive tumor, pancreas, and intestines as well as in background tissue and clearance organs were found to be in agreement with our previous results obtained with this BN

Table 2.

Group	study	PC-295		PC-82		PC-310		PC-3	
		% of control	(n)	% of control	(n)	% of control	(n)	% of control	(n)
control	uptake $^{111}\text{In-Cmp 3}$	100 ± 31	(11)	100 ± 31	(14)	100 ± 19	(4)	100 ± 33	(12)
	binding $^{125}\text{I-GRP}$	100 ± 19		100 ± 37		100 ± 67		100 ± 53	
	binding $^{111}\text{In-BN}$	100 ± 36		100 ± 54		100 ± 25		100 ± 42	
cas 2	uptake $^{111}\text{In-Cmp 3}$	124 ± 29	(5)	109 ± 37	(3)				
	binding $^{125}\text{I-GRP}$	72 ± 6.9*		67 ± 26		nd		nd	
	binding $^{111}\text{In-BN}$	55 ± 17*		67 ± 28					
cas 4	uptake $^{111}\text{In-Cmp 3}$	22 ± 7.3*	(5)	56 ± 30	(3)				
	binding $^{125}\text{I-GRP}$	11 ± 8.1*		29 ± 27*		nd		nd	
	binding $^{111}\text{In-BN}$	6.5 ± 6.4*		27 ± 30					
cas 7	uptake $^{111}\text{In-Cmp 3}$	27 ± 22*	(12)	46 ± 17*	(8)	59 ± 4.0*	(5)	141 ± 24*	(5)
	binding $^{125}\text{I-GRP}$	3.4 ± 1.9*		12 ± 5.3*		55 ± 14		123 ± 54	
	binding $^{111}\text{In-BN}$	1.5 ± 0.8*		7.7 ± 3.8*		52 ± 28		120 ± 19	
cas 7 T 2	uptake $^{111}\text{In-Cmp 3}$	35.8 ± 11	(5)	62 ± 10	(3)				
	binding $^{125}\text{I-GRP}$	20 ± 6.0**		33 ± 4.6**		nd		nd	
	binding $^{111}\text{In-BN}$	14 ± 6.5**		28 ± 6.4**					
cas 7 T 4	uptake $^{111}\text{In-Cmp 3}$	40 ± 9.4**	(4)	107 ± 12**	(3)				
	binding $^{125}\text{I-GRP}$	30 ± 9.7**		60 ± 23**		nd		nd	
	binding $^{111}\text{In-BN}$	17 ± 6.3**		56 ± 10**					
cas 7 T 14	uptake $^{111}\text{In-Cmp 3}$			86 ± 46	(8)	99 ± 30**	(5)	95 ± 47	(5)
	binding $^{125}\text{I-GRP}$	nd		91 ± 30**		50 ± 19		112 ± 76	
	binding $^{111}\text{In-BN}$			87 ± 40**		83 ± 21		125 ± 49	

Note; Biodistribution results are average tumor uptake of $^{111}\text{In-Cmp 3}$ (% injected dose/ gram) as percentage of intact animals (control, 100%). *In vitro* autoradiography results are average GRP receptor-mediated binding (net Density Light Units/ mm^2 of total binding minus non-specific binding) as percentage of the intact animals (control, 100%) of $^{125}\text{I-GRP}$ and $^{111}\text{In-[DTPA-Pro}^1\text{,Tyr}^4\text{]BN}$. cas = castration for 2, 4 or 7 days; T = testosterone supplementation for 2, 4, or 14 days; nd= not determined. * = significantly different from control group ($P < 0.05$); ** = significantly different from castration for 7 days ($P < 0.05$).

analog in male nude NMRI mice bearing PC-3 tumors [1]. The uptake of ^{111}In -labeled Cmp-3 peptide is indicated in table 2. All androgen-dependent PC tumors demonstrated a significant growth inhibition after androgen ablation with a consistent reduction in tumor uptake at 7 days after castration of tumor-bearing mice. This decline was strongest in PC-295 showing a decrease in tumor uptake of 73% ($p=0.0002$). Supplementing testosterone to castrated mice resulted in a partial reversal of the uptake in all 3 androgen-dependent tumor models. Peptide uptake in PC-295 tumors after 4 days of testosterone administration increased from 27% before testosterone supplementation to 40% after supplementation ($p=0.05$). The reduction in peptide uptake in androgen depleted PC-82 and PC-310 tumors was less pronounced than in PC-295, although still significant (54% and 41% respectively, $p<0.016$). Resupplementation of these mice

with testosterone resulted in a recovery of uptake to almost control level (86% and 99% for PC-82 and PC-310, respectively).

Growth of the androgen-independent PC-3 model was not affected by ablation treatment. Interestingly, tumor uptake of the ^{111}In -BN analog was increased up to 141% after ablation, which was normalized after testosterone supplementation.

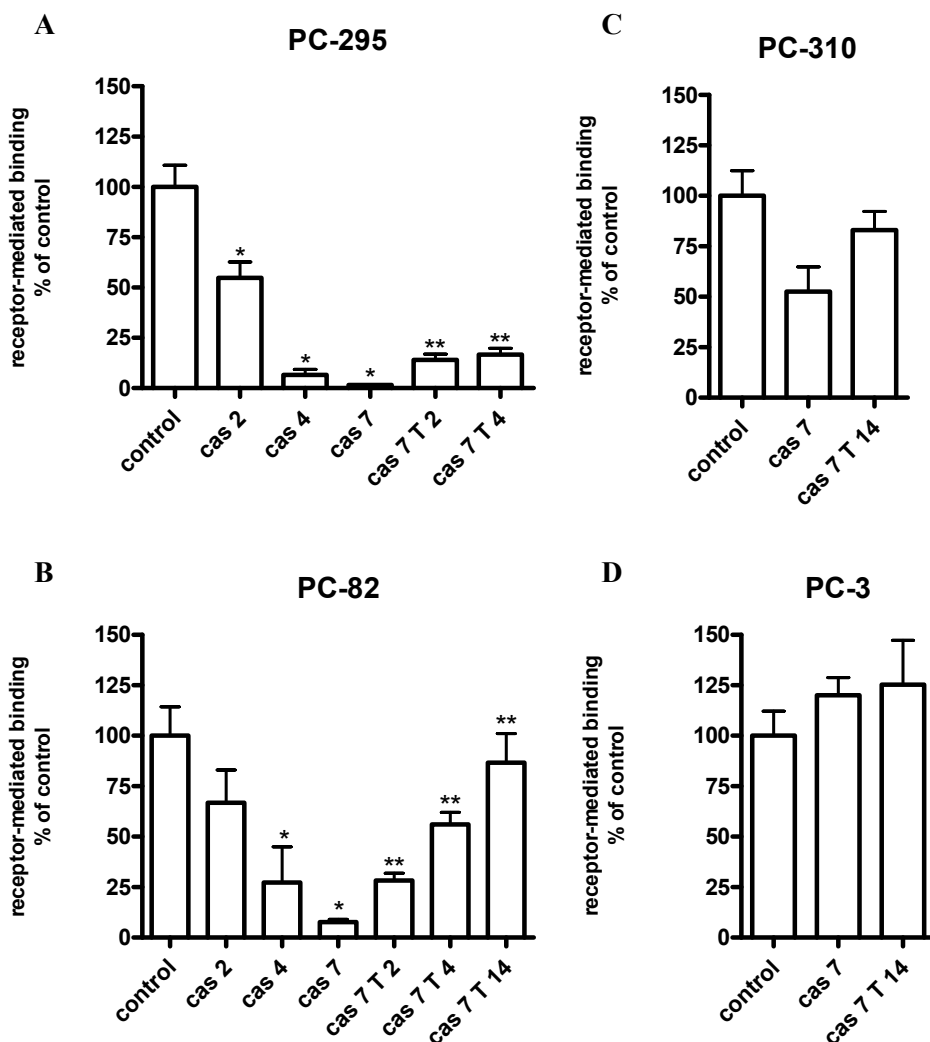


Figure 2. Receptor-mediated binding of ^{111}In -[DTPA-Pro¹,Tyr⁴] to androgen-dependent PC-295 (A), PC-310 (B), PC-82 (C), and androgen-independent PC-3 (D) xenograft sections. Xenografts were derived from biodistribution study (Table 1). Results are average receptor-mediated binding (net Density Light Units/mm² of total binding minus non-specific binding) as percentage of the control group (100%) (n = 4-14 xenografts / group (see Table 1), 2 sections / xenograft). cas = castration for 2, 4 or 7 days; T = testosterone supplementation for 2, 4, or 14 days; * = significantly different from control group (P < 0.05); ** = significantly different from cas 7 group (P < 0.05).

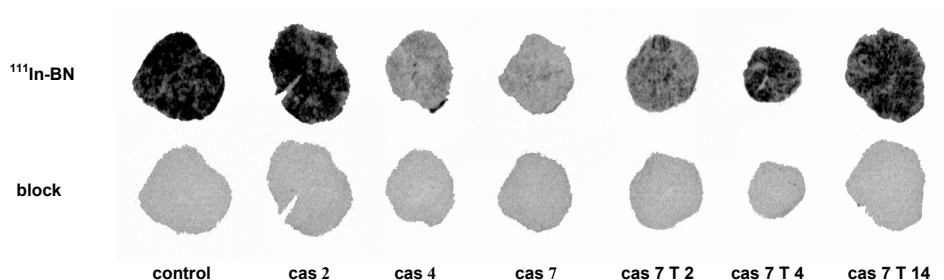


Figure 3. *In vitro* autoradiograms of PC-82 tumor sections incubated with 10^{-10} M ^{111}In -[DTPA-Pro¹,Tyr⁴]BN with (*block*) or without (^{111}In -BN) additional 10^{-6} M Tyr⁴-BN. Xenografts were derived from biodistribution study (Table 1).

Frozen sections of the PC xenografts derived from the biodistribution study were used for autoradiography of GRP receptor-binding with the GRP receptor-binding peptides ^{125}I -GRP and ^{111}In -[DTPA-Pro¹,Tyr⁴]BN. Results are shown in table 2 and figures 2 and 3. The effect of androgen ablation on GRP receptor-mediated tumor uptake as determined in the biodistribution study could be confirmed by autoradiography: GRP receptor-binding of both ^{125}I -GRP and the ^{111}In -BN analog appeared to be suppressed due to the ablation. In compliance with the biodistribution results, PC-295 showed the strongest response to ablation treatment with >94% reduction of GRP receptor-binding ($P > 0.0001$), compared to >88% for PC-82 and >45% for PC-310. Recovery of GRP receptor-binding after testosterone supplementation was again more rapid for PC-82 than for PC-295; 17% versus 56% of control value at 4 days after re-implantation for PC-295 and PC-82 respectively. PC-82 showed near complete restoration of receptor-binding of up to 91% at 14 days of testosterone administration. In contrast, GRP receptor recovery in the PC-310 was incomplete.

Consistent with the biodistribution data, the androgen-independent PC-3 tumor demonstrated a slight, non-significant, increase of GRP receptor-binding after testosterone ablation, which was restored to control levels after testosterone supplementation.

DISCUSSION

Due to early screening for PC with prostate-specific antigen (PSA) tests, more patients are being diagnosed when tumors are still confined to the prostate and surgical intervention is still an option. However, the (micro)metastatic stage of these tumors is often uncertain. Metastatic disease has a significant impact on the prognosis and determines therapy options. Reliable and sensitive diagnostic tools are highly wanted to improve staging quality at time of diagnosis.

It has been reported that the GRP receptor is expressed in high density on PC cells [6-9]. Markwalder and Reubi described high GRP receptor-expression in primary PC and prostatic intraepithelial neoplasias (PIN), whereas normal prostate tissue and, in most cases, prostatic hyperplasia expressed no, or only very low levels of GRP receptors [6]. They also found GRP receptor-expression in 4 out of 7 bone metastases derived from hormone-refractory patients albeit very diverse receptor densities. Bombesin (BN) is a neuropeptide with high affinity for the GRP receptor. Radiolabeled analogs of these BN-like peptides are being developed as promising new radiopharmaceuticals for imaging and therapy of GRP receptor-expressing tumors, such as PC [26-31].

Evaluation of GRP receptor expression throughout the different stages of human prostate tumor development using a panel of 12 well established human PC xenograft models has shown that GRP receptors are predominantly expressed in the androgen-dependent xenografts. GRP receptor binding largely disappeared in androgen-independent but responsive and completely androgen-independent tumors. Also, castration (androgen ablation) of mice bearing androgen-dependent PC xenografts resulted in strongly reduced *in vitro* GRP receptor-binding. These results indicated that GRP receptor-expression is androgen-regulated [19].

To further study androgen regulation of the GRP receptor we used three androgen responsive prostate cancer models. We hypothesized that if reduced GRP receptor-expression was induced by androgen ablation in de androgen-dependent xenograft bearing mice the expression could be reversed by restoring the hormonal status of the animals. *In vitro* ¹²⁵I-labeled peptide binding studies supported our hypothesis; complete recovery of GRP receptor-mediated binding after supplementing testosterone in androgen ablated mice bearing androgen-dependent PC-295 and PC-82 xenografts. The recovery rate was incomplete, however in the case of the third androgen-dependent PC-310 tumor. This may be explained by a shorter testosterone supplementation period (13 days versus 38 and 22 days for PC-295 and PC-82 respectively), suggesting that restoration of GRP receptor expression is a relatively slow process (Figure 1).

In vivo biodistribution studies were performed with the previously evaluated ¹¹¹In-Cmp 3 BN analog [1]. Consistent with previous *in vitro* results, ¹¹¹In-BN analog uptake was significantly reduced in castrated mice in all three androgen-dependent xenografts. Supplementation of mice with testosterone induced significant recovery of tumor uptake in all three xenograft models. *In vitro* autoradiography confirmed the *in vivo* biodistribution results.

As expected, GRP receptor-expression in the androgen-independent PC-3 model was not regulated by androgens. These results underline the fact that the PC-3 xenograft is a useful model for the general testing of new GRP receptor-targeting

compounds, the model does not behave like early stage androgen responsive prostate cancer and thus is of low clinical relevance as model for prostate cancer [20].

CONCLUSION

The results of this study show that expression of GRP receptors in androgen responsive human PC xenograft models is androgen-regulated. Clinically, this would imply that PC patients having received standard hormonal therapy may have very low tumor expression of GRP receptors and therefore, GRP receptor based technologies may not be relevant in patients that have been pre-treated by hormonal therapy. On the other hand, this study shows that the GRP-receptor seems to be a very good alternative target for new imaging and- treatment modalities in early stage, hormonally naïve, untreated patients. Studies are now underway to further validate GRP receptor density in tumor tissue derived from both hormonally treated and –untreated patients as well as from patients at different stages of tumor progression.

ACKNOWLEDGEMENTS

The authors thank Erik de Blois for radiolabeling of the BN peptides and Nanda Wildeman for her help with the autoradiographic experiments.

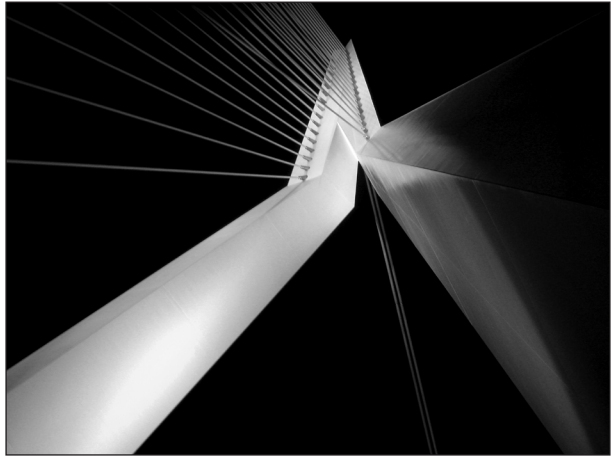
REFERENCES

1. de Visser, M., H.F. Bernard, J.L. Erion, et al., Novel (111)In-labelled bombesin analogues for molecular imaging of prostate tumours. *Eur J Nucl Med Mol Imaging* 2007; 34(8): 1228.
2. Jemal, A., R. Siegel, E. Ward, et al., Cancer statistics, 2007. *CA Cancer J Clin* 2007; 57(1): 43.
3. Scherr, D., P.W. Swindle and P.T. Scardino, National Comprehensive Cancer Network guidelines for the management of prostate cancer. *Urology* 2003; 61(2 Suppl 1): 14.
4. Mancuso, A., S. Oudard and C.N. Sternberg, Effective chemotherapy for hormone-refractory prostate cancer (HRPC): present status and perspectives with taxane-based treatments. *Crit Rev Oncol Hematol* 2007; 61(2): 176.
5. Oudard, S., E. Banu, P. Beuzebec, et al., Multicenter randomized phase II study of two schedules of docetaxel, estramustine, and prednisone versus mitoxantrone plus prednisone in patients with metastatic hormone-refractory prostate cancer. *J Clin Oncol* 2005; 23(15): 3343.
6. Markwalder, R. and J.C. Reubi, Gastrin-releasing peptide receptors in the human prostate: relation to neoplastic transformation. *Cancer Res* 1999; 59(5): 1152.
7. Reubi, J.C., S. Wenger, J. Schmuckli-Maurer, et al., Bombesin receptor subtypes in human cancers: detection with the universal radioligand (125)I-[D-TYR(6), beta-ALA(11), PHE(13), NLE(14)] bombesin(6-14). *Clin Cancer Res* 2002; 8(4): 1139.
8. Sun, B., G. Halmos, A.V. Schally, et al., Presence of receptors for bombesin/gastrin-releasing peptide and mRNA for three receptor subtypes in human prostate cancers. *Prostate* 2000; 42(4): 295.
9. Xiao, D., J. Wang, L.L. Hampton, et al., The human gastrin-releasing peptide receptor gene structure, its tissue expression and promoter. *Gene* 2001; 264(1): 95.
10. Spindel, E.R., E. Giladi, P. Brehm, et al., Cloning and functional characterization of a complementary DNA encoding the murine fibroblast bombesin/gastrin-releasing peptide receptor. *Mol Endocrinol* 1990; 4(12): 1956.
11. Wada, E., J. Way, H. Shapira, et al., cDNA cloning, characterization, and brain region-specific expression of a neuromedin-B-preferring bombesin receptor. *Neuron* 1991; 6(3): 421.
12. Nagalla, S.R., B.J. Barry, K.C. Creswick, et al., Cloning of a receptor for amphibian [Phe13] bombesin distinct from the receptor for gastrin-releasing peptide: identification of a fourth bombesin receptor subtype (BB4). *Proc Natl Acad Sci U S A* 1995; 92(13): 6205.
13. Fathi, Z., M.H. Corjay, H. Shapira, et al., BRS-3: a novel bombesin receptor subtype selectively expressed in testis and lung carcinoma cells. *J Biol Chem* 1993; 268(8): 5979.
14. Ferris, H.A., R.E. Carroll, D.L. Lorimer, et al., Location and characterization of the human GRP receptor expressed by gastrointestinal epithelial cells. *Peptides* 1997; 18(5): 663.
15. Rettenbacher, M. and J.C. Reubi, Localization and characterization of neuropeptide receptors in human colon. *Naunyn Schmiedebergs Arch Pharmacol* 2001; 364(4): 291.
16. Erspamer, V., G.F. Erpamer and M. Inselvini, Some pharmacological actions of alytesin and bombesin. *J Pharm Pharmacol* 1970; 22(11): 875.
17. van Weerden, W.M., C.M. de Ridder, C.L. Verdaasdonk, et al., Development of seven new human prostate tumor xenograft models and their histopathological characterization. *Am J Pathol* 1996; 149(3): 1055.
18. van Weerden, W.M. and J.C. Romijn, Use of nude mouse xenograft models in prostate cancer research. *Prostate* 2000; 43(4): 263.
19. de Visser, M., W.M. van Weerden, C.M. de Ridder, et al., Androgen-dependent expression of the gastrin-releasing Peptide receptor in human prostate tumor xenografts. *J Nucl Med* 2007; 48(1): 88.
20. van der Kwast, T.H., J. Schalken, J.A. Ruizeveld de Winter, et al., Androgen receptors in endocrine-therapy-resistant human prostate cancer. *Int J Cancer* 1991; 48(2): 189.

21. van Steenbrugge, G.J., M. Groen, F.H. de Jong, et al., The use of steroid-containing Silastic implants in male nude mice: plasma hormone levels and the effect of implantation on the weights of the ventral prostate and seminal vesicles. *Prostate* 1984; 5(6): 639.
22. Bakker, W.H., E.P. Krenning, W.A. Breeman, et al., Receptor scintigraphy with a radioiodinated somatostatin analogue: radiolabeling, purification, biologic activity, and in vivo application in animals. *J Nucl Med* 1990; 31(9): 1501.
23. Breeman, W.A., M. De Jong, B.F. Bernard, et al., Pre-clinical evaluation of [(111)In-DTPA-Pro(1), Tyr(4)]bombesin, a new radioligand for bombesin-receptor scintigraphy. *Int J Cancer* 1999; 83(5): 657.
24. Breeman, W.A., L.J. Hofland, M. de Jong, et al., Evaluation of radiolabelled bombesin analogues for receptor-targeted scintigraphy and radiotherapy. *Int J Cancer* 1999; 81(4): 658.
25. Breeman, W.A., E. de Blois and K. E.P. Effects of quenchers on the radiochemical purity of 111In-labeled peptides. in *SNM annual meeting 2007* 2007. Washington DC.
26. De Vincentis, G., F. Scopinaro, A. Varvarigou, et al., Phase I trial of technetium [Leu13] bombesin as cancer seeking agent: possible scintigraphic guide for surgery? *Tumori* 2002; 88(3): S28.
27. Panigone, S. and A.D. Nunn, Lutetium-177-labeled gastrin releasing peptide receptor binding analogs: a novel approach to radionuclide therapy. *Q J Nucl Med Mol Imaging* 2006; 50(4): 310.
28. Smith, C.J., W.A. Volkert and T.J. Hoffman, *Radiolabeled peptide conjugates for targeting of the bombesin receptor superfamily subtypes*, in *Nucl Med Biol*. 2005. p. 733.
29. Smith, C.J., W.A. Volkert and T.J. Hoffman, Gastrin releasing peptide (GRP) receptor targeted radiopharmaceuticals: a concise update. *Nucl Med Biol* 2003; 30(8): 861.
30. Van de Wiele, C., F. Dumont, R. Vanden Broecke, et al., Technetium-99m RP527, a GRP analogue for visualisation of GRP receptor- expressing malignancies: a feasibility study. *Eur J Nucl Med* 2000; 27(11): 1694.
31. De Vincentis, G., F. Scopinaro, A. Varvarigou, et al., Phase I trial of technetium [Leu13] bombesin as cancer seeking agent: possible scintigraphic guide for surgery? *Tumori* 2002; 88(3): S28.

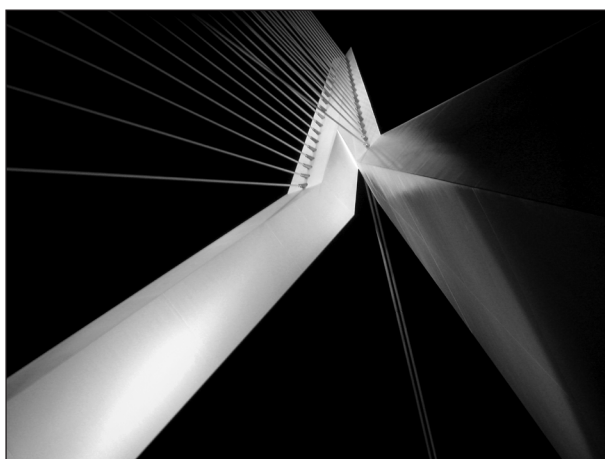
IV

Epilogue



8

Summary and general discussion



Radiolabeled receptor-binding peptides have been shown to be powerful tools for imaging and therapy of tumors. Especially analogs of somatostatin were proven to be effective in receptor-targeted localization, staging and treatment of ss_{t_2} -expressing neuroendocrine tumors. However, much profit can still be gained with the development of radiopharmaceuticals targeting other types of cancer which do not over-express ss_{t_2} receptors in sufficiently high levels. In this project we therefore aimed to develop and evaluate radiolabeled peptide analogs of neurotensin (NT) for targeting neurotensin receptor-1 (NTR-1) expressing exocrine pancreatic tumors (**Part I**) and analogs of bombesin (BN) for gastrin releasing peptide (GRP) receptor-targeted scintigraphy of prostate cancer (**Part II**). In addition, we evaluated the expression of GRP receptors throughout the different stages of prostate cancer development (**Part III**). Below we summarize our results and discuss the potential of radiolabeled BN and NT peptides for clinical application.

Part I: Neurotensin analogs for *in vivo* targeting of exocrine pancreatic cancer

The expression of NT receptors was shown in several human cancers, such as Ewing's sarcomas, astrocytomas, meningiomas, and in 75% of exocrine ductal pancreatic adenocarcinomas. The latter is of particular clinical interest due to the poor prognosis and the lack of ss_{t_2} -expression. Due to its extremely rapid progression and the late revelation of symptoms, exocrine pancreatic cancer is rarely curable by surgical intervention at the time of diagnosis. Therefore, novel clinical tools are urgently needed for its early diagnosis and therapy.

The presence of NT receptors in these human tumors versus their absence or minimal expression in surrounding healthy tissue and pancreatitis provides the molecular basis for developing radiolabeled NT analogs for targeted diagnostic imaging and radionuclide therapy.

Aiming towards this goal, we developed new NT analogs with modified lysine and arginine derivatives to enhance stability and coupled these analogs to either the DTPA or the DOTA chelating system (**chapters 2 and 3**). *In vitro*, the NTR-1 binding affinity of the ^{111}In -labeled NT analogs was not compromised by the modifications in the peptide sequence and the attachment of the chelator, whereas the *in vitro* stability in human serum was successfully improved. In addition, the NT analogs showed rapid receptor-mediated internalization into receptor-positive tumor cells with analog [^{111}In -DTPA](Pip)Gly-Pro-(PipAm)Gly-Arg-Pro-Tyr-tBuGly-Leu-OH (^{111}In -MP2530) and its DOTA-conjugated counterpart, [^{111}In -DOTA](Pip)Gly-Pro-(PipAm)Gly-Arg-Pro-Tyr-tBuGly-Leu-OH (^{111}In -MP2656), as the leading compounds. *In vivo* biodistribution studies confirmed the *in vitro* results and showed highest tumor uptake and rapid clearance from background tissues and blood for ^{111}In -MP2530 and ^{111}In -MP2656. The relatively high kidney retention could not be reduced by

co-administration of lysine, which is probably due to the lack of lysine residues in the peptide sequence of these NT analogs.

Although pre-clinically the NT analogs seemed promising, initial patient studies performed in our institute may suggest otherwise. Out of seven patients with proven adenocarcinoma of the pancreas who underwent ^{111}In -MP2530 scintigraphy, none showed pathological uptake on the scintigraphic images [1]. *In vitro* autoradiography of tumor tissue derived after surgery (five patients) showed low NTR-1-expression in only one moderately differentiated tumor, this low incidence being in contrast to the findings of Reubi et al., showing NT receptors in 75% of pancreatic adenocarcinomas. The results of our study might however be influenced by the fact that the patients in our study had poorly to moderately differentiated tumors, whereas Reubi et al. observed NT receptors more often in differentiated than in poorly differentiated tumors [2]. The lack of ^{111}In -MP2530 uptake in the receptor-positive tumor of the pancreas in this patient *in vivo*, might be ascribed to the rapid degradation of the compound that was found in the patients studied here. Next to the unexpected low incidence of NT receptors on exocrine pancreatic tumors, the observed relatively high accumulation in the kidneys and bone marrow might argue the prospect of NT receptor-targeted peptide receptor radionuclide therapy (PRRT). This conclusion is strengthened by another clinical evaluation study by Buchegger et al. using a $^{99\text{m}}\text{Tc}$ -labeled NT analog ($^{99\text{m}}\text{Tc}$ -NT-XI) [3], showing only moderate pathological uptake in one out of four exocrine pancreatic cancer patients. Tumors from two out of these four patients were shown receptor-negative.

In summary, stabilization of the NT analogs in patients might improve the scintigraphic potential of the peptides to image NTR-1-expressing tumors. On the other hand, clinical imaging studies have shown that the incidence and receptor density of NT receptors on exocrine pancreatic tumors may be lower than was expected, suggesting that the NTR-1 might not be an optimal target for peptide receptor scintigraphy (PRS) and PRRT using radiolabeled peptide analogs. Additional imaging studies with a more stable NTR-1 targeting compound in exocrine pancreatic cancer patients, including patients with more differentiated tumors, are necessary to further assess the clinical relevance of NTR-1 targeted PRS and PRRT.

Part II: Bombesin analogs for *in vivo* targeting of prostate cancer.

Prostate cancer is the second leading cause of cancer-related deaths and the most frequently diagnosed cancer in men in Western countries. Prostate cancer will increase to be a major health problem due to the aging of people in the western world. In general, tumor that is confined to the prostate gland should be curable; the odds of cure diminish considerably when the malignancy has penetrated the capsule, invaded the seminal vesicles, or metastasized to the lymph nodes. The three standard treatment

strategies for men with early stage (organ-confined) prostate cancer are radical prostatectomy, radiation therapy (external beam radiation therapy, brachytherapy, or both), and active surveillance.

Metastatic disease, on the other hand, is a major oncological problem and is not curable but temporary tumor reduction can be achieved by hormone deprivation therapy. However, prostate cancer patients will eventually relapse, the majority of these patients even within 1-2 years. After failure of hormone therapy, taxane-based treatment strategies have shown to moderately improve the chances of survival. However, most patients will eventually die of progressive, hormone-independent disease within a few years.

Early screening for prostate cancer (prostate specific antigen (PSA) testing) has resulted in a sharp increase in the detection rate of locally confined tumors, the micro-metastatic stage of these tumors is often uncertain. Accurate staging is essential for treatment planning, for unnecessary invasive surgery might be prevented. Currently, all men with prostate cancer are assigned a pathological stage of disease based upon evaluation of the digital rectal examination (DRE) and pathologist evaluation of the surgical biopsy specimen. Adjunctive studies may be used to further predict the likelihood of organ-confined disease including a radionuclide bone scan, abdominal-pelvic computed tomography (CT), magnetic resonance imaging (MRI) of the prostate gland, and single-photon emission computed tomographic (SPECT) imaging using a murine monoclonal antibody that targets prostate specific membrane antigen (PSMA) (ProstaScint). There is, however, still need for sensitive imaging modalities that combine localization and staging of the disease with differentiation between benign and malignant prostate tissue.

GRP receptors are over-expressed on several human tumors including prostate tumors. In **chapter 4** we describe the synthesis of 5 new BN peptide analogs, all based on the C-terminal octapeptide sequence of BN and including non-natural amino acids. The BN analogs were conjugated to the DTPA chelating system which enabled stable radiolabeling with ^{111}In . These new BN analogs were evaluated for their *in vitro* and *in vivo* GRP receptor-targeting characteristics. In animal studies [^{111}In -DTPA-ACMpip⁵,Tha⁶, β Ala¹¹,Tha¹³,Nle¹⁴]BN(5-14) (^{111}In -Cmp 3) showed good uptake in both rat and human GRP receptor-expressing tumor models with favorable tumor-to-non tumor ratios of radioactivity. ^{111}In -Cmp 3 is therefore a good candidate for molecular SPECT imaging of GRP receptor-positive tumors, like prostate tumors. Replacing DTPA by the DOTA chelating system in the Cmp 3 peptide structure would enable radiolabeling with β -particle emitters like ^{177}Lu and ^{90}Y , which may permit the use of Cmp 3 in PRRT of GRP receptor-expressing tumors. The DOTA chelator also enables radiolabeling with positron-emitters like ^{68}Ga , ^{86}Y and ^{64}Cu for PET-imaging.

PET is a rising new imaging modality with high potential for diagnosis, staging, and follow up of cancer patients. Advantages of PET over SPECT imaging include a higher spatial resolution in clinical cameras and the possibility to quantitate more accurately the uptake in the tumor and the normal organs. ^{18}F -FDG is a well known PET tracer, and often used for tumor imaging. ^{18}F -FDG is being used to visualize increased glucose metabolism, which is a characteristic of many fast growing tumors. However, studies have shown that ^{18}F -FDG is in general not a suitable PET tracer for diagnosing prostate cancer as, unlike many other tumor types, prostate cancer often does not display increased glucose metabolism. Early studies showed little difference between FDG uptake in prostate cancer and benign prostatic hyperplasia [4, 5]. The over-expression of GRP receptors in prostate tumors is restricted to only the malignant cells, as normal and hyperplastic prostate tissue were shown to be GRP receptor-negative [6]. GRP receptor-targeted imaging strategies are therefore capable of designating malignant from non malignant neoplasms.

Chapter 5 describes a study evaluating the previously published DOTA-BN analog, $[\text{DOTA}^0\text{-Pro}^1, \text{Tyr}^4]\text{BN}$, radiolabeled with ^{86}Y and ^{64}Cu as candidates for non-invasive detection of GRP receptor-positive tumors using PET. Both the ^{64}Cu and ^{86}Y -labeled DOTA-BN peptides were able to clearly delineate the human prostate tumor model *in vivo* in mice. Superior microPET images were obtained using the ^{86}Y -labeled compound due to lower accumulation of radioactivity in the clearance organs and background tissues. The latter compound is therefore promising as a GRP receptor-targeting PET tracer.

Part III: GRP receptor-expression during prostate cancer development.

A typical feature of prostate cancer is the transition of an initially androgen-responsive characteristic, towards androgen-independent tumor growth in more progressed stages of tumor development. Expression of GRP receptors in human prostate tumors is, however, primarily evaluated in early stages of tumor development and therefore expression in more progressed prostate tumors is uncertain. As a result, it is unclear whether GRP receptor-mediated SPECT and PET imaging and PRRT are suitable imaging and treatment modalities in all stages of the disease. In **chapters 6 and 7** we aimed to assess more information on GRP receptor expression in different stages of prostate cancer development. We therefore used a panel of 12 well established human prostate cancer xenograft models representing the various stages of prostate tumor progression, ranging from early, androgen-dependent stages, to late stage androgen-independent disease. *In vitro* autoradiographic receptor-binding studies showed GRP receptor-mediated binding of radiolabeled BN analogs only in androgen-dependent and not in androgen-independent xenografts representing the more advanced stages of prostate tumor development (**chapter 6**). These results suggest that GRP receptor

expression is directly or indirectly related to the state of androgen-dependency of the tumor.

As the majority of prostate cancer patients are initially androgen sensitive, androgen ablation treatment is a commonly used effective treatment strategy. However, along with the transition from androgen-dependent to androgen-independent tumor growth, ablation treatment becomes ineffective, and patients cope with hormone refractory prostate cancer (HFPC). In chapters 6 and 7 we evaluated the effect of androgen ablation on GRP receptor expression. Mice bearing the androgen sensitive and GRP receptor-positive xenografts were ablated from testosterone by castration. Subsequently, GRP receptor expression was determined *in vitro* (autoradiography) and *in vivo* (biodistribution) using a radiolabeled BN analog. All androgen-dependent tumor models demonstrated a significant reduction in tumor uptake after castration of tumor-bearing mice which could be confirmed *in vitro*. In addition, ending ablation treatment via testosterone supplementation in the castrated tumor-bearing mice resulted in recovery of the GRP receptor expression level (**chapter 7**). These results provide strong support for androgen-dependent GRP receptor-expression. Further studies evaluating GRP receptor-expression in human prostate tumor samples (primary tumors, involved lymph nodes, and metastases) before and after hormone treatment are ongoing. Results of these studies might be more conclusive on the potentially androgen-regulated expression of GRP receptors.

The outcome of the studies described above could have serious consequences for the clinical application of GRP receptor-targeted strategies. Androgen-independent prostate cancer might not express sufficient levels of GRP receptors, and consequently, tumor visualization and treatment using radiolabeled BN analogs might have no value in these patients. In addition, androgen ablation treatment in patients with early stage androgen-sensitive prostate cancer might induce GRP receptor down-regulation and might therefore hamper GRP receptor-targeted tumor imaging and therapy in these patients.

Nevertheless, non-invasive imaging techniques for diagnosis, localization, and staging of prostate cancer patients are still urgently needed, especially imaging techniques that can differentiate between benign and malignant prostate tissue. Early detection and accurate staging at time of diagnosis is essential and determines the treatment options available, as the presence of lymph node metastasis will make local treatment needless. The results of this study provide strong support for the use of GRP receptors for a sensitive new image modality for prostate cancer patients at the earliest time possible. Also, a significant number of patients that have been treated locally by radical prostatectomy or radiation therapy will sooner or later show increasing levels of PSA of unknown origin and require additional therapy. These patients who have not yet been treated with additional hormonal therapy, who are

faced with generally low volume metastases, may benefit from new systemic treatments using GRP receptor-based, radiolabeled therapeutic BN analogs.

CONCLUSION

In pre-clinical studies the novel ^{111}In -labeled DTPA- and DOTA-conjugated NT analogs seemed promising for imaging and treatment of exocrine pancreatic adenocarcinomas. However, results from an initial patient study showed low *in vivo* stability of the compound used, low incidence of NTR-1-expressing tumors, and no detectable pathologic uptake in one receptor-positive lesion *in vivo*. These findings, together with the high accumulation of radioactivity in the patient's kidneys and bone marrow, might suggest that the NTR-1 is not an appropriate target for PRS and PRRT of exocrine pancreatic tumors. Additional patient studies with a more stable NT analog are necessary to assess the clinical relevance of NTR-1 targeted PRS and PRRT. At present, NTR-1-targeting using radiolabeled NT analogs is not further evaluated in our institute.

In contrast to NTR-1, GRP receptor-based imaging modalities using radiolabeled BN analogs have shown positive tumor visualization in a few patient studies. Currently, ongoing pre-clinical studies in our institute comparing the *in vivo* characteristics of several reported BN analogs, will establish the most promising GRP receptor-targeting compound for further clinical evaluation in cancer patients.

Whether the GRP receptor is an appropriate target in the more advanced, androgen-independent, stages of prostate cancer remains as yet undecided, as is the relevance of GRP-receptor-targeted modalities in hormonally treated patients. Although our pre-clinical results suggest androgen-regulation of the GRP receptor, evaluation of GRP receptor-expression in human tumor samples will provide more insight.

REFERENCES

1. Froberg, A., C. van Eijck, M. Verdijseldonck, et al., Use of neurotensin analogue In-111-neurotensin (In-111-MP2530) in diagnosis of pancreatic adenocarcinoma. *Eur J Nucl Med Mol Imaging* 2004; 31, suppl 2: S392.
2. Reubi, J.C., B. Waser, H. Friess, et al., Neurotensin receptors: a new marker for human ductal pancreatic adenocarcinoma. *Gut* 1998; 42(4): 546.
3. Buchegger, F., F. Bonvin, M. Kosinski, et al., Radiolabeled neurotensin analog, ^{99m}Tc-NT-XI, evaluated in ductal pancreatic adenocarcinoma patients. *J Nucl Med* 2003; 44(10): 1649.
4. Hofer, C., C. Laubenbacher, T. Block, et al., Fluorine-18-fluorodeoxyglucose positron emission tomography is useless for the detection of local recurrence after radical prostatectomy. *Eur Urol* 1999; 36(1): 31.
5. Salminen, E., A. Hogg, D. Binns, et al., Investigations with FDG-PET scanning in prostate cancer show limited value for clinical practice. *Acta Oncol* 2002; 41(5): 425.
6. Markwalder, R. and J.C. Reubi, Gastrin-releasing peptide receptors in the human prostate: relation to neoplastic transformation. *Cancer Res* 1999; 59(5): 1152.

9

Nederlandse samenvatting
voor niet-ingewijden



NEDERLANDSE SAMENVATTING VOOR NIET-INGEWIJDEN

De ontwikkeling van nieuwe behandelingsmethoden voor kankerpatiënten gaat snel. Desondanks zijn er vele soorten van kanker die vaak te laat geconstateerd worden en daardoor onbehandelbaar zijn. Het onderzoeksproject, dat wordt beschreven in dit proefschrift, was gericht op de ontwikkeling van nieuwe technieken voor het diagnosticeren en behandelen van patiënten met prostaat­kanker en patiënten met exocrine pancreas(alvleesklier)tumoren. In dit hoofdstuk wordt een korte inleiding gegeven, gevolgd door een samenvatting van de resultaten van het onderzoek.

Receptoren zijn eiwitten die zich op het membraan van cellen bevinden. Peptiden zijn kleine eiwitten die zich kunnen binden aan deze receptoren. Elke peptide bindt aan een specifieke receptor op een manier die vergelijkbaar is met een sleutel en een slot. Deze peptide-receptor bindingen zorgen in het lichaam voor de communicatie tussen cellen. Tumorcellen brengen vaak bepaalde receptoren in overvloed tot expressie.

In de nucleaire geneeskunde wordt deze zogenaamde “overexpressie” van receptoren gebruikt om de tumorcellen in het lichaam te traceren. Hierbij wordt gebruik gemaakt van gesynthetiseerde peptiden welke zijn gekoppeld aan een radioactief molecuul. Deze radioactief “gelabelde” peptiden binden in het lichaam de receptoren op de tumorcellen waarna met behulp van speciale camera’s de locatie van de radioactieve peptiden in beeld gebracht kan worden. Deze methode van tumorvisualisatie wordt ook wel peptide-receptor scintigrafie (PRS) genoemd. De koppeling van het peptide aan een radioactief molecuul, dat in staat is tumorcellen te beschadigen, maakt tevens behandeling van de tumor mogelijk. Deze behandelingsmethode wordt ook wel peptide-receptor radionuclide therapie genoemd (PRRT).

Radioactief gelabelde peptiden worden succesvol gebruikt voor de visualisatie en behandeling van tumoren. Met name derivaten (afgeleide producten) van het peptide somatostatine zijn bewezen effectief in het lokaliseren en behandelen van neuroendocriene tumoren. Deze somatostatine derivaten zijn al sterk geoptimaliseerd, terwijl er op het gebied van tumoren, die andere receptoren dan de somatostatine receptoren tot expressie brengen, nog veel progressie geboekt kan worden.

Dit project was gericht op de ontwikkeling van radioactief gelabelde peptide derivaten van neurotensine (NT) voor de visualisatie en behandeling van exocrine pancreastumoren (**Deel I**) en op de ontwikkeling van radioactief gelabelde peptide derivaten van bombesine (BN) voor de visualisatie van prostaat tumoren (**Deel II**).

Zoals hierboven beschreven staat, binden deze peptide derivaten zich aan een receptor die op tumorcellen tot expressie wordt gebracht. In het geval van NT gaat het om de neurotensine receptor-1 (NTR-1) en in het geval van BN gaat het om de

gastrin-releasing peptide (GRP) receptor. De aanwezigheid van deze receptoren is van essentieel belang voor deze methode van tumorvisualisatie en -behandeling. In **deel III** van dit onderzoeksproject hebben we onderzocht of de GRP receptor in alle stadia van prostaatkankerontwikkeling door de tumorcellen tot expressie wordt gebracht. Hieronder wordt een samenvatting gegeven van de resultaten van dit onderzoeksproject.

Deel I: Neurotensine derivaten voor visualisatie en behandeling van exocrine pancreastumoren

In de literatuur staat beschreven dat NT receptoren tot overexpressie worden gebracht op 75% van alle exocrine pancreastumoren. Deze vorm van kanker is zeer progressief (snelle groei) en wordt, bij patiënten die deze tumoren dragen, vaak pas laat geconstateerd. Als gevolg hiervan is op het moment van diagnose een operatieve verwijdering van de tumor nog maar zelden een optie. Nieuwe methoden voor een vroege diagnose en behandeling zijn essentieel voor een betere prognose voor deze patiënten.

Het natuurlijke NT peptide, zoals dit voor komt in het menselijk lichaam, wordt snel afgebroken door enzymen in het bloed. In deze natuurlijke vorm zou het gelabelde peptide, na toediening aan de patiënt, afbreken vóór het de tumorcellen kan bereiken.

De **Hoofdstukken 2 en 3** van dit proefschrift beschrijven de evaluatie van nieuwe gestabiliseerde derivaten van NT. In experimenten met tumorcellen is gebleken dat, ondanks de veranderingen die zijn aangebracht in de samenstelling van de gestabiliseerde NT derivaten, de affiniteit (bindingssterkte) voor de NT receptor nog steeds voldoende hoog is. Ook hebben we middels internalisatie studies aangetoond dat de nieuwe NT derivaten via binding aan de NT receptor de tumorcel in getransporteerd worden. Vervolgens zijn de nieuwe NT derivaten getest in tumordragende muizen in een zogenaamde biodistributie studie, een studie naar de verdeling van het peptide in het lichaam.

Uit deze studies in tumorcellen en tumordragende muizen zijn twee NT derivaten geselecteerd met de hoogste receptor affiniteit, beste internalisatie in de tumorcellen en meest gunstige biodistributie in tumordragende muizen. Eén van deze twee geselecteerde NT derivaten, $^{111}\text{In-MP2530}$, is getest in 5 patiënten met exocrine pancreastumoren. In tegenstelling tot onze verwachtingen konden we in geen van deze patiënten de tumor visualiseren met behulp van het radioactief gelabelde NT derivaat. Na operatie van deze patiënten bleek dat de tumorcellen in 4 van de 5 patiënten geen NT receptoren tot expressie brachten, en er in 1 patiënt slechts een lage hoeveelheid NT receptoren op de tumorcellen aanwezig was. Deze lage incidentie van de NT receptoren op exocrine pancreastumoren is ook gevonden door een andere onderzoeksgroep. Deze bevindingen zouden kunnen betekenen

dat NT receptor niet in zoveel patiënten tot expressie wordt gebracht dan in eerste instantie werd gedacht (75%), waardoor de NT receptor mogelijk niet geschikt is voor PRS en PRRT. Door het lage aantal patiënten in deze studie met het nieuwe NT derivaat kunnen we uit de bevindingen geen harde conclusies trekken.

Het feit dat we in de patiënt met een lage hoeveelheid NT receptoren de tumor niet konden visualiseren, kan betekenen dat het gestabiliseerde NT derivaat toch wordt afgebroken in het bloed vóór het de tumorcellen bereikt. Studies in meer patiënten met exocrine pancreastumoren met meer stabiele NT derivaten, zou mogelijk duidelijkheid kunnen verschaffen over de expressie van NT receptoren op de tumoren, en de potentie van deze PRS en PRRT met NT derivaten.

Deel II: Bombesine derivaten voor visualisatie van prostaatkanker

Prostaatkanker is de meest voorkomende vorm van kanker onder westerse mannen. Over het algemeen is prostaatkanker goed te genezen wanneer de tumor gelokaliseerd is binnen de prostaat. Echter, wanneer de tumor de wand van de prostaat doorbreekt en/of metastaseert (uitzaait) naar de nabij gelegen lymfeklieren, daalt de kans op genezing aanzienlijk.

Gemetastaseerd prostaatkanker is niet te genezen, maar kan wel onderdrukt worden middels hormoonbehandeling. Bij deze therapie wordt het mannelijke geslachtshormoon testosteron, een androgeen, onderdrukt. Helaas is deze therapie slechts tijdelijk effectief en zal de tumor uiteindelijk opnieuw gaan groeien, in de meeste gevallen binnen 1-2 jaar na de start van de hormoonbehandeling. Deze nieuwe tumorgroei is vervolgens ongevoelig voor de hormoonbehandeling. Een alternatief voor deze hormoonongevoelige patiënten is chemotherapie, maar ook deze behandeling is tijdelijk en matig effectief.

Vroege screening op prostaatkanker bij mannen heeft geresulteerd in een stijging van het aantal diagnoses van binnen de prostaat gelegen tumoren. Op het moment van de screening blijft echter onduidelijk of er wel of geen micrometastasen aanwezig zijn. Een accurate bepaling van het stadium van prostaatkanker waarin de patiënt zich bevindt (wel/niet gemetastaseerd) is essentieel voor de bepaling van de behandelingsstrategie, zodat een onnodige en ingrijpende operatie vermeden kan worden. Op dit moment is er sterke behoefte aan een diagnostische techniek die accuraat het stadium van prostaatkankerontwikkeling kan bepalen.

GRP receptoren worden tot overexpressie gebracht op prostaattumorcellen. Bombesine is een peptide dat een hoge bindingsaffiniteit heeft voor de GRP receptor. Net als bij derivaten van somatostatine en NT zouden radioactief gelabelde derivaten van BN mogelijk gebruikt kunnen worden voor PRS en PRRT van prostaattumoren.

Hoofdstuk 4 van dit proefschrift beschrijft de evaluatie van nieuwe radioactief gelabelde BN derivaten voor de visualisatie van prostaattumoren. Studies in tumorcellen

hebben laten zien dat enkele van deze nieuwe BN derivaten een hoge bindingsaffiniteit hebben voor de GRP receptor en deze via de GRP receptor de cel kunnen binnendringen (internaliseren). Op basis van deze resultaten is één derivaat, ^{111}In -Cmp 3, geselecteerd voor verdere karakterisering in tumordragende proefdieren. De resultaten van deze experimenten tonen aan dat ^{111}In -Cmp 3 een veelbelovende kandidaat is voor het visualiseren van prostaattumoren in patiënten. Studies met ^{111}In -Cmp 3 in prostaatkanker patiënten zijn nog niet uitgevoerd.

Het camerasysteem waarmee ^{111}In -Cmp 3 in de patiënt gedetecteerd kan worden in de patiënt is de zogenaamde SPECT (single-photon emission computed tomography) camera. Een recent ontwikkeld camerasysteem voor PRS is de PET (positron emission tomography) camera. Deze PET camera heeft ten opzichte van de SPECT camera een aantal voordelen, waaronder een hogere resolutie van de scans. In **hoofdstuk 5** is een bestaand BN derivaat gekoppeld aan een radioactief molecuul welke gedetecteerd kan worden met behulp van de PET camera. Studies met tumordragende muizen hebben aangetoond dat het BN derivaat, ^{86}Y -DOTA-Pro¹,Tyr⁴BN, veelbelovend is voor PRS van prostaattumoren met behulp van een PET camera.

Deel III: Expressie van GRP receptoren gedurende prostaatkankerontwikkeling.

Een typische eigenschap van prostaatkanker is de overgang van hormoonongevoelige tumorgroei in een vroeg stadium, naar hormoonongevoelige tumorgroei in een meer gevorderd stadium van ontwikkeling. De overexpressie van GRP receptoren op prostaattumoren, welke noodzakelijk is voor de toepassing van radioactieve BN derivaten, is voornamelijk getest op tumorweefsel van patiënten in een vroeg stadium van tumorontwikkeling. Hierdoor is de receptor expressie op de hormoonongevoelige prostaattumoren nog onduidelijk. In **hoofdstuk 6 en 7** hebben we daarom de GRP receptor expressie in de vroege én late stadia onderzocht. Hiervoor is gebruik gemaakt van 12 tumormodellen die samen de verschillende stadia van prostaatkankerontwikkeling representeren. De resultaten van het onderzoek wezen uit dat de GRP receptor alléén tot expressie komt op de vroege, hormoonongevoelige modellen, en niet op de late, hormoonongevoelige modellen. Daarnaast is geconstateerd dat de eerder genoemde hormoonbehandeling, welke wordt toegepast bij patiënten met hormoonongevoelige tumorgroei, een negatief effect heeft op het aantal GRP receptoren op de tumormodellen.

De resultaten van deze studie suggereren dat de expressie van GRP receptoren afhankelijk is van de hormoonongevoeligheid van de tumor én de aanwezigheid van het hormoon testosteron. Voor prostaatkanker patiënten zou dit kunnen betekenen dat de radioactieve BN derivaten onbruikbaar zijn wanneer de tumor zich heeft ontwikkeld tot een hormoonongevoelig stadium. Omdat de experimenten echter zijn uitgevoerd met behulp van prostaattumormodellen, is verder onderzoek met

tumorweefsel dat afkomstig is van prostaatkankerpatiënten noodzakelijk om de resultaten te verifiëren. Het feit dat de GRP receptor wel aanwezig is in een vroeg stadium van prostaatkankerontwikkeling maakt PRS met behulp van radioactieve BN derivaten voor diagnose en tumorlokalisatie veelbelovend.

CONCLUSIES

De studies in dit proefschrift hebben bijgedragen aan de ontwikkeling van nieuwe visualisatie- en behandelingsmethoden voor prostaatkankerpatiënten en patiënten met exocrine pancreastumoren.

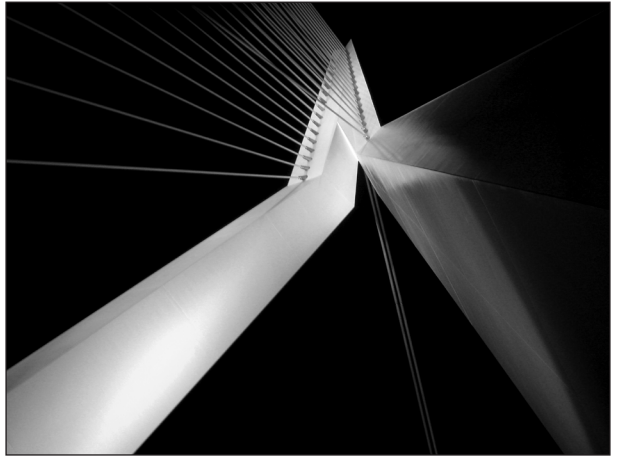
Nieuwe NT derivaten werden geselecteerd na aanleiding van positieve resultaten uit studies in cellijnen en muizen. Een veelbelovend NT derivaat, is vervolgens in een kleine groep patiënten met exocrine pancreastumoren getest. In tegenstelling tot onze muizen studies, konden we in geen van deze patiënten de tumor visualiseren. Vervolg onderzoek toonde aan dat het NT derivaat snel werd afgebroken in het lichaam van de patiënten én dat het merendeel van de patiënten, in tegenstelling tot de literatuur, geen NT receptoren tot expressie brachten. Hierdoor zijn vervolgstudies met meer stabiele NT derivaten en onderzoek naar de expressie van NT receptoren noodzakelijk om uitsluitsel te kunnen geven over de geschiktheid van de NT receptor voor PRS en PRRT in patiënten met exocrine pancreastumoren.

Uit verschillende studies in cellen en muizen is gebleken dat de BN derivaten, ^{111}In -Cmp 3 en [^{86}Y -DOTA-Pro¹,Tyr⁴]BN, veelbelovend zijn voor PRS van prostaattumoren in patiënten. Op dit moment zijn er binnen onze onderzoeksgroep experimenten gaande waarin verschillende BN derivaten van onze én andere onderzoeksgroepen vergeleken worden. Het beste BN derivaat zal vervolgens in prostaatkankerpatiënten getest gaan worden.

Vervolgstudies naar de expressie van GRP receptoren in de verschillende stadia van prostaatkankerontwikkeling worden momenteel verricht. Als aanvulling op de prostaattumormodellen die zijn gebruikt in dit onderzoeksproject, maken we in de vervolgstudies gebruik van prostaattumorweefsels afkomstig van patiënten. Deze studies zouden mogelijk meer inzicht kunnen geven in de toepasbaarheid van radioactief gelabelde BN derivaten voor PRS in hormoonongevoelige prostaatkankerpatiënten.

D

Dankwoord



DANKWOORD

Hier is het dan: het lang verwachte proefschrift! Ik heb me wel eens afgevraagd of het er ooit zou komen, maar dankzij de hulp en steun van velen is het toch gelukt. Ik wil hiervoor een aantal mensen bijzonder bedanken:

Allereerst mijn beide promotoren: Prof. Dr. Ir. Marion de Jong en Prof. Dr. Eric P. Krenning.

Marion, wat jij allemaal meemaakt in binnen- of buitenland is echt waanzinnig en de heerlijke anekdotes die daaruit voortkwamen, maakten de besprekingen altijd erg gezellig!

Op professioneel gebied was je voor mij een onuitputtelijke bron van wetenschappelijke informatie en een orakel op het gebied van “what to do next”. Maar wat ik in het bijzonder aan wil halen is je geduld. Het schrijven van manuscripten ging niet altijd even snel, maar je hebt me desondanks telkens weer gestimuleerd om op eigen kracht en op eigen tempo door te gaan. Daarbij wist je op cruciale momenten de chaos in mijn hoofd te reorganiseren en de benodigde rust terug te brengen.

In momenten van twijfel over het afronden van dit promotieproject, heb je mij weten te overtuigen om toch door te zetten. Je hebt daarbij voor mij vele obstakels uit de weg geruimd. Ik wil je ontzettend bedanken voor al je geduld en alles wat je voor me hebt gedaan.

Beste Prof. Krenning, ik kwam binnen bij Nucleaire Geneeskunde als één van “de meisjes” en ben halverwege het promotietraject doorgeschoven naar één van “de mama’s”. U heeft mij vervolgens de gelegenheid gegeven om het traject, op een voor mij prettige manier, voort te zetten. Zonder uw medewerking was dit proefschrift er nooit gekomen. Ik dank u voor mijn aanstelling als AIO en ik dank u voor uw ondersteuning.

Alle leden van de preklinische groep, iedereen heeft mij in de afgelopen jaren wel ergens mee geholpen, een gróot “BEDANKT” daarvoor. Maar dat is niet alles, hieronder volgen nog wat persoonlijkere woorden van dank:

Ria, bedankt voor de rustgevende gesprekken, ik heb je wijze raad en adviezen altijd erg gewaardeerd. En niet te vergeten, bedankt voor *AL* die krantenknipsels, Martijn en ik hebben ervan genoten!

Magda, met jou kon ik tijdens de koffie soms even lekker kletsen over van alles en nog wat, belangrijk of onbelangrijk, werk of privé, serieus of hilarisch, even mijn gedachten verzetten. Ik vond je medeleven en interesse altijd erg prettig!

Bert, ik kon met alle vragen bij je terecht, je maakte altijd tijd voor me. Wat ik mij vooral zal herinneren zijn je bezorgde, vaderlijke blikken. Ik heb je bezorgdheid en behulpzaamheid altijd zeer gewaardeerd en vind het erg jammer dat je ons gaat verlaten vanwege je FPU. Bert, ik wens je heel veel geluk toe en succes met al je plannen voor de toekomst.

Marleen, jij bent voor mij hét voorbeeld van een goede AIO. Ik heb veel respect voor hoe je werkt en ik wou dat ik aan je kon tippen! Ik kijk er dan ook naar uit om met je samen te werken aan jouw eigen promotieonderzoek en ik wens je veel succes!

Cristina, I did not get a chance to really work with you. That's a pity because you are a "Scientist" with a capital "S". Good luck with your career back in Switzerland.

Erik, bedankt voor al je labelingen! Dat klinkt onderhand oersaai, maar ja, zonder jouw labelingen had ik de experimenten simpelweg niet uit kunnen voeren. Dus, dankjewel Erik!

Wout, jij natuurlijk óók bedankt voor alle labelingen, maar ook voor het lezen en becommentariëren van mijn manuscripten. Daarnaast zal jouw nuchtere kijk op alles mij altijd bijblijven: "Wout Breeman? Ja die ken ik wel, die kon altijd zo héérlijk droog uit de hoek komen."

Rogier en Stefan, jullie zijn allebei halve NUGE-naren, maar hebben intussen wel ieder een héle plek ingenomen in mijn preklinisch NUGE-hart. Heel veel succes met jullie promotieonderzoeken en ik hoop er straks bij jullie promotie ook bij te zijn! En Rogier, als jij er nu even voor zorgt dat de GRP receptor in alle patiëntenweefsels kan worden aangetoond.....

Maarten, Edgar, Flavio en Ingrid, ik wil jullie, als ex-NUGE-naren, bedanken voor de alle gezelligheid. Ik wens jullie veel succes met jullie carrières.

Lideke, bedankt dat je me steeds hebt betrokken bij de patiëntenstudies. Ook bedankt voor het snelle lezen van manuscripten en het snel, uitgebreid en duidelijk beantwoorden van mijn vragen. Als ik nog iets terug kan doen?

Alle NUGE-naren op de L-vleugel, ik schaam me dat ik me het afgelopen anderhalf jaar bijna niet heb laten zien. Tijdens de lunch was het altijd gezellig en ik moet toegeven: ik mis het. Na 12 december zal ik proberen mijn leven te beteren!

Deel III van dit proefschrift is volledig in samenwerking met de afdeling Experimentele Urologie tot stand gekomen. Dr. Wytse M. van Weerden, Wytse, bedankt voor je begeleiding in dit deel van het project. Je hebt het enorm druk, maar desondanks heb ik bij jou nooit het gevoel gekregen dat je geen tijd voor me had. In tegendeel zelfs, je hebt heel veel tijd gestoken in het optimaliseren van mijn manuscripten en

nog eens zoveel tijd in het bespreken ervan. Corrina en Suzanne, deel III had niet bestaan zonder jullie inzet. Het voorbereidend werk dat jullie hebben verricht aan de tumordragende muizen was méér werk dan het experiment op zich, super!

Jack Erion, you have put a lot of effort in reading and revising some of my manuscripts, thank you very much for that!

Jason Lewis and Gráinne Biddlecombe, thank you for all the efforts you have put in the development of the PET-tracers (chapter 5), nice work!

Nanda Wildeman, bedankt voor al je hulp bij de autoradiografie experimenten, het was massaproductie! Ik vond het reuze gezellig toen je bij ons werkte... waarom duurt zo'n stage geen 3 jaar?

Héél veel dank ben ik verschuldigd aan mijn paranimfen Arthur en Maria. Zij hebben op alle vlakken geholpen aan dit proefschrift én aan de promotie: van het aanvragen van offertes van drukkers, receptie en dinerlocaties, het lezen van onderdelen uit het proefschrift, tot aan het houden van opbeurende peptalks en het fungeren als mentale boksbal in barre tijden. Samengevat wil ik zeggen: "Vrienden, dankjulliewel."

Wendy, als iemand weet wat "het druk hebben" inhoudt, dan ben jij dat. We hebben het allebei zó druk gehad dat we de vriendschap een beetje hebben laten versloffen. Toch weet ik dat jij er altijd bent als ik je nodig heb en dat gaf mij rust in deze hectische tijd. Dankjewel dat je mijn vriendin bent.

Suzanne, wij kwamen samen binnen als analist, gingen samen naar ons eerste congres, zijn samen AIO geworden, "samen" mama geworden, samen verhuisd naar het Sv-gebouw en gaan nu ook samen promoveren. Het is dan ook niet zo vreemd dat wij op het werk als onafscheidelijk worden beschouwd. Onze vriendschap is héél bijzonder, wij zijn namelijk zó verschillend en toch ook zó hetzelfde! Ik denk dan ook dat dát nu juist onze kracht is, waardoor we samen zó hard kunnen lachen en ook zo onbeschaamd kunnen huilen. Ik ben blij dat jij de afgelopen jaren aan mijn zijde hebt gestaan en ik ben er trots op dat ik op 12 december aan jouw zijde mag staan!

Mijn lieve ouders, ik heb de afgelopen jaren enorm veel steun van jullie gekregen, zo waren jullie regelmatig een flexibel kinderdagverblijf en meerdere malen een full-service verhuisbedrijf..., je zult toch maar zo'n dochter hebben. Ik heb veel respect voor jullie betrokkenheid bij het wel en wee van jullie kinderen, schoonkinderen en kleinkinderen. Papa en mama, jullie zijn mijn rotsen in de branding!

Hé broeder, lieve Marcel, ik vind het jammer dat ik er niet helemaal voor je kon zijn wanneer je me het hardst nodig had. Gelukkig zijn we broer en zus... *so you're stuck with me, brother!* We zijn intussen wel wat gewend van elkaar, maar ik beloof je dat ik vanaf nu weer een betere zus voor je zal zijn (en dat staat nu dus zwart op wit!).

Joyce, jij was de enige in de hele familie die precies begreep wat het schrijven van een proefschrift inhield. Tegen jou kon ik dan ook lekker klagen als het voor mijn gevoel maar weer eens niet opschoot. Dank je daarvoor en voor je hulp bij het corrigeren van de Nederlandse samenvatting.

Mijn schoonouders, Henk en Ingrid, bedankt voor jullie luisterende oren, jullie begrip en jullie geduld.

Susanne en Rieks, Gijs, Jasper, Linda, jullie waren een gezellige afleiding, bedankt!

Martijn, wij zijn bij elkaar sinds de start van mijn promotieonderzoek. Alles wat we tot nu toe hebben bereikt was echt team-work; allebei een opleiding, een AIO en een HAIO, en tegelijkertijd de zorg voor onze prachtige dochter Nicole. Toch verdien jij de 1ste prijs! Jij hebt me de afgelopen jaren gestimuleerd om keuzes te maken en daarvoor te gaan, maar vooral ook om naar mezelf te luisteren en mijn hart te volgen. Dit heeft mij de kracht gegeven om door te gaan wanneer dat even moeilijk was. Jij bent mijn "Mount Everest" in de branding! Lieve Martijn, ik heb goed nieuws: ik ben klaar! Maar pas op, nu ga ik voor de beker!

Nicole, jouw stralende kracht als zonnetje in huis, is mijn brandstof voor het leven.

Monique

SPONSORING

Financiële ondersteuning voor de totstandkoming van dit proefschrift werd verleend door onderstaande sponsoren, waarvoor hartelijk dank!

J.E. Jurriaanse Stichting

Harlan Netherlands B.V.

Tyco Healthcare/Mallinckrodt Medical B.V.

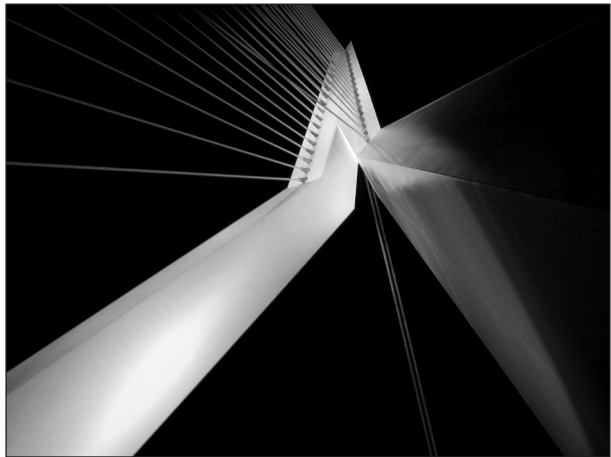
Siemens Nederland N.V.

Veenstra Instruments B.V.

Bioscan Inc.

CV

Curriculum Vitae
Publicatielijst



CURRICULUM VITAE

Monique de Visser werd geboren op 12 oktober 1978 te Bergen op Zoom. In 1996 behaalde zij haar HAVO diploma aan het Roncalli Scholengemeenschap te Bergen op Zoom, waarna zij begon aan de hogere laboratoriumopleiding (HLO) aan de Hogeschool Brabant te Etten-Leur, afstudeerrichting Biochemie. Na een stage bij de afdeling Target Discovery van N.V. Organon te Oss (begeleider: Dr. K.J. Dechering) studeerde zij in juli 2000 af. In datzelfde jaar werd zij aangesteld als research-analist in de groep van Prof. Dr. Ir. M. de Jong bij de afdeling Nucleaire Geneeskunde van het Erasmus MC (hoofd: Prof. Dr. E.P. Krenning).

Vanaf december 2002 werkte zij binnen dezelfde groep als assistent in opleiding (AIO) aan de ontwikkeling van nieuwe peptide derivaten voor de visualisatie en behandeling van tumoren. De resultaten van het onderzoek zijn beschreven in dit proefschrift.

PUBLICATIES

M. de Visser, P.J.J.M. Janssen, A. Srinivasan, J.C. Reubi, B. Waser, J. L. Erion, M. A. Schmidt, E.P. Krenning, M. de Jong. Stabilised ^{111}In -labelled DTPA- and DOTA-conjugated neurotensin analogues for imaging and therapy of exocrine pancreatic cancer. *Eur J Nucl Med Mol Imaging* 2003, 30: 1134.

M. de Visser, H.F. Bernard, J. L. Erion, M. A. Schmidt, A. Srinivasan, B. Waser, J.C. Reubi, E.P. Krenning, M. de Jong. Novel ^{111}In -labelled bombesin analogues for molecular imaging of prostate tumours. *Eur J Nucl Med Mol Imaging* 2007, 34(8);1228-38.

M. de Visser, W.M. van Weerden, C.A. de Ridder, S. Reneman, M. Melis, E.P. Krenning, M. de Jong. Androgen-dependent expression of the gastrin-releasing peptide receptor in human prostate tumor xenografts. *J Nucl Med* 2007; 48(1):88-93.

M. de Visser, W.M. van Weerden, C.A. de Ridder, S. Reneman, M. Melis, W.A.P. Bree-man, E.P. Krenning, M. de Jong. Androgen-regulated gastrin-releasing peptide receptor Expression in human prostate tumor xenograft bearing nude mice. (*submitted*)

M. de Visser*, **S.M. Verwijnen***, R. Valkema, D.J. Kwekkeboom, A.C. Fröberg, E.P. Krenning, M. de Jong. Improvement strategies for Peptide Receptor Scintigraphy and Radionuclide Therapy. *Cancer Biother. Radiopharm.* 2007; *in press*

P.J.J.M. Janssen*, **M. de Visser***, S.M. Verwijnen, H.F. Bernard, A. Srinivasan, J.L. Erion, W.A.P. Breeman, A.G. Vulto, E.P. Krenning, M. de Jong. Five stabilized ^{111}In -labeled neurotensin analogs in nude mice bearing HT29 tumors. *Cancer Biother. Radiopharm.* 2007, 22(3);374-382.

G.B. Biddlecombe, B.E. Rogers, **M. de Visser**, J.J. Parry, M. de Jong, J.L. Erion, J.S. Lewis. Molecular imaging of gastrin-releasing peptide receptor-positive tumors in mice using ^{64}Cu - and ^{86}Y -DOTA-(Pro¹,Tyr⁴)-bombesin(1-14). *Bioconjugate Chemistry* 2007, 18;724-730.

E.J. Rolleman, E.P. Krenning, H.F. Bernard, **M. de Visser**, M. Bijster, T.J. Visser, M. Vermeij, J. Lindemans, M. de Jong. Long-term toxicity of [^{177}Lu -DOTA⁰,Tyr³]octreotate in rats. *Eur J Nucl Med Mol Imaging* 2007;34(2):219-227

M. Melis, E.P. Krenning, H.F. Bernard, **M. de Visser**, E.J. Rolleman, M. de Jong. Renal uptake and retention of radiolabelled somatostatin, bombesin, neurotensin, minigastrin and CCK analogues: species and gender differences. *Nucl. Med. Biol.* 2007;34(6):633-641